AD_____

Award Number: DAMD17-02-1-0418

TITLE: Role of the Neddylation Enzyme Uba3, a New Estrogen Receptor Corepressor in Breast Cancer

PRINCIPAL INVESTIGATOR: Kenneth P. Nephew, Ph.D.
Meiyun Fan, Ph.D.
Teresa Craft
Annie Park

CONTRACTING ORGANIZATION: Indiana University School of Medicine
Bloomington, IN 47405-4401

REPORT DATE: September 2006

TYPE OF REPORT: Annual Summary

PREPARED FOR: U.S. Army Medical Research and Materiel Command
Fort Detrick, Maryland 21702-5012

REPORT DOCUMENTATION PAGE

Form Approved
OMB No. 0704-0188

1. REPORT DATE	2. REPORT TYPE	3. DATES COVERED
01-09-2006	Annual Summary	1 Sep 2002 – 31 Aug 2006

4. TITLE AND SUBTITLE

Role of the Neddylation Enzyme Uba3, a New Estrogen Receptor Corepressor in Breast Cancer

5a. CONTRACT NUMBER

5b. GRANT NUMBER
DAMD17-02-1-0418

5c. PROGRAM ELEMENT NUMBER

6. AUTHOR(S)
Kenneth P. Nephew, Ph.D
Meiyun Fan, Ph.D.
Teresa Craft
Annie Park

5d. PROJECT NUMBER

5e. TASK NUMBER

5f. WORK UNIT NUMBER

7. PERFORMING ORGANIZATION NAME(S) AND ADDRESS(ES)

Indiana University School of Medicine
Bloomington, IN 47405-4401

8. PERFORMING ORGANIZATION REPORT NUMBER

9. SPONSORING / MONITORING AGENCY NAME(S) AND ADDRESS(ES)
U.S. Army Medical Research and Materiel Command
Fort Detrick, Maryland 21702-5012

10. SPONSOR/MONITOR'S ACRONYM(S)

11. SPONSOR/MONITOR'S REPORT NUMBER(S)

12. DISTRIBUTION / AVAILABILITY STATEMENT
Approved for Public Release; Distribution Unlimited

13. SUPPLEMENTARY NOTES
Original contains colored plates: ALL DTIC reproductions will be in black and white.

14. ABSTRACT

Estrogens play important roles in both the onset and malignant progression of breast cancer. The content of estrogen receptors in breast tumors is a valuable predictor of whether a patient will respond to therapy with antiestrogens, such as tamoxifen and fulvestrant (ICI 182,780). Expression and activity of ER can be lost or impaired in antiestrogen-resistant breast cancer. The proposed studies are designed to test the overall hypothesis that the ubiquitin-like NEDD8 protein modification pathway represses estrogen action by facilitating degradation of ER protein. Perturbation of this pathway may prove instrumental in breast tumor progression; alternatively, activation of this pathway may prove to be a valid target for novel therapeutics. This study on mechanisms that regulate ER levels and activity are highly relevant to the development and progression breast cancer, including tumor progression to states of hormone independence and antiestrogen resistance. Thus, understanding how the estrogen receptor is regulated is an area of research critical to understanding the tissue selective pharmacology of estrogens. In addition, tamoxifen and other selective estrogen receptor modulators target the estrogen receptor, and this study is of the utmost relevance to those important therapies.

15. SUBJECT TERMS
Estrogen Receptor, Corepressor, Ubiquitination, Nuclear Receptors, Transcription

16. SECURITY CLASSIFICATION OF:				18. NUMBER OF PAGES	19a. NAME OF RESPONSIBLE PERSON
					USAMRMC
a. REPORT	b. ABSTRACT	c. THIS PAGE			19b. TELEPHONE NUMBER *(include area code)*
U	U	U	UU	131	

Table of Contents

INTRODUCTION

Estrogen regulates diverse biological processes through estrogen receptors (ERα and ERβ) (1). Receptor levels and dynamics have a profound influence on target tissue responsiveness and sensitivity to estrogen, and receptor turnover rates provide estrogen target cells with the capacity for rapid regulation of receptor levels and thus dynamic hormone responses (2-5). Furthermore, several experimental results have recently demonstrated that receptor degradation is a key component of the response of cancer cells, including breast cancer cells, to antiestrogen therapy (6, 7). In advanced stage breast cancers, estrogen receptor expression and activity can be lost or impaired, and the tumors are often resistant to endocrine therapies, such as the steroidal antiestrogens, ICI 182,780 and ICI 164,384 (6, 7). Our findings during the funding period have raised the intriguing possibility for a role of ubiquitin and ubiquitin-like pathways, including the NEDD8 pathway, in ERα ubiquitination and degradation and suggest that disruptions in such pathways may contribute to the development of antiestrogen-resistance in human breast cancer. The overall hypothesis that ubiquitin protein modification pathways repress estrogen action by facilitating degradation of ER protein was tested. Our experimental results suggest that perturbation of this pathway may prove instrumental in breast tumor progression; alternatively, activation of ubiquitin protein modification pathways may prove to be valid targets for novel therapeutics.

BODY

Task 1 was to determine the effect of Uba3 on breast cancer cell proliferation. We attempted to generate breast cancer cell lines stably expressing the dominant negative Uba3 (C216S), a mutant that we had used previously to block the NEDD8 pathway (8). However, blocking this pathway in MCF7 breast cancer cells was lethal and the cells died. We then attempted to an inducible promoter to control C216S expression levels, but these efforts were similarly unsuccessful. We conclude that the NEDD8 is essential for cell survival. To further address this task, we generated a breast cancer cell line stably expressing a dominant negative Ubc12. The results of this investigation are described in Fan et al. (8 and manuscript in appendix), and some of the key findings are highlighted here. We established the stable cell line MCF7/ Ubc12C111S, which contains an impaired NEDD8 pathway and examined the effect of the antiestrogen on ERα degradation in these cells. Expression of Ubc12C111S inhibited ICI 182,780-induced ERα down-regulation (Fig. 5A). We then examined the growth inhibitory effect of ICI 182,780 in MCF/C111S cells. No significant difference was observed in basal cell proliferation rates between MCF7/C111S and MCF7/Vec cells in hormone-free medium (data not shown). Treatment with the antiestrogen inhibited basal cell growth of MCF7 and MCF7/Vec cells (Fig. 6A). In contrast, MCF7/C111S cells were partially resistant to ICI 182,780 (Fig. 6A, Left panel). Dose-response analysis showed that MCF7/C111S cells were resistant to a broad range of ICI 182,780 concentrations (Fig. 6A, Right panel). On the other hand, estradiol-induced proliferation of MCF7/C111S and control cells was similar (2-fold increase in cell number over a 6-day treatment period; data not shown). The effect of 4-OHT on MCF7/C111S and MCF7/Vec cell proliferation was examined in a time- and dose-response analysis. The response of the cell lines to 4-OHT was similar (Fig. 6B), suggesting that Ubc12C111S expression did not confer cells resistance to growth inhibitory effect of antiestrogens in general. These results suggest that the expression of Ubc12C111S conferred resistance of MCF7 cells to the growth inhibitory effects of ICI 182,780, but disrupting the NEDD8 pathway had no effect on the mitogenic response of MCF7 breast cancer cells to estradiol or the growth inhibitory effects of 4-OHT. Task one has been completed.

The second task of the project was to determine the molecular mechanisms of ERα corepression by the NEDD8 pathway. Toward this goal, we constructed Uba3 deletion constructs lacking one or both of the presumptive nuclear receptor interacting motifs (the NR boxes). GST-pulldown assays were conducted to determine which receptor domains mediate the interactions between ERα with Uba3. We were unable to detect direct interaction of the deletion mutant constructs with estrogen receptor (data not shown), suggesting that the NR boxes are essential for Uba3-ER interaction. However, this could also be due to important changes in protein conformation due to the removal of amino acid sequences. Thus, we took an alternative approach and generated point mutations within the NR boxes and then proposed to examine direct interactions of the mutant proteins with ER. Constructs were made and sequenced. However, we were unable to express proteins from the new constructs, for reasons that are unclear at this time. We speculate that perhaps the mutations made the protein unstable. Nonetheless, although mostly negative results were obtained, Task 2 has been completed.

Task 3 was to determine if ERα and ERα function is modified by APP-BP1 and Ubc12 and an NEDD8 target protein. First, we took a direct approach and determined if ERα is an NEDD8 target protein using co-transfection experiments, co-immunoprecipitation assays and Western blot analysis and looked for NEDD8-ER conjugates. We included various other components of the NEDD8 pathway, including co-transfecting Uba3, APPBP1, Ubc12 and various Cullin family members. We were unable to detect neddylated receptor (data not shown); therefore, we concluded that ER is not a direct substrate for modification by NEDD8. Next, we tested the hypothesis that the neddylation pathway may act to restrict

ERα activity by indirectly modulating receptor degradation. The results of this investigation are described in the manuscript in the appendix (8), and some of the key findings are highlighted below.

Coexpression of Uba3 decreased ERα protein level (Fig. 1A), and treatment with MG132, a specific proteasome inhibitor, blocked Uba3-stimulated down-regulation of ERα (Fig. 1B), confirming that the Uba3-induced ERα degradation is through the 26S proteasome. Overexpression of APP-BP1 or Ubc12 had no significant effect on ERα protein levels (data not shown), a result consistent with our previous observation that Uba3 is the limiting factor in neddylation-associated inhibition of ERα transcriptional activity (25). Next, to test the hypothesis that the neddylation pathway is required for ligand-mediated degradation of ERα, we used the dominant negative mutant of Ubc12, Ubc12C111S. Treatment of ERα transfected HeLa cells with estradiol resulted in a time-dependent decrease in ERα protein levels (Fig. 2A). In contrast, the effects of estradiol on receptor levels were less dramatic in cells expressing Ubc12C111S (Fig. 2A). Consistent with this observation, Uba3C216S, a dominant negative mutant of Uba3, also inhibited estradiol-induced ERα down regulation (Fig. 2B). Addition of the proteasome inhibitor MG132 prior to estradiol treatment completely abolished ligand-induced down-regulation of ERα (Fig. 2B), confirming that ERα undergoes proteasome-dependent degradation in response to estradiol. Collectively, these results demonstrate that a functional NEDD8 pathway is required for efficient, ligand-induced, proteasome-mediated degradation of ERα. Having established a role for the NEDD8 pathway in ERα down-regulation, we examined the effect of NEDD8 on receptor ubiquitination. Expression of dominant negative Ubc12C111S or Uba3C216S markedly decreased ERα ubiquitination in either the absence (Fig. 3, left panel) or presence of estradiol and MG132 (Fig. 3, right panel), compared to cells transfected with control vector or wild type Ubc12 or Uba3. These results suggest that a functional neddylation pathway is required for the efficient ubiquitination of ERα.

Having completed task 3, we continued to perform further investigations into the roles of ubiquitin-like pathway NEDD8 in the responses to estradiol and antiestrogens (deemed a logical extension of the SOW in previous Summary Reports and within the scope of the fundamental questions underlying the SOW). Thus, the role of the ubiquitin-proteasome pathway in ERα-mediated transcriptional responses in breast cancer cells was investigated. Genetic and pharmacologic approaches were utilized to disrupt ERα ubiquitination, proteasome-mediated proteolysis and thus ERα degradation, including a dominant negative mutant of the NEDD8 conjugation enzyme (Ubc12C111S), the 20S proteasome inhibitor MG132, a ubiquitin mutant with all of its lysines mutated to arginine (UbK0), and the partial agonist/antagonist tamoxifen. To investigate the effect of blocking ERα degradation on estradiol-induced transcriptional responses, estrogen receptor-responsive reporter assays and expression of endogenous ER-target genes in MCF7 human breast cancer cells were utilized. The results of this study are described in *Fan et al*. (ref. 9; appendix); key findings are highlighted below.

We show that proteasomal degradation is not essential for transcriptional activity of ERα and suggest that the ubiquitin-proteasome system functions to limit estradiol-induced transcriptional output. The results demonstrate that blocking polyubiquitination of ERα stabilizes the receptor, resulting in the prolonged expression of ERα-responsive genes (Fig.1B,C). Inhibiting the proteasome enhanced ERα transcriptional activity in MCF7 human breast cancer cells (Fig. 5A,B), indicating that ERα degradation plays a key role in limiting estradiol-induced transcriptional responses in these cells. The results further suggest that in cells containing low levels of ERα, proteasome-mediated receptor degradation plays a role in limiting estradiol-induced transcriptional responsiveness (Figure 1B). While blocking ERα degradation increased the magnitude of estradiol-induced gene transcription, no effect on hormone sensitivity was observed (Fig. 2). However, inhibiting the proteasome increased both the magnitude and duration of estradiol-induced expression of an ERα-target gene in breast cancer cells (Fig. 5A). Overall, the data support the hypothesis that proteasome-mediated degradation of ERα serves as a means to limit the duration of estradiol signaling in receptor positive breast cancer cells. The important implication of this study is that the estradiol-induced transcriptional response is limited by receptor degradation through the ubiquitin-proteasome system, and defects in proteasome-mediated degradation of ERα could lead to an enhanced cellular response to estradiol in breast cancer cells.

Abnormal expression of ERα has long been associated with both the initiation and progression of breast cancer (10). An increase in the number of ERα-positive cells, as well as increased individual cell ERα content, have frequently been detected in malignant breast tumors (11). Furthermore, increased ERα content has been shown to augment the magnitude of estrogen-stimulated gene expression, providing a growth advantage to breast cancer cells (2, 8, 9,12). Collectively, these observations indicate that alterations in ERα degradation pathways may contribute to deregulation of ERα, perhaps leading to enhanced estrogen action in breast tumors.

We (described above) and others have clearly shown degradation of unliganded ERα is mediated by the ubiquitin-proteasome pathway, regulation of this pathway, at the molecular level, remains unclear. One potential mechanism involves CHIP, the carboxyl terminus of Hsc70-interacting protein, previously shown to target Hsp90 interacting proteins for ubiquitination and proteasomal degradation. We investigated a role for CHIP in degradation of unliganded ERα (ref.

13; appendix). In HeLa cells transfected with ERα and CHIP, ERα is downregulated through a ubiquitination dependent pathway, while ERα-mediated gene transcription decreased (Fig. 1 and Fig 2A). In contrast, siRNA inhibition of CHIP expression resulted in increased ERα accumulation and reporter gene transactivation (Fig 1B and Fig 2B). Transfection of mutant CHIP constructs demonstrated that both the U-box (containing ubiquitin ligase activity) and the tetratricopeptide repeat (TPR, essential for chaperone binding) CHIP domains are required for CHIP-mediated ERα downregulation (Fig 3). In addition, coimmunoprecipitation assays demonstrated that ERα and CHIP associate through the CHIP TPR domain (Fig 3). In ERα-positive breast cancer MCF7 cells, CHIP overexpression resulted in decreased levels of endogenous ERα protein and attenuation of ERα-mediated gene expression (Fig 4 and Fig 5). Furthermore, ERα-CHIP interaction was induced by the Hsp90 inhibitor geldanamycin (GA), resulting in enhanced ER-alpha degradation; this GA effect was further enhanced by CHIP overexpression, but was abolished by CHIP-siRNA (Fig 6-7). Finally, ERα dissociation from CHIP by various ERα ligands, including estradiol, tamoxifen, and ICI 182,780 interrupted CHIP-mediated ERα degradation (Fig 8). These results demonstrate a role for CHIP in both basal and GA-induced ERα degradation. Furthermore, based on our observations that CHIP promotes ERα degradation and attenuates receptor-mediated gene transcription, we suggest that CHIP, by modulating ERα stability, contributes to the regulation of functional receptor levels, and thus hormone responsiveness, in estrogen target cells. Thus, based on our results, the chaperone/CHIP pathway, by regulating ERα, levels, likely contributes to the development/progression of breast cancer. We believe that such a possible role for CHIP in breast cancer merits further examination. Towards this objective, we generated and characterized antiestrogens-resistant cell lines (*Fan et al*., ref. 14; appendix, Fig. 1) and examined gene expression profiles using microarray technology (Figs 2, 3). We demonstrated that genes in our in vitro models are relevant to published gene expression data for human breast cancer tumors, *i.e*., genes known to associate with recurrence on tamoxifen (Table 1). In addition, during the funding period, we examined the mechanism of antiestrogen action and ERα degradation (*Long and Nephew*, ref. 15, appendix) and showed that that fulvestrant induces ERα to interact with CK8 and CK18 (Fig. 6), drawing the receptor into close proximity to nuclear matrix-associated proteasomes that facilitate ERα turnover (Figs 7, 8). We also contributed to collaborative projects on the regulation of ER target genes in breast cancer and novel antiestrogen compounds, resulting in co-authored publications (ref. 16-18; appendix).

KEY RESEARCH ACCOMPLISHMENTS

- Showed that the neddylation pathway is required for ligand-mediated degradation of ERα
- Discovered that the NEDD8 pathway is required for efficient ubiquitination of ERα
- Established that disrupting the NEDD8 pathway confers antiestrogen resistance in breast cancer cells
- Provided evidence that allowed us to speculate that disruptions in the NEDD8 pathway may provide a mechanism by which breast cancer cells acquire ICI 182,780 resistance while retaining expression of ERα.
- Showed that that ERα degradation plays a key role in limiting estradiol-induced transcriptional responses in MCF7 human breast cancer cells.
- Demonstrated that inhibiting the proteasome increased estradiol-induced expression of an ERα-target gene in breast cancer cells.
- Determined that proteasomal degradation is not essential for transcriptional activity of ERα and that the ubiquitin-proteasome system appears to function to limit estradiol-induced transcriptional output.
- Provided evidence to suggest that defects in proteasome-mediated degradation of ERα could lead to an enhanced cellular response to estradiol in breast cancer cells.
- Demonstrated that CHIP promotes ERα degradation and attenuates receptor-mediated gene transcription.
- Provided evidence to suggest that CHIP, by modulating ERα stability, contributes to the regulation of functional receptor levels, and thus hormone responsiveness, in estrogen target cells.
- Provided evidence to suggest the chaperone/CHIP pathway, by regulating ERα, levels, may contribute to the development/progression of breast cancer.

REPORTABLE OUTCOMES

Manuscripts

1. *Fan M, Bigsby RM, **Nephew KP** 2003 The NEDD8 pathway is required for proteasome mediated degradation of human estrogen receptor-α and essential for the antiproliferation activity of ICI 182,780 in ER-positive breast cancer cells Mol Endocrinol 17:356-365 (cover article)
2. *Fan M, Nakshatri H, **Nephew KP**. 2004. Inhibiting proteasomal proteolysis sustains estrogen receptor-alpha activation. Mol Endocrinol 18:2603-2615
3. *Fan M, Park A, **Nephew KP**. 2005 Interactions between estrogen receptor and the COOH terminus of the Hsp70-interacting protein (CHIP) Mol Endocrinol 19:2901-14

4. *Fan M, Yan PS, Hartman-Frey C, Chen L, Paik H, Abbosh PH, Cheng ASL, Li L, Huang T H-M, **Nephew KP**. Diverse gene expression and DNA methylation profiles correlate with differential adaptation of breast cancer cells to the antiestrogens tamoxifen and fulvestrant. Cancer Res (under revision)
5. *Long X, **Nephew KP.** 2006 Fulvestrant (ICI 182,780)-dependent interacting proteins mediate immobilization and degradation of estrogen receptor-α. J Biol Chem, 281:9607-15
6. *Leu YW, Yan PS, Fan W, Jin VX, Liu CJ, Curran EM, Welshons WV, Wei HS, Davuluri RV, Plass C, **Nephew KP,** Huang TH-M. 2004. Loss of estrogen signaling triggers epigenetic silencing of downstream targets Cancer Res 64:8184-8192 (cover article).
7. *Cheng ASL, Jin VX, PYan PS, Fan M, Leu YW, Chan MWY, Plass C, **Nephew KP,** Davuluri RV, Huang TH-M. 2006 Combinatorial analysis of transcription factor partners reveals recruitment of c-MYC to estrogen receptorα- responsive promoters Mol Cell, 3:393-404
8. *Fan M, Rickert EL, Chen L, Aftab SA, **Nephew KP**, Weatherman R. Characterization of the molecular and structural determinants of selective estrogen receptor downregulators. Breast Cancer Res Treat (*in press*).

*This DOD award is acknowledged in these publications.

Presentations

1. Fan M, Long X, Bailey JA, Reed CA, Gize EA, Osborne E, Kirk EA, Bigsby RM, **Nephew KP** The activating enzyme of NEDD8 inhibits steroid receptor function. Keystone Symposium on Nuclear Receptor Superfamily, April, 2002
2. Fan M, Bigsby RM, **Nephew KP** 2002 Role for the neddylation pathway in estrogen receptor ubiquitination and degradation. 84th Annual Meeting of the Endocrine Society, June 19-22, San Francisco, CA (platform talk)
3. Fan M, Bigsby RM, **Nephew KP** 2002 Role for the neddylation pathway in estrogen receptor ubiquitination and degradation. Midwest Regional Molecular Endocrinology Conference, Indiana University, Bloomington, IN (platform talk)
4. Fan M, Nakshatri H, **Nephew KP** The role of proteasome-mediated estrogen receptor-α (ER) degradation in estrogen responsiveness 94th annual meeting of the American Association for Cancer Research, Toronto, Ontario, Canada (poster/discussion).
5. Fan M, Nakshatri H, **Nephew KP** 2003 The role of proteasome-mediated degradation of estrogen receptor-α in estrogen-induced transcriptional response. Elwood Jensen Symposium on Nuclear Receptors and Endocrine Disorders. University of Cincinnati, December 5-7 (platform talk).
6. Fan M, Park A, **Nephew KP** 2005 CHIP (Carboxyl Terminus of Hsc70-Interacting Protein) promotes basal and geldanamycin-induced degradation of estrogen receptor-α. 87th annual Meeting of The Endocrine Society, San Diego, CA (platform talk).

CONCLUSIONS

The antiestrogen ICI 182,780 is a drug is used as a second-line endocrine agent in patients who have developed tamoxifen-resistant breast cancer. Despite its potent antitumor effects, the drug does not circumvent the development of antiestrogen resistance (19-21). Moreover, the fact that most tumors acquiring ICI 182,780 resistance do so while retaining expression of ERα and estrogen responsiveness (22-24), suggests that administration of the antiestrogen may possibly lead to the selection of tumor cells defective in ERα down-regulation pathway(s), which in turn may confer a proliferative advantage in either the presence or absence of estrogens. In this context, mechanism underlying persistent expression of ERα in tumors with acquired resistance, such as disruptions in the NEDD8, CHIP or other ubiquitin or ubiquitin-associated/protein receptor degradation pathways, may thus present an important therapeutic target for future drug intervention.

For the "so what section" (evaluates the knowledge as a scientific or medical product to also be included in the conclusion of this report), the loss of ERα degradation pathway(s) may provide a mechanism by which breast cancer cells acquire antiestrogen resistance while retaining expression of ERα. Pathways that utilize the ubiquitin-proteasome system could serve as a therapeutic targets for breast cancer.

In summary, all three tasks have been completed. .

List of personnel receiving pay from the research effort: Kenneth P. Nephew, Ph.D., Principal Investigator; Meiyun Fan, Ph.D., Postdoctoral Fellow; Teresa Craft, M.S., Research Associate, Annie Park, B.S., Research Associate, Xinghua Long, Graduate Student.

REFERENCES CITED

1. Barkhem T, Nilsson S, Gustafsson JA 2004 Molecular mechanisms, physiological consequences and pharmacological implications of estrogen receptor action. Am J Pharmacogenomics 4:19-28
2. Webb P, Lopez GN, Greene GL, Baxter JD, Kushner PJ 1992 The limits of the cellular capacity to mediate an estrogen response. Mol Endocrinol 6:157-67
3. Klinge CM 2000 Estrogen receptor interaction with co-activators and co-repressors. Steroids 65:227-51.
4. Reid G, Denger S, Kos M, Gannon F 2002 Human estrogen receptor-alpha: regulation by synthesis, modification and degradation. Cell Mol Life Sci 59:821-31
5. Eckert RL, Mullick A, Rorke EA, Katzenellenbogen BS 1984 Estrogen receptor synthesis and turnover in MCF-7 breast cancer cells measured by a density shift technique. Endocrinology 114:629-37
6. Dauvois S, Danielian PS, White R, Parker MG 1992 Antiestrogen ICI 164,384 reduces cellular estrogen receptor content by increasing its turnover. Proc Natl Acad Sci U S A 89:4037-41
7. Dauvois S, White R, Parker MG 1993 The antiestrogen ICI 182780 disrupts estrogen receptor nucleocytoplasmic shuttling. J Cell Sci 106:1377-88
8. Fan M, Bigsby RM, **Nephew KP** 2003 The NEDD8 pathway is required for proteasome mediated degradation of human estrogen receptor-α and essential for the antiproliferation activity of ICI 182,780 in ER-positive breast cancer cells Mol Endocrinol 17:356-365
9. Fan M, Nakshatri H, **Nephew KP**. 2004. Inhibiting proteasomal proteolysis sustains estrogen receptor-alpha activation. Mol Endocrinol 18:2603-2615
10. Anderson E 2002 The role of oestrogen and progesterone receptors in human mammary development and tumorigenesis. Breast Cancer Res 4:197-201
11. Sommer S, Fuqua SA 2001 Estrogen receptor and breast cancer. Semin Cancer Biol 11:339-52
12. Fowler AM, Solodin N, Preisler-Mashek MT, Zhang P, Lee AV, Alarid ET 2004 Increases in estrogen receptor-alpha concentration in breast cancer cells promote serine 118/104/106-independent AF-1 transactivation and growth in the absence of estrogen. Faseb J 18:81-93
13. Fan M, Park A, **Nephew KP**. 2005 Interactions between estrogen receptor and the COOH terminus of the Hsp70-interacting protein (CHIP) Mol Endocrinol 19:2901-14
14. Fan M, Yan PS, Hartman-Frey C, Chen L, Paik H, Abbosh PH, Cheng ASL, Li L, Huang T H-M, **Nephew KP**. Diverse gene expression and DNA methylation profiles correlate with differential adaptation of breast cancer cells to the antiestrogens tamoxifen and fulvestrant. Cancer Res (under revision)
15. Long X, **Nephew KP.** 2006 Fulvestrant (ICI 182,780)-dependent interacting proteins mediate immobilization and degradation of estrogen receptor-α. J Biol Chem, 281:9607-15
16. Leu YW, Yan PS, Fan W, Jin VX, Liu CJ, Curran EM, Welshons WV, Wei HS, Davuluri RV, Plass C, **Nephew KP,** Huang TH-M. 2004. Loss of estrogen signaling triggers epigenetic silencing of downstream targets Cancer Res 64:8184-8192 (cover article).
17. Cheng ASL, Jin VX, PYan PS, Fan M, Leu YW, Chan MWY, Plass C, **Nephew KP,** Davuluri RV, Huang TH-M. 2006 Combinatorial analysis of transcription factor partners reveals recruitment of c-MYC to estrogen receptorα- responsive promoters Mol Cell, 3:393-404
18. Fan M, Rickert EL, Chen L, Aftab SA, **Nephew KP**, Weatherman R. Characterization of the molecular and structural determinants of selective estrogen receptor downregulators. Breast Cancer Res Treat (*in press*)
19. Howell A, Osborne CK, Morris C, Wakeling AE 2000 ICI 182,780 (Faslodex): development of a novel, "pure" antiestrogen. Cancer 89:817-25
20. Lykkesfeldt AE, Larsen SS, Briand P 1995 Human breast cancer cell lines resistant to pure anti-estrogens are sensitive to tamoxifen treatment. Int J Cancer 61:529-34
21. Osborne CK, Coronado-Heinsohn EB, Hilsenbeck SG, Osborne CK, Coronado-Heinsohn EB, Hilsenbeck SG, McCue BL, Wakeling AE, McClelland RA, Manning DL, Nicholson RI 1995 Comparison of the effects of a pure steroidal antiestrogen with those of tamoxifen in a model of human breast cancer. J Natl Cancer Inst 87:746-50
22. Dumont JA, Bitonti AJ, Wallace CD, Baumann RJ, Cashman EA, Cross-Doersen DE 1996 Progression of MCF-7 breast cancer cells to antiestrogen-resistant phenotype is accompanied by elevated levels of AP-1 DNA-binding activity. Cell Growth Differ 7:351-9

23. Larsen SS, Heiberg I, Lykkesfeldt AE 2001 Anti-oestrogen resistant human breast cancer cell lines are more sensitive towards treatment with the vitamin D analogue EB1089 than parent MCF-7 cells. Br J Cancer 84:686-90.
24. Brunner N, Boysen B, Jirus S, Skaar TC, Holst-Hansen C, Lippman J, Frandsen T, Spang-Thomsen M, Fuqua SA, Clarke R 1997 MCF7/LCC9: an antiestrogen-resistant MCF-7 variant in which acquired resistance to the steroidal antiestrogen ICI 182,780 confers an early cross-resistance to the nonsteroidal antiestrogen tamoxifen. Cancer Res 57:3486-93

APPENDICES

Reprints:

1. *Fan M, Bigsby RM, **Nephew KP** 2003 The NEDD8 pathway is required for proteasome mediated degradation of human estrogen receptor-α and essential for the antiproliferation activity of ICI 182,780 in ER-positive breast cancer cells Mol Endocrinol 17:356-365 (cover article)
2. *Fan M, Nakshatri H, **Nephew KP**. 2004. Inhibiting proteasomal proteolysis sustains estrogen receptor-alpha activation. Mol Endocrinol 18:2603-2615
3. *Fan M, Park A, **Nephew KP**. 2005 Interactions between estrogen receptor and the COOH terminus of the Hsp70-interacting protein (CHIP) Mol Endocrinol 19:2901-14
4. *Fan M, Yan PS, Hartman-Frey C, Chen L, Paik H, Abbosh PH, Cheng ASL, Li L, Huang T H-M, **Nephew KP**. Diverse gene expression and DNA methylation profiles correlate with differential adaptation of breast cancer cells to the antiestrogens tamoxifen and fulvestrant. Cancer Res (under revision)
5. *Long X, **Nephew KP.** 2006 Fulvestrant (ICI 182,780)-dependent interacting proteins mediate immobilization and degradation of estrogen receptor-α. J Biol Chem, 281:9607-15
6. *Leu YW, Yan PS, Fan W, Jin VX, Liu CJ, Curran EM, Welshons WV, Wei HS, Davuluri RV, Plass C, **Nephew KP,** Huang TH-M. 2004. Loss of estrogen signaling triggers epigenetic silencing of downstream targets Cancer Res 64:8184-8192 (cover article).
7. *Cheng ASL, Jin VX, PYan PS, Fan M, Leu YW, Chan MWY, Plass C, **Nephew KP,** Davuluri RV, Huang TH-M. 2006 Combinatorial analysis of transcription factor partners reveals recruitment of c-MYC to estrogen receptorα- responsive promoters Mol Cell, 3:393-404
8. *Fan M, Rickert EL, Chen L, Aftab SA, **Nephew KP**, Weatherman R. 2006 Characterization of the molecular and structural determinants of selective estrogen receptor downregulators. Breast Cancer Res Treat (*in press*).

*This DOD award is acknowledged in these publications.

0888-8809/03/$15.00/0
Printed in U.S.A.

Molecular Endocrinology 17(3):356–365

doi: 10.1210/me.2002-0323

The NEDD8 Pathway Is Required for Proteasome-Mediated Degradation of Human Estrogen Receptor (ER)-α and Essential for the Antiproliferative Activity of ICI 182,780 in ERα-Positive Breast Cancer Cells

MEIYUN FAN, ROBERT M. BIGSBY, AND KENNETH P. NEPHEW

Medical Sciences (M.F., K.P.N.), Indiana University School of Medicine, Bloomington, Indiana 47405; and Departments of Obstetrics & Gynecology (R.M.B., K.P.N.) and of Cellular and Integrative Physiology (R.M.B., K.P.N.), Indiana University Cancer Center (R.M.B., K.P.N.), Indiana University School of Medicine, Indianapolis, Indiana 46202

Steroid hormone receptors, including estrogen receptor-α (ERα), are ligand-activated transcription factors, and hormone binding leads to depletion of receptor levels via preteasome-mediated degradation. NEDD8 (neural precursor cell-expressed developmentally down-regulated) is an ubiquitin-like protein essential for protein processing and cell cycle progression. We recently demonstrated that ubiquitin-activating enzyme (Uba)3, the catalytic subunit of the NEDD8-activating enzyme, inhibits ERα transcriptional activity. Here we report that Uba3-mediated inhibition of ERα transactivation function is due to increased receptor protein turnover. Coexpression of Uba3 with ERα increased receptor degradation by the 26S proteasome. Inhibition of NEDD8 activation and conjugation diminished polyubiquitination of ERα and blocked proteasome-mediated degradation of receptor protein. The antiestrogen ICI 182,780 is known to induce ER degradation. In human MCF7 breast cancer cells modified to contain a disrupted NEDD8 pathway, ICI 182,780 degradation of ERα was impaired, and the antiestrogen was ineffective at inhibiting cell proliferation. This study provides the first evidence linking nuclear receptor degradation with the NEDD8 pathway and the ubiquitin-proteasome system, suggesting that the two pathways can act together to modulate ERα turnover and cellular responses to estrogens. Based on our observation that an intact NEDD8 pathway is essential for the antiproliferation activity of the ICI 182,780 in ERα positive breast cancer cells, we propose that disruptions in the NEDD8 pathway provide a mechanism by which breast cancer cells acquire antiestrogen resistance while retaining expression of ERα. (*Molecular Endocrinology* 17: 356–365, 2003)

ESTROGEN REGULATES DIVERSE biological processes through estrogen receptors (ERα and ERβ) (1). Receptor levels and dynamics have a profound influence on target tissue responsiveness and sensitivity to estrogen (2). ERα is a short-lived protein with a half-life of about 4 h, which is reduced to 3 h by 17β-estradiol (estradiol), and to less than 1 h by the steroidal antiestrogens, ICI 182,780 and ICI 164,384 (3, 4). Receptor turnover rates provide estrogen target cells with the capacity for rapid regulation of receptor levels and thus dynamic hormone responses. An attenuated transcriptional response has been associated with down-regulation of ERα, and receptor up-regulation has been shown to enhance the cellular response to estrogen (2). Nonetheless, mechanisms governing ERα protein levels remain poorly understood.

It has recently been shown that degradation of ERα and other members of the nuclear receptor superfamily occurs through the ubiquitin-proteasome pathway (5). Ubiquitination is a multistep process involving the action of a ubiquitin-activating enzyme (E1 or Uba), a ubiquitin conjugation enzyme (E2 or Ubc), and a ubiquitin ligase (E3) (6). Because the high specificity for target proteins is primarily conferred by E3, regulation of E3 activity may play a crucial role in governing protein degradation *in vivo*. A large number of E3s are cullin-based ubiquitin ligases (7), including SCF (Skp1/Cul1/F-box/ROC1) and VCB (von Hippel-Lindau-Cul2/elongin B/elongin C) complexes. One important level of regulation of these cullin-based ubiquitin ligases involves modification of the cullin subunit with NEDD8, an ubiquitin-like protein (7).

NEDD8 conjugation (neddylation) resembles ubiquitination and involves the action of amyloid precursor protein-binding protein (APP-BP1)/Uba3, a heterodimeric E1-like enzyme, and Ubc12, an E2-like enzyme (8).

Abbreviations: APP-BP1, Amyloid precursor protein-binding protein; AR, androgen receptor; csFBS, charcoal-stripped FBS; E2, ubiquitin conjugation enzyme; E3, ubiquitin ligase; ER, estrogen receptor; estradiol, 17β-estradiol; FBS, fetal bovine serum; HA, hemagglutinin; GAPDH, glyceraldehyde phosphate dehydrogenase; GFP, green fluorescent protein; MTT, 3-(4,5-dimethylthiazol-2-yl)-2,5-diphenyltetrazolium bromide; NEDD8, neural precursor cell-expressed developmentally down-regulated; 4-OHT, 4-hydroxytamoxifen; PR, progesterone receptor; Uba, ubiquitin-activating enzyme; Ubc, ubiquitin-conjugation enzyme.

Whether a ligase is required for neddylation is unknown. To date, the only known substrates of NEDD8 are cullin family members (9, 10). Cullin neddylation is conserved and plays an important regulatory role for cullin-based E3 activity in yeast, plant, and mammalian cells (7, 11–13). Interrupting NEDD8 modification of cullins in mammalian cells has been shown to block ubiquitination of certain proteins involved in different cellular functions, including p27, IκBα, HIFα, and NFκB precursor p105 (14–19). Recent studies have revealed that cullin neddylation is a tightly controlled dynamic process (20–24), and the effect of neddylation on protein polyubiquitination appears to be specific (17, 18).

We recently identified the NEDD8 activating enzyme, Uba3 as an ER-interacting protein and inhibitor of transactivation by steroid nuclear receptors (25). We further demonstrated that an intact neddylation pathway is required for Uba3-mediated inhibition of ER transcriptional activity (25). Taken together with recent reports linking the ubiquitin and NEDD8 pathways (7), our findings raise the intriguing possibility for a role of neddylation in ERα ubiquitination and degradation. Here we show that Uba3 enhances ERα degradation by the 26S proteasome, and expression of dominant-negative mutants of Uba3 or Ubc12 impaired ERα ubiquitination and ligand-induced ERα degradation. Blocking the neddylation pathway with the dominant-negative Ubc in ERα-positive human breast cancer cells inhibited both receptor degradation and the growth inhibitory effect of the antiestrogen ICI 182,780 (known clinically as Faslodex or Fulvestrant). Collectively, these data show that the NEDD8 pathway plays an essential role in ubiquitination and proteasomal degradation of ERα and indicate that disruptions in the pathway may contribute to the development of antiestrogen resistance in human breast cancer.

RESULTS

Uba3 Enhances Proteasomal Degradation of ERα

To test the hypothesis that the neddylation pathway restricts ERα activity by modulating receptor degradation, we transfected HeLa cells with ERα, alone or in combination with an expression vector for Uba3, APP-BP1, or Ubc12, or with an empty vector (pcDNA3.1, Invitrogen, Carlsbad, CA); a green fluorescence protein (GFP) expression vector was cotransfected to serve as a means of normalizing transfection efficiency and sample preparations. Steady-state levels of ERα protein were determined by Western blot analysis. Coexpression of Uba3 decreased ERα protein level but had no effect on GFP expression (Fig. 1A). Treatment of the transfected HeLa cells with MG132, a specific proteasome inhibitor, blocked Uba3-stimulated down-regulation of ERα (Fig. 1B), confirming that the Uba3-induced ERα degradation is through the 26S proteasome. Overexpression of APP-BP1 or Ubc12 had no significant effect on ERα protein levels (data not shown), a result consistent with our previous observation that Uba3 is the limiting factor in neddylation-associated inhibition of ERα transcriptional activity (25).

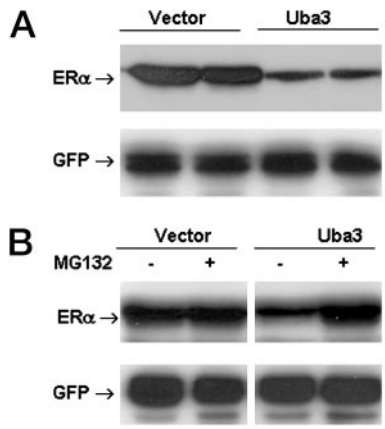

Fig. 1. Uba3 Enhances Proteasomal Degradation of ERα

A, Coexpression of Uba3 decreases ERα protein level in transfected HeLa cells. HeLa cells were transfected with pSG5-ER and pcDNA-Uba3 or pcDNA vector. Whole cell extracts were prepared 24 h post transfection and analyzed by Western blotting to determine ERα protein level. B, Proteasome inhibitor MG132 restores expression level of ERα in cells transfected with Uba3. Transfected HeLa cells (same as in A) were treated with 20 μM MG132 for 6 h before protein extracts and ERα level analysis. GFP was used as an internal control to correct for transfection efficiency and SDS-PAGE loading. Representative results of three independent experiments are shown.

The Neddylation Pathway Is Required for Ligand-Mediated Degradation of ERα

Estradiol stimulates ERα degradation through the ubiquitin-proteasome pathway (26–30). Having established a role for Uba3 in this process, it was important to assess whether neddylation pathway is required for ligand-induced degradation of ERα. To address this issue, we used a dominant-negative mutant of Ubc12 (Ubc12C111S). Due to a single Cys-to-Ser substitution at the active Cys residue, Ubc12C111S forms a stable complex with NEDD8, resulting in sequestration of NEDD8 and inhibition of subsequent NEDD8 conjugation (31, 32). Dominant-negative inhibition of NEDD8 conjugation by Ubc12C111S has been shown to impair efficient ubiquitination and protein degradation (14, 15, 17, 18). Treatment of ERα-transfected HeLa cells with estradiol resulted in a time-dependent decrease in ERα protein levels; receptor levels were reduced by 80% at 6–8 h. (Fig. 2A). In contrast, the effects of estradiol on receptor levels were less dramatic in cells expressing Ubc12C111S, producing a reduction of only 40% by 6–8 h (Fig. 2A). Consistent with this observation, Uba3C216S, a dominant-negative mutant of Uba3 (31, 32), also inhibited estradiol-induced ERα down-regulation (Fig. 2B). Addition of the proteasome inhibitor MG132 before estradiol treatment completely abolished ligand-induced down-regulation of ERα (Fig. 2B), con-

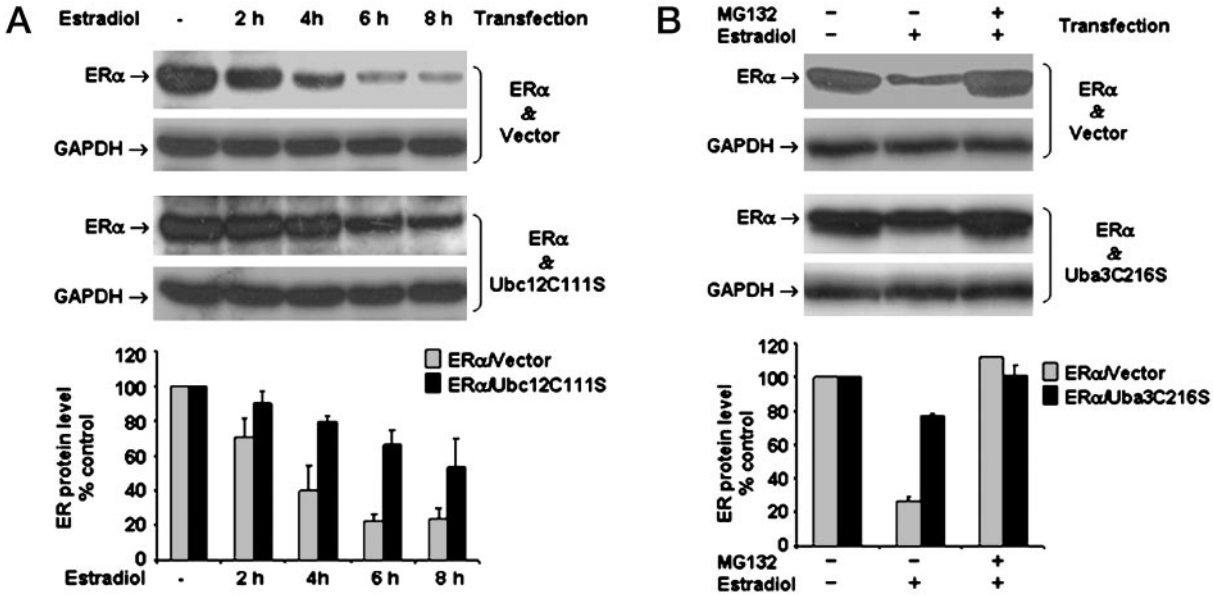

Fig. 2. Expression of Ubc12C111S or Uba3C216S Inhibits Ligand-Induced ERα Degradation

A, HeLa cells were transfected with pSG5-ER and pcDNA vector (*upper panel*) or pcDNA-Ubc12C111S (*lower panel*). Twenty-four hours after transfection, cells were treated with 100 nM estradiol for the indicated times and analyzed for ERα protein level using Western blotting. Relative ERα levels in cells cotransfected with vector (*gray*) or Ubc12C111S (*black*) from two independent experiments are shown in corresponding histogram. B, HeLa cells were transfected with pSG5-ER and pcDNA vector (*upper panel)* or pcDNA-Uba3C216S (*lower panel*). Twenty-four hours after transfection, cells were treated with vehicle or 20 μM MG132 for 1 h followed by incubation with vehicle or 100 nM estradiol for 6 h, as indicated. ERα protein levels were analyzed by immunoblotting. Relative ERα levels in cells cotransfected with vector (*gray*) or Uba3C216S (*black*) from three independent experiments are shown in corresponding histogram. GAPDH was used as an internal control to correct SDS-PAGE loading.

firming that exogenous ERα in HeLa cells undergoes proteasome-dependent degradation in response to estradiol. Collectively, these results demonstrate that a functional NEDD8 pathway is required for efficient, ligand-induced, proteasome-mediated degradation of ERα.

The NEDD8 Pathway Is Required for Efficient Ubiquitination of ERα

Having established a role for Uba3 and Ubc12 in ERα down-regulation, it was important to examine the effect of NEDD8 on receptor ubiquitination. HeLa cells were cotransfected with ERα and hemagglutinin (HA)-tagged ubiquitin, along with wild-type Ubc12 or Uba3 or the corresponding mutant forms of these neddylation enzymes (Ubc12C111S or Uba3C216S). At 24 h post transfection, cells were treated with MG132 or vehicle, followed by estradiol treatment. Immunoprecipitation assays using an anti-ERα antibody were performed and the levels of ubiquitinated ERα in the precipitated immunocomplex were assessed by Western blotting with an anti-HA antibody. The polyubiquitinated ERα exhibited a ladder of higher molecular weight species on the blot membrane (Fig. 3). Expression of dominant-negative Ubc12C111S or Uba3C216S markedly decreased ERα ubiquitination in either the absence (Fig. 3, *left panel*) or presence of estradiol and MG132 (Fig. 3, *right panel*), compared with cells transfected with control vector or wild-type Ubc12 or Uba3. These results suggest that a functional neddylation pathway is required for the efficient ubiquitination of ERα.

ERα Protein Levels in MCF7 Breast Cancer Cell Lines Stably Expressing Dominant-Negative Ubc12C111S

MCF7 human breast cancer cells express high levels of ERα and proliferate in response to estrogen treatment (33, 34), providing a model to study endogenous ERα function. To further investigate the role of neddylation in ERα function under physiological relevant conditions, we transfected Ubc12C111S into MCF7 cells and established the stable cell line MCF7/C111S. As a control, MCF7/Vec (MCF7 cells stably transfected with empty vector) was also established. Expression of the Ubc12C11S mutant protein in MCF7/C111S cells was confirmed by Western blotting and, consistent with a previous report (31), the mutant was detected as 26- and 31-kDa proteins (Fig. 4, lanes 3–8). In the regular growth medium containing phenol red and 10% fetal bovine serum (FBS), the level of ERα in MCF7/Vec cells was very low; after 3 d of culture in hormone-free medium containing 3% dextran-coated charcoal-stripped FBS (cs-FBS) and no phenol red, ERα expression was dramatically increased (Fig. 4, lanes 1 and 2). The culture medium (regular growth medium *vs.* hormone-free me-

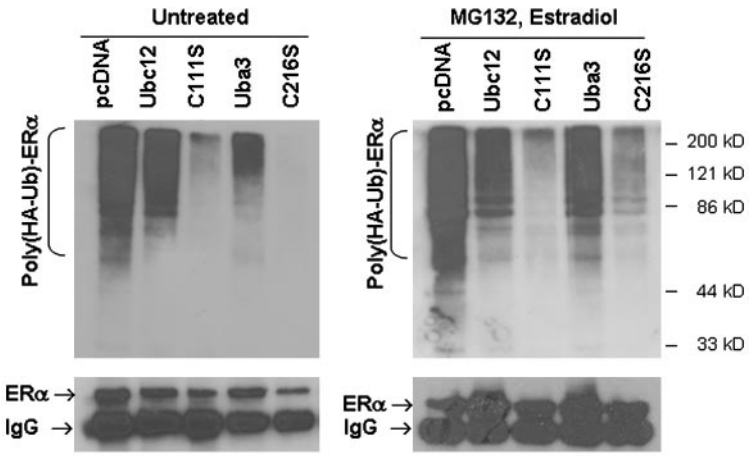

Fig. 3. An Intact NEDD8 Pathway Is Required for Efficient ERα Ubiquitination

HeLa cells were transfected with pSG5-ER, and pcDNA-HA-Ubiquitin, alone with indicated construct. Twenty-four hours after transfection, cells were either untreated (*left panel*) or treated with 20 μM MG132 for 1 h followed by 100 nM estradiol exposure for 3 h (*right panel*). Protein extracts were prepared and subjected to immunoprecipitation using anti-ERα antibody. Polyubiquitinated ERα was detected by Western blotting using anti-HA antibody, and was visualized as a ladder of higher molecular weight species on the blot. The blot was striped and reprobed by anti-ERα antibody to assess the amount of precipitated ERα (*lower panels*). The heavy chain of the anti-ERα IgG used for immunoprecipitation exhibits a 57-kDa band in the ERα blot. Representative results of three independent experiments are shown.

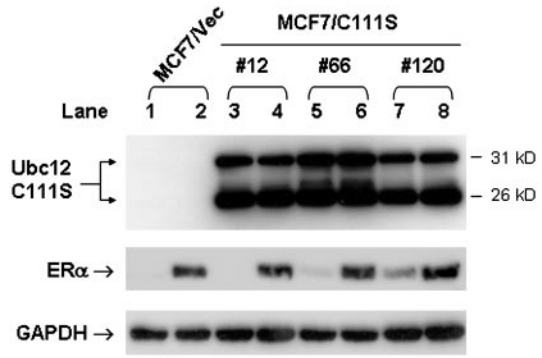

Fig. 4. The Expression of Ubc12C111S and ERα in Three Independent MCF7/C111S Clones

MCF7/C111S cells stably expressing mutant Ubc12C111S were maintained in growth medium (lanes 1, 3, 5, and 7) or hormone-free medium for 3 d (lanes 2, 4, 6, and 8) and analyzed by immunoblotting using anti-HA (*upper panel*) or anti-ERα (*lower panel*) antibodies, respectively. GAPDH was used as an internal control to correct for SDS-PAGE loading.

dium) showed no effect on the expression level of Ubc12C111S. In three MCF7/C111S clones, receptor levels varied among the clones and, when cultured in growth medium, detectable ERα was seen in two of the three clones (Fig. 4, lanes 5 and 7). When cultured in estrogen-free medium, however, ERα levels were high in all three clones (Fig. 4, lanes 4, 6, 8).

Ubc12C111S Inhibits ICI 182,780-Induced Down-Regulation of ERα

In contrast to estradiol, which down-regulates ERα in target tissues through both transcriptional and posttranslational mechanism (35, 36), the pure antiestrogen ICI 182,780 causes ERα protein degradation without affecting ERα mRNA levels (3, 36). Based on our observations that the NEDD8 pathway is essential for ERα degradation in transfected HeLa cells (Fig. 2), it was of interest to examine the effect of the antiestrogen on ERα degradation in MCF7/C111S cells. Cells were cultured in hormone-free medium for 3 d before ICI 182,780 treatment. Under this condition, comparable amounts of ERα were observed in MCF7/C111S and MCF7/Vec cells (compare 0-h lanes in Fig. 5A). Treatment with ICI 182,780 rapidly (by 1 h) decreased ERα levels in the MCF7/Vec cells; by 4 h post treatment, the levels of ERα were reduced by 95% (Fig. 5A). In the MCF7/C111S cells, the effects of ICI 182,780 on ERα levels were much less dramatic (Fig. 5A). Thus, although ER degradation was not completely inhibited by expression of the dominant-negative Ubc12C111S, these results confirm our observations using transient transfection in HeLa cells and further suggest that the NEDD8 pathway is required for efficient degradation of endogenous ERα. To examine the effect of another antiestrogen on ERα degradation in this system, cells were cultured in the presence of various doses of 4-hydroxytamoxifen (4-OHT) and ERα levels were examined. In both MCF7/Vec and MCF7/C111S cells, ERα levels remained unchanged or were slightly increased after treatment with 4-OHT (Fig. 5B). Stabilization of ERα by tamoxifen has been reported by others (30), perhaps due to inhibition of the basal rate of ER degradation by the antiestrogen.

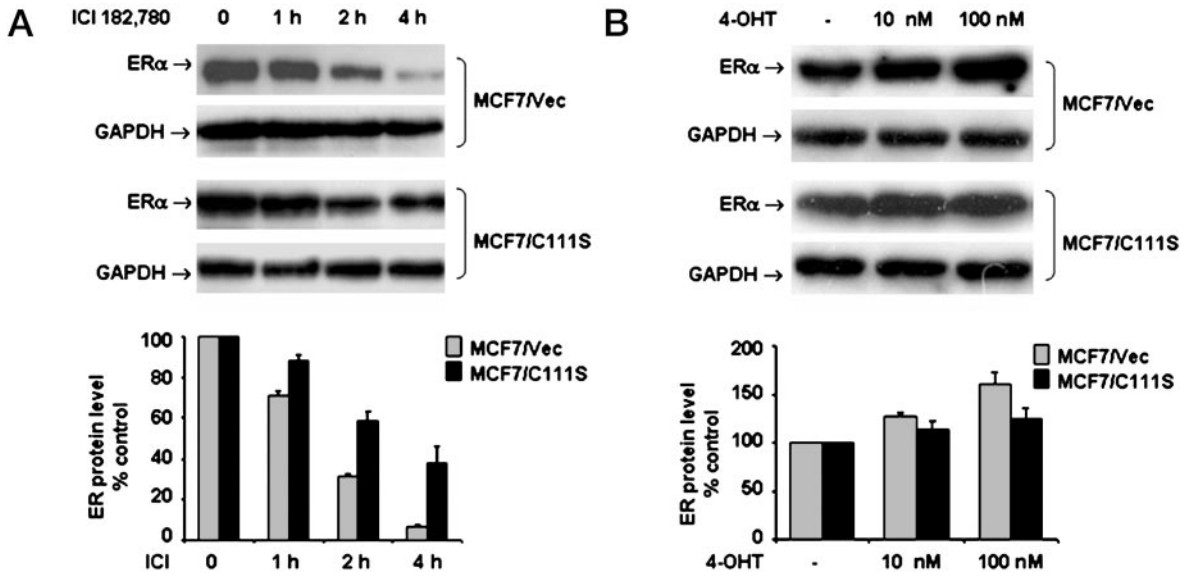

Fig. 5. ERα Degradation Is Impaired in MCF7/C111S Cells

A, ICI 182,780-induced ERα degradation is impaired in MCF7/C111S cells. MCF7/Vec (*upper panel*) and MCF7/C111S cells (*lower panel*) were cultured in hormone-free medium for 3 d and treated with 1 nM ICI 182,780 for the indicated times. B, 4-OHT does not cause ERα degradation in MCF7 cells. MCF7/Vec (*upper panel*) and MCF7/C111S cells (*lower panel*) were cultured in hormone-free medium for 3 d and treated with indicated doses of 4-OHT for 6 h. ERα protein levels were determined by Western blotting with anti-ERα antibody. The histogram shows the relative ERα levels after ICI 182,780 or 4-OHT treatment. Relative ERα levels in MCF7/vec (*gray*) from three independent experiments or MCF7/C111S (*black*) from three independent MCF7/C111S clones are shown in corresponding histogram. GAPDH was used as an internal control to correct SDS-PAGE loading.

Disrupting the NEDD8 Pathway Confers Antiestrogen Resistance in Breast Cancer Cells

Estradiol is mitogenic in MCF7 cells and stimulates cell proliferation through activation of ERα (37). The pure antiestrogen ICI 182,780, on the other hand, blocks ERα-mediated transactivation and induces ERα protein degradation, resulting in growth inhibition of breast cancer cells (38). Because expression of Ubc12C111S inhibited ICI 182,780-induced ERα down-regulation (Fig. 5A), we examined the growth inhibitory effect of ICI 182,780 in MCF7/C111S cells. No significant difference was observed in basal cell proliferation rates between MCF7/C111S and MCF7/Vec cells in hormone-free medium (data not shown). Treatment with the antiestrogen (1 nM) inhibited the basal cell growth of MCF7 and MCF7/Vec cells (Fig. 6A). In contrast, MCF7/C111S cells were partially resistant to ICI 182,780. Specifically, over an 8-d period, the antiestrogen inhibited the growth of control cells by 50% compared with 20–25% growth inhibition of the MCF7/C111S cells (Fig. 6A, *left panel*). Dose-response analysis showed that MCF7/C111S cells were resistant to a broad range (0.01–10 nM) of ICI 182,780 concentrations (Fig. 6A, *right panel*). On the other hand, estradiol-induced proliferation of MCF7/C11S and control cells was similar (2-fold increase in cell number over a 6-d treatment period; data not shown). The effect of 4-OHT on MCF7/C111S and MCF7/Vec cell proliferation was examined in a time- and dose-response analysis. The response of the cell lines to 4-OHT was similar (Fig. 6B), suggesting that Ubc12C111S expression did not confer cells resistance to growth inhibitory effect of antiestrogens in general. These results suggest that the expression of Ubc12C111S conferred resistance of MCF7 cells to the growth inhibitory effects of ICI 182,780, but disrupting the NEDD8 pathway had no effect on the mitogenic response of MCF7 breast cancer cells to estradiol or the growth inhibitory effects of 4-OHT.

DISCUSSION

ERα is a short-lived protein whose degradation is primarily mediated by the ubiquitin-proteasome pathway (26–30). The recently described ubiquitin-like pathways, including the NEDD8 and SUMO (small ubiquitin-like modifier) conjugation systems (39), have been implicated in nuclear receptor regulation (40–44) and the NEDD8 pathway has been shown to enhance protein polyubiquitination (12, 14–19, 45–47). Our previous investigation into the role of the NEDD8 pathway in nuclear hormone receptor regulation showed that Uba3, the catalytic subunit of the NEDD8 activating enzyme complex, interacts with ERα and inhibits receptor function (25). Here we report that Uba3-mediated inhibition of ERα transactivation is due to increased receptor turnover and that an intact neddylation pathway is essential for ERα ubiquitination and degradation. By impairing the NEDD8 path-

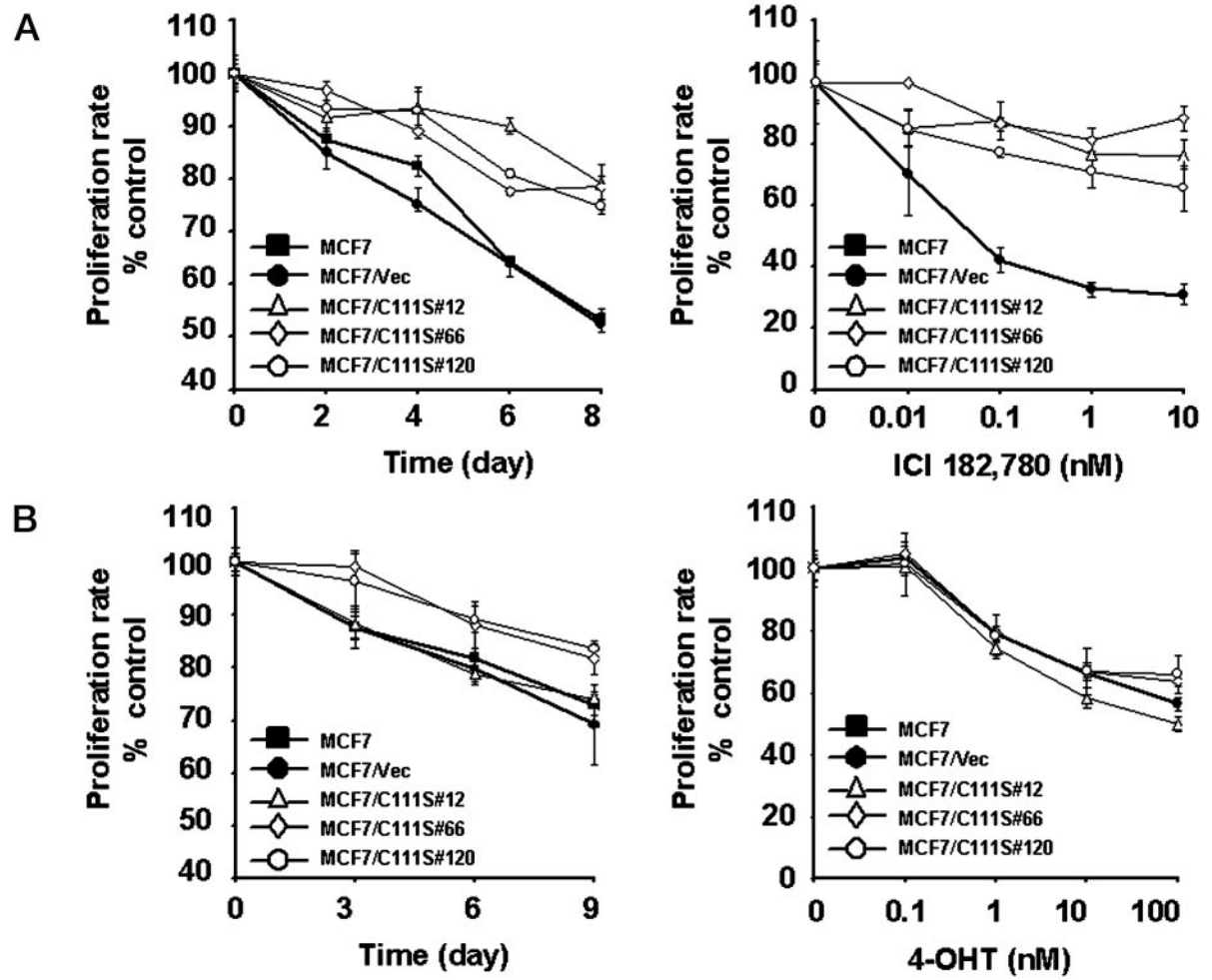

Fig. 6. Interruption of the NEDD8 Pathway Confers Resistance to ICI 182,780 in Human Breast Cancer Cells

A, Time- and dose-dependent growth inhibition of ICI 182,780. For time-response analysis, cells were treated with 1 nM ICI 182,780 and cell numbers were determined 0, 2, 4, 6, and 8 d after drug exposure. For dose-response assay, cells were treated with indicated doses of ICI 182,780 and cell numbers were determined on d 7. B, Time- and dose-dependent antiproliferative effect of 4-OHT. For time-response analysis, cells were treated with 10 nM 4-OHT and cell numbers were determined 0, 3, 6, and 9 d later. For the dose-response assay, cells were treated with indicated doses of 4-OHT and cell numbers were determined on d 7. For all assays, cells were cultured in hormone-free medium for 3 d before treatment and cell numbers were determined by MTT assay. Relative proliferation rate was expressed as percentage of cells grown in hormone-free medium. Each experiment was repeated three times in quadruplicate.

way in human MCF7 breast cancer cells, we demonstrated that the cells became resistant to the growth inhibitory effects of ICI 182,780. Thus, our data suggest that neddylation plays an important role in ERα degradation and we speculate that alterations in the NEDD8 pathway may provide a mechanism by which tumors can acquire antiestrogen resistance.

Several recent studies have focused on the role of the ubiquitin-proteasome pathway in nuclear receptor down-regulation (26–30). Enhancement of ERα ubiquitination by estradiol was first reported by Nirmala and Thampan (48), and Nawaz *et al*. (27) showed that a functional ubiquitin-proteasome system is required for ERα degradation. Both basal and ligand-induced ERα ubiquitination occurs at the nuclear matrix (49), but how ERα is targeted for ubiquitination has not been fully established. Previously, we had shown that Uba3 interacts directly with ER and that this interaction is augmented by estradiol (25). Here, we show that overexpression of Uba3 enhanced degradation of ERα and that disruption of Uba3 activity reduces estradiol-induced receptor degradation. Taken together, these data support a role for Uba3 in the regulation of basal as well as ligand-induced ERα turnover.

The present study is the first to link the NEDD8 pathway to ubiquitination of ERα. The exact mechanism connecting the two pathways, however, remains unclear. The only known substrates for direct neddylation are members of the cullin family (10). Some of the cullins have been identified as core subunits of specific ubiquitin ligase complexes (7). Mechanistically, conjugation of NEDD8 to cullins may up-regulate

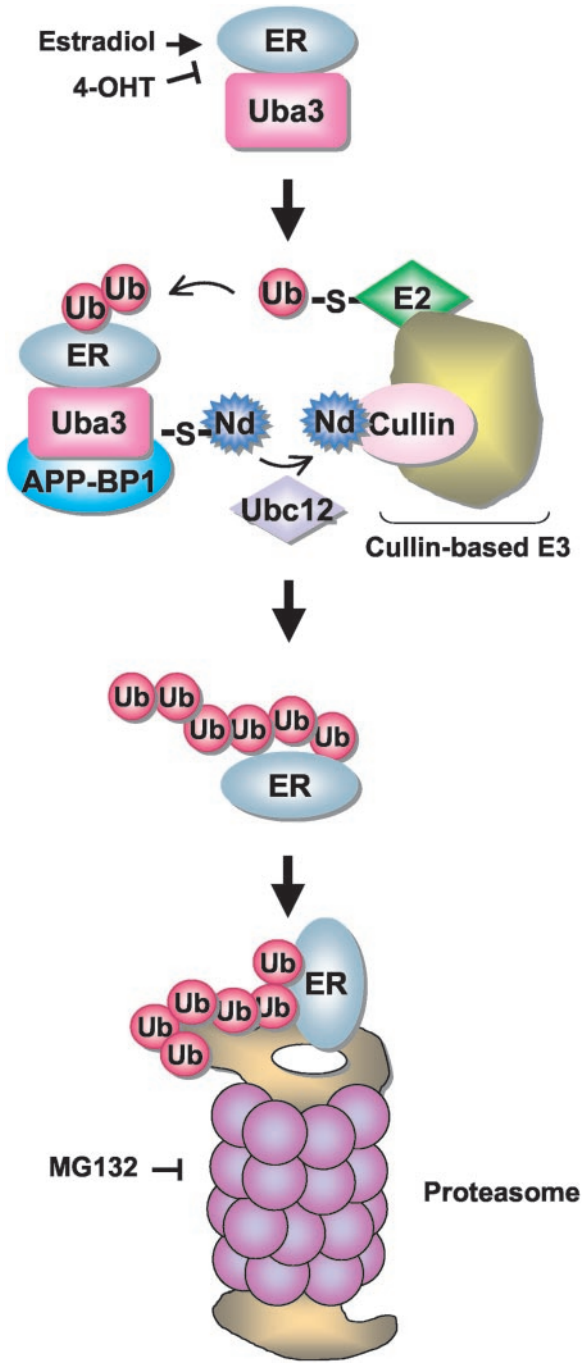

Fig. 7. Hypothetical Model Depicting the Role of Neddylation Pathway in Proteasome-Mediated Degradation of ERα

The physical interaction between Uba3 and ERα promotes the functional recruitment and activation of a cullin-based ubiquitin-protein ligase to augment receptor polyubiquitination. Uba3 and APP-BP1, the heterodimeric activating enzyme for NEDD8, and Ubc12, the NEDD8 conjugating enzyme, promote cullin NEDD8 modification of specific ubiquitin E3 ligases. Neddylated cullins enhance the formation and activity of the ubiquitin E2-E3 complex. The potency of ERα-Uba3 interaction appears to correlate with ERα turnover rate. In the absence of ligand, ERα interacts weakly with Uba3, resulting in basal ubiquitination and degradation of ERα; however, estradiol augments the ERα-Uba3 interaction to enhance ERα ubiquitination. On the other hand, 4-OHT interrupts the ERα-Uba3 interaction and stabilizes ERα, and MG132 blocks ERα degradation by inhibiting proteasome activity. APP-BP1, Amyloid precursor protein-binding protein; E2, ubiquitin conjugation enzyme; E3, ubiquitin protein ligase; estradiol, 17β-estradiol; Nd, neural precursor cell-expressed developmentally down-regulated (NEDD8); ↓ and ⊥, Stimulation and inhibition, respectively.

ubiquitin ligase activity of specific E3s by facilitating the formation of an ubiquitin E2-E3 complex (45). In this regard, the interaction between Uba3 and ERα could result in the functional recruitment and activation of a cullin-based ubiquitin-protein ligase, which, in turn, targets ERα for degradation by the ubiquitin-proteasome system. The hypothetical model depicting the role of neddylation pathway in proteasome-mediated degradation of ERα is shown in Fig. 7. Together with our previously reported data (25), these observations indicate that such targeted degradation of ERα leads to reduced hormonal responsiveness.

In addition to its effect on ERα, Uba3 inhibits the transactivation function of other steroid receptors, ERβ, androgen receptor (AR) and progesterone receptor (PR) (25). Others have reported that NEDD8 interacts with aryl hydrocarbon receptor and the interaction affects the transcriptional activity and stability of the receptor protein (40). Furthermore, the NEDD8 protein has been found to colocalize with AR (50). Together with the observations that turnover of ER, AR, PR, and aryl hydrocarbon receptor occurs via degradation by the 26S proteasome (28, 51–53), these results provide compelling evidence for integration of the neddylation and ubiquitin-proteasome pathways in steroid hormone action. Because receptor levels can have a profound influence on target tissue responsiveness to hormone, NEDD8 and ubiquitin pathways, by modulating receptor protein turnover, could play important roles in determining and perhaps limiting cellular responses to steroid hormones and antihormones.

The antiestrogen ICI 182,780 is a 7α-alkylsulfinyl analog of estradiol lacking agonist activity (54). The drug is used as a second-line endocrine agent in patients who have developed tamoxifen-resistant breast cancer (38). Although the drug clearly displays complex pharmacology, rapid degradation of ERα protein has been associated with the antiproliferative effects of ICI 182,780 on breast cancer cells (38, 54). Despite its potent antitumor effects, the drug does not circumvent the development of antiestrogen resistance (55–58). Moreover, the fact that most tumors acquiring ICI 182,780 resistance do so while retaining expression of ERα and estrogen responsiveness (55, 59) suggests that administration of the antiestrogen may possibly lead to the selection of tumor cells defective in ERα down-regulation pathway(s), which in turn may confer a proliferative advantage in either the presence or absence of estrogens. Mechanism underlying persistent expression of ERα in tumors with acquired resis-

tance may thus present an important therapeutic target for future drug intervention. In this context, the loss of NEDD8 expression during malignant transformation of prostate cancer was recently reported (60). Because our results show an intact NEDD8 pathway is essential for ERα ubiquitination and degradation, we speculate that disruptions in the NEDD8 pathway may provide a mechanism by which breast cancer cells acquire ICI 182,780 resistance while retaining expression of ERα.

MATERIALS AND METHODS

Materials

The following antibodies and reagents were used in this study: anti-ER (HC20; Santa Cruz Biotechnology, Inc., Santa Cruz, CA); anti-HA (3F10; Roche Molecular Biochemicals, Indianapolis, IN); anti-GFP (GFP01, NeoMarkers, Inc., Fremont, CA); anti-GAPDH (glyceraldehyde phosphate dehydrogenase; Chemicon International, Inc., Temecula, CA); anti-rabbit IgG and protein G-agarose beads (Oncogene Research Products, San Diego, CA); SuperSignal West Pico Chemiluminescent Substrate (Pierce Chemical Co., Rockford, IL); protease inhibitor cocktail set III (Calbiochem-Novabiochem Corp., San Diego, CA); Bio-Rad Laboratories, Inc. (Hercules, CA) protein assay kit; FBS and csFBS (HyClone Laboratories, Inc., Logan, UT); LipofectAMINE Plus Reagent, geneticin, and other cell culture reagents were from Life Technologies, Inc. (Rockville, MD). Estradiol, 4-OHT, MG132, and 3-(4, 5-dimethylthiazol-2-yl)-2,5-diphenyltetrazolium bromide (MTT) were from Sigma (St. Louis, MO). ICI 182,780 was purchased from Tocris Cookson Ltd. (Ellisville, MO).

Plasmid Construction

The construction of pSG5-ER(HEGO), pcDNA-Uba3, pcDNA-HA-Uba3C216S, pcDNA-HA-Ubc12, and pcDNA-HA-Ubc12C111S was described previously (25). The pcDNA-HA-ubiquitin was kindly provided by Y. Xiong (61). The pCMV (cytomegalovirus)-GFP was purchased (Promega Corp., Madison, WI).

Cell Lines

The human cervical carcinoma cell line, HeLa, and the breast cancer cell line, MCF-7 were purchased from ATCC (Manassas, VA). HeLa cells were maintained in MEM with 2 mM L-glutamine, 1.5 g/liter sodium bicarbonate, 0.1 mM nonessential amino acids, 1.0 mM sodium pyruvate, 50 U/ml penicillin, 50 μg/ml streptomycin, and 10% FBS. MCF7 cells were maintained in MEM with 2 mM L-glutamine, 0.1 mM nonessential amino acids, 50 U/ml penicillin, 50 μg/ml streptomycin, 6 ng/ml insulin, and 10% FBS. Before experiments involving in transient transfection and hormone treatment, cells were cultured in hormone-free medium (phenol red-free MEM with 3% csFBS) for 3 d.

Transient Transfection Assays

HeLa cells were cultured in hormone-free medium for 3 d and transfected with equal amount of total plasmid DNA (adjusted by corresponding empty vectors) by using LipofectAMINE Plus Reagent according to the manufacturer's guidelines. Five hours later, the DNA/LipofectAMINE mixture was removed and cells were cultured in hormone-free medium. All cells were also cotransfected with pCMV-GFP as internal control to correct for transfection efficiency and SDS-PAGE loading.

Stable Transfection

MCF7 cells were transfected with pcDNA-HA-Ubc12C111S or empty vector by using LipofectAMINE Plus Reagent and selected in growth medium containing 0.5 mg/ml geneticin for 3 wk. Drug-resistant colonies were chosen and expanded in growth medium containing 0.3 mg/ml geneticin. The expression of HA-Ubc12C111S in the stable cell lines (MCF7/C111S) was detected by Western blotting with anti-HA antibody. Geneticin-resistant clones from vector transfectants (MCF7/Vec) were pooled, maintained in growth medium containing 0.3 mg/ml geneticin, and used as control cells.

Preparation of Cell Extracts and Immunoblotting

Whole cell extracts were prepared by suspending cells ($\sim 2 \times 10^6$) in 0.1 ml of ice-cold lysis buffer (25 mM HEPES, pH 7.5; 0.3 M NaCl; 0.2% sodium dodecyl sulfate; 0.5% sodium deoxycholate; 0.2 mM EDTA; 0.5 mM dithiothreitol; 0.1% Triton X-100; 10 μl protease inhibitor cocktail set III). After 15 min on ice, extracts were sonicated (3×10 sec), insoluble material was removed by centrifugation (15 min at 12,000 $\times$ *g*), and protein concentration in the supernatant was determined using the Bio-Rad Laboratories, Inc. protein assay kit. The protein extracts were mixed with 1/4 vol of 5$\times$ electrophoresis sample buffer and boiled for 5 min at 90 C. Protein extract (50 μg per lane) was then fractionated by SDS-PAGE, transferred to polyvinylidene difluoride membrane, and probed with antibodies. Primary antibody was detected by horseradish peroxidase-conjugated second antibody and visualized using enhanced SuperSignal West Pico Chemiluminescent Substrate. The band density of exposed films was evaluated with ImageJ software (http://rsb.info.nih.gov/ij/).

Immunoprecipitation

For immunoprecipitation, 500 μg whole cell extract was diluted to protein concentration of 1 μg/μl using PBS containing protease inhibitor cocktail and incubated with 5 μl anti-rabbit IgG and 20 μl protein G-agarose beads for 1 h at 4 C. After centrifugation at 12,000 $\times$ *g* for 15 sec, the precleared supernatants were incubated with 5 μl anti-ER antibody overnight at 4 C, followed by another 1-h incubation with 30 μl protein G-agarose beads. The beads were then pelleted by brief centrifugation, washed three times with PBS and once with PBS containing 0.4 M NaCl, and resuspended in 30 μl SDS-PAGE loading buffer for SDS-PAGE and Western blotting.

Cell Proliferation Assays

To assess the effects of estradiol, ICI 182,780, or 4-OHT on cell proliferation, cells (1000/well) were plated in 96-well dishes in hormone-free medium for 3 d before drug exposure. For time-response analysis, cell numbers were determined by MTT assay (62) at indicated times after drug treatment; and for dose-response analysis, cell number was determined by MTT assay at d 7.

Acknowledgments

Received September 13, 2002. Accepted December 11, 2002.

Address all correspondence and requests for reprints to: Kenneth P. Nephew, Ph.D., Medical Sciences, Indiana

University School of Medicine, 302 Jordan Hall, 1001 East Third Street, Bloomington, Indiana 47405-4401. E-mail: knephew@indiana.edu.

The authors gratefully acknowledge the following agencies for supporting this work: NIH Grants CA-74748 (to K.P.N.) and HD-37025 (to R.M.B.); the U.S. Army Medical Research Acquisition Activity, Award Numbers DAMD 17-02-1-0418 and DAMD17-02-1-0419 (to K.P.N.); American Cancer Society Research Grant TBE-104125 (to K.P.N.), the Walther Cancer Institute (to M.F.); and Hoosiers Outrun Cancer/Bloomington Hospital Foundation (to K.P.N.).

REFERENCES

1. McKenna NJ, O'Malley BW 2001 Nuclear receptors, coregulators, ligands, and selective receptor modulators: making sense of the patchwork quilt. Ann NY Acad Sci 949:3–5
2. Webb P, Lopez GN, Greene GL, Baxter JD, Kushner PJ 1992 The limits of the cellular capacity to mediate an estrogen response. Mol Endocrinol 6:157–167
3. Dauvois S, Danielian PS, White R, Parker MG 1992 Antiestrogen ICI 164,384 reduces cellular estrogen receptor content by increasing its turnover. Proc Natl Acad Sci USA 89:4037–4041
4. Eckert RL, Mullick A, Rorke EA, Katzenellenbogen BS 1984 Estrogen receptor synthesis and turnover in MCF-7 breast cancer cells measured by a density shift technique. Endocrinology 114:629–637
5. Dennis AP, Haq RU, Nawaz Z 2001 Importance of the regulation of nuclear receptor degradation. Front Biosci 6:D954–D959
6. Pickart CM 2001 Mechanisms underlying ubiquitination. Annu Rev Biochem 70:503–533
7. Deshaies RJ 1999 SCF and Cullin/Ring H2-based ubiquitin ligases. Annu Rev Cell Dev Biol 15:435–467
8. Gong L, Yeh ET 1999 Identification of the activating and conjugating enzymes of the NEDD8 conjugation pathway. J Biol Chem 274:12036–12042
9. Wada H, Yeh ET, Kamitani T 1999 Identification of NEDD8-conjugation site in human cullin-2. Biochem Biophys Res Commun 257:100–105
10. Hori T, Osaka F, Chiba T, Miyamoto C, Okabayashi K, Shimbara N, Kato S, Tanaka K 1999 Covalent modification of all members of human cullin family proteins by NEDD8. Oncogene 18:6829–6834
11. Lammer D, Mathias N, Laplaza JM, Jiang W, Liu Y, Callis J, Goebl M, Estelle M 1998 Modification of yeast Cdc53p by the ubiquitin-related protein rub1p affects function of the SCFCdc4 complex. Genes Dev 12:914–926
12. Liakopoulos D, Busgen T, Brychzy A, Jentsch S, Pause A 1999 Conjugation of the ubiquitin-like protein NEDD8 to cullin-2 is linked to von Hippel-Lindau tumor suppressor function. Proc Natl Acad Sci USA 96:5510–5515
13. del Pozo JC, Estelle M 1999 The Arabidopsis cullin AtCUL1 is modified by the ubiquitin-related protein RUB1. Proc Natl Acad Sci USA 96:15342–15347
14. Morimoto M, Nishida T, Honda R, Yasuda H 2000 Modification of cullin-1 by ubiquitin-like protein Nedd8 enhances the activity of SCF(skp2) toward p27(kip1). Biochem Biophys Res Commun 270:1093–1096
15. Podust VN, Brownell JE, Gladysheva TB, Luo RS, Wang C, Coggins MB, Pierce JW, Lightcap ES, Chau V Luo RS, Wang C, Coggins MB, Pierce JW, Lightcap ES, Chau V 2000 A Nedd8 conjugation pathway is essential for proteolytic targeting of p27Kip1 by ubiquitination. Proc Natl Acad Sci USA 97:4579–4584
16. Read MA, Brownell JE, Gladysheva TB, Hottelet M, Parent LA, Coggins MB, Pierce JW, Podust VN, Luo RS, Chau V, Palombella VJ 2000 Nedd8 modification of cul-1 activates SCF(β(TrCP))-dependent ubiquitination of IκBα. Mol Cell Biol 20:2326–2333
17. Ohh M, Kim WY, Moslehi JJ, Chen Y, Chau V, Read MA, Kaelin Jr WG 2002 An intact NEDD8 pathway is required for Cullin-dependent ubiquitylation in mammalian cells. EMBO Rep 3:177–182
18. Amir RE, Iwai K, Ciechanover A 2002 The NEDD8 pathway is essential for SCF(β-TrCP)-mediated ubiquitination and processing of the NF-κ B precursor p105. J Biol Chem 277:23253–23259
19. Yang X, Menon S, Lykke-Andersen K, Tsuge T, Di X, Wang X, Rodriguez-Suarez RJ, Zhang H, Wei N 2002 The COP9 signalosome inhibits p27(kip1) degradation and impedes G1-S phase progression via deneddylation of SCF Cul1. Curr Biol 12:667–672
20. Lyapina S, Cope G, Shevchenko A, Serino G, Tsuge T, Zhou C, Wolf DA, Wei N, Deshaies RJ 2001 Promotion of NEDD-CUL1 conjugate cleavage by COP9 signalosome. Science 292:1382–1385
21. Schwechheimer C, Serino G, Callis J, Crosby WL, Lyapina S, Deshaies RJ, Gray WM, Estelle M, Deng XW 2001 Interactions of the COP9 signalosome with the E3 ubiquitin ligase SCFTIRI in mediating auxin response. Science 292:1379–1382
22. Kito K, Yeh ET, Kamitani T 2001 NUB1, a NEDD8-interacting protein, is induced by interferon and down-regulates the NEDD8 expression. J Biol Chem 276: 20603–20609
23. Kamitani T, Kito K, Fukuda-Kamitani T, Yeh ET 2001 Targeting of NEDD8 and its conjugates for proteasomal degradation by NUB1. J Biol Chem 276:46655–46660
24. Zhou C, Seibert V, Geyer R, Rhee E, Lyapina S, Cope G, Deshaies RJ, Wolf DA 2001 The fission yeast COP9/signalosome is involved in cullin modification by ubiquitin-related Ned8p. BMC Biochem 2:7 (http://www.biomedcentral.com/1471-2091/2/7)
25. Fan M, Long X, Bailey JA, Reed CA, Osborne E, Gize EA, Kirk EA, Bigsby RM, Nephew KP 2002 The activating enzyme of NEDD8 inhibits steroid receptor function. Mol Endocrinol 16:315–330
26. Alarid ET, Bakopoulos N, Solodin N 1999 Proteasome-mediated proteolysis of estrogen receptor: a novel component in autologous down-regulation. Mol Endocrinol 13:1522–1534
27. Nawaz Z, Lonard DM, Dennis AP, Smith CL, O'Malley BW 1999 Proteasome-dependent degradation of the human estrogen receptor. Proc Natl Acad Sci USA 96: 1858–1862
28. Lonard DM, Nawaz Z, Smith CL, O'Malley BW 2000 The 26S proteasome is required for estrogen receptor-α and coactivator turnover and for efficient estrogen receptor-α transactivation. Mol Cell 5:939–948
29. El Khissiin A, Leclercq G 1999 Implication of proteasome in estrogen receptor degradation. FEBS Lett 448: 160–166
30. Wijayaratne AL, McDonnell DP 2001 The human estrogen receptor-α is a ubiquitinated protein whose stability is affected differentially by agonists, antagonists, and selective estrogen receptor modulators. J Biol Chem 276:35684–35692
31. Wada H, Yeh ET, Kamitani T 2000 A dominant-negative UBC12 mutant sequesters NEDD8 and inhibits NEDD8 conjugation *in vivo*. J Biol Chem 275:17008–17015
32. Chen Y, McPhie DL, Hirschberg J, Neve RL 2000 The amyloid precursor protein-binding protein APP-BP1 drives the cell cycle through the S-M checkpoint and causes apoptosis in neurons. J Biol Chem 275: 8929–8935
33. Brooks SC, Locke ER, Soule HD 1973 Estrogen receptor in a human cell line (MCF-7) from breast carcinoma. J Biol Chem 248:6251–6253

34. Levenson AS, Jordan VC 1997 MCF-7: the first hormone-responsive breast cancer cell line. Cancer Res 57: 3071–3078
35. Nephew KP, Long X, Osborne E, Burke KA, Ahluwalia A, Bigsby RM 2000 Effect of estradiol on estrogen receptor expression in rat uterine cell types. Biol Reprod 62: 168–177
36. Pink JJ, Jordan VC 1996 Models of estrogen receptor regulation by estrogens and antiestrogens in breast cancer cell lines. Cancer Res 56:2321–2330
37. Lippman M, Bolan G, Huff K 1976 The effects of estrogens and antiestrogens on hormone-responsive human breast cancer in long-term tissue culture. Cancer Res 36:4595–4601
38. Howell A, Osborne CK, Morris C, Wakeling AE 2000 ICI 182,780 (Faslodex): development of a novel, "pure" antiestrogen. Cancer 89:817–825
39. Yeh ET, Gong L, Kamitani T 2000 Ubiquitin-like proteins: new wines in new bottles. Gene 248:1–14
40. Antenos M, Casper RF, Brown TJ 2002 Interaction with NEDD8, a ubiquitin-like protein, enhances the transcriptional activity of the aryl hydrocarbon receptor. J Biol Chem 277:44028–44034
41. Kaul S, Blackford Jr JA, Cho S, Simons Jr SS 2002 Ubc9 is a novel modulator of the induction properties of glucocorticoid receptors. J Biol Chem 277:12541–12549
42. Kotaja N, Aittomaki S, Silvennoinen O, Palvimo JJ, Janne OA 2000 ARIP3 (androgen receptor-interacting protein 3) and other PIAS (protein inhibitor of activated STAT) proteins differ in their ability to modulate steroid receptor-dependent transcriptional activation. Mol Endocrinol 14: 1986–2000
43. Poukka H, Aarnisalo P, Karvonen U, Palvimo JJ, Janne OA 1999 Ubc9 interacts with the androgen receptor and activates receptor-dependent transcription. J Biol Chem 274:19441–19446
44. Poukka H, Karvonen U, Janne OA, Palvimo JJ 2000 Covalent modification of the androgen receptor by small ubiquitin-like modifier 1 (SUMO-1). Proc Natl Acad Sci USA 97:14145–14150
45. Kawakami T, Chiba T, Suzuki T, Iwai K, Yamanaka K, Minato N, Suzuki H, Shimbara N, Hidaka Y, Osaka F, Omata M, Tanaka K 2001 NEDD8 recruits E2-ubiquitin to SCF E3 ligase. EMBO J 20:4003–4012
46. Osaka F, Saeki M, Katayama S, Aida N, Toh EA, Kominami K, Toda T, Suzuki T, Chiba T, Tanaka K, Kato S 2000 Covalent modifier NEDD8 is essential for SCF ubiquitin-ligase in fission yeast. EMBO J 19:3475–3484
47. Wu K, Chen A, Pan ZQ 2000 Conjugation of Nedd8 to CUL1 enhances the ability of the ROC1-CUL1 complex to promote ubiquitin polymerization. J Biol Chem 275: 32317–32324
48. Nirmala PB, Thampan RV 1995 Ubiquitination of the rat uterine estrogen receptor: dependence on estradiol. Biochem Biophys Res Commun 213:24–31
49. Stenoien DL, Patel K, Mancini MG, Dutertre M, Smith CL, O'Malley BW, Mancini MA 2001 FRAP reveals that mobility of oestrogen receptor-α is ligand- and proteasome-dependent. Nat Cell Biol 3:15–23
50. Stenoien DL, Cummings CJ, Adams HP, Mancini MG, Patel K, DeMartino GN, Marcelli M, Weigel NL, Mancini MA 1999 Polyglutamine-expanded androgen receptors form aggregates that sequester heat shock proteins, proteasome components and SRC-1, and are suppressed by the HDJ-2 chaperone. Hum Mol Genet 8:731–741
51. Lange CA, Shen T, Horwitz KB 2000 Phosphorylation of human progesterone receptors at serine-294 by mitogen-activated protein kinase signals their degradation by the 26S proteasome. Proc Natl Acad Sci USA 97: 1032–1037
52. Okino ST, Whitlock Jr JP 2000 The aromatic hydrocarbon receptor, transcription, and endocrine aspects of dioxin action. Vitam Horm 59:241–264
53. Sheflin L, Keegan B, Zhang W, Spaulding SW 2000 Inhibiting proteasomes in human HepG2 and LNCaP cells increases endogenous androgen receptor levels. Biochem Biophys Res Commun 276:144–150
54. Howell A, DeFriend DJ, Robertson JF, Blamey RW, Anderson L, Anderson E, Sutcliffe FA, Walton P 1996 Pharmacokinetics, pharmacological and anti-tumour effects of the specific anti-oestrogen ICI 182780 in women with advanced breast cancer. Br J Cancer 74:300–308
55. Lykkesfeldt AE, Larsen SS, Briand P 1995 Human breast cancer cell lines resistant to pure anti-estrogens are sensitive to tamoxifen treatment. Int J Cancer 61:529–534
56. Osborne CK, Coronado-Heinsohn EB, Hilsenbeck SG, McCue BL, Wakeling AE, McClelland RA, Manning DL, Nicholson RI 1995 Comparison of the effects of a pure steroidal antiestrogen with those of tamoxifen in a model of human breast cancer. J Natl Cancer Inst 87:746–750
57. Dumont JA, Bitonti AJ, Wallace CD, Baumann RJ, Cashman EA, Cross-Doersen DE 1996 Progression of MCF-7 breast cancer cells to antiestrogen-resistant phenotype is accompanied by elevated levels of AP-1 DNA-binding activity. Cell Growth Differ 7:351–359
58. Larsen SS, Heiberg I, Lykkesfeldt AE 2001 Anti-oestrogen resistant human breast cancer cell lines are more sensitive towards treatment with the vitamin D analogue EB1089 than parent MCF-7 cells. Br J Cancer 84: 686–690
59. Brunner N, Boysen B, Jirus S, Skaar TC, Holst-Hansen C, Lippman J, Frandsen T, Spang-Thomsen M, Fuqua SA, Clarke R 1997 MCF7/LCC9: an antiestrogen-resistant MCF-7 variant in which acquired resistance to the steroidal antiestrogen ICI 182,780 confers an early cross-resistance to the nonsteroidal antiestrogen tamoxifen. Cancer Res 57:3486–3493
60. Meehan KL, Holland JW, Dawkins HJ 2002 Proteomic analysis of normal and malignant prostate tissue to identify novel proteins lost in cancer. Prostate 50:54–63
61. Furukawa M, Zhang Y, McCarville J, Ohta T, Xiong Y 2000 The CUL1 C-terminal sequence and ROC1 are required for efficient nuclear accumulation, NEDD8 modification, and ubiquitin ligase activity of CUL1. Mol Cell Biol 20:8185–8197
62. Alley MC, Scudiero DA, Monks A, Hursey ML, Czerwinski MJ, Fine DL, Abbott BJ, Mayo JG, Shoemaker RH, Boyd MR 1988 Feasibility of drug screening with panels of human tumor cell lines using a microculture tetrazolium assay. Cancer Res 48:589–601

0888-8809/04/$15.00/0
Printed in U.S.A.

Molecular Endocrinology 18(11):2603–2615

doi: 10.1210/me.2004-0164

Inhibiting Proteasomal Proteolysis Sustains Estrogen Receptor-α Activation

MEIYUN FAN, HARIKRISHNA NAKSHATRI, AND KENNETH P. NEPHEW

Medical Sciences (M.F., K.P.N.), Indiana University School of Medicine, Bloomington, Indiana 47405; Department of Surgery (H.N.), Department of Biochemistry and Molecular Biology, Walther Oncology Center; Indiana University Cancer Center (H.N., K.P.N.); and Department of Cellular and Integrative Physiology (K.P.N.), Indiana University School of Medicine, Indianapolis, Indiana 46202

Estrogen receptor-α (ERα) is a ligand-dependent transcription factor that mediates physiological responses to 17β-estradiol (E2). Ligand binding rapidly down-regulates ERα levels through proteasomal proteolysis, but the functional impact of receptor degradation on cellular responses to E2 has not been fully established. In this study, we investigated the effect of blocking the ubiquitin-proteasome pathway on ERα-mediated transcriptional responses. In HeLa cells transfected with ERα, blocking either ubiquitination or proteasomal degradation markedly increased E2-induced expression of an ER-responsive reporter. Time course studies further demonstrated that blocking ligand-induced degradation of ERα resulted in prolonged stimulation of ER-responsive gene transcription. In breast cancer MCF7 cells containing endogenous ERα, proteasome inhibition enhanced E2-induced expression of endogenous pS2 and cathepsin D. However, inhibiting the proteasome decreased expression of progesterone receptor (PR), presumably due to the heterogeneity of the PR promoter, which contains multiple regulatory elements. In addition, in endometrial cancer Ishikawa cells overexpressing steroid receptor coactivator 1, 4-hydroxytamoxifen displayed full agonist activity and stimulated ERα-mediated transcription without inducing receptor degradation. Collectively, these results demonstrate that proteasomal degradation is not essential for ERα transcriptional activity and functions to limit E2-induced transcriptional output. The results further indicate that promoter context must be considered when evaluating the relationship between ERα transcription and proteasome inhibition. We suggest that the transcription of a gene driven predominantly by an estrogen-responsive element, such as pS2, is a more reliable indicator of ERα transcription activity than a gene like PR, which contains a complex promoter requiring cooperation between ERα and other transcription factors. (*Molecular Endocrinology* 18: 2603–2615, 2004)

THE ACTIONS OF estrogens are mediated primarily through estrogen receptors (ERα and ERβ) (1), ligand-dependent transcription factors that interact directly with estrogen response elements (EREs) in the promoters of target genes (1). Cellular levels of ERα (2), along with a large number of receptor coregulator complexes (3), play key roles in controlling appropriate physiological responses in estrogen target tissues, such as breast and uterus. Levels of ERα mRNA and protein are regulated primarily by its cognate ligand, 17β-estradiol (E2) (4–6). E2 binding results in rapid turnover of ERα protein through the ubiquitin (Ub)-proteasome pathway (7–11), which has been implicated in both the overall control of gene transcription (12–16) and transactivation function of ERα and other nuclear receptors (7, 17–24).

The Ub-proteasome system consists of the 26S proteasome, a complex composed of a 20S catalytic core for protein proteolysis and two ATPase-containing 19S regulatory particles that recognize polyubiquitin-tagged substrates (25). Like many other transcription factors, stimulation of ERα transcriptional activation appears to be associated with receptor ubiquitination and proteasomal degradation (11, 26). Several proteins possessing Ub ligase activity (*e.g.* E6AP, p300, BRCA1, and MDM2), as well as SUG1, a component of the 19S proteasome, have been shown to associate with ERα and modulate receptor signaling (27–34). These observations suggest that proteasome-mediated receptor degradation is important for ER function.

Recent studies have demonstrated that inhibiting proteasomal degradation increases transcriptional activity of many, but not all, nuclear receptors, indicating a receptor-specific effect of proteasome inhibition (17–24). Blocking ERα turnover by a proteasome-

Abbreviations: CAT, Chloramphenicol acetyltransferase; DMSO, dimethylsulfoxide; E2, 17β-estradiol; ER, estrogen receptor; ERE, estrogen response elements; GR, glucocorticoid receptor; hnRNA, heterogeneous nuclear RNA; Luc, firefly luciferase; 4-OHT, 4-hydroxytamoxifen; p-Pol II, phosphorylated RNA pol II; PR, progesterone receptor; Q-PCR, real-time quantitative reverse transcription-PCR; RSV, Rous sarcoma virus; SRC, steroid receptor coactivator; SV40, simian virus 40; Ub, ubiquitin; Ubc, ubiquitin-conjugation enzyme; Vit, vitellogenin.

***Molecular Endocrinology* is published monthly by The Endocrine Society (http://www.endo-society.org), the foremost professional society serving the endocrine community.**

specific inhibitor, MG132, results in decreased expression of an ERα-responsive luciferase reporter, implicating that proteasomal degradation of ERα is required for its transactivation function (7, 35). However, MG132, and other proteasome inhibitors, have recently been shown to deleteriously affect production of a functional firefly luciferase enzyme (36), complicating the assessment of studies utilizing only ERα-responsive reporters expressing luciferase, in combination with 20S proteasome inhibitors. In addition, several studies have recently suggested that receptor degradation may not be required for ERα-mediated transcription. Frasor *et al.* (11, 37) reported that the partial agonist/antagonist 4-hydroxytamoxifen (4-OHT), which protects ERα from proteasomal degradation, stimulates ER-mediated transcription of a group of genes in MCF7 cells (38). Dissociation of ERα activation from degradation has also been reported in pituitary tumor cells (39, 40).

In the present study, we investigated the role of the Ub-proteasome pathway in ERα-mediated transcriptional responses. Genetic and pharmacological approaches were used to disrupt ERα ubiquitination, proteasome-mediated proteolysis, and thus ERα degradation, including the 20S proteasome inhibitor MG132, a dominant-negative mutant of the NEDD8 conjugation enzyme (Ubc12C111S) (41, 42), a Ub mutant with all of its lysines mutated to arginine (UbK0) (43), and the partial agonist/antagonist 4-OHT. To determine the effect of blocking ERα degradation on E2-induced transcriptional responses, ER-responsive reporter assays and expression of endogenous ER-target genes were used. The results demonstrate that proteasomal degradation is not essential for transcriptional activity of ERα and indicate that the Ub-proteasome system functions to limit E2-induced transcriptional output.

RESULTS

Inhibiting the Proteasome Increases ERα Transcriptional Output

The enzymatic activity of chloramphenicol acetyltransferase (CAT), luciferase (Luc) or β-galactosidase (Gal) reporter proteins is commonly used for assessing transcriptional activity of nuclear receptors in the presence of proteasome inhibitors. Recent studies with breast cancer T47D cells revealed that proteasome inhibitors (MG132, lactacystin, and proteasome inhibitor I) interfere with the production of luciferase and galactosidase proteins by a posttranscriptional mechanism, whereas the enzymatic activity of CAT remains unaffected (36). To verify these observations in our experimental systems, we examined the effect of MG132 on expression of these reporter enzymes from constitutively active constructs in cervical carcinoma HeLa and breast cancer MCF-7 cells. Cells were transfected with Rous sarcoma virus (RSV)-CAT, simian virus 40 (SV40)-Luc, or cytomegalovirus (pCMV)-β-gal and then treated with vehicle [dimethylsulfoxide (DMSO)] or MG132 (1 μM) for 24 h. Reporter enzyme activity was determined using standard assays for luciferase, CAT, and galactosidase. Treatment of HeLa cells with MG132 had no effect on CAT activity but decreased luciferase and galactosidase activity by 80% and 30%, respectively (Fig. 1A, *left panel*). Essentially similar results were obtained using MCF7 cells (Fig. 1A, *right panel*). These results agree with a previous report demonstrating that proteasome inhibitors have deleterious effects on the enzymatic activities of luciferase and galactosidase reporter proteins (36).

Previously, we and others showed that E2 induces ERα degradation in transiently transfected HeLa cells and MG132 abolishes such degradation (8, 9, 42). Based on the above results, we further investigated the relationship between ERα turnover and E2-induced transcriptional response using an E2-responsive CAT reporter. HeLa cells were transiently transfected with ERE-vitellogenin (Vit)-CAT and different doses of ERα-expressing construct (0.1–5 ng pSG5-ERα/10^5 cells). Cells were treated with vehicle (DMSO) or MG132 (1 μM) for 1 h followed by E2 (10 nM). CAT activity was measured 24 h after E2 treatment. Basal CAT activity increased, proportional to the amount of pSG5-ERα (Fig. 1B; *open bars*). As expected, E2 markedly induced CAT activity (Fig. 1B; *gray bars*); however, treatment with MG132 plus E2 resulted in greater CAT activity, compared with E2 alone (Fig. 1B; *black vs. gray bars*). Cells treated with MG132 alone exhibited slightly higher CAT activity than the DMSO control (Fig. 1B, *hatched bars*). A synergistic effect of MG132 plus E2 was observed in cells transfected with lower levels of ERα (0.1–0.3 ng pSG5-ERα/10^5 cells). For example, the combined treatment of MG132 and E2 increased ERE-CAT activity by about 7.4-fold in cells transfected with 0.1 ng pSG5-ERα/10^5 cells, whereas MG132 or E2 alone increased ERE-CAT activity by 1.82- or 3.10-fold, respectively (*table* in Fig. 2B). Immunoblot analysis showed that pretreatment with MG132 effectively blocked E2-induced ERα down-regulation in HeLa cells (Fig. 1C). Taken together, these observations demonstrate that ERα retains the capacity to activate transcription in the absence of proteasomal degradation, and blocking ERα turnover increases E2-induced transcriptional output. The results further suggest that, in cells containing low levels of ERα, proteasome-mediated receptor degradation plays a role in limiting E2-induced transcriptional responsiveness.

Effect of Inhibiting the Proteasome on E2 Sensitivity

Based on the observation that preventing receptor protein turnover increases ERα-mediated transcription, we examined the effect of inhibiting the proteasome on hormone sensitivity. HeLa cells were transfected with ERE-Vit-CAT and pSG5-ERα,

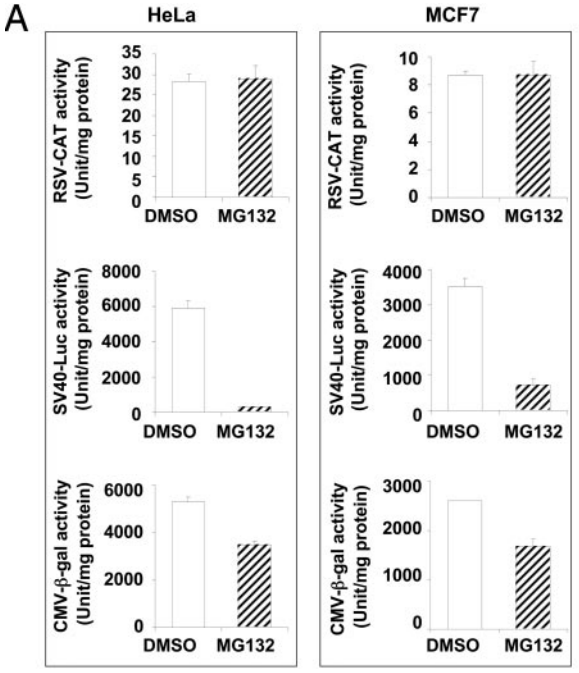

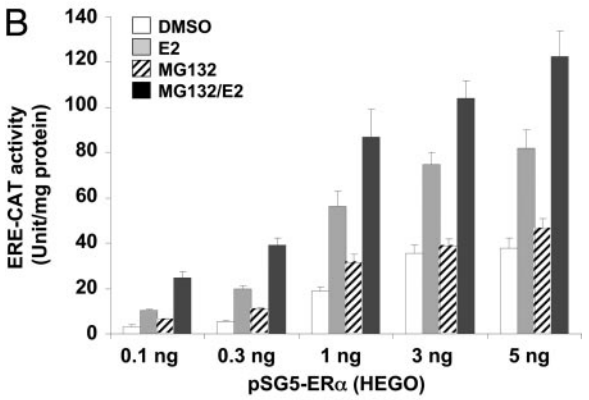

The fold increases of ERE-CAT (relative to DMSO)

	pSG5-ERα				
	0.1 ng	0.3 ng	1 ng	3 ng	5 ng
DMSO	1.00	1.00	1.00	1.00	1.00
E2	3.10	3.70	3.00	2.09	2.17
MG132	1.82	2.01	1.68	1.08	1.22
MG132/E2	7.40	7.31	4.63	2.91	3.23

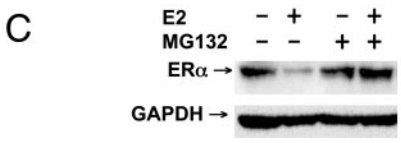

Fig. 1. Proteasome Inhibition Enhances E2-Induced CAT Reporter Gene Expression in HeLa Cells Transfected with ERα

A, Effect of proteasome inhibition by MG132 on expression of reporter enzymes from constitutively active promoters. HeLa cells (*left panel*) were plated on 12-well dishes at a density of 1×10^5 cells per well and cultured in hormone-free medium for 3 d. The cells were transfected with 100 ng RSV-CAT, 100 ng SV40-Luc, or 5 ng pCMV-β-gal using LipofectAMINE Plus Reagent. The DNA/LipofectAMINE mixture was removed 5 h later and cells were placed in hormone free medium containing either 0.1% vehicle (DMSO) or 1 μM MG132 for 24 h. Similarly, MCF7 cells (*right panel*) were plated at a density of 1.2×10^5 cells per well, transfected with 250 ng RSV-CAT, 250 ng SV40-Luc, or 10 ng pCMV-β-gal and then treated with DMSO or MG132 for 24 h. Reporter enzyme activities were normalized against total cellular protein and expressed as the mean ± SD from three independent experiments, each in triplicate. B, Effect of MG132 on ERα-mediated CAT expression. HeLa cells were plated in 12-well dishes at a density of 1×10^5 cells per well and cultured in hormone-free medium for 2 d. The cells were transfected with 100 ng ERE-Vit-CAT and the indicated amount of pSG5-ERα using LipofectAMINE Plus reagent. The DNA/LipofectAMINE mixture was removed 5 h later and cells were placed in hormone-free medium for 24 h. Transfected cells were treated with DMSO or MG132 (1 μM) for 1 h and then treated with 10 nM E2 for 24 h. CAT activity was determined using the colorimetric CAT ELISA kit and normalized against total cellular protein. CAT activity is expressed as the mean ± SD of three independent experiments, each performed in triplicate. Fold increases in ERE-CAT in the presence of E2 ± MG132 are presented in the *table*. C, Effect of MG132 on E2-induced down-regulation of ERα. HeLa cells were plated in 60-mm dishes at a density of 3×10^5 cells per dish and cultured in hormone-free medium for 2 d. Cells were transfected with 100 ng pSG5-ERα using LipofectAMINE Plus reagent. The DNA/LipofectAMINE mixture was removed 5 h later, and cells were placed in hormone-free medium for 24 h. The transfected cells were treated with DMSO or MG132 (1 μM) for 1 h and then treated with 10 nM E2 for 8 h. Whole-cell lysates were prepared and subjected to immunoblotting analysis using an anti-ERα antibody (Chemicon, Temecula, CA). Glyceraldehyde-3-phosphate dehydrogenase (GAPDH) was used as a loading control.

treated with DMSO or MG132 for 1 h, and then treated with various doses of E2 (1×10^{-15} to 1×10^{-8} M). CAT activity was determined 24 h after the addition of ligand. In cells transfected with 0.3 ng (Fig. 2A) or 1 ng pSG5-ERα (Fig. 2B), a hyperbolic dose response to E2 was observed; the lowest dose of hormone that induced CAT activity was 1×10^{-11} M E2. Increasing ERα expression (0.3 ng *vs.* 1 ng pSG5-ERα) and pretreatment with MG132 augmented maximal CAT induction by E2, but no effect on E2 sensitivity was observed. The minimal dose of E2 required to induce CAT was 1×10^{-11} M under all experiment conditions, and the EC_{50} was not different (Fig. 2). These results demonstrate that blocking ERα degradation increases the magnitude of E2-induced gene transcription but has no effect on hormone sensitivity.

Inhibiting the Proteasome Extends the Duration of E2-Induced Gene Transcription

The results of the above experiments suggest that inhibiting the proteasome may extend the half-life of ligand-activated ERα and thus increase receptor transcriptional output. To test the possibility that MG132 treatment would subsequently extend the duration of an E2-induced transcriptional response, we performed a time course analysis using luciferase as a reporter protein. The half-life of CAT in mammalian cells is about 50 h (44);

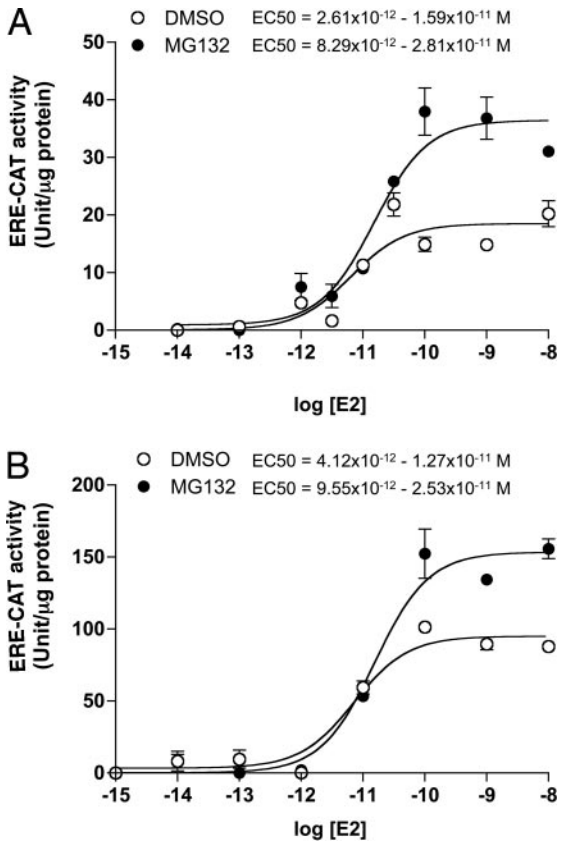

Fig. 2. Effect of MG132 on E2 Dose-Dependent Induction of Reporter Gene Expression in HeLa Cells

HeLa cells were plated in 12-well dishes at a density of 1×10^5 cells per well and cultured in hormone-free medium for 2 d. The cells were transfected with 100 ng ERE-Vit-CAT and 0.3 ng (A) or 1 ng (B) of pSG5-ERα using LipofectAMINE Plus reagent. The DNA/LipofectAMINE mixture was removed 5 h later and cells were placed in hormone-free medium for 24 h. The transfected cells were treated with DMSO or MG132 (1 μM) for 1 h and then treated with the indicated concentration of E2 for 24 h. CAT activities were normalized against total cellular protein and expressed as mean ± SD of three independent experiments, each performed in triplicate. EC_{50} range was calculated with a 95% confidence.

in contrast, luciferase has an intracellular half-life of about 3 h (44), making it well suited for performing a dynamic analysis of promoter activation. Thus, we used HeLa cells transfected with ERα and ERE-pS2-Luc to study the effect of proteasome inhibition on E2-induced transcription in a time-dependent manner. In transfected HeLa cells, E2 induced a transient induction of luciferase activity, maximal at 6 h (Fig. 3A, *solid circles*). Pretreatment with MG132 decreased E2-induced luciferase expression at the early time points (1.5–6 h), but markedly increased E2-induced luciferase expression from 9–20 h (Fig. 3A, *solid triangles*).

As mentioned above, MG132 can inhibit luciferase production. To determine the effect of MG132 on luciferase synthesis in general, we transfected HeLa cells with a constitutively active luciferase construct (SV40-Luc). In contrast to what we observed using ERE-pS2-Luc, MG132 consistently decreased the expression of SV40-Luc during the 20-h period (Fig. 4B), excluding the possibility that MG132 enhances ERE-luc activity by stabilizing luciferase protein. To subtract the general inhibitory effect of MG132 on luciferase synthesis, at each time point shown in Fig. 3C, ERα-mediated luciferase expression in the presence of MG132 was normalized to luciferase activity from the SV40-Luc construct [normalized ERE-Luc activity in the presence of MG132 = ERE-Luc activity in the presence of MG132 × (SV40-Luc activity/SV40-Luc activity in the presence of MG132)]. The adjusted results clearly demonstrate that blocking receptor degradation with MG132 increases both the magnitude and duration of E2-induced gene transcription, suggesting that the duration of gene transcription induced by E2 is limited by ERα degradation through the 26S proteasome.

Inhibiting ERα Ubiquitination Prolongs E2-Induced Gene Transcription

In a previous study, we used a dominant-negative mutant of the NEDD8 conjugation enzyme, Ubc12C111S, to inhibit ERα ubiquitination and degradation (42). Here we used Ubc12C111S as a means to investigate the role of ERα turnover in ERα transactivation function and to corroborate our observations using MG132. The impact of Ubc12C111S on the time-dependent induction of a reporter gene by ERα was investigated. HeLa cells were transfected with pSG5-ERα and ERE-pS2-Luc, along with a control vector (pcDNA) or a construct expressing the mutant Ubc12 (pcDNA-Ubc12C111S). In cells transfected with pcDNA, E2 transiently induced luciferase expression, and maximal induction was observed at 5 h (Fig. 3D, *solid circles*). However, in cells transfected with pcDNA-Ubc12C111S, a delay in peak expression of E2-induced luciferase activity was observed (9 h; Fig. 3D, *solid triangles*), and luciferase expression remained elevated, even 20 h after E2 treatment. No effect of Ubc12C111S on maximal E2-induced luciferase activity was observed (Fig. 3D, *solid circles vs. solid triangles*). To confirm that the observed effect of Ubc12C111S on ERα-mediated luciferase expression was specific, luciferase activity in cells cotransfected with SV40-Luc and Ubc12C111S was assessed over time. No effect of Ubc12C111S on SV40-Luc expression was seen at 6 and 12 h after transfection; a slight increase in luciferase expression was observed at 20 h (1.3-fold; Fig. 3E). Overall, these results demonstrate that inhibiting ERα ubiquitination prolongs ERα-mediated transcription, supporting the hypothesis that proteasome-mediated degradation of ERα serves as a means to limit the duration of E2 signaling.

Blocking Polyubiquitination Sustains E2-Induced Gene Expression

To determine the effect of blocking polyubiquitination on ERα-mediated transcription, we used a Ub mutant,

UbK0, which has all of its lysines replaced by arginine. This mutant competes with endogenous ubiquitin and terminates ubiquitin chains, resulting in the accumulation of short ubiquitin conjugates that cannot be degraded efficiently by the proteasome (43). First, we examined the effect of overexpressing UbK0 on E2-

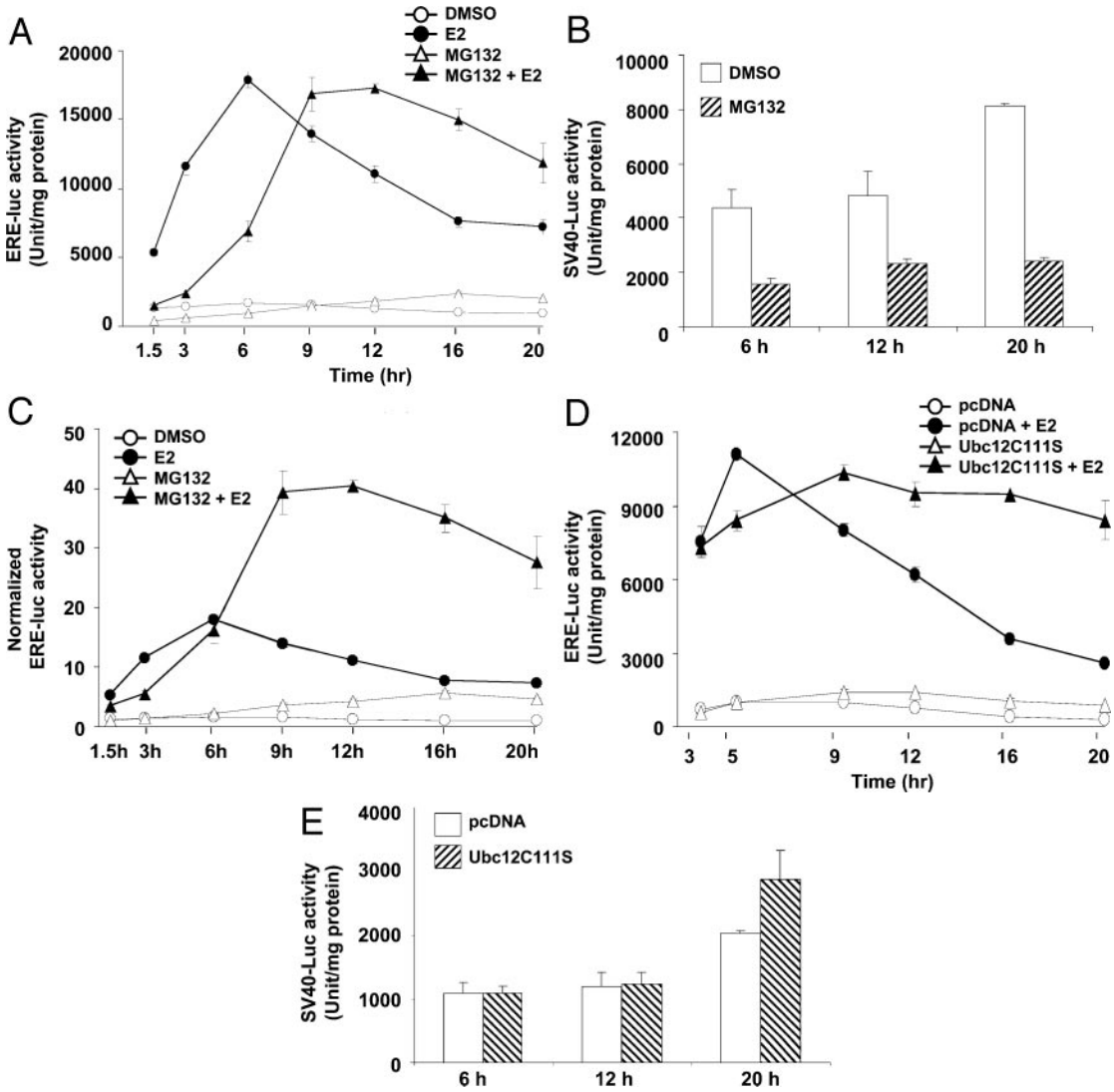

Fig. 3. Effect of Blocking ERα Turnover on Time-Dependent Induction of Reporter Gene Expression by E2 in HeLa Cells

A, Effect of MG132 on E2-induced expression of reporter gene. HeLa cells were plated in 12-well dishes at a density of 1×10^5 cells per well and cultured in hormone-free medium for 2 d. The cells were transfected with 250 ng ERE-pS2-Luc and 1 ng of pSG5-ERα using LipofectAMINE Plus reagent. The DNA/LipofectAMINE mixture was removed 5 h later, and cells were placed in hormone-free medium for 24 h. The transfected cells were treated with DMSO or MG132 (5 μM) for 1 h and then treated with 10 nM E2 for the indicated time period. Luciferase activity was determined using the Luciferase Assay System, normalized against total cellular protein. B, Effect of MG132 on SV40-Luc expression. HeLa cells were transfected with 100 ng SV40-Luc. The DNA/LipofectAMINE mixture was removed 5 h later and cells were placed in hormone-free medium containing either 0.1% vehicle (DMSO) or MG132 (5 μM) for the indicated time period. Luciferase activity was determined and normalized against total cellular protein. C, Normalized ERE-Luc activities. ERα-mediated luciferase activity in the presence of MG132 was normalized to luciferase activity from the SV40-Luc construct [Normalized ERE-Luc activity in the presence of MG132 = ERE-Luc activity in the presence of MG132 × (SV40-Luc activity/SV40-Luc activity in the presence of MG132)]. D, Effect of overexpressing Ubc12C111S on E2-induced reporter gene expression. HeLa cells were transfected with 250 ng ERE-pS2-Luc, 1 ng pSG5-ERα, along with 100 ng pcDNA or pcDNA-Ubc12C111S, and treated with 10 nM E2 for the indicated period of time. Luc activities were normalized against total cellular protein. E, Effect of overexpressing Ubc12C111S on SV40-Luc expression. HeLa cells were transfected with 100 ng SV40-Luc, along with 100 ng pcDNA-Ubc12C111S or control vector pcDNA. The DNA/LipofectAMINE mixture was removed 5 h later, and cells were placed in hormone-free medium for the indicated time period. Luc activities were normalized against total cellular protein. For all assays, Luc activities are expressed as mean ± SD from three independent experiments, each performed in triplicate.

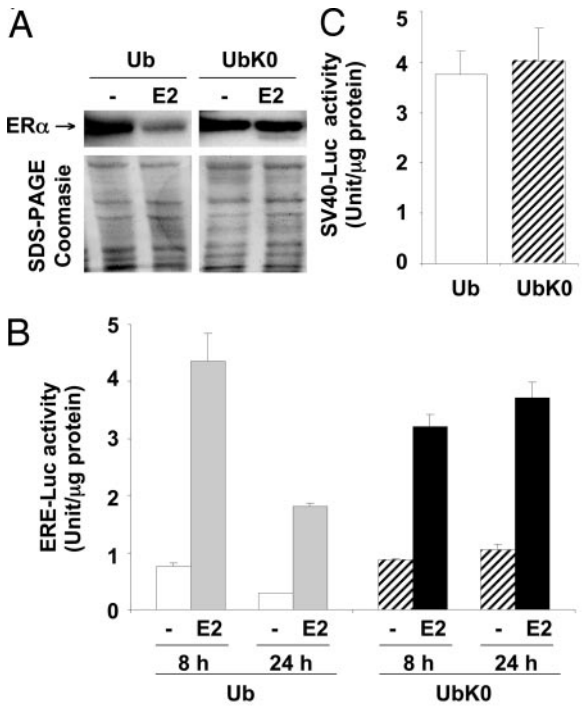

Fig. 4. Ub Mutant Blocks ER Degradation and Sustained E2-Induced Gene Expression

A, Overexpression of UbK0 blocks E2-induced ERα degradation. HeLa cells were plated in 60-mm dishes at a density of 3×10^5 cells per dish and cultured in hormone-free medium for 2 d. The cells were transfected with 150 ng pSG5-ERα, along with 150 ng pcDNA-Ub or pCS2-UbK0, using LipofectAMINE Plus reagent. The DNA/LipofectAMINE mixture was removed 5 h later, and cells were placed in hormone-free medium for 24 h before treatment with DMSO or 10 nM E2 for 8 h. Whole-cell lysates were prepared and subjected to immunoblotting analysis using an anti-ERα antibody. The Coomasie-stained SDS-PAGE gels show that equal amounts of cell lysates were loaded. B, Effect of UbK0 on ERα-mediated luciferase expression. HeLa cells stably transfected with ERα were plated in 12-well dishes at a density of 1×10^5 cells per well and cultured in hormone-free medium for 2 d. The cells were transfected with 250 ng ERE-pS2-Luc, along with 100 ng pcDNA-Ub or pCS2-UbK0 as indicated, using LipofectAMINE Plus reagent. The DNA/LipofectAMINE mixture was removed 5 h later, and cells were placed in hormone-free medium for 24 h before treatment with DMSO or 10 nM E2 for the indicated time period. C, Effect of UbK0 on luciferase expression from SV40-Luc. HeLa cells stably transfected with ERα were transfected with 100 ng SV40-Luc, along with 100 ng pcDNA-Ub or pCS2-UbK0. Five hours later, the DNA/LipofectAMINE mixture was removed, and cells were placed in hormone-free medium for the indicated time period. Luciferase activity was normalized against total cellular protein and expressed as the mean ± SD from three independent experiments, each performed in triplicate.

induced ERα degradation. In HeLa cells cotransfected with wild-type Ub and ERα, the level of receptor protein decreased markedly after E2 treatment (Fig. 4A), accompanied by transient E2-induced expression of an ER-responsive luciferase reporter gene (Fig. 4B, 8 h *vs.* 24 h). In contrast, cells transfected with UbK0 showed sustained E2-induced luciferase expression (Fig. 4B), and no decrease in ERα protein levels was observed (Fig. 4A). Furthermore, the effect of UbK0 on ERα-induced luciferase was specific, as UbK0 showed no effect on expression of the SV40-Luc construct (Fig. 4C). These results demonstrate that blocking polyubiquitination of ERα stabilizes the receptor, resulting in the prolonged expression of an ERα-responsive gene.

Proteasome Inhibition Enhances ERα-Mediated Transcription in MCF7 Breast Cancer Cells

To further investigate the role of ERα degradation in receptor transactivation ability under physiologically relevant conditions, we examined the effect of inhibiting the proteasome in MCF7 breast cancer cells, which endogenously express ERα. First, we examined the effect of MG132 on ERE-Vit-CAT expression in MCF7 cells. MCF7 cells were transiently transfected with ERE-Vit-CAT and then treated with DMSO or MG132 (1 μM) for 1 h before E2 (10 nM) treatment. CAT activity was determined 24 h after E2 treatment. A 17.8 ± 1.7 fold increase in CAT expression was seen in MCF7 cells treated with E2, compared with the control; treatment with MG132 further increased E2-induced CAT activity to 25.6 ± 2.5 fold. Therefore, inhibiting the proteasome enhanced ERα transcriptional activity in MCF7 cells, indicating that ERα degradation plays a key role in limiting E2-induced transcriptional responses in breast cancer cells.

To determine the effect of proteasome inhibition on transcription of ERα-target genes in breast cancer cells, we pretreated MCF7 cells with MG132 and examined E2-induced pS2 gene expression. ERα regulates pS2 transcription through an imperfect palindromic ERE at position −405 to −393 of its promoter region (45); pS2 expression is considered a reliable indicator of ERα transcriptional activity (46). Time-dependent effects of MG132 on heterogeneous nuclear pS2 RNA (pS2 hnRNA) levels, which reflect the rates of pS2 gene transcription (47–50), were examined. Primers amplifying the conjoining sequence between the first intron and second exon of the pS2 gene were used, and expression of pS2 hnRNA was assessed by real-time quantitative RT-PCR (Q-PCR). After administration of E2, levels of pS2 hnRNA increased by 3 h, peaked at 12 h, and then declined by 70% during the next 8 h (Fig. 5A, *gray bars*). However, at all time points examined, E2-induced expression of pS2 hnRNA was markedly enhanced by pretreatment with MG132 (Fig. 5A, *black vs. gray bars*), and pS2 hnRNA levels declined only by 15% from 12–20 h after the combined treatment (Fig. 5A, *black bars*). MG132 alone showed no effect on basal pS2 hnRNA expression (Fig. 5A, *hatched bars*). In agreement with what we observed with pS2 hnRNA, the combined treatment of MG132 plus E2 resulted in greater expression of pS2 mRNA after 6 h, compared with E2 treatment

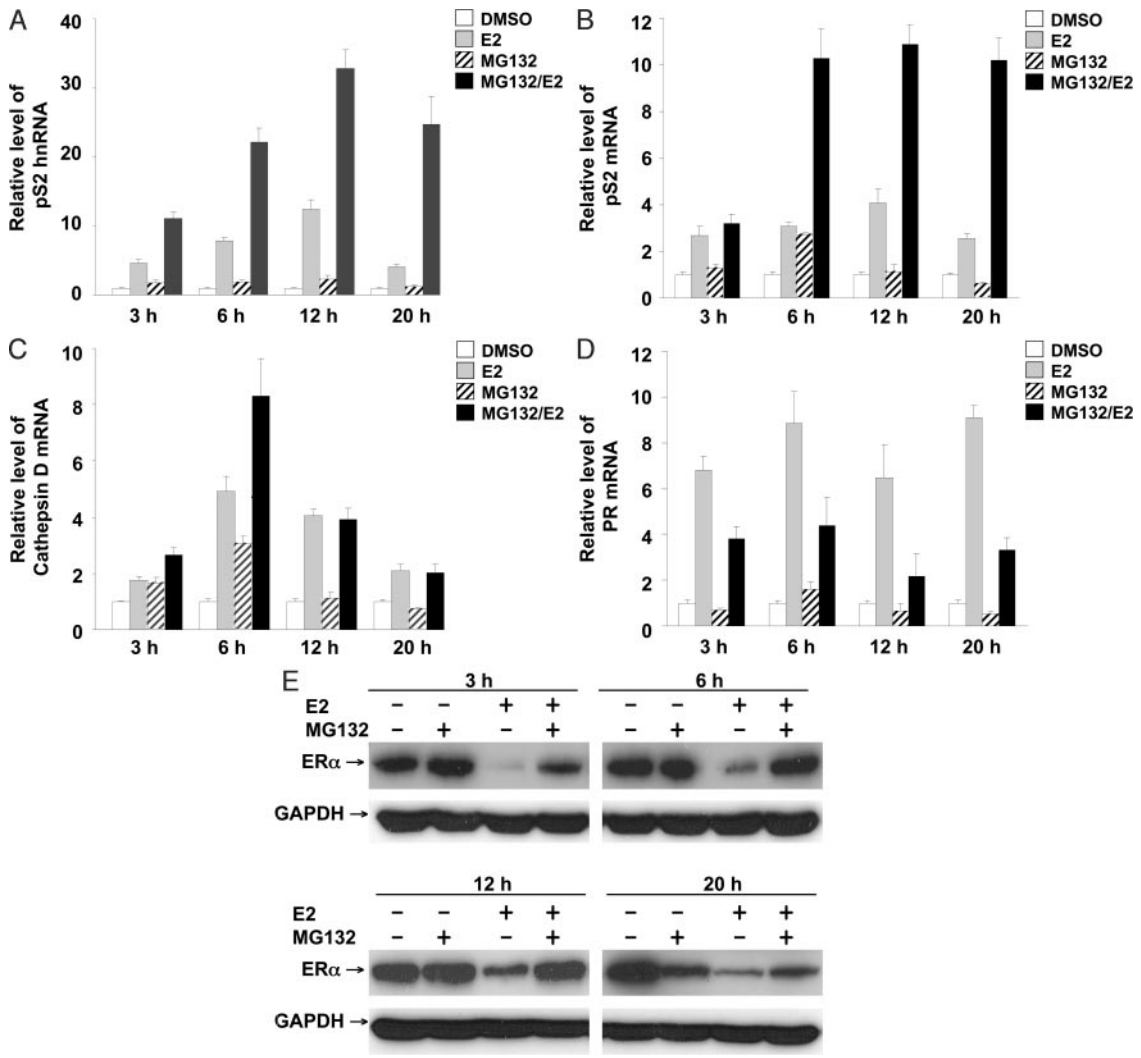

Fig. 5. Effects of MG132 on ERα-Mediated Transcription of Endogenous Target Genes in MCF7 Cells

MCF7 cells were plated at a density of 3×10^6 per 10-cm dish and allowed to grow in hormone-free medium for 3 d. The cells were pretreated with MG132 (5 μM) for 1 h and then treated with 10 nM E2 for the indicated time periods. Total RNA was prepared and subjected to Q-PCR analysis to determine the expression levels of pS2 hnRNA (A), pS2 mRNA (B), cathepsin D mRNA (C), and PR mRNA (D). For all Q-PCR assays, the relative levels of mRNA were normalized with β-actin mRNA and standardized such that values obtained in cells treated with vehicle (DMSO) only were set to 1. The results were expressed as mean ± SD from two independent experiments, each in duplicate. To determine the effect of MG132 on E2-induced ER degradation, MCF7 cells were treated as in panel A and subjected to whole-cell lysate preparation and immunoblotting with an anti-ER antibody (E). Glyceraldehyde-3-phosphate dehydrogenase (GAPDH) was used as a loading control.

alone (Fig. 5B, *black vs. gray bars*); pS2 mRNA levels remained markedly elevated up to 20 h, the last time point examined (Fig. 5B, *black bars*). The coordinate increase in E2-induced expression of both pS2 hnRNA and pS2 mRNA by MG132 excludes the possibility that MG132 inhibits the hnRNA splicing process or stabilizes pS2 mRNA. Therefore, it seems reasonable to conclude that blocking the proteasome with MG132 enhances E2-induced pS2 transcription initiation. Together, these results demonstrate that inhibiting the proteasome increases both the magnitude and duration of E2-induced expression of the endogenous pS2 gene in breast cancer cells.

We also examined the effect of MG132 on mRNA expression of cathepsin D and progesterone receptor (PR), two well-known E2-regulated genes, in MCF7 cells. As shown in Fig. 5C, a transient increase in cathepsin D mRNA expression was observed after treatment with E2. Pretreatment with MG132 enhanced both basal and E2-induced cathepsin D expression at 3 and 6 h (Fig. 5C, *black vs. gray bars*); however, at 12 and 24 h, the effect of MG132 was no longer apparent. Treatment of MCF7 cells with E2 increased PR mRNA levels 7-fold by 3 h, and PR mRNA levels remained elevated throughout the experiment period (Fig. 5D, *gray bars*). MG132 pretreatment

decreased E2-induced expression of PR mRNA by more than 50% at all time points examined (Fig. 5D, *black vs. gray bars*), which agrees with a recent report that MG132 inhibits ERα-induced increase in PR protein levels (7). The differential effects of MG132 on these ERα-target genes demonstrate that promoter context must be considered when evaluating MG132 regulation of ERα-mediated transcription. Immunoblotting analysis showed that pretreatment with MG132 efficiently blocked E2-induced ERα down-regulation in MCF7 cells (Fig. 5E).

4-OHT Stimulates ERα-Mediated Transcription without Inducing ERα Degradation

The antiestrogen 4-OHT has been shown to up-regulate ERα levels by blocking ERα degradation (37), and previous studies have shown that 4-OHT functions as an ERα agonist in Ishikawa endometrial cancer cells (51, 52). To further examine the relationship between receptor stability and ERα-mediated transcription, we stably transfected ERα-negative Ishikawa cells with ERα. The ERα(+) Ishikawa cells were then transfected with a luciferase reporter construct containing the human C3 promoter (C3T1-Luc) and then treated with either E2 (10 nM) or 4-OHT (1 μM) for 16 h. After E2 administration, a 2-fold increase in luciferase activity was observed (Fig. 6A), accompanied by a marked decrease in ERα protein level (Fig. 6B). Treatment with 4-OHT also stimulated expression of luciferase (80% of E2-stimulated luciferase expression) (Fig. 6A), but the antiestrogen did not down-regulate ERα (Fig. 6B). Thus, these results demonstrate that the partial agonist activity of 4-OHT and ERα degradation are not coupled in endometrial cancer cells. It has been reported that steroid receptor coactivator 1 (SRC-1), by stimulating transcription activity of 4-OHT liganded ERα (53), can convert 4-OHT to a full agonist. We reasoned that if receptor degradation is essential for ERα to initiate transcription, SRC1 should enhance 4-OHT-stimulated ERα transactivation activity and, in parallel, induce proteasomal degradation of 4-OHT-liganded ERα. To test this reasoning, the ERα(+)Ishikawa cells

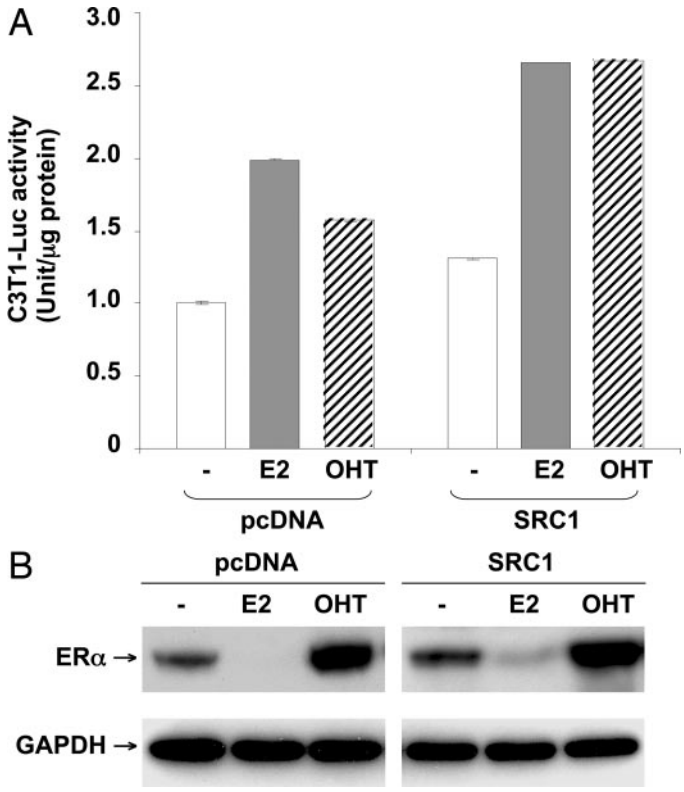

Fig. 6. Uncoupling of 4-OHT-Induced ERα Activation and ERα Degradation

A, 4-OHT stimulates ERα-mediated gene expression in Ishikawa cells. Ishikawa cells stably transfected with ERα were plated in 12-well dishes at a density of 1×10^5 cells per well and cultured in hormone-free medium for 2 d. The cells were transfected with 250 ng C3T1-Luc, along with 100 ng pcDNA or pcDNA-SRC1, using LipofectAMINE Plus reagent. The DNA/LipofectAMINE mixture was removed 5 h later, and cells were placed in hormone-free medium for 24 h before treatment with 10 nM E2 or 1 μM 4-OHT for 16 h. Luciferase activity was normalized against total cellular protein and expressed as mean ± SD from three independent experiments, each performed in triplicate. B, Effect of 4-OHT on ERα protein level. Ishikawa cells stably transfected with ERα were plated in 60-mm dishes at a density of 3×10^5 cells per dish and cultured in hormone-free medium for 3 d before treatment with 10 nM E2 or 1 μM 4-OHT for 16 h. Whole-cell lysates were prepared and subjected to immunoblotting analysis using an anti-ER antibody. GAPDH was used as a loading control.

were cotransfected with a construct expressing SRC1 and C3T1-Luc and then treated with either E2 (10 nM) or 4-OHT (1 μM) for 16 h. As expected, overexpressing SRC1 resulted in similar 4-OHT- and E2-stimulated ERα activity (Fig. 6A); however, 4-OHT did not induce receptor down-regulation (Fig. 6B). Thus, under these experimental conditions, 4-OHT, even when behaving as a full agonist in the presence of an increased level of SRC-1, did not induce ERα degradation. Taken together, these results demonstrate that ERα-mediated gene transactivation can be uncoupled from receptor degradation.

DISCUSSION

Like other rapidly turned over transcription factors, engagement of ERα in transactivation is coupled to ERα degradation by the Ub-proteasome pathway (7–11, 35). However, the functional impact of ERα degradation on cellular responses to E2 has not been well established. In this study, we analyzed the effect of blocking ERα degradation on E2-induced transcriptional output. We demonstrate that blocking ERα turnover prolongs the ability of ERα to transactivate target genes and increases the output of E2-induced gene transcription. We also show that 4-OHT can act as a full agonist in Ishikawa cells overexpressing SRC-1 to stimulate ERα transcriptional activity, without inducing receptor degradation. Furthermore, proteasome inhibition by MG132 increases ERα-mediated reporter gene expression, as well as expression of endogenous ERα-target genes (pS2 and cathepsin D), in MCF7 breast cancer cells. These data demonstrate that proteasomal degradation is not essential for ERα transcriptional activity; ERα remains functional after escaping ubiquitination and proteasomal proteolysis. An important implication of this study is that the E2-induced transcriptional response is limited by receptor degradation through the Ub-proteasome system, and defects in proteasome-mediated degradation of ERα could lead to an enhanced cellular response to E2.

In this study, several approaches targeting different steps in ubiquitination/proteasome proteolysis were used to block ERα degradation. MG132 was used to inhibit ERα proteolysis by specifically blocking activity of the 20S proteasome. A dominant-negative mutant (Ubc12C111S) of the NEDD8 conjugation enzyme was used to block ERα ubiquitination by inhibiting Ub ligase activity (41, 42). A Ub mutant with all of its lysines mutated to arginine (UbK0) was used to block ERα polyubiquitination by terminating polyubiquitin chains (43). One concern regarding the use of these approaches is a lack of specificity, such that the observed effect on enhanced E2-induced transcriptional output could be due to stabilization of multiple regulatory proteins, in addition to ERα. However, several observations suggest that this is not the case. MG132, Ubc12C111S, and UbK0 substantially enhance E2-induced, but not basal, expression of ERE reporter genes or the endogenous pS2 gene, suggesting that the effect of these inhibitors on ERα target gene expression is hormone dependent and thus receptor dependent. Furthermore, a time-dependent effect on E2-induced gene transcription was observed, which agrees with the ability of these inhibitors to block ligand-induced ERα degradation. Finally, no time-dependent effect on SV40-Luc expression was observed, in contrast to ERE-Luc, suggesting that these inhibitors do not broadly affect gene transcription in a time-dependent manner. Therefore, we conclude that MG132, Ubc12C111S, and UbK0 enhance E2-induced gene transcription primarily by extending the lifetime of functional ERα.

Consistent with our ERα findings, proteasome inhibition has been shown to enhance the transcriptional response mediated by other nuclear receptors, including the glucocorticoid receptor (GR) (17, 24), aryl hydrocarbon receptor (18), peroxisome proliferator-activated receptor α (19), retinoid receptors (20), and the vitamin D_3 receptor (21). However, it has also been reported that MG132 decreases transcriptional activity of PR and androgen receptor (22, 23), indicating that the effect of proteasome inhibition on transcriptional activity could be receptor specific. This is presumably due to the involvement of mechanisms other than modulation of receptor levels; for example, MG132 inhibited androgen receptor activity by eliminating androgen-induced nuclear translocation and coactivator recruitment (22, 23).

In MCF7 cells, we observed differential effects of MG132 on E2-induced transcription of endogenous pS2, cathepsin D, and PR gene, suggesting that proteasome inhibition can have promoter-specific effects on gene transcription. Although the reason for this is not clear, these observations raise the intriguing possibility of a differential requirement of ERα turnover in gene transcription, such that ERα degradation is required for PR transcription, but not for pS2 and cathepsin D. However, another attractive possibility is that multiple regulatory elements, other than an ERE, could be differentially regulated by proteasome inhibition; the different structures of the PR, pS2, and cathepsin D promoters may favor this possibility. For endogenous genes, the effect of estrogen is usually mediated through cross-talk between the ERE and nearby regulatory elements, and there appears to be an inverse correlation between the influence of nearby elements and the strength of the ERE (54). The ERE sequence in pS2 promoter deviates from the consensus palindromic ERE by 1 bp and, when isolated from surrounding sequences, is able to mediate estrogen responsiveness (45); however, for the cathepsin D promoter, although the ERE-like sequence deviates from the consensus ERE by only 2 bp, it is unable to confer estrogen regulation alone and must cooperate with other regulatory elements (54). In the case of the PR promoter, only a half-site ERE is found, and estrogen induction of PR appears to require cooperation with nearby Sp1 and AP-1 sites (55). Based on the obser-

vation that ERE-Vit-CAT (Fig. 1B) and ERE-pS2-Luc (Fig. 2) activities correlate with cellular concentrations of ERα, we suggest that ERα levels are the determining factor for the transcription activity of genes controlled exclusively by ERE. We further suggest that transcriptional activity of endogenous genes driven predominantly by an ERE (*e.g*. pS2) may depend upon the availability of ERα. In contrast, the level of ERα is unlikely to be the sole determining factor for the transcription of genes without a consensus ERE in their complex promoters (*e.g*. PR). In support of this notion, it has been reported that E2-induced transcription of the PR gene does not parallel ERα occupancy (55). Therefore, it is possible that MG132 inhibits PR expression through other protein factors, either directly or indirectly. In this respect, when evaluating the transcriptional activity of ERα, after escaping proteasome degradation, promoter context must be considered. Based on our own and the results of others (50), it is plausible that the transcription rate of a gene driven predominantly by an ERE is a more reliable readout of ERα transcription activity than a gene containing a complex promoter requiring ERα plus other transcription factors.

Our results differ from a previous study by Reid *et al.* (35), showing that MG132 prevented recruitment of phosphorylated RNA pol II (p-Pol II) to the pS2 promoter. This is most likely due to different experimental conditions and endpoints used in the two studies. For example, in their study Reid *et al.* used a higher dose (10 μM) and longer pretreatment (7 h) with MG132. However, under that condition, it is not clear whether the drug had any effect on p-Pol II recruitment to non-estrogen-responsive promoters. In addition, although α-amantin was used to clean the pS2 promoter before p-Pol II recruitment analysis, it is not clear that gene transcription resumed immediately (within a 2 h period) after α-amantin treatment. Thus, whether the differential recruitment of p-Pol II, in the absence or presence of MG132 after α-amantin pretreatment, is correlated with pS2 gene transcription remains an open question. However, the observation by Reid *et al.* (35) that the 20S proteolytic subunit does not associate with the pS2 promoter in response to E2 stimulation, agrees with numerous studies showing that the 20S proteasome subunit is not required for transcription initiation and elongation (56–60). Our observation further shows that 20S proteasome activity is not essential for ERα-mediated gene transcription.

Although the mechanism(s) by which the proteasome modulates ERα-mediated transactivation remains to be fully elucidated, chromatin immunoprecipitation assays have demonstrated that both unliganded and liganded receptors constantly cycle on and off estrogen-responsive promoters (35). MG132 appears to halt this cyclic interaction, leading to prolonged occupancy of ERα on EREs (35). The cyclic turnover of ERα could be a mechanism used by cells to prevent multiple rounds of transcription initiation from a single promoter, thus ensuring an appropriate cellular response to changes in circulating concentrations of hormone. To support this explanation, recent studies of GR show that proteasome inhibition dramatically increases both the residence time of GR on its target promoter and transcriptional output (24). In addition to extending the half-life of ligand-activated ERα, other factors, such as increased cellular concentration of receptor coactivators, could contribute to the enhancement of transcription by proteasome inhibition. Several ERα coactivators, including the steroid receptor coactivator family members (SRC1, SRC2, and SRC3) and cAMP response element binding protein (CREB)-binding protein/p300, are substrates of proteasomal degradation; proteasome inhibition appears to increase cellular concentrations of these coactivators (61).

We found that blocking ERα degradation (using MG132, Ubc12C111S, or UbK0) decreases E2-induced ERE-pS2-Luc expression at earlier time points (1.5–6 h) after E2 treatment (Figs. 3 and 4). Although the reason for this is unknown, one possibility is that ubiquitination and 20S proteasome activity are required for optimal ERα activation, perhaps by facilitating the release of ERα from preexisting corepressor complexes. To fully elucidate the physiological role(s) of ubiquitination, identification of the primary Ub ligase(s) for ERα, as well as the ubiquitination site(s) in this receptor, will be necessary.

In target tissues where ERα levels are limiting, the magnitude of the response to E2 is correlated with cellular ERα concentrations (2, 62). The Ub-proteasome pathway, by modulating receptor protein turnover, could play an important role in determining cellular responses to circulating E2 levels. Our results indicate that both the magnitude and duration of E2-induced gene transcription are limited by proteasome-mediated degradation of ERα; therefore, it seems reasonable to speculate that defects in ERα degradation could lead to enhanced cellular responsiveness to estrogens. In support of this possibility, it has been demonstrated that thyroid hormone and insulin, by blocking ligand-induced ERα degradation, can augment E2-stimulated cell proliferation (39, 63). Therefore, our future studies will examine the functional impact of proteasome-mediated ERα degradation on complex biological responses to estrogens, such as mammary gland development. In addition, aberrant ERα expression and estrogen responsiveness have been linked to breast tumor pathogenesis and development (64–66). Our previous studies demonstrate that blocking ERα degradation render breast cancer cells insensitive to the growth-inhibitory effects of ICI 182,780, a potent ERα down-regulator (42). Whether defects in the ERα degradation pathway contribute to deregulated estrogen signaling in breast cancer cells and play a role in disease progression to antiestrogen resistance remains to be elucidated.

MATERIALS AND METHODS

Plasmid Construction

The construction of pSG5-ERα(HEGO), ERE2-pS2-Luc, pcDNA-HA-Ubc12C111S, C3T1-Luc, pcDNA-SRC1, pCS2-UbK0, and ERE-Vit-CAT has been described previously (43, 67, 68).

Cell Lines

The human cervical carcinoma cell line HeLa and the breast cancer cell line MCF-7 were purchased from ATCC (Manassas, VA). The ERα-negative endometrial Ishikawa cell line was kindly provided by Dr. S. Hyder (University of Missouri, Columbia, MO). HeLa and Ishikawa cells were maintained in MEM with 2 mM L-glutamine, 1.5 g/liter sodium bicarbonate, 0.1 mM nonessential amino acids, 1.0 mM sodium pyruvate, 50 U/ml penicillin, 50 μg/ml streptomycin, and 10% fetal bovine serum. MCF7 cells were maintained in the same medium with the addition of 6 ng/ml insulin. Before experiments involving hormone treatment, cells were cultured in hormone-free medium (phenol red-free MEM with 3% dextran-coated charcoal-stripped fetal bovine serum) for 3 d.

Transient Transfection and Reporter Enzyme Assays

Cells (80% confluence) were transfected with an equal amount of total plasmid DNA (adjusted by corresponding empty vectors) by using LipofectAMINE Plus Reagent (Invitrogen, Carlsbad, CA) according to the manufacturer's guidelines. The DNA/LipofectAMINE mixture was removed 5 h later and cells were placed in hormone-free medium. Unless stated otherwise, 24 h after transfection, cells were treated with vehicle (DMSO) or MG132 (Sigma Chemical Co., St. Louis, MO) for 1 h before E2 (Sigma) treatment. At the end of the experiment, cell lysates were prepared for reporter enzyme assays. Luciferase activity was determined using the Luciferase Assay System (Promega Corp., Madison, WI), Gal activity was determined using a chemiluminescent reporter assay (PE Applied Biosystems, Foster City, CA), and CAT activity was determined using the colorimetric CAT ELISA kit (Roche Molecular Biochemicals, Indianapolis, IN). Total cellular protein was determined by using the Protein Assay Kit (Bio-Rad Laboratories, Inc., Hercules, CA). Reporter activities were expressed as relative light units normalized to total cellular protein.

Q-PCR

MCF7 cells were plated at a density of 3×10^6 per 10-cm dish and allowed to grow in hormone-free medium for 3 d. The cells were pretreated with MG132 (5 μM) for 1 h before E2 (10 nM) treatment. Total RNA was prepared by a RNAeasy Mini Kit (QIAGEN, Valencia, CA), according to the manufacturer's protocol. RNA (2 μg) was reverse transcribed in a total volume of 40 μl containing 400 U Moloney murine leukemia virus (M-MLV) reverse transcriptase (New England Biolabs, Beverly, MA), 400 ng random hexamers (Promega), 80 U RNase Inhibitor, and 1 mM deoxynucleotide triphosphates. The resulting cDNA was used in subsequent Q-PCR reactions, performed in 1× iQ SYBR Green Supermix (Bio-Rad) with 5 pmol forward and reverse primers. The primers used in the Q-PCR were, for pS2 mRNA: forward primer, 5′-ATACCATCGACGTCCCTCCA-3′; and reverse primer, 5′-AAGCGTGTCTGAGGTGTCCG-3′ (69); for pS2 hnRNA: forward primer, 5′-TTGGAGAAGGAAGCTGGATGG-3′ (start position 3997, within the intron); reverse primer, 5′-ACCACAATTCTGTCTTTCACGG-3′ (start position 4126, within the second exon); for PR: forward primer, 5′-TCAGTGGGCAGATGC TGTATTT-3′; and reverse primer, 5′-GCCACATGGTAAGGCATAATGA-3′ (70); for cathepsin D: forward primer, 5′-GTACATGATCCCCTGTGAGAAGGT-3′; reverse primer, 5′-GGGACAGCTTGTAGCCTTTGC-3′ (71); and for β-actin: forward primer, 5′-TGCGTGACATTAAGGAGAAG-3′; and reverse primer, 5′-GCTCGTAGCT CTTCTCCA-3′. Q-PCR was performed in 96-well optical plates (Bio-Rad) using an iCycler system (Bio-Rad) for 40 cycles (94 C for 10 sec, 60 C for 40 sec), after an initial 3-min denaturation at 94 C. The relative concentration of RNA was calculated using the ΔΔCt method according to Relative Quantitation of Gene Expression (Applied Biosystems User Bulletin) with β-actin mRNA as an internal control. Results were expressed as relative RNA levels standardized such that values obtained in cells treated with vehicle (DMSO) only were set to 1.

Acknowledgments

We thank Teresa Craft and Annie Park for excellent technical assistance; Dr. Curt Balch for critical review of this manuscript; Dr. Michele Pagano for providing the pCS2-UbK0 construct; and Dr. Wenlin Shao and Dr. Myles Brown for the Q-PCR primers of pS2 hnRNA.

Received April 19, 2004. Accepted July 21, 2004.

Address all correspondence and requests for reprints to: Kenneth P. Nephew, Ph.D., Medical Sciences, Indiana University School of Medicine, 302 Jordan Hall, 1001 East 3rd Street, Bloomington, Indiana 47405-4401. E-mail: knephew@indiana. edu.

This work was supported by the United States Army Medical Research Acquisition Activity, Award Nos. DAMD 17-02-1-0418 and DAMD17-02-1-0419 (to K.P.N.); American Cancer Society Research and Alaska Run for Woman Grant TBE-104125 (to K.P.N.); American Cancer Society Grant RPG-00-122-01-TBE and National Institutes of Health Grant CA89153 (to H.N.); and the Walther Cancer Institute (to M.F.).

REFERENCES

1. McKenna NJ, O'Malley BW 2001 Nuclear receptors, coregulators, ligands, and selective receptor modulators: making sense of the patchwork quilt. Ann NY Acad Sci 949:3–5
2. Webb P, Lopez GN, Greene GL, Baxter JD, Kushner PJ 1992 The limits of the cellular capacity to mediate an estrogen response. Mol Endocrinol 6:157–167
3. Klinge CM 2000 Estrogen receptor interaction with coactivators and co-repressors. Steroids 65:227–251
4. Saceda M, Lippman ME, Chambon P, Lindsey RL, Ponglikitmongkol M, Puente M, Martin MB 1988 Regulation of the estrogen receptor in MCF-7 cells by estradiol. Mol Endocrinol 2:1157–1162
5. Pink JJ, Jordan VC 1996 Models of estrogen receptor regulation by estrogens and antiestrogens in breast cancer cell lines. Cancer Res 56:2321–2330
6. Nephew KP, Long X, Osborne E, Burke KA, Ahluwalia A, Bigsby RM 2000 Effect of estradiol on estrogen receptor expression in rat uterine cell types. Biol Reprod 62: 168–177
7. Lonard DM, Nawaz Z, Smith CL, O'Malley BW 2000 The 26S proteasome is required for estrogen receptor-α and coactivator turnover and for efficient estrogen receptor-α transactivation. Mol Cell 5:939–948
8. Nawaz Z, Lonard DM, Dennis AP, Smith CL, O'Malley BW 1999 Proteasome-dependent degradation of the human estrogen receptor. Proc Natl Acad Sci USA 96: 1858–1862

9. Alarid ET, Bakopoulos N, Solodin N 1999 Proteasome-mediated proteolysis of estrogen receptor: a novel component in autologous down-regulation. Mol Endocrinol 13:1522–1534
10. El Khissiin A, Leclercq G 1999 Implication of proteasome in estrogen receptor degradation. FEBS Lett 448: 160–166
11. Wijayaratne AL, McDonnell DP 2001 The human estrogen receptor-α is a ubiquitinated protein whose stability is affected differentially by agonists, antagonists, and selective estrogen receptor modulators. J Biol Chem 276:35684–35692
12. Muratani M, Tansey WP 2003 How the ubiquitin-proteasome system controls transcription. Nat Rev Mol Cell Biol 4:192–201
13. Conaway RC, Brower CS, Conaway JW 2002 Emerging roles of ubiquitin in transcription regulation. Science 296: 1254–1258
14. Tansey WP 2001 Transcriptional activation: risky business. Genes Dev 15:1045–1050
15. Salghetti SE, Muratani M, Wijnen H, Futcher B, Tansey WP 2000 Functional overlap of sequences that activate transcription and signal ubiquitin-mediated proteolysis. Proc Natl Acad Sci USA 97:3118–3123
16. Salghetti SE, Caudy AA, Chenoweth JG, Tansey WP 2001 Regulation of transcriptional activation domain function by ubiquitin. Science 293:1651–1653
17. Wallace AD, Cidlowski JA 2001 Proteasome-mediated glucocorticoid receptor degradation restricts transcriptional signaling by glucocorticoids. J Biol Chem 276: 42714–42721
18. Pollenz RS 2002 The mechanism of AH receptor protein down-regulation (degradation) and its impact on AH receptor-mediated gene regulation. Chem Biol Interact 141:41–61
19. Blanquart C, Barbier O, Fruchart JC, Staels B, Glineur C 2002 Peroxisome proliferator-activated receptor α (PPARα) turnover by the ubiquitin-proteasome system controls the ligand-induced expression level of its target genes. J Biol Chem 277:37254–37259
20. Boudjelal M, Voorhees JJ, Fisher GJ 2002 Retinoid signaling is attenuated by proteasome-mediated degradation of retinoid receptors in human keratinocyte HaCaT cells. Exp Cell Res 274:130–137
21. Li XY, Boudjelal M, Xiao JH, Peng ZH, Asuru A, Kang S, Fisher GJ, Voorhees JJ 1999 1,25-Dihydroxyvitamin D_3 increases nuclear vitamin D_3 receptors by blocking ubiquitin/proteasome-mediated degradation in human skin. Mol Endocrinol 13:1686–1694
22. Kang Z, Pirskanen A, Janne OA, Palvimo JJ 2002 Involvement of proteasome in the dynamic assembly of the androgen receptor transcription complex. J Biol Chem 277:48366–48371
23. Lin HK, Altuwaijri S, Lin WJ, Kan PY, Collins LL, Chang C 2002 Proteasome activity is required for androgen receptor transcriptional activity via regulation of androgen receptor nuclear translocation and interaction with coregulators in prostate cancer cells. J Biol Chem 277: 36570–36576
24. Stavreva DA, Muller WG, Hager GL, Smith CL, McNally JG 2004 Rapid glucocorticoid receptor exchange at a promoter is coupled to transcription and regulated by chaperones and proteasomes. Mol Cell Biol 24: 2682–2697
25. Ciechanover A, Orian A, Schwartz AL 2000 Ubiquitin-mediated proteolysis: biological regulation via destruction. Bioessays 22:442–451
26. Molinari E, Gilman M, Natesan S 1999 Proteasome-mediated degradation of transcriptional activators correlates with activation domain potency in vivo. EMBO J 18:6439–6447
27. Nawaz Z, Lonard DM, Smith CL, Lev-Lehman E, Tsai SY, Tsai MJ, O'Malley BW 1999 The Angelman syndrome-associated protein, E6-AP, is a coactivator for the nuclear hormone receptor superfamily. Mol Cell Biol 19: 1182–1189
28. Grossman SR, Deato ME, Brignone C, Chan HM, Kung AL, Tagami H, Nakatani Y, Livingston DM 2003 Polyubiquitination of p53 by a ubiquitin ligase activity of p300. Science 300:342–344
29. Hanstein B, Eckner R, DiRenzo J, Halachmi S, Liu H, Searcy B, Kurokawa R, Brown M 1996 p300 is a component of an estrogen receptor coactivator complex. Proc Natl Acad Sci USA 93:11540–11545
30. Ruffner H, Joazeiro CA, Hemmati D, Hunter T, Verma IM 2001 Cancer-predisposing mutations within the RING domain of BRCA1: loss of ubiquitin protein ligase activity and protection from radiation hypersensitivity. Proc Natl Acad Sci USA 98:5134–5139
31. Fan S, Wang J, Yuan R, Ma Y, Meng Q, Erdos MR, Pestell RG, Yuan F, Auborn KJ, Goldberg ID, Rosen EM 1999 BRCA1 inhibition of estrogen receptor signaling in transfected cells. Science 284:1354–1356
32. Fraser RA, Rossignol M, Heard DJ, Egly JM, Chambon P 1997 SUG1, a putative transcriptional mediator and subunit of the PA700 proteasome regulatory complex, is a DNA helicase. J Biol Chem 272:7122–7126
33. Saji S, Okumura N, Eguchi H, Nakashima S, Suzuki A, Toi M, Nozawa Y, Hayashi S 2001 MDM2 enhances the function of estrogen receptor α in human breast cancer cells. Biochem Biophys Res Commun 281:259–265
34. Masuyama H, Hiramatsu Y 2004 Involvement of suppressor for Gal 1 in the ubiquitin/proteasome-mediated degradation of estrogen receptors. J Biol Chem 279: 12020–12026
35. Reid G, Hubner MR, Metivier R, Brand H, Denger S, Manu D, Beaudouin J, Ellenberg J, Gannon F 2003 Cyclic, proteasome-mediated turnover of unliganded and liganded ERα on responsive promoters is an integral feature of estrogen signaling. Mol Cell 11:695–707
36. Deroo BJ, Archer TK 2002 Proteasome inhibitors reduce luciferase and β-galactosidase activity in tissue culture cells. J Biol Chem 277:20120–20123
37. Laios I, Journe F, Laurent G, Nonclercq D, Toillon RA, Seo HS, Leclercq G 2003 Mechanisms governing the accumulation of estrogen receptor α in MCF-7 breast cancer cells treated with hydroxytamoxifen and related antiestrogens. J Steroid Biochem Mol Biol 87:207–221
38. Frasor J, Stossi F, Danes JM, Komm B, Lyttle CR, Katzenellenbogen BS 2004 Selective estrogen receptor modulators: discrimination of agonistic versus antagonistic activities by gene expression profiling in breast cancer cells. Cancer Res 64:1522–1533
39. Alarid ET, Preisler-Mashek MT, Solodin NM 2003 Thyroid hormone is an inhibitor of estrogen-induced degradation of estrogen receptor-α protein: estrogen-dependent proteolysis is not essential for receptor transactivation function in the pituitary. Endocrinology 144:3469–3476
40. Schreihofer DA, Resnick EM, Lin VY, Shupnik MA 2001 Ligand-independent activation of pituitary ER: dependence on PKA-stimulated pathways. Endocrinology 142: 3361–3368
41. Wada H, Yeh ET, Kamitani T 2000 A dominant-negative UBC12 mutant sequesters NEDD8 and inhibits NEDD8 conjugation in vivo. J Biol Chem 275:17008–17015
42. Fan M, Bigsby RM, Nephew KP 2003 The NEDD8 pathway is required for proteasome-mediated degradation of human estrogen receptor (ER)-α and essential for the antiproliferative activity of ICI 182,780 in ERα-positive breast cancer cells. Mol Endocrinol 17:356–365
43. Bloom J, Amador V, Bartolini F, DeMartino G, Pagano M 2003 Proteasome-mediated degradation of p21 via N-terminal ubiquitinylation. Cell 115:71–82
44. Thompson JF, Hayes LS, Lloyd DB 1991 Modulation of firefly luciferase stability and impact on studies of gene regulation. Gene 103:171–177

45. Berry M, Nunez AM, Chambon P 1989 Estrogen-responsive element of the human pS2 gene is an imperfectly palindromic sequence. Proc Natl Acad Sci USA 86: 1218–1222
46. Brown AM, Jeltsch JM, Roberts M, Chambon P 1984 Activation of pS2 gene transcription is a primary response to estrogen in the human breast cancer cell line MCF-7. Proc Natl Acad Sci USA 81:6344–6348
47. Lipson KE, Baserga R 1989 Transcriptional activity of the human thymidine kinase gene determined by a method using the polymerase chain reaction and an intron-specific probe. Proc Natl Acad Sci USA 86:9774–9777
48. Tian Y, Ke S, Thomas T, Meeker RJ, Gallo MA 1998 Transcriptional suppression of estrogen receptor gene expression by 2,3,7,8-tetrachlorodibenzo-p-dioxin (TCDD). J Steroid Biochem Mol Biol 67:17–24
49. Elferink CJ, Reiners Jr JJ 1996 Quantitative RT-PCR on CYP1A1 heterogeneous nuclear RNA: a surrogate for the in vitro transcription run-on assay. Biotechniques 20: 470–477
50. Delany AM 2001 Measuring transcription of metalloproteinase genes. Nuclear run-off assay vs analysis of hnRNA. Methods Mol Biol 151:321–333
51. Anzai Y, Holinka CF, Kuramoto H, Gurpide E 1989 Stimulatory effects of 4-hydroxytamoxifen on proliferation of human endometrial adenocarcinoma cells (Ishikawa line). Cancer Res 49:2362–2365
52. Jamil A, Croxtall JD, White JO 1991 The effect of anti-oestrogens on cell growth and progesterone receptor concentration in human endometrial cancer cells (Ishikawa). J Mol Endocrinol 6:215–221
53. Shang Y, Brown M 2002 Molecular determinants for the tissue specificity of SERMs. Science 295:2465–2468
54. Barkhem T, Haldosen LA, Gustafsson JA, Nilsson S 2002 pS2 Gene expression in HepG2 cells: complex regulation through crosstalk between the estrogen receptor α, an estrogen-responsive element, and the activator protein 1 response element. Mol Pharmacol 61:1273–1283
55. Lee YJ, Gorski J 1996 Estrogen-induced transcription of the progesterone receptor gene does not parallel estrogen receptor occupancy. Proc Natl Acad Sci USA 93: 15180–15184
56. Makino Y, Yogosawa S, Kayukawa K, Coin F, Egly JM, Wang Z, Roeder RG, Yamamoto K, Muramatsu M, Tamura T 1999 TATA-binding protein-interacting protein 120, TIP120, stimulates three classes of eukaryotic transcription via a unique mechanism. Mol Cell Biol 19: 7951–7960
57. Russell SJ, Johnston SA 2001 Evidence that proteolysis of Gal4 cannot explain the transcriptional effects of proteasome ATPase mutations. J Biol Chem 276:9825–9831
58. Ferdous A, Gonzalez F, Sun L, Kodadek T, Johnston SA 2001 The 19S regulatory particle of the proteasome is required for efficient transcription elongation by RNA polymerase II. Mol Cell 7:981–991
59. Gonzalez F, Delahodde A, Kodadek T, Johnston SA 2002 Recruitment of a 19S proteasome subcomplex to an activated promoter. Science 296:548–550
60. Ferdous A, Kodadek T, Johnston SA 2002 A nonproteolytic function of the 19S regulatory subunit of the 26S proteasome is required for efficient activated transcription by human RNA polymerase II. Biochemistry 41: 12798–12805
61. Yan F, Gao X, Lonard DM, Nawaz Z 2003 Specific ubiquitin-conjugating enzymes promote degradation of specific nuclear receptor coactivators. Mol Endocrinol 17: 1315–1331
62. Katzenellenbogen BS, Kendra KL, Norman MJ, Berthois Y 1987 Proliferation, hormonal responsiveness, and estrogen receptor content of MCF-7 human breast cancer cells grown in the short-term and long-term absence of estrogens. Cancer Res 47:4355–4360
63. Panno ML, Salerno M, Pezzi V, Sisci D, Maggiolini M, Mauro L, Morrone EG, Ando S 1996 Effect of oestradiol and insulin on the proliferative pattern and on oestrogen and progesterone receptor contents in MCF-7 cells. J Cancer Res Clin Oncol 122:745–749
64. Clarke RB, Howell A, Potten CS, Anderson E 1997 Dissociation between steroid receptor expression and cell proliferation in the human breast. Cancer Res 57: 4987–4991
65. Shoker BS, Jarvis C, Clarke RB, Anderson E, Hewlett J, Davies MP, Sibson DR, Sloane JP 1999 Estrogen receptor-positive proliferating cells in the normal and precancerous breast. Am J Pathol 155:1811–1815
66. Shoker BS, Jarvis C, Clarke RB, Anderson E, Munro C, Davies MP, Sibson DR, Sloane JP 2000 Abnormal regulation of the oestrogen receptor in benign breast lesions. J Clin Pathol 53:778–783
67. Fan M, Long X, Bailey JA, Reed CA, Osborne E, Gize EA, Kirk EA, Bigsby RM, Nephew KP 2002 The activating enzyme of NEDD8 inhibits steroid receptor function. Mol Endocrinol 16:315–330
68. Klein-Hitpass L, Tsai SY, Greene GL, Clark JH, Tsai MJ, O'Malley BW 1989 Specific binding of estrogen receptor to the estrogen response element. Mol Cell Biol 9:43–49
69. Rajendran RR, Nye AC, Frasor J, Balsara RD, Martini PG, Katzenellenbogen BS 2003 Regulation of nuclear receptor transcriptional activity by a novel DEAD box RNA helicase (DP97). J Biol Chem 278:4628–4638
70. Aerts JL, Christiaens MR, Vandekerckhove P 2002 Evaluation of progesterone receptor expression in eosinophils using real-time quantitative PCR. Biochim Biophys Acta 1571:167–172
71. Augereau P, Miralles F, Cavailles V, Gaudelet C, Parker M, Rochefort H 1994 Characterization of the proximal estrogen-responsive element of human cathepsin D gene. Mol Endocrinol 8:693–703

Molecular Endocrinology **is published monthly by The Endocrine Society (http://www.endo-society.org), the foremost professional society serving the endocrine community.**

0888-8809/05/$15.00/0
Printed in U.S.A.

Molecular Endocrinology 19(12):2901–2914

doi: 10.1210/me.2005-0111

CHIP (Carboxyl Terminus of Hsc70-Interacting Protein) Promotes Basal and Geldanamycin-Induced Degradation of Estrogen Receptor-α

Meiyun Fan, Annie Park, and Kenneth P. Nephew

Medical Sciences (M.F., A.P., K.P.N.), Indiana University School of Medicine, Bloomington, Indiana 47405; and Indiana University Cancer Center (K.P.N.) and Department of Cellular and Integrative Physiology (K.P.N.), Indiana University School of Medicine, Indianapolis, Indiana 46202

In estrogen target cells, estrogen receptor-α (ERα) protein levels are strictly regulated. Although receptor turnover is a continuous process, dynamic fluctuations in receptor levels, mediated primarily by the ubiquitin-proteasome pathway, occur in response to changing cellular conditions. In the absence of ligand, ERα is sequestered within a stable chaperone protein complex consisting of heat shock protein 90 (Hsp90) and cochaperones. However, the molecular mechanism(s) regulating ERα stability and turnover remain undefined. One potential mechanism involves CHIP, the carboxyl terminus of Hsc70-interacting protein, previously shown to target Hsp90-interacting proteins for ubiquitination and proteasomal degradation. In the present study, a role for CHIP in ERα protein degradation was investigated. In ER-negative HeLa cells transfected with ERα and CHIP, ERα proteasomal degradation increased, whereas ERα-mediated gene transcription decreased. In contrast, CHIP depletion by small interference RNA resulted in increased ERα accumulation and reporter gene transactivation. Transfection of mutant CHIP constructs demonstrated that both the U-box (containing ubiquitin ligase activity) and the tetratricopeptide repeat (TPR, essential for chaperone binding) domains within CHIP are required for CHIP-mediated ERα down-regulation. In addition, coimmunoprecipitation assays demonstrated that ERα and CHIP associate through the CHIP TPR domain. In ERα-positive breast cancer MCF7 cells, CHIP overexpression resulted in decreased levels of endogenous ERα protein and attenuation of ERα-mediated gene expression. Furthermore, the ERα-CHIP interaction was stimulated by the Hsp90 inhibitor geldanamycin (GA), resulting in enhanced ERα degradation; this GA effect was further augmented by CHIP overexpression but was abolished by CHIP depletion. Finally, ERα dissociation from CHIP by various ERα ligands, including 17β-estradiol, 4-hydroxytamoxifen, and ICI 182,780, interrupted CHIP-mediated ERα degradation. These results demonstrate a role for CHIP in both basal and GA-induced ERα degradation. Furthermore, based on our observations that CHIP promotes ERα degradation and attenuates receptor-mediated gene transcription, we suggest that CHIP, by modulating ERα stability, contributes to the regulation of functional receptor levels, and thus hormone responsiveness, in estrogen target cells. (*Molecular Endocrinology* 19: 2901–2914, 2005)

THE PRIMARY MEDIATORS of 17β-estradiol (E2) action, the major female sex steroid hormone, are the estrogen receptors ERα and ERβ. These receptors function as ligand-activated transcription factors, regulating expression of genes coordinating most physiological and many pathophysiological processes in estrogen target tissues (1). Tissue sensitivity, and the overall magnitude of response to E2 and other estrogens, is strongly influenced by a combination of factors, including cellular levels of ERα and its various coactivators and corepressors (2, 3).

To strictly control cellular responses, the cellular synthesis and turnover of the ERα protein dynamically fluctuates with changing cellular environments (4). For example, in the absence of ligand, ERα is a short-lived protein (half-life of 4–5 h) and undergoes constant degradation (5). In the presence of ligand, by contrast, the turnover rate of ERα can be increased or decreased, depending upon the ligand, thus modulating receptor protein levels. Turnover-inducing factors and conditions include the cognate ligand E2, pure antiestrogens [ICI 164,384, ICI 182,780 (ICI), RU 58,668], heat shock protein (Hsp) 90 inhibitors [geldanamycin (GA) and radicicol], ATP depletion (oligomycin and hypoxia) and aryl hydrocarbon agonists; these all induce degradation and rapid down-regulation of ERα

First Published Online July 21, 2005

Abbreviations: CHIP, Carboxyl terminus of Hsc70-interacting protein; CHIPi, CHIP-siRNA expression construct; CMV, cytomegalovirus promoter; DMSO, dimethylsulfoxide; E2, 17β-estradiol; ERα, estrogen receptor-α; ERE, estrogen response element; FBS, fetal bovine serum; GA, geldanamycin; GAPDH, glyceraldehyde-3-phosphate dehydrogenase; GFP, green fluorescent protein; HA, hemagglutinin; Hsp, heat shock protein; ICI, ICI 182,780; Luc, firefly luciferase; OHT, 4-hydroxytamoxifen; siRNA, small interference RNA; SV40, simian virus 40 promoter; TPR, tetratricopeptide repeat.

***Molecular Endocrinology* is published monthly by The Endocrine Society (http://www.endo-society.org), the foremost professional society serving the endocrine community.**

levels (6–12). In contrast, the partial agonist/antagonist 4-hydoxytamoxifen (OHT), thyroid hormone, and protein kinase K activators (forskolin, 8-bromo-cAMP) all block receptor degradation, subsequently increasing ERα protein levels (13–15).

Although both basal and ligand-induced ERα degradation are mediated by the ubiquitin-proteasome pathway (12, 13, 16–21), regulation of this pathway, at the molecular level, remains unclear. Emerging evidence suggests that multiple ERα degradation pathways exist, and the engagement of one pathway over another depends on the nature of the stimulus (19, 21–23). For example, E2-induced receptor degradation is coupled with transcription and requires new protein synthesis (17, 19, 22, 24); conversely, neither ERα transcriptional activity nor new protein synthesis are needed for ICI-induced ERα degradation (19, 20, 22). In addition, various stimuli induce distinct changes in the conformation and cellular compartmentalization of ERα (22, 25–27), and these may be associated with receptor ubiquitination.

Like other members of the steroid receptor superfamily, unliganded ERα, by associating with various Hsp90-based chaperone complexes, is maintained in a ligand-binding competent conformation (28). Although these associations do not influence ERα ligand-binding affinity, Hsp90 chaperone complexes appear to regulate ERα stability because Hsp90 disruption induces rapid ERα degradation through the ubiquitin proteasome pathway (9, 28, 29). For regulation of such complexes, recent studies have identified the carboxyl terminus of Hsc70-interacting protein (CHIP) as a ubiquitin ligase that directs chaperone substrates for ubiquitination and proteasomal degradation (30, 31). CHIP interacts with Hsp/Hsc70 and Hsp90 through an amino-terminal TPR domain and catalyzes ubiquitin conjugation through a carboxyl-terminal U-box domain (30). As recent observations demonstrate that CHIP targets a number of Hsp70/90-associated proteins for ubiquitination and degradation, including the glucocorticoid receptor, androgen receptor, Smad1/4, and ErbB2 (30–33), we investigated a regulatory role for CHIP in ERα stability. Our results demonstrate that CHIP, likely through a chaperone intermediate, associates with ERα and consequently facilitates both basal and GA-induced receptor degradation in human cancer cells.

RESULTS

CHIP Overexpression Decreases and CHIP Knockdown Increases ERα Protein Levels

To investigate the effect of CHIP overexpression on steady-state levels of ERα, ER-negative HeLa cells were cotransfected with constructs expressing CHIP (pcDNA-His6-CHIP) and ERα (pSG5-ERα). ERα protein levels were subsequently determined by immunoblot analysis. Overexpression of CHIP decreased ERα protein levels in a dose-dependent manner (Fig. 1A). To control for transfection efficiency, the green fluorescent protein (GFP) was also included in transfection. No effect of CHIP on GFP expression level was observed (Fig. 1A), demonstrating that CHIP-induced down-regulation of ERα was specific. Next, we examined whether CHIP-induced ERα down-regulation could be inhibited by CHIP-specific small interference RNA (siRNA). Compared with cells transfected with CHIP only, cotransfection of pBS/U6/CHIPi, a CHIP-siRNA expression construct (33), dramatically decreased the level of exogenous CHIP (Fig. 1B, *upper*

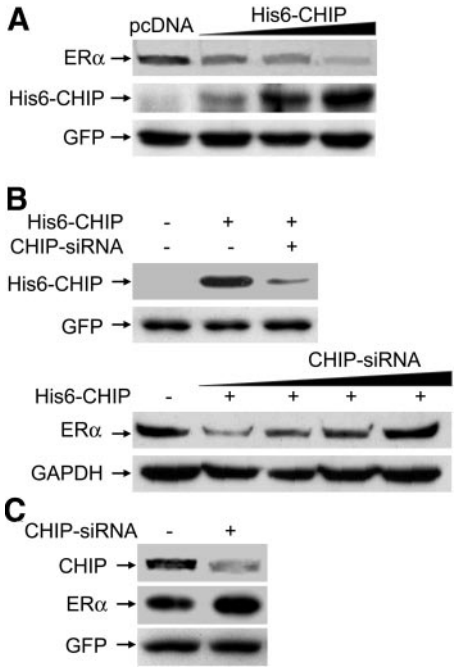

Fig. 1. CHIP Overexpression Decreases and CHIP Knockdown Increases ERα Protein Levels

A, Overexpression of CHIP down-regulates ERα protein levels. HeLa cells were transfected with 250 ng pSG5-ERα, 100 ng CMV-GFP, and various amounts (0, 50, 100, and 250 ng) of pcDNA-his6-CHIP. B, Expression of CHIP-siRNA attenuates CHIP-induced ERα down-regulation. In the *upper panel*, HeLa cells were transfected with 250 ng pcDNA-his6-CHIP, with or without 250 ng pBS/U6/CHIPi, as indicated. In the lower panel, HeLa cells were transfected with 250 ng pSG5-ERα, 250 ng pcDNA-his6-CHIP, and various doses (150, 300, 500, and 1000 ng) of pBS/U6/CHIPi. C, Knockdown of endogenous CHIP increases ERα level. HeLa cells were transfected with 250 ng pSG5-ERα and either 250 ng pcDNA-his6-CHIP or 250 ng pBS/U6/CHIPi, as indicated. For all experiments, 3×10^5 HeLa cells were plated in 60-mm dishes, cultured in hormone-free medium for 3 d, and then transfected with LipofectAMINE Plus Reagent. Cell lysates were prepared 24 h after transfection. Protein levels were determined by immunoblotting with specific antibodies. Exogenous His6-CHIP and endogenous CHIP were detected by anti-His6 and anti-CHIP, respectively. GFP and GAPDH were used as transfection control and SDS-PAGE loading controls, respectively. Representative results of two independent experiments, each performed in duplicate, are shown.

panel). However, pBS/U6/CHIPi had no effect on GFP level, confirming that the CHIP-siRNA specifically blocks CHIP expression (Fig. 1B). The effect of CHIP-siRNA on CHIP-induced ERα down-regulation was then examined. As shown in Fig. 1B (*lower panel*), cotransfection of CHIP-siRNA, in a dose-dependent fashion, attenuated ERα down-regulation induced by exogenous CHIP. Collectively, these results demonstrate that CHIP overexpression can down-regulate ERα protein level in HeLa cells.

To examine a role for endogenous CHIP in regulation of ERα protein levels, HeLa cells, which are known to express CHIP (30), were cotransfected with pBS/U6/CHIPi and ERα. Expression of CHIP-siRNA decreased the level of endogenous CHIP by 60%, and correspondingly increased ERα protein level by 1.6-fold (Fig. 1C), indicating that endogenous CHIP plays a role in controlling ERα level in HeLa cells.

CHIP Down-Regulates ERα Levels through the Ubiquitin Proteasome Pathway

To determine whether proteasome activity is required for CHIP-induced ERα down-regulation, HeLa cells were cotransfected with pcDNA-His6-CHIP and pSG5-ERα, treated with the protease inhibitor MG132, and subjected to immunoblotting. As shown in Fig. 2A, a 6-h treatment with MG132 completely blocked CHIP-induced down-regulation of ERα. To examine whether polyubiquitination is required for CHIP-induced ERα degradation, a mutant ubiquitin, UbK0, with all lysines replaced by arginines (34), was used. Previously, we showed that the UbK0 protein could efficiently block E2-induced ERα degradation (35). Expression of UbK0, but not wild-type ubiquitin, restored ERα protein levels (Fig. 2B), demonstrating that CHIP stimulates ERα degradation through the ubiquitin and proteasome pathway.

CHIP Targets Mature ERα for Degradation

It has been proposed that CHIP functions as a general ubiquitin ligase, responsible for ubiquitinating unfolded or misfolded proteins in a chaperone-dependent process (31). To examine whether ERα down-regulation by CHIP was due to the selective ubiquitination of unfolded or misfolded receptor protein, we examined the effect of OHT, a selective ER modulator, on CHIP-mediated ERα degradation. It has been shown that OHT can dissociate ERα from its chaperone complex and protect the receptor from both basal turnover and degradation induced by Hsp90-binding agents (8, 13, 21). We reasoned that if CHIP selectively targets immature or misfolded ERα (with no functional OHT-binding pocket), then, in the presence of CHIP, OHT treatment should not restore ERα levels. On the other hand, if CHIP targets mature ERα, OHT treatment should rescue the receptor protein from CHIP-induced degradation. HeLa cells were thus cotransfected with pcDNA-His6-CHIP and pSG5-ERα and treated with OHT for 6 h before lysate preparation. OHT treatment completely abolished CHIP-

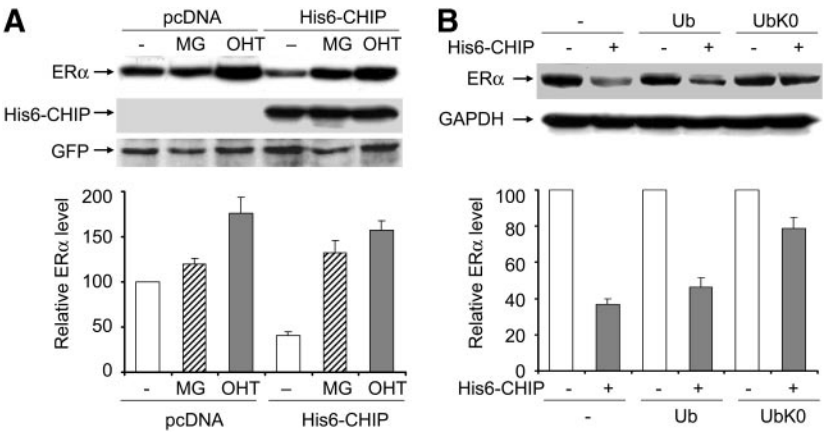

Fig. 2. The Proteasome Inhibitor MG132, Partial ERα-Antagonist OHT, and Ubiquitin Mutant UbK0, All Block CHIP-Induced ERα Degradation

A, The proteasome inhibitor MG132 and the partial ERα antagonist OHT block CHIP-induced ERα down-regulation. HeLa cells were transfected with 250 ng pSG5-ERα and 100 ng CMV-GFP, along with 250 ng pcDNA (vector control) or pcDNA-His6-CHIP, then treated with DMSO (vehicle), 10 μM MG312 or 1 μM OHT for 6 h before immunoblot analysis. Protein levels of ERα, CHIP and GFP were determined by immunoblotting with anti-ERα, anti-His6, and anti-GFP, respectively. GFP was used as a control for transfection efficiency and SDS-PAGE loading. B, Expression of the ubiquitin mutant UbK0 blocks CHIP-induced ERα down-regulation. HeLa cells were transfected with 250 ng pSG5-ERα, with or without 250 ng pcDNA-His6-CHIP, pcDNA-Ub, or pCS2-UbK0, as indicated. ERα protein levels were determined by immunoblotting with anti-ERα. GAPDH was used as a loading control for SDS-PAGE. For all experiments, 3×10^5 HeLa cells were plated in 60-mm dishes, cultured in hormone-free medium for 3 d, and then transfected with LipofectAMINE Plus Reagent. Cell lysates were prepared 24 h after transfection. The band density of exposed films was evaluated with ImageJ software. Relative ERα levels were presented as the mean ± SE of three independent experiments, each performed in duplicate.

induced ERα down-regulation (Fig. 2A) but had no effect on protein levels of CHIP and GFP excluding the possibility that OHT treatment affects protein degradation in general. These results demonstrate that CHIP induces degradation of correctly folded, ligand-binding competent ERα.

Both the TPR and U-Box Domains Are Essential for CHIP-Induced ERα Down-Regulation

To examine whether the ubiquitin ligase activity and chaperone interaction domain are required for CHIP-induced ERα degradation, two mutant CHIP constructs were used: 1) CHIP(K30A), a TPR domain mutant unable to interact with Hsp/Hsc70 or Hsp90; and 2) CHIP(H260Q), a U-box domain mutant unable to catalyze protein ubiquitin conjugation (36). In contrast to wild-type CHIP, neither CHIP(K30A) nor CHIP(H260Q) overexpression decreased ERα protein levels (Fig. 3A). These results establish that both the chaperone interaction and ubiquitin ligase activity of CHIP are required for CHIP-targeted degradation of ERα protein.

The TPR Domain of CHIP Is Required for the CHIP-ERα Interaction

As CHIP appears to be linked to ERα degradation, we investigated whether CHIP associates with the receptor. HeLa cells were cotransfected with ERα and CHIP, and coimmunoprecipitation analysis performed using an ERα-specific antibody. The results revealed a complex containing both CHIP and ERα (Fig. 3B). Because CHIP(K30A) exhibited no effect on ERα turnover (Fig. 3A), we examined whether the TPR domain is required for the CHIP-ERα interaction. In HeLa cells cotransfected with ERα and CHIP(K30A), the CHIP mutant was not detected in the precipitated ERα complex (Fig. 3B), demonstrating a requirement for the TPR domain in the CHIP-ERα interaction. Because it is known that CHIP interacts with Hsp90 or Hsc/Hsp70 through the TPR domain (30), our results suggest that a chaperone intermediate is involved in CHIP-induced ERα degradation.

CHIP Interacts with Endogenous ERα, in Breast Cancer Cells, to Induce Receptor Ubiquitination and Degradation

Having demonstrated a role for CHIP (possibly in association with chaperones) in degradation of exogenous ERα in HeLa cells, it was of interest to examine the effect of CHIP on stability and function of endogenous ERα in breast cancer cells. In human breast cancer MCF7 cells, overexpression of CHIP resulted in a dose-dependent ERα down-regulation (Fig. 4A). Coimmunoprecipitation analysis of MCF7 cells transfected with pcDNA-His6-CHIP revealed both CHIP and ERα in the immunocomplexes precipitated by either an ERα-specific or anti-His6 antibody (Fig. 4B), suggesting that CHIP associates with endogenous

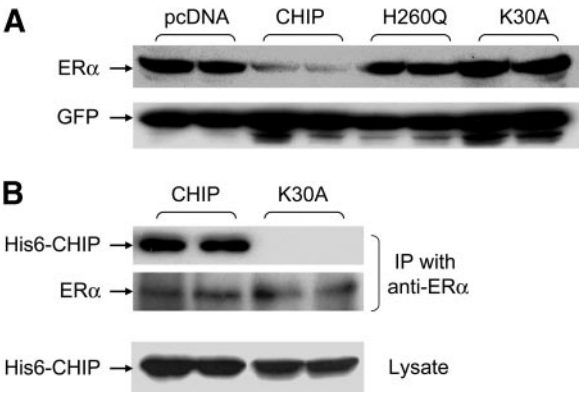

Fig. 3. Both the TPR and U-Box Domains Are Required for CHIP-Induced ERα Down-Regulation

A, Both the TRP and U-box domains are required for CHIP to down-regulate ERα. HeLa cells were transfected with 250 ng pSG5-ERα, 100 ng CMV-GFP, along with 250 pcDNA (control) or various CHIP constructs, as indicated. ERα and GFP protein levels were determined by immunoblotting with anti-ERα and anti-GFP, respectively. GFP was used as control for transfection efficiency and SDS-PAGE loading. B, The TRP domain is required for CHIP-ERα interaction. HeLa cells were transfected with 250 ng pSG5-ERα, along with 250 ng pcDNA-His6-CHIP or pcDNA-His6-CHIP(K30A). ERα protein in cell lysates was precipitated with anti-ERα. The presence of CHIP in the precipitated ERα complex was determined by immunoblotting with anti-His6. The same blot was reprobed with anti-ERα to assess the amount of ERα in the precipitated immunocomplex. The expression levels of CHIP or CHIP(K30A) in whole cell lysates was determined by immunoblotting with anti-His6 (*lower panel*). For all experiments, HeLa cells were plated in 60-mm dishes at a density of 3×10^5 cells/dish, cultured in hormone-free medium for 3 d, and then transfected with LipofectAMINE Plus Reagent. Cell lysates were prepared 24 h after transfection. Representative results of two independent experiments, each performed in duplicate, are shown. IP, Immunoprecipitation.

ERα. In addition, both Hsc70 and Hsp90 were detected in the precipitated ERα complex (Fig. 4B). These results indicate that CHIP can associate with endogenous ERα-Hsp90/Hsc70 complexes to down-regulate ERα level in breast cancer cells.

To determine whether CHIP promotes polyubiquitination of endogenous ERα, we examined the ubiquitination status of ERα in MCF7 cells transfected with hemagglutinin-tagged ubiquitin (HA-Ub), plus a vector control (pcDNA) or a CHIP-expressing construct. To block proteasomal degradation of polyubiquitinated proteins, transfected cells were treated with MG132 for 6 h before lysate preparation. An ERα-specific antibody was then used for immunoprecipitation, and the presence of ubiquitinated ERα in the immunocomplex was detected by immunoblotting with an HA antibody. To assess overall levels of protein ubiquitination, whole cell lysates were immunoblotted using an HA antibody. The polyubiquitinated ERα exhibited a typical high-molecular-weight smear on the blot membrane, and overexpression of CHIP markedly increased smear intensity, suggesting elevated receptor

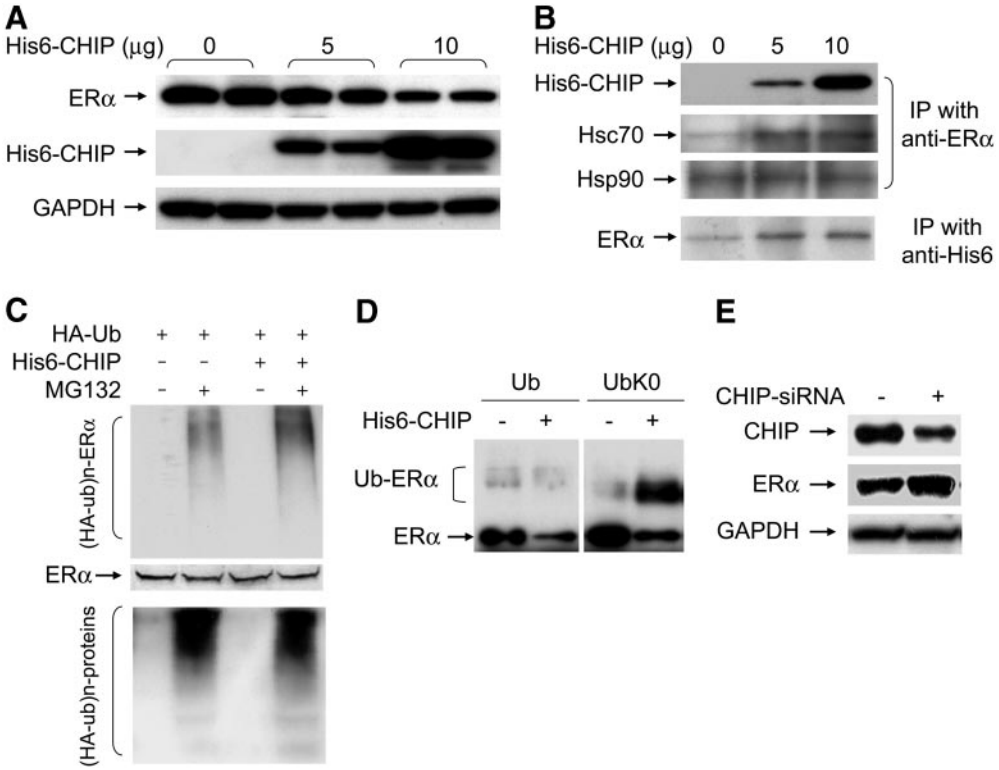

Fig. 4. CHIP Interacts with Endogenous ERα and Induces ERα Ubiquitination and Degradation in Breast Cancer MCF7 Cells

A, Overexpression of CHIP down-regulates endogenous ERα levels in MCF7 cells. MCF7 cells were plated in 100-mm dishes at a density of 1×10^6 cells/dish, cultured in hormone-free medium for 3 d, and transfected with various amounts (0, 5, or 10 μg) of pcDNA-His6-CHIP using FuGENE. Twenty-four hours after transfection, whole cell lysates were prepared, and protein levels of ERα and CHIP determined by immunoblotting with anti-ERα and anti-His6, respectively. GAPDH was used as an SDS-PAGE loading control. B, CHIP associates with ERα-Hsp complex in MCF7 cells. MCF7 cells were transfected as in panel A and subjected to coimmunoprecipitation analysis. ERα and CHIP were precipitated with anti-ERα and anti-His6, respectively. The presence of CHIP, Hsc70, Hsp90, or ERα in the precipitated complexes was determined by immunoblotting with anti-His6, anti-Hsc70, anti-Hsp90, or anti-ERα, respectively. C, Expression of CHIP enhances endogenous ERα polyubiquitination in MCF7 cells. MCF7 cells were plated in 60-mm dishes at a density of 5×10^5 cells/dish cultured in hormone-free medium for 3 d, and transfected with 250 ng pcDNA-HA-Ub and 250 ng pcDNA or pcDNA-His6-CHIP. Twenty-four hours after transfection, whole cell lysates were prepared and ERα protein was precipitated with anti-ERα. The presence of ubiquitin-conjugated ERα in the immunocomplex was detected by immunoblotting with anti-HA (*upper panel*). The same membrane was reprobed with anti-ERα to assess the amount of precipitated ERα (*middle panel*). Whole cell lysates were separated by SDS-PAGE and probed with HA antibody to determine the amount of total ubiquitinated proteins (*lower panel*). D, CHIP increases ERα ubiquitination in MCF7 cells expressing UbK0. MCF7 cells were plated as in panel C and transfected with 500 ng pcDNA-HA-Ub or 500 ng pCS2-UbK0, along with 250 ng pcDNA or pcDNA-His6-CHIP, as indicated. Twenty-four hours after transfection, whole cell lysates were prepared and ERα protein was detected by immunoblotting with anti-ERα. E, Knockdown of endogenous CHIP increases ERα level. MCF7 cells were plated as in panel C and transfected with 2 μg vector or pBS/U6/CHIPi using FuGENE. Forty-eight hours after transfection, whole cell lysates were prepared, and protein levels of CHIP and ERα were determined by immunoblotting with anti-CHIP and anti-ERα, respectively. GAPDH was used as an SDS-PAGE loading control. For all experiments, representative results of two independent experiments, each performed in duplicate, are shown. IP, Immunoprecipitation.

polyubiquitination (Fig. 4C, *upper panel*). In contrast, CHIP had no effect on overall protein ubiquitination (Fig. 4C, *lower panel*).

A possible limitation of *in vivo* ubiquitination assays is that the immunocomplex may contain multiple polyubquitinated species, not just the target protein of interest. To corroborate the observation that CHIP promotes ERα ubiquitination, we examined the effect of CHIP on ERα-ubiquitination in MCF7 cells transfected with UbK0. This mutant ubiquitin competes with endogenous ubiquitin and terminates ubiquitin chains, resulting in the accumulation of oligoubiquitin-ERα conjugates, which upon immunoblotting with ERα antibody can be detected as mobility-shifted bands. In MCF7 cells transfected with wild-type ubiquitin, overexpression of CHIP had no effect on the intensity of ERα-ubiquitination (Fig. 4D, *left panel*), presumably due to the rapid degradation of polyubiquitinated ERα. However, in cells transfected with UbK0, overexpression of CHIP remarkably increased the amount of oligoubiquitinated ERα (Fig. 4D, *right panel*), confirming that overexpression of CHIP promotes ERα ubiquiti-

nation. Together, these results suggest that CHIP, by facilitating receptor ubiquitination, targets endogenous ERα for proteasome-mediated degradation.

Knockdown of Endogenous CHIP by siRNA Increases ERα Level in MCF7 Cells

The above experiments showed that overexpression of CHIP promotes ERα polyubiquitination and degradation in breast cancer cells. Conversely, we wanted to examine whether knockdown of endogenous CHIP protein by CHIP-siRNA could increase endogenous ERα level. Transfection of MCF7 cells with pBS/U6/CHIPi decreased the level of endogenous CHIP by 60% (Fig. 4E, *upper panel*) and increased the level of ERα level by 1.5-fold (Fig. 4E, *lower panel*), indicating that endogenous CHIP plays a role in basal turnover of ERα in breast cancer cells.

CHIP Down-Regulates ERα-Mediated Gene Expression

Having established a role for CHIP in ERα ubiquitination and receptor turnover, we next examined the effect of CHIP on ERα-mediated gene transactivation. HeLa cells were transiently transfected with ERα and an estrogen-responsive reporter (ERE-pS2-Luc), plus various CHIP (CHIP, H260Q, K30A, CHIP-siRNA) or control (pcDNA) constructs. Twenty-four hours after transfection, cells were treated for 6 h with vehicle [dimethylsulfoxide (DMSO)] or E2 (10 nM) and luciferase activity then measured. In a parallel experiment, a constitutive reporter [simian virus 40 promoter-firefly luciferase (SV40-Luc)] was used to monitor transcription efficiency, as well as any general effects of the various CHIP constructs might have on luciferase expression. The ERE-pS2-Luc activities were then normalized to the corresponding SV40-Luc activities. Expression of wild-type CHIP decreased ($P < 0.05$) E2-induced ERE-pS2-Luc expression, whereas the CHIP mutants had no effect on ERα-mediated gene transactivation (Fig. 5A). Conversely, depletion of endogenous CHIP by siRNA increased both basal and E2-induced ERE-pS2-Luc expression ($P < 0.05$, Fig. 5B). Similarly, in MCF7 cells, overexpression of CHIP, but not U-box or TPR mutant, attenuated ERα-mediated reporter gene expression (Fig. 6A), whereas knockdown of endogenous CHIP by siRNA augmented ERα-mediated reporter gene expression (Fig. 6B). To examine the effect of knocking down CHIP on the expression of an endogenous ERα target gene, MCF7 cells were transfected with CHIP-siRNA, and *pS2* mRNA levels were examined. As shown in Fig. 6C, both basal and E2-induced expression of *pS2* mRNA were significantly increased. Together, these results demonstrate that CHIP coordinately regulates ERα protein levels and ERα-mediated gene transactivation.

GA Induces ERα Degradation through a CHIP-Dependent Mechanism

The Hsp90 inhibitor, GA, binds to the amino-terminal ATP/ADP-binding domain of Hsp90, locking this chaperone protein in its ADP-bound conformation (9, 29, 37). CHIP has been reported to play a role in GA-induced degradation of ErbB2, a Hsp90 client protein (36, 38), and recent studies have shown that GA stimulates ERα degradation through the ubiquitin-proteasome pathway (9, 29, 37). Whether CHIP plays a role in GA-induced ERα degradation has not been previously investigated. Thus, we examined the effects of CHIP overexpression and depletion on GA-induced ERα degradation. In HeLa cells transfected with ERα, GA treatment resulted in a time-dependent ERα down-regulation (Fig. 7A); this effect was enhanced by CHIP overexpression (Fig. 7A). Conversely, CHIP depletion by siRNA completely abolished GA-induced ERα down-regulation (Fig. 7A).

To investigate the effect of GA on the CHIP-ERα interaction, HeLa cells were transfected with ERα and

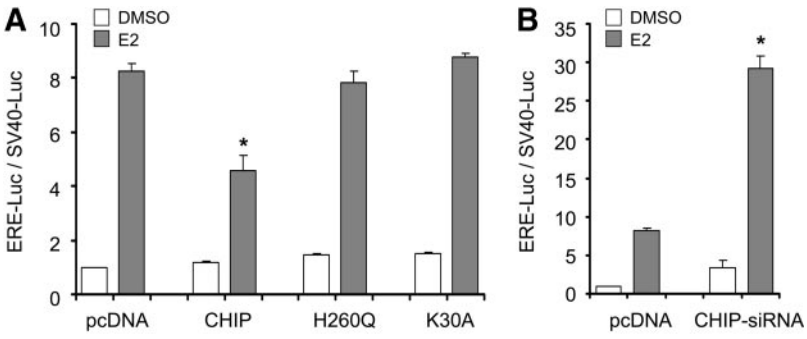

Fig. 5. CHIP Down-Regulates ERα-Mediated Reporter Gene Expression in HeLa Cells

HeLa cells were plated in 12-well dishes at a density of 1×10^5/well, grown in hormone-free medium for 3 d, and transfected with 10 ng pSG5-ERα, 250 ng ERE-pS2-Luc, 250 ng various CHIP constructs (A) or pBS/U6/CHIPi (B). Twenty-four hours after transfection, cells were treated for 6 h with DMSO or 10 nM E2 and then assayed for luciferase activity. The ERE-pS2-Luc activity was normalized to SV40-Luc activity, which was determined in a parallel experiment where ERE-pS2-Luc was replaced with SV40-Luc. The results are expressed as means ± SE from three independent experiments, with each performed in quadruplicate. *, $P < 0.05$ (Student's *t* test, *vs.* pcDNA treated with E2).

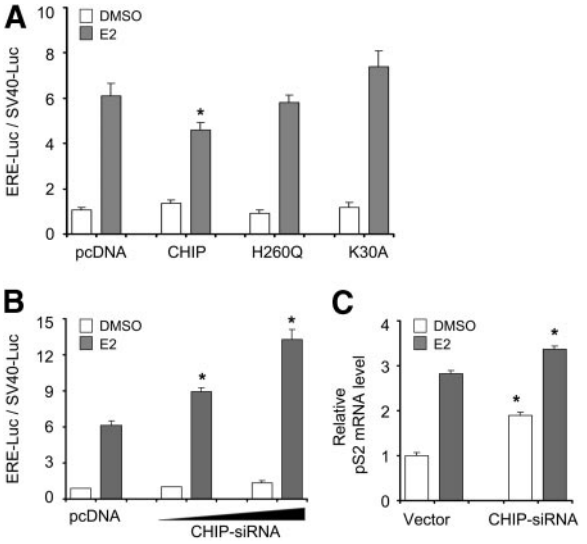

Fig. 6. CHIP Down-Regulates ERα-Mediated Gene Expression in MCF7 Cells

A, Overexpression of CHIP Inhibits ERα-Mediated Reporter Gene Expression. MCF7 cells were plated in 12-well dishes at a density of 1×10^5/well, grown in hormone-free medium for 3 d, and transfected with 250 ng ERE-pS2-Luc, along with 250 ng various CHIP constructs. Twenty-four hours after transfection, cells were treated with DMSO or 10 nM E2 for 6 h and then assayed for luciferase. The ERE-pS2-Luc activity was normalized to SV40-Luc activity (determined in a parallel experiment where ERE-pS2-Luc was replaced with SV40-Luc). Results are expressed as the mean ± SE from three independent experiments, each performed in quadruplicate. *, $P < 0.05$ (Student's *t* test, *vs.* pcDNA treated with E2). B, Knockdown of CHIP by siRNA increases ERα-mediated reporter gene expression. MCF7 cells were plated as in panel A and transfected with 250 ng ERE-pS2-Luc and various amounts (0, 250, and 500 ng) of pBS/U6/CHIPi. Twenty-four hours after transfection, cells were treated and subjected to luciferase analysis, as in panel A. C, Knockdown of CHIP by siRNA increases expression of pS2 mRNA. MCF7 cells were plated in 100 mm dishes at a density of 1×10^6/dish, grown in hormone-free medium for 3 d, and transfected with 5 μg vector or pBS/U6/CHIPi using FuGENE. Forty-eight hours after transfection, cells were treated for 6 h with DMSO or 10 nM E2. The mRNA level of pS2 was determined by real-time quantitative PCR. The relative pS2 mRNA levels were normalized with β-actin mRNA and expressed as mean ± SE from three independent experiments, each performed in duplicate. *, $P < 0.05$ (Student's *t* test, CHIP-siRNA *vs.* pcDNA).

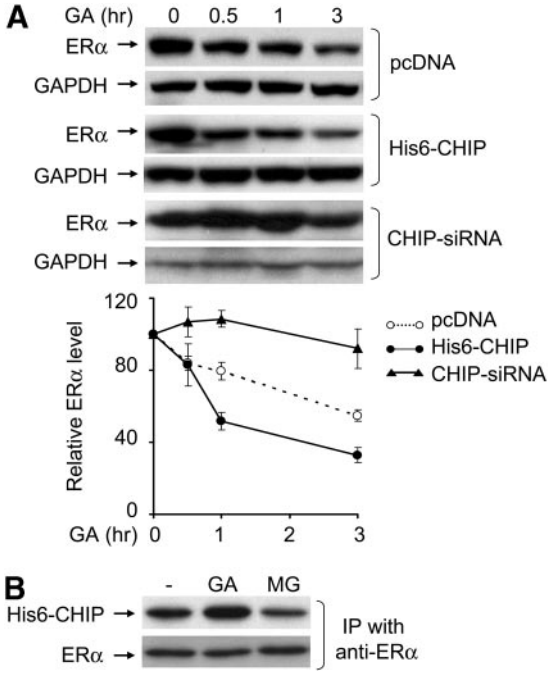

Fig. 7. Disruption of Hsp90 Function Induces ERα Degradation through a CHIP-Dependent Mechanism in HeLa Cells

A, CHIP overexpression augments and CHIP depletion by siRNA blocks GA-induced ERα degradation. HeLa cells were plated in 60-mm dishes at a density of 3×10^5 cells/dish, cultured in hormone-free medium for 3 d, and transfected with 250 ng pSG5-ERα, along with 250 ng pcDNA, pcDNA-His6-CHIP or pBS/U6/CHIPi by using LipofectAMINE Plus Reagent. Twenty-four hours after transfection, the cells were treated with 1 μM GA for 0, 0.5, 1, and 3 h. Cell lysates were immunoblotted with anti-ERα. GAPDH was used as an SDS-PAGE loading control. The band density of exposed films was evaluated with ImageJ software. Relative ERα levels were presented as mean ± SE from three independent experiments. B, GA enhances CHIP-ERα interaction. HeLa cells were plated as in panel A and transfected with 250 ng pSG5-ERα and 250 ng pcDNA-His6-CHIP. Twenty-four hours after transfection, cells were untreated or treated with 1 μM GA or 10 mM MG132 for 1 h before lysate preparation. ERα protein was precipitated by anti-ERα and the presence of CHIP determined by immunoblotting with anti-His6. The same membrane was then reprobed with anti-ERα to assess the amount of precipitated ERα in the same complex. Representative results of three independent experiments, each performed in duplicate, are shown. IP, Immunoprecipitation.

CHIP, and coimmunoprecipitation was performed with an ERα-specific antibody. The amount of CHIP in the precipitated ERα complex increased after a 1-h GA treatment (Fig. 7B), suggesting that GA promotes ERα degradation by recruiting CHIP to the chaperone-ERα complex. Because CHIP can associate with ubiquitinated proteins through its U-box domain (31), ERα ubiquitination may play a role in the GA-induced ERα-CHIP interaction. We thus examined the interaction between ERα and CHIP in the presence of the proteasome inhibitor MG132. We reasoned that if CHIP preferentially interacts with ubiquitinated ERα, then MG132, by enhancing the accumulation of polyubiquitinated ERα, would increase the ERα-CHIP interaction. However, MG132 treatment did not increase the amount of CHIP precipitated with the ERα complex (Fig. 7B), suggesting that the GA-induced ERα-CHIP interaction occurs before ERα polyubiquitination.

To establish a role for CHIP in GA-induced ERα degradation under physiologically relevant conditions, the consequence of knocking down endogenous CHIP by siRNA on ERα degradation was examined in MCF7 cells. GA induced rapid ERα down-regulation in MCF7

cells transfected with a pcDNA control plasmid (Fig. 8A), consistent with previous reports (9, 29). However, expression of CHIP-siRNA significantly impaired GA-induced ERα down-regulation (Fig. 8A). In addition, we performed a coimmunoprecipitation analysis to examine the effect of GA treatment on the association between endogenous CHIP and ERα. As shown in Fig. 8B, GA treatment increased the amount of CHIP that coimmunoprecipitated with ERα. Based on these results, we suggest that GA induces ERα degradation by enhancing the recruitment of CHIP to ERα-chaperone complexes.

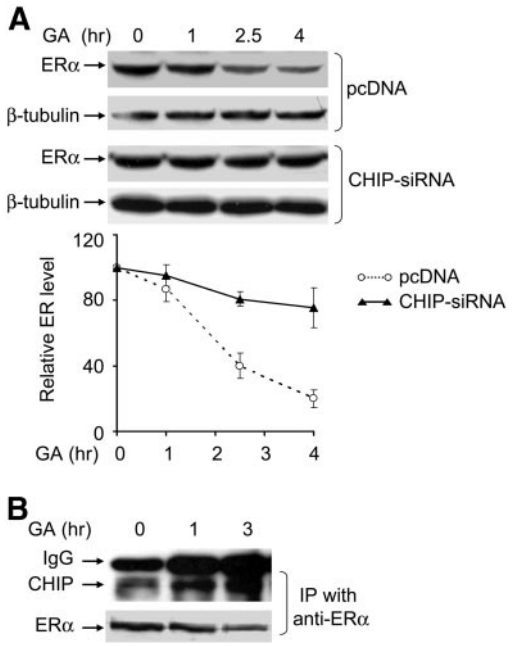

Fig. 8. CHIP Is Required for GA-Induced ERα Degradation in Breast Cancer MCF7 Cells

A, CHIP depletion by CHIP-siRNA eliminates GA-induced ERα degradation. MCF7 cells were plated in 60-mm dishes at a density of 3×10^5 cells/dish, cultured in hormone-free medium for 3 d, and transfected with 500 ng pcDNA (control) or pBS/U6/CHIPi. Twenty-four hours after transfection, cells were treated with 1 μM GA for 0, 1, 2.5, and 4 h, and subjected to immunoblotting with anti-ERα. β-Tubulin was used as SDS-PAGE loading control. The band density of exposed films was evaluated with ImageJ software. Relative ERα levels are presented as mean ± SE from three independent experiments (*lower panel*). B, GA stimulates CHIP-ERα interaction. MCF7 cells were plated at 1×10^6 cells in 100-mm dishes, cultured in hormone-free medium for 3 d, and treated with 1 μM GA for 0, 1, and 3 h before lysate preparation. ERα protein was precipitated by anti-ERα and the presence of CHIP examined by immunoblotting with anti-CHIP. The same membrane was then reprobed with ERα antibody to assess the amount of precipitated ERα in the same complex. Representative results of two independent experiments, each performed in duplicate, are shown. IP, Immunoprecipitation.

Effects of Ligand Binding on GA-Induced ERα Degradation

Ligand binding results in disassembly of the ERα-Hsp90 chaperone complex, due to competition for overlapping binding sites and conformational changes within the ERα protein (28). Because GA stimulated the CHIP-ERα interaction (Figs. 7B and 8B), we investigated whether ligand binding, by interrupting the CHIP-ERα interaction, could interfere with GA-induced ERα degradation. Toward this, ERα protein levels were examined in MCF7 cells: 1) exposed to E2, ICI or GA alone; 2) pretreated with vehicle, E2, OHT, or ICI for 30 min, followed by a 6-h treatment with GA; and 3) pretreated with vehicle or GA for 30 min, followed by a 5.5-h treatment with E2, OHT, or ICI. As expected, E2, ICI and GA treatment, but not OHT, dramatically down-regulated ERα levels in MCF7 cells (Fig. 9A, *upper panel*). Exposure to E2 or OHT, either before (Fig. 9A, *middle panel*) or shortly after (Fig. 9A, *lower panel*) GA treatment, completely abolished GA-induced ERα degradation. In contrast to what was observed with E2 and OHT, ICI exposure, neither before (Fig. 9A, *middle panel*) nor shortly after (Fig. 9A, *lower panel*) GA treatment, failed to protect ERα against degradation.

To examine the effect of these ligands on the CHIP-ERα interaction, coimmunoprecipitation analysis was performed on MCF7 cells transfected with CHIP. Cells were pretreated with GA for 30 min, followed by a 30-min treatment with E2, OHT, or ICI. GA treatment alone increased the amount of CHIP detected in the precipitated ERα complex; however, this amount was substantially reduced by treatment with E2, OHT, or ICI (Fig. 9B). These results demonstrate that all three ligands can interfere with the interaction between CHIP and ERα. Because these ligands have dramatically different effects on ERα stability, our results indicate that after dissociation from the Hsp90 chaperone complex, distinct downstream pathways exist for ERα degradation. Because E2 alone can induce ERα degradation through a transcription coupled mechanism (17, 19, 22, 24), it was somewhat unexpected to observe that ERα was stable during the combined treatment of GA and E2 (Fig. 9A). One explanation is that Hsp90 activity (inhibited by GA) is required for transcription-coupled ERα degradation. The OHT-ERα complex lacks transcriptional activity in MCF7 cells and thus is not a substrate for the transcription-coupled degradation pathway. Consequently, the ability of OHT to block GA-induced ERα degradation is likely due to disruption of the CHIP-ERα interaction (Fig. 9B). ICI also interrupts the GA-induced CHIP-ERα interaction (Fig. 9B) but fails to stabilize ERα (Fig. 9A), suggesting that the ERα-ICI complex is targeted for degradation through a CHIP-independent, GA-insensitive pathway.

Effect of CHIP and GA on ER α Cellular Localization

CHIP and Hsp90 are located primarily in the cytoplasm (30), whereas ERα is primarily a nuclear-localized pro-

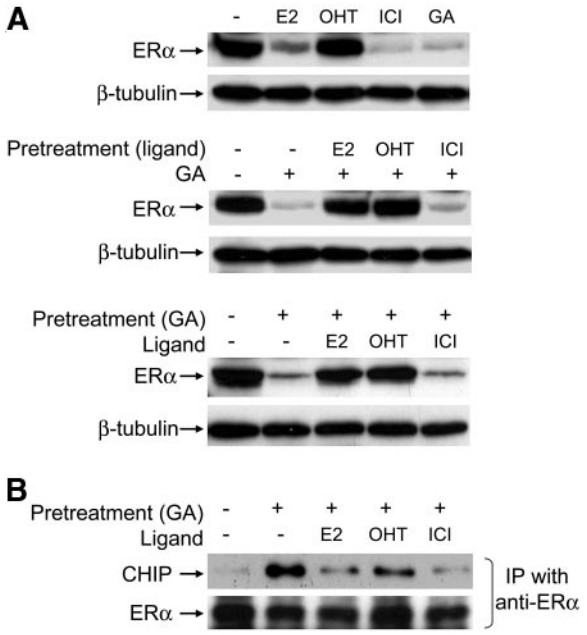

Fig. 9. Effect of Ligand Binding on Geldanamycin-Induced ERα Degradation

A, ERα protein levels in MCF7 cells treated with GA before or after ligand exposure. MCF7 cells were plated in 60-mm dishes at a density of 3×10^5 cells/dish and cultured in hormone-free medium for 3 d. *Upper panel*, Cells were treated with vehicle, 10 nM E2, 1 μM OHT, 100 nM ICI or 1 μM GA for 6 h; *middle panel*, cells were exposed to indicated ligand for 30 min before a 6-h GA treatment; *lower panel*, 30 min after GA treatment, cells were exposed to indicated ligand for 5.5 h. For all experiments, ERα levels were determined by immunoblotting with anti-ERα. β-Tubulin was used as SDS-PAGE loading control. B, Effect of ligands on GA-induced CHIP-ERα interaction. MCF7 cells were plated in 100-mm dishes at a density of 1×10^6 cells/dish, cultured in hormone-free medium for 3 d, and then transfected with 5 μg pcDNA-His6-CHIP by using FuGENE. Twenty-four hours after transfection, the cells were treated with 1 μM GA for 30 min, followed by a 30-min treatment with indicated ligands (100 nM E2, 1 μM OHT, and 100 nM ICI). ERα protein from the cell lysates was precipitated using anti-ERα. CHIP presence in the precipitated ERα complex was determined by immunoblotting with anti-His6. The same membrane was reprobed with ERα antibody to assess the amount of precipitated ERα. Representative results of two independent experiments, each performed in duplicate, are shown. IP, Immunoprecipitation.

tein (39). To determine whether CHIP overexpression, or GA treatment, could affect the cellular distribution of ERα, HeLa cells were transfected with a GFP-ERα fusion protein (40) and the cellular distribution of green fluorescence was examined. In control cells, fluorescence was restricted to the nuclei (Fig. 10A, *top left panel*). CHIP coexpression or GA treatment did not affect the nuclear localization of GFP-ERα (Fig. 10A). In contrast, ICI treatment, either alone or in the presence of transfected CHIP, resulted in the appearance of green fluorescence in the cytoplasm (Fig. 10A, *bottom two panels*). This observation is consistent with a previous study by Dauvois *et al.* (7) showing that ICI induces cytoplasmic retention of ERα. In addition, in HeLa cells transfected with GFP-ERα only, treatment with GA resulted in the appearance of GFP foci in the nuclei of approximately 20% of transfected cells (Fig. 10A, *left middle panel*). These GFP foci were not observed in GA-treated cells cotransfected with CHIP (Fig. 10A, *right middle panel*). Although the identity of the GFP foci is unknown, one possibility is that these represent aggregated GFP-ERα, resulting from the combined effect of Hsp90 inhibition and high expression levels of GFP-ERα. CHIP overexpression may promote both basal and GA-induced ERα degradation, preventing GFP-ERα aggregate formation. Consistent with this interpretation, we found that expression of CHIP decreased the number of GFP-ERα-expressing cells (Fig. 10B). Based on our results, and a recent finding that a small fraction of nuclear-localized CHIP can promote nuclear protein degradation (41), we suggest that CHIP-mediated ERα degradation occurs within the nucleus.

DISCUSSION

The cellular level of ERα determines both estrogen sensitivity and responsiveness (2, 35, 42). Steady-state levels of ERα protein are tightly regulated through a rapid balance between receptor synthesis and turnover, according to changing cellular conditions (4). Although it has been well documented that ERα degradation is primarily mediated by the ubiquitin proteasome pathway, the molecular mechanism(s) by which cells regulate ERα stability are largely unknown. Here we report that the Hsc70/Hsp90-interacting protein CHIP plays a key role in both basal and Hsp90 inhibitor-induced ERα turnover. Furthermore, CHIP-induced receptor degradation occurs through the ubiquitin proteasome pathway. Overexpression of CHIP promotes ERα degradation, accompanied by a decrease in ERα-mediated gene transactivation. Conversely, inhibition of CHIP by siRNA increases ERα levels and up-regulates ERα-mediated gene transactivation. Thus, this is the first report that CHIP, by modulating the cellular concentration of ERα, plays a role in regulating estrogen action.

During the preparation of this report, Tateishi and colleagues (43) reported a similar finding, that CHIP plays a role in basal ERα turnover. Our findings agree with several conclusions from that study, including: 1) CHIP, through its TPR domain, associates with ERα-chaperone complexes; 2) CHIP promotes, through its TPR and U-box domains, both polyubiquitination and proteasomal degradation of unliganded ERα; 3) CHIP-mediated ERα degradation occurs in the nucleus; and 4) ligand binding blocks CHIP-mediated ERα degradation by disrupting CHIP-ERα interaction. Here, we further extend the study of Tateishi *et al.* (43) in two significant aspects: 1) CHIP is required for Hsp90 in-

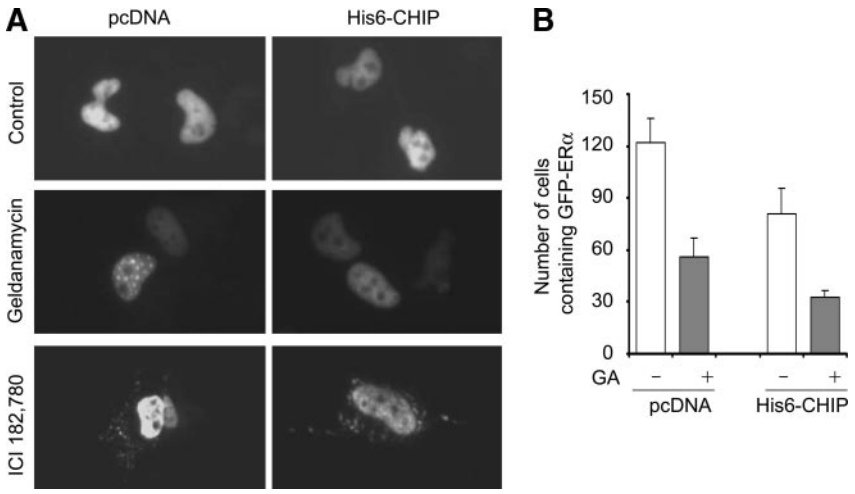

Fig. 10. Effect of CHIP and GA on ERα Cellular Localization

HeLa cells were plated in six-well dishes at a density of 1×10^5 cells/dish, cultured in hormone-free medium for 3 d, and transfected with 250 ng GFP-ERα and 250 ng pcDNA or pcDNA-His6-CHIP by using LipofectAMINE Plus Reagent. Twenty-four hours after transfection, the transfected cells were treated with 1 μM GA or 100 nM ICI for 6 h. The fluorescence of GFP-ERα was then examined using an inverted microscope (Axiovert 40 CFL) (A). The number of cells expressing GFP-ERα from 10 microscope fields is shown in the histogram (B). Representative results of two independent experiments, each performed in triplicate, are shown. *Open bar*, Vehicle-treated controls; *gray bar*, GA treatment (1 μM, 6 h).

hibitor-induced ERα degradation; and 2) CHIP targets functional ERα (correctly folded, ligand-binding competent receptor protein) for degradation.

Several lines of evidence from our study support the conclusion that CHIP targets functional ERα for degradation. First, OHT treatment completely blocked CHIP-induced ERα degradation, suggesting that ERα reaches a correctly folded conformation, competent for ligand binding, before CHIP-directed degradation. Secondly, CHIP overexpression down-regulated ERα levels and decreased ERα-mediated gene expression, whereas CHIP depletion by siRNA up-regulated ERα levels and increased ERα-mediated gene transcription. This coordinate regulation of ERα levels and activity suggests that CHIP targets functional ERα for degradation. Thirdly, CHIP plays a role in GA-induced ERα degradation by primarily targeting Hsp90-associated, transcriptionally competent ERα (29). Although originally believed to function as a general ubiquitin ligase, responsible for ubiquitinating unfolded or misfolded proteins in a chaperone-dependent process (31), more recent studies have demonstrated that CHIP also targets mature Hsp90 client proteins for degradation (33, 36).

Tateishi *et al.* (43) observed that CHIP overexpression increased ERα transcriptional activity. Although this was not observed in our study, the use of different estrogen response element (ERE) and control reporter constructs for the functional analyses of ERα could account for this discrepancy. In the present study, an estrogen-responsive reporter construct (ERE-pS2-Luc), possessing two ERE copies within the pS2 promoter (44), was used. Our previous study demonstrated a close correlation between ERE-pS2-Luc expression and cellular concentration of ERα (35). In the present study, we also used a constitutively active construct, SV40-Luc, to monitor and normalize the effects of both CHIP and CHIP-siRNA on transfection efficiency and luciferase expression. In the study by Tateishi *et al.* (43), pRSVβGal was used as an internal control. When we used a similar construct, CMVβGal, we found that overexpression of either wild-type CHIP or TPR mutant (K30A), but not U-box mutant (H260Q), dramatically decreased CMVβGal expression in a dose-dependent manner (data not shown). Based on these observations, we suggest that βGal is not a suitable control reporter for studying the effect of CHIP on gene transcription.

Our results, with data from Tateishi *et al.* (43), suggest a role for the Hsp90 chaperone complex in the regulation of cellular ERα levels. A summary of distinct ERα degradation pathways is depicted in Fig. 11. Nascent ERα is translocated into nucleus, and by associating with Hsp90, receptor protein is maintained in a ligand-binding competent conformation, ready for subsequent activation (28). In the absence of ligand or other activation signals, CHIP constantly targets chaperone-associated ERα for degradation, thereby limiting cellular concentrations of receptor protein. Ligand binding disassembles the ERα-Hsp90 complex and thus protects ERα from CHIP-mediated degradation. However, depending on the ligand, ERα stability can vary considerably, suggesting that different downstream destructive pathways exist. Furthermore, the ERα-ligand interaction could play a definitive role in pathway use. For example, when activated by E2, ERα is degraded through a transcription-coupled mechanism (17, 19, 22, 24). Pretreatment with GA, however, abolished E2-induced ERα degradation (Fig. 9A), suggesting that Hsp90 activity is required for transcrip-

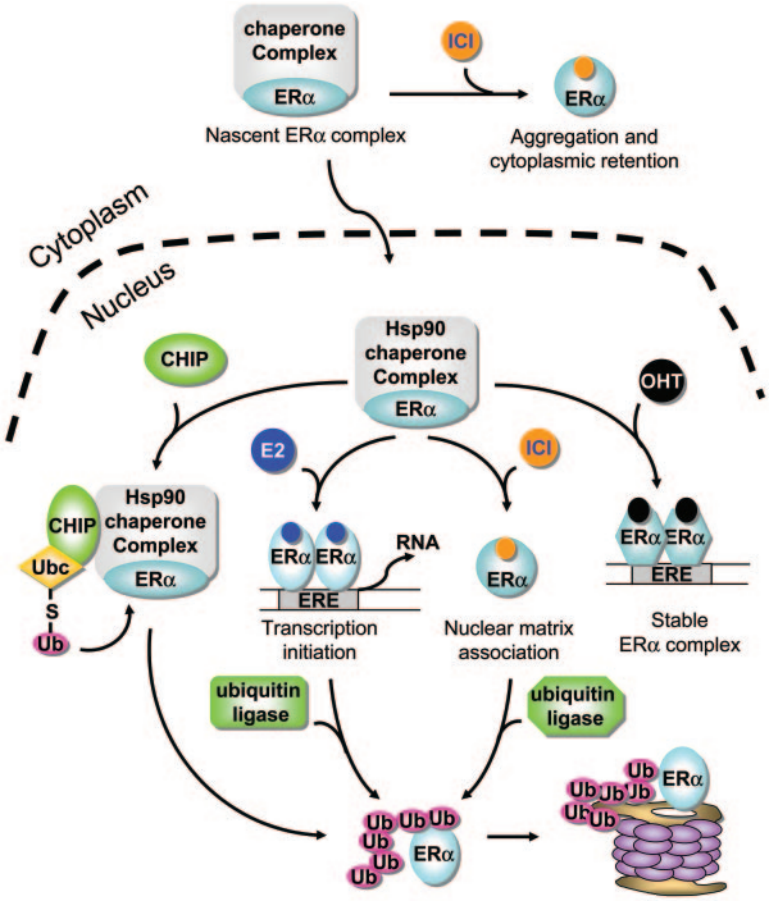

Fig. 11. Schematic Summary of Distinct ERα Degradation Pathways

Nascent ERα is translocated into nucleus. There, by associating with Hsp90, the receptor is maintained in a ligand-binding competent conformation, ready for subsequent activation. In the absence of ligand or other activation signals, CHIP constantly targets Hsp90-associated ERα for degradation. Ligand binding disassembles the ERα-Hsp90 complex and thus protects ERα from CHIP-mediated degradation. However, depending upon the ligand, distinct downstream destructive pathways are engaged in the degradation of liganded ERα. When activated by E2, ERα is degraded through a transcription-coupled mechanism. In response to ICI, nuclear ERα-ICI complex is immobilized to the nuclear matrix and undergoes rapid proteasomal degradation. In addition, ICI induces cytoplasmic retention and aggregation of nascent ERα OHT-ERα complexes are stable, likely due to the lack of transcriptional activity.

tion-coupled ERα degradation. In support of this possibility, the Hsp90-p23 complex has been shown to play a role in disassembling the nuclear receptor transcriptional complex from chromatin, a process believed to be a prerequisite for degradation of activated transcription factors (45–47). Conversely, through an unknown mechanism, the nuclear ERα-ICI complex is immobilized to the nuclear matrix and undergoes rapid degradation, in association with cytoplasmic retention of aggregated nascent ERα (7, 8, 22, 27, 40, 48). Although it is not clear how intracellular localization influences receptor degradation, the unique distribution pattern of ERα after treatment with ICI-182,780, together with the fact that ICI-induced receptor degradation is independent of ERα transcription activity, support the possibility that the pure antiestrogen and E2 use distinct degradation pathways for ERα. Taken together with our previous observation that an intact NEDD8 conjugation pathway is essential for ICI-induced ERα degradation in breast cancer cells (49), we suggest that destruction of the ICI-liganded receptor requires a cullin-based ubiquitin ligase.

Abnormal expression of ERα has long been associated with both the initiation and progression of breast cancer (50). An increase in the number of ERα-positive cells, as well as increased individual cell ERα content, have frequently been detected in malignant breast tumors (42). Furthermore, increased ERα content has been shown to augment the magnitude of estrogen-stimulated gene expression, providing a growth advantage to breast cancer cells (2, 35, 49, 51). A recent study demonstrated a correlation between the loss of ERK7, a regulator of estrogen-induced ERα degradation, and breast cancer progression (52). Collectively, these observations indicate that alterations in ERα degradation pathways may contribute to deregulation of ERα, perhaps leading to enhanced estrogen action in breast tumors. Based on our results, the chaperone/

CHIP pathway, by regulating ERα levels, likely contributes to the development/progression of that disease; and such a possible role merits further examination.

MATERIALS AND METHODS

Materials

The following antibodies and reagents were used in this study: anti-ERα (HC20) and anti-β-tubulin (SC9104) (Santa Cruz Biotechnology, Santa Cruz, CA); anti-HA tag (3F10; Roche Molecular Biochemicals, Indianapolis, IN); anti-ERα (Ab-10) and anti-GFP (GFP01) (NeoMarkers, Inc., Fremont, CA); anti-GAPDH (glyceraldehyde-3-phosphate dehydrogenase) (Chemicon International, Inc., Temecula, CA); anti-CHIP (PA1-015, Affinity Bioreagents, Golden, CO); anti-Hsp90 (SPA-830) and anti-Hsc70 (SPA-816) (Stressgene, Victoria, British Columbia, Canada); anti-His6 (8906-1, BD Biosciences, Palo, Alto, CA); protein G-agarose beads (Oncogene Research Products, San Diego, CA); horseradish peroxidase-conjugated second antibodies and SuperSignal West Pico Chemiluminescent Substrate (Pierce, Rockford, IL); protein assay kit (Bio-Rad Laboratories Inc., Hercules, CA); protease inhibitor cocktail set III (Calbiochem-Novabiochem Corp., San Diego, CA); LipofectAMINE Plus Reagent (Life Technologies, Inc., Logan, UT); FuGENE (Roche Molecular Biochemicals, Indianapolis, IN); 17β-estradiol, OHT, GA and MG132 (Sigma Chemical Co., St. Louis, MO); ICI (Tocris Cookson Ltd., Ellisville, MO); passive lysis buffer and luciferase assay system (Promega Corp., Madison, WI); fetal bovine serum (FBS) and dextran-coated charcoal-stripped FBS (Hyclone Laboratories, Inc., Logan, UT); cell culture supplementary reagents (Life Technologies, Inc., Rockville, MD).

Plasmid Construction

The construction of pSG5-ERα(HEGO), ERE2-pS2-Luc, SV40-Luc, pcDNA-HA-Ub, pCS2-UbK0 and cytomegalovirus promoter (CMV)-GFP have all been described previously (35). The pcDNA-His6-CHIP, pcDNA-His6-CHIP(K30A), and pcDNA-CHIP(H260Q) constructs were kindly provided by Drs. Neckers and Patterson (36), the pBS/U6/CHIPi construct by Dr. Chang (33), and the GFP-ERα construct by Dr. Stenoien (40).

Cell Lines and Transient Transfection

The human cervical carcinoma cell line HeLa and the breast cancer cell line MCF-7 were purchased from ATCC (Manassas, VA). HeLa cells were maintained in MEM with 2 mM L-glutamine, 1.5 g/liter sodium bicarbonate, 0.1 mM nonessential amino acids, 1.0 mM sodium pyruvate, 50 U/ml penicillin, 50 μg/ml streptomycin, and 10% FBS. MCF7 cells were maintained in the same medium, with the addition of 6 ng/ml insulin. Before experiments, cells were cultured in hormone-free medium (phenol red-free MEM with 3% dextran-coated charcoal-stripped FBS) for 3 d. For transfection, cells (80% confluence) were transfected with an equal amount of total plasmid DNA (adjusted with the corresponding empty vectors) by using LipofectAMINE Plus Reagent or FuGENE according to the manufacturer's guidelines.

Immunoblotting, Immunoprecipitation, and Luciferase Assay

For immunoblot analysis, whole cell extracts were prepared by suspending cells ($\sim 2 \times 10^6$) in 0.1 ml SDS lysis buffer [62 mM Tris (pH 6.8), 2% SDS, 10% glycerol, and protease inhibitor cocktail III]. After 15 min incubation on ice, extracts were sonicated (3 × 20 sec), insoluble material removed by centrifugation (15 min at 12,000 × *g*), and supernatant protein concentration determined using a Bio-Rad protein assay kit. Five percent β-mercaptoethanol was added to the protein extracts before heating at 90 C for 5 min. Protein extracts (50 μg per lane) were fractionated by SDS-PAGE, transferred to polyvinylidene difluoride membranes, and probed with antibodies. Primary antibody was detected by horseradish peroxidase-conjugated second antibody and visualized using an enhanced SuperSignal West Pico Chemiluminescent Substrate. The band density of exposed films was evaluated with National Institutes of Health ImageJ software (http://rsb.info.nih.gov/ij/). Immunoprecipitation was performed as described previously (49). For luciferase assays, cell lysates were prepared with passive lysis buffer and luciferase activity determined using the Luciferase Assay System.

CHIP siRNA Construct

The pBS/U6/CHIPi construct was kindly provided by Dr. Zhijie Chang (33). The siRNA expressed by the pBS/U6/CHIPi construct starts with GGG (position 233–251 bp relative to the ATG start site in the CHIP cDNA).

Quantitative Real-Time PCR

Total RNA was prepared by a RNAeasy Mini Kit (QIAGEN, Valencia, CA), according to the manufacturer's protocol. RNA (2 μg) was reverse-transcribed in a total volume of 40 μl containing 400 U Moloney murine leukemia virus reverse transcriptase (New England Biolabs, Beverly, MA), 400 ng random hexamers (Promega), 80 U ribonuclease inhibitor and 1 mM deoxynucleotide triphosphates. The resulting cDNA was used in subsequent quantitative real-time PCRs, performed in 1× iQ SYBR Green Supermix (Bio-Rad) with 5 pmol forward and reverse primers as previously described (35).

Acknowledgments

The authors gratefully acknowledge Drs. Len Neckers (National Cancer Institute, Rockville, MD) and Cam Patterson (University of North Carolina, Chapel Hill, NC) for providing pcDNA-His6-CHIP, pcDNA-His6-CHIP(K30A) and pcDNA-CHIP(H260Q); Dr. Zhijie Chang (Tsinghua University, Beijing, China) for pBS/U6/CHIPi; Dr. Michele Pagano (New York University Cancer Institute, New York, NY) for pCS2-UbK0 and Dr. Michael A. Mancini (Baylor College of Medicine, Houston, TX) for GFP-ERα. We thank Dr. Curt Balch (Indiana University School of Medicine) for his critical review of this manuscript.

Received March 4, 2005. Accepted July 14, 2005.

Address all correspondence and requests for reprints to: Kenneth P. Nephew, Ph.D., Medical Sciences, Indiana University School of Medicine, 302 Jordan Hall, 1001 East 3rd Street, Bloomington, Indiana 47405-4401. E-mail: knephew@indiana.edu.

This work was supported by the U.S. Army Medical Research Acquisition Activity, award numbers DAMD 17-02-1-0418 and DAMD17-02-1-0419; American Cancer Society Research and Alaska Run for Woman Grant TBE-104125; and the Walther Cancer Institute.

REFERENCES

1. Barkhem T, Nilsson S, Gustafsson JA 2004 Molecular mechanisms, physiological consequences and pharma-

cological implications of estrogen receptor action. Am J Pharmacogenom 4:19–28
2. Webb P, Lopez GN, Greene GL, Baxter JD, Kushner PJ 1992 The limits of the cellular capacity to mediate an estrogen response. Mol Endocrinol 6:157–167
3. Klinge CM 2000 Estrogen receptor interaction with co-activators and co-repressors. Steroids 65:227–251
4. Reid G, Denger S, Kos M, Gannon F 2002 Human estrogen receptor-α: regulation by synthesis, modification and degradation. Cell Mol Life Sci 59:821–831
5. Eckert RL, Mullick A, Rorke EA, Katzenellenbogen BS 1984 Estrogen receptor synthesis and turnover in MCF-7 breast cancer cells measured by a density shift technique. Endocrinology 114:629–637
6. Dauvois S, Danielian PS, White R, Parker MG 1992 Antiestrogen ICI 164,384 reduces cellular estrogen receptor content by increasing its turnover. Proc Natl Acad Sci USA 89:4037–4041
7. Dauvois S, White R, Parker MG 1993 The antiestrogen ICI 182780 disrupts estrogen receptor nucleocytoplasmic shuttling. J Cell Sci 106:1377–1388
8. Devin-Leclerc J, Meng X, Delahaye F, Leclerc P, Baulieu EE, Catelli MG 1998 Interaction and dissociation by ligands of estrogen receptor and Hsp90: the antiestrogen RU 58668 induces a protein synthesis-dependent clustering of the receptor in the cytoplasm. Mol Endocrinol 12:842–854
9. Bagatell R, Khan O, Paine-Murrieta G, Taylor CW, Akinaga S, Whitesell L 2001 Destabilization of steroid receptors by heat shock protein 90-binding drugs: a ligand-independent approach to hormonal therapy of breast cancer. Clin Cancer Res 7:2076–2084
10. Stoner M, Saville B, Wormke M, Dean D, Burghardt R, Safe S 2002 Hypoxia induces proteasome-dependent degradation of estrogen receptor α in ZR-75 breast cancer cells. Mol Endocrinol 16:2231–2242
11. Wormke M, Stoner M, Saville B, Safe S 2000 Crosstalk between estrogen receptor α and the aryl hydrocarbon receptor in breast cancer cells involves unidirectional activation of proteasomes. FEBS Lett 478:109–112
12. Alarid ET, Bakopoulos N, Solodin N 1999 Proteasome-mediated proteolysis of estrogen receptor: a novel component in autologous down-regulation. Mol Endocrinol 13:1522–1534
13. Laios I, Journe F, Laurent G, Nonclercq D, Toillon RA, Seo HS, Leclercq G 2003 Mechanisms governing the accumulation of estrogen receptor α in MCF-7 breast cancer cells treated with hydroxytamoxifen and related antiestrogens. J Steroid Biochem Mol Biol 87:207–221
14. Alarid ET, Preisler-Mashek MT, Solodin NM 2003 Thyroid hormone is an inhibitor of estrogen-induced degradation of estrogen receptor-α protein: estrogen-dependent proteolysis is not essential for receptor transactivation function in the pituitary. Endocrinology 144:3469–3476
15. Tsai HW, Katzenellenbogen JA, Katzenellenbogen BS, Shupnik MA 2004 Protein kinase A activation of estrogen receptor α transcription does not require proteasome activity and protects the receptor from ligand-mediated degradation. Endocrinology 145:2730–2738
16. El Khissiin A, Leclercq G 1999 Implication of proteasome in estrogen receptor degradation. FEBS Lett 448: 160–166
17. Lonard DM, Nawaz Z, Smith CL, O'Malley BW 2000 The 26S proteasome is required for estrogen receptor-α and coactivator turnover and for efficient estrogen receptor-α transactivation. Mol Cell 5:939–948
18. Nawaz Z, Lonard DM, Dennis AP, Smith CL, O'Malley BW 1999 Proteasome-dependent degradation of the human estrogen receptor. Proc Natl Acad Sci USA 96: 1858–1862
19. Wijayaratne AL, McDonnell DP 2001 The human estrogen receptor-α is a ubiquitinated protein whose stability is affected differentially by agonists, antagonists, and selective estrogen receptor modulators. J Biol Chem 276:35684–35692
20. Reid G, Hubner MR, Metivier R, Brand H, Denger S, Manu D, Beaudouin J, Ellenberg J, Gannon F 2003 Cyclic, proteasome-mediated turnover of unliganded and liganded ERα on responsive promoters is an integral feature of estrogen signaling. Mol Cell 11:695–707
21. Nonclercq D, Journe F, Body JJ, Leclercq G, Laurent G 2004 Ligand-independent and agonist-mediated degradation of estrogen receptor-α in breast carcinoma cells: evidence for distinct degradative pathways. Mol Cell Endocrinol 227:53–65
22. Stenoien DL, Patel K, Mancini MG, Dutertre M, Smith CL, O'Malley BW, Mancini MA 2001 FRAP reveals that mobility of oestrogen receptor-α is ligand- and proteasome-dependent. Nat Cell Biol 3:15–23
23. Marsaud V, Gougelet A, Maillard S, Renoir JM 2003 Various phosphorylation pathways, depending on agonist and antagonist binding to endogenous estrogen receptor α (ERα), differentially affect ERα extractability, proteasome-mediated stability, and transcriptional activity in human breast cancer cells. Mol Endocrinol 17: 2013–2027
24. Shao W, Keeton EK, McDonnell DP, Brown M 2004 Coactivator AIB1 links estrogen receptor transcriptional activity and stability. Proc Natl Acad Sci USA 101: 11599–11604
25. Brzozowski AM, Pike AC, Dauter Z, Hubbard RE, Bonn T, Engstrom O, Ohman L, Greene GL, Gustafsson JA, Carlquist M 1997 Molecular basis of agonism and antagonism in the oestrogen receptor. Nature 389:753–758
26. Wijayaratne AL, Nagel SC, Paige LA, Christensen DJ, Norris JD, Fowlkes DM, McDonnell DP 1999 Comparative analyses of mechanistic differences among antiestrogens. Endocrinology 140:5828–5840
27. Htun H, Holth LT, Walker D, Davie JR, Hager GL 1999 Direct visualization of the human estrogen receptor α reveals a role for ligand in the nuclear distribution of the receptor. Mol Biol Cell 10:471–486
28. Pratt WB, Toft DO 1997 Steroid receptor interactions with heat shock protein and immunophilin chaperones. Endocr Rev 18:306–360
29. Lee MO, Kim EO, Kwon HJ, Kim YM, Kang HJ, Kang H, Lee JE 2002 Radicicol represses the transcriptional function of the estrogen receptor by suppressing the stabilization of the receptor by heat shock protein 90. Mol Cell Endocrinol 188:47–54
30. Ballinger CA, Connell P, Wu Y, Hu Z, Thompson LJ, Yin LY, Patterson C 1999 Identification of CHIP, a novel tetratricopeptide repeat-containing protein that interacts with heat shock proteins and negatively regulates chaperone functions. Mol Cell Biol 19:4535–4545
31. Connell P, Ballinger CA, Jiang J, Wu Y, Thompson LJ, Hohfeld J, Patterson C 2001 The co-chaperone CHIP regulates protein triage decisions mediated by heat-shock proteins. Nat Cell Biol 3:93–96
32. He B, Bai S, Hnat AT, Kalman RI, Minges JT, Patterson C, Wilson EM 2004 An androgen receptor NH2-terminal conserved motif interacts with the COOH terminus of the Hsp70-interacting protein (CHIP). J Biol Chem 279: 30643–30653
33. Li L, Xin H, Xu X, Huang M, Zhang X, Chen Y, Zhang S, Fu XY, Chang Z 2004 CHIP mediates degradation of Smad proteins and potentially regulates Smad-induced transcription. Mol Cell Biol 24:856–864
34. Bloom J, Amador V, Bartolini F, DeMartino G, Pagano M 2003 Proteasome-mediated degradation of p21 via N-terminal ubiquitinylation. Cell 115:71–82
35. Fan M, Nakshatri H, Nephew KP 2004 Inhibiting proteasomal proteolysis sustains estrogen receptor-α activation. Mol Endocrinol 18:2603–2615
36. Xu W, Marcu M, Yuan X, Mimnaugh E, Patterson C, Neckers L 2002 Chaperone-dependent E3 ubiquitin li-

gase CHIP mediates a degradative pathway for c-ErbB2/Neu. Proc Natl Acad Sci USA 99:12847–12852
37. Grenert JP, Sullivan WP, Fadden P, Haystead TA, Clark J, Mimnaugh E, Krutzsch H, Ochel HJ, Schulte TW, Sausville E, Neckers LM, Toft DO 1997 The amino-terminal domain of heat shock protein 90 (hsp90) that binds geldanamycin is an ATP/ADP switch domain that regulates hsp90 conformation. J Biol Chem 272:23843–23850
38. Zhou P, Fernandes N, Dodge IL, Reddi AL, Rao N, Safran H, DiPetrillo TA, Wazer DE, Band V, Band H 2003 ErbB2 degradation mediated by the co-chaperone protein CHIP. J Biol Chem 278:13829–13837
39. King WJ, Greene GL 1984 Monoclonal antibodies localize oestrogen receptor in the nuclei of target cells. Nature 307:745–747
40. Stenoien DL, Mancini MG, Patel K, Allegretto EA, Smith CL, Mancini MA 2000 Subnuclear trafficking of estrogen receptor-α and steroid receptor coactivator-1. Mol Endocrinol 14:518–534
41. Huang Z, Nie L, Xu M, Sun XH 2004 Notch-induced E2A degradation requires CHIP and Hsc70 as novel facilitators of ubiquitination. Mol Cell Biol 24:8951–8962
42. Sommer S, Fuqua SA 2001 Estrogen receptor and breast cancer. Semin Cancer Biol 11:339–352
43. Tateishi Y, Kawabe Y, Chiba T, Murata S, Ichikawa K, Murayama A, Tanaka K, Baba T, Kato S, Yanagisawa J 2004 Ligand-dependent switching of ubiquitin-proteasome pathways for estrogen receptor. EMBO J 23: 4813–4823
44. Fan M, Long X, Bailey JA, Reed CA, Osborne E, Gize EA, Kirk EA, Bigsby RM, Nephew KP 2002 The activating enzyme of NEDD8 inhibits steroid receptor function. Mol Endocrinol 16:315–330
45. Freeman BC, Yamamoto KR 2002 Disassembly of transcriptional regulatory complexes by molecular chaperones. Science 296:2232–2235
46. Wochnik GM, Young JC, Schmidt U, Holsboer F, Hartl FU, Rein T 2004 Inhibition of GR-mediated transcription by p23 requires interaction with Hsp90. FEBS Lett 560: 35–38
47. Morimoto RI 2002 Dynamic remodeling of transcription complexes by molecular chaperones. Cell 110:281–284
48. Pink JJ, Jordan VC 1996 Models of estrogen receptor regulation by estrogens and antiestrogens in breast cancer cell lines. Cancer Res 56:2321–2330
49. Fan M, Bigsby RM, Nephew KP 2003 The NEDD8 pathway is required for proteasome-mediated degradation of human estrogen receptor (ER)-α and essential for the antiproliferative activity of ICI 182,780 in ERα-positive breast cancer cells. Mol Endocrinol 17:356–365
50. Anderson E 2002 The role of oestrogen and progesterone receptors in human mammary development and tumorigenesis. Breast Cancer Res 4:197–201
51. Fowler AM, Solodin N, Preisler-Mashek MT, Zhang P, Lee AV, Alarid ET 2004 Increases in estrogen receptor-α concentration in breast cancer cells promote serine 118/104/106-independent AF-1 transactivation and growth in the absence of estrogen. FASEB J 18:81–93
52. Henrich LM, Smith JA, Kitt D, Errington TM, Nguyen B, Traish AM, Lannigan DA 2003 Extracellular signal-regulated kinase 7, a regulator of hormone-dependent estrogen receptor destruction. Mol Cell Biol 23:5979–5988

Molecular Endocrinology **is published monthly by The Endocrine Society (http://www.endo-society.org), the foremost professional society serving the endocrine community.**

Diverse Gene Expression and DNA Methylation Profiles Correlate with Differential Adaptation of Breast Cancer Cells to the Antiestrogens Tamoxifen and Fulvestrant

Meiyun Fan[1], Pearlly S. Yan[2], Cori Hartman-Frey[1], Lei Chen[1], Henry Paik[1], Samuel L. Oyer[1], Jonathan D. Salisbury[1], Alfred S.L. Cheng[2], Lang Li[3], Phillip H. Abbosh[1], Tim H-M. Huang[2], Kenneth P. Nephew[1, 4, 5]

[1]Medical Sciences, Indiana University School of Medicine, Bloomington, IN 47405; [2]Division of Human Cancer Genetics, Comprehensive Cancer Center, Ohio State University, Columbus, OH 43210; [3]Division of Biostatistics, [3]Department of Medicine, [4]Department of Cellular and Integrative Physiology, Indiana University School of Medicine Indianapolis, IN, 46202; and [4]Indiana University Cancer Center, Indianapolis, IN 46202.

Funding: The authors gratefully acknowledge the following agencies for supporting this work: American Cancer Society Research and Alaska Run for Woman Grant TBE-104125; US National Institutes of Health (N.I.H.), National Cancer Institute Grants CA 085289 (to K. P. N.), CA 113001 (to T. H-M. H.), and Student Research Program in Academic Medicine, (N.I.H. 2T35HL07584; to F. Pavalko); U.S. Army Medical Research Acquisition Activity, Award Numbers DAMD 17-02-1-0418 and DAMD17-02-1-0419; Walther Cancer Institute; Lilly Endowment, Inc (to the Center for Medical Genomics, Indiana University School of Medicine);

Acknowledgements: We thank Dr. Curtis Balch for help with manuscript preparation, Ronald E. Jerome and Chunxiao Zhu for technical help with microarrays, and Dr. Bert Vogelstein, Johns Hopkins University, for kindly providing TOP-FLASH and FOP-FLASH plasmids.

[5]To whom correspondence should be addressed:

Kenneth P. Nephew, Ph.D.

Medical Sciences

Indiana University School of Medicine

302 Jordan Hall

1001 E. 3rd St.

Bloomington, Indiana 47405-4401

Phone: (812) 855-9445

FAX: (812) 855-4436

E-mail:knephew@indiana.edu

ABSTRACT

The development of targeted therapies for antiestrogen-resistant breast cancer requires a detailed understanding of its molecular characteristics. To further elucidate the molecular events underlying acquired resistance to the antiestrogens tamoxifen and fulvestrant, we established drug-resistant sublines from a single colony of hormone-dependent breast cancer MCF7 cells. These model systems allowed us to examine the cellular and molecular changes induced by antiestrogens in the context of a uniform clonal background. Global changes in both basal and estrogen-induced gene expression profiles were determined, in hormone-sensitive and hormonal-resistant sublines, using Affymetrix Human Genome U133 Plus 2.0 Arrays. Changes in DNA methylation were assessed by differential methylation hybridization, a high-throughput promoter CpG-island microarray analysis. By comparative studies, we found distinct gene expression and promoter DNA methylation profiles associated with acquired resistance to fulvestrant *vs*. tamoxifen. Fulvestrant resistance was characterized by pronounced upregulation of multiple growth-stimulatory pathways, resulting in ERα-independent, autocrine-regulated proliferation. Conversely, acquired resistance to tamoxifen correlated with maintenance of the estrogen receptor-α (ERα)-positive phenotype, although receptor-mediated gene regulation was altered. Activation of growth-promoting genes, due to promoter hypomethylation, was more frequently observed in antiestrogen resistant cells, compared to gene inactivation by promoter hypermethylation, revealing an unexpected insight into the molecular changes associated with endocrine resistance. In summary, this study provides an in-depth understanding of the molecular changes specific to acquired resistance to clinically important antiestrogens. Such knowledge of resistance-associated

mechanisms could allow for identification of therapy targets and strategies for resensitization to these well-established antihormonal agents.

INTRODUCTION

The steroid hormone estrogen is strongly implicated in the development and progression of breast cancer (1). The primary mediator of estrogen action in breast cancer cells is estrogen receptor alpha (ERα), a ligand-activated transcription factor (1). Consequently, the leading drugs used for endocrine therapy of breast cancer all block ERα activity, including antiestrogens (*i.e.*, tamoxifen and fulvestrant) and aromatase inhibitors (AIs) (2). Despite the efficacy and favorable safety profile of these agents, the use of endocrine therapy is limited by the onset of drug resistance, in which most patients who initially respond to endocrine therapy eventually relapse (2).

In breast cancer cells, ERα can mediate "genomic" regulation of gene transcription and "non-genomic" activation of various protein kinase cascades (*e.g.*, Shc/Grb2/SOS/MAPK, PI3K/AKT, and cAMP/PKA pathways) (3). As the transcriptional activity and target gene specificity of ERα and subsequent cellular response(s) to ligands are determined by complex combinatorial associations of ERα with coregulators, other transcription factors, and membrane-initiated signaling pathways (3-6, 7), a myriad of receptor interactions may become altered during the acquisition of antiestrogen resistance.

ERα transcriptional activity is mediated by a constitutively active AF-1 and a ligand-regulated AF-2 (8). 17β-estradiol (E2), the primary ligand for ERα, binds to the ligand-binding domain (LBD) and induces a conformational change in the AF2 domain, resulting in coregulator recruitment and transcription regulation, followed by rapid ERα degradation (8, 9). The antiestrogen tamoxifen, which competes with E2 for LBD binding, induces a conformational change distinct from the E2-ERα complex, leading to

inactivation of the AF-2 domain and receptor stabilization (10, 11). However, tamoxifen-bound ERα is capable of binding to DNA and regulating gene transcription, either directly, through the AF-1 domain, or indirectly, by sequestering coregulators away from other transcription factors (12). In addition, tamoxifen can act as an agonist to elicit non-genomic signaling through membrane ERα (13). These observations suggest that the action of tamoxifen is not limited to diminished estrogen-induced gene regulation. However, the mechanism(s) remains unclear of how the complex, multifactorial actions of this drug on gene expression and non-genomic signaling contribute to the acquisition of breast cancer tamoxifen resistance.

In contrast to tamoxifen, the antiestrogen fulvestrant is recommended for use in postmenopausal women whose disease has progressed after first-line endocrine therapies (such as tamoxifen and AIs). The mechanism of action of this so-called "pure antagonist" differs markedly from tamoxifen. Fulvestrant inhibits cytoplasm-to-nucleus ERα translocation, dimerization, and DNA binding of ERα, as well as inducing its cytoplasmic aggregation, immobilization to the nuclear matrix, and proteasomal degradation (14). As a consequence of these actions, both ERα-mediated genomic gene regulation and non-genomic signaling are attenuated, leading to complete suppression of ERα signaling pathways (14, 15). Despite the potent effects of fulvestrant, tumors eventually develop resistance to this SERD (16), although the underlying mechanism(s) of this phenomenon remains poorly understood.

Interrupting ERα function by antistrogens can result in epigenetic modification of chromatin and altered gene expression (17, 18). DNA methylation occurs in CpG dinucleotides, which are concentrated to form CpG islands (CpGi) in the promoter region

of ~70% of human genes (19). Hypermethylation of CpGi in gene promoters often leads to inactivation of transcription, and an inverse relationship between promoter methylation levels and transcriptional activity has been well documented (20). Our recent studies demonstrate that depleting ERα with siRNA in breast cancer cells triggers repressive chromatin modifications and DNA methylation in a set of ERα-target promoters, resulting in transcriptional silencing of the corresponding genes (17). Whether interrupting ERα function by tamoxifen or fulvestrant can similarly affect DNA methylation patterns has not been explored.

The purpose of the current study was to identify molecular changes associated with acquired tamoxifen or fulvestrant resistance. To achieve this objective, we compared gene expression and DNA methylation profiles in estrogen-responsive MCF7 human breast cancer cells and tamoxifen- and fulvestrant-resistant MCF7 derivatives. Collectively, our results indicate that significant changes in downstream ERα target gene networks contribute to the acquisition of tamoxifen resistance; in contrast, loss of ERα signaling pathways, activation of compensatory growth-stimulatory cascades, and global remodeling of gene expression patterns underlie acquired resistance to fulvestrant. Finally, we report, for the first time, a prominent role for promoter hypomethylation of oncogenes in the acquisition of breast cancer antiestrogen resistance.

EXPERIMENTAL PROCEDURES

Reagents. ERα antibody (HC20; Santa Cruz Biotechnology, Santa Cruz, CA); GAPDH antibody (Chemicon International, Inc., Temecula, CA); EGFR and ERBB2 antibodies (Cell Signaling Technology, Inc, Danvers, MA); β-catenin antibody, AG879, PD153035 and 4557W (EMD Biosciences, Inc. La Jolla, CA); fetal bovine serum (FBS) and dextran-coated charcoal-stripped FBS (csFBS) (Hyclone laboratories, Inc., Logan, Utah); Topflash and Fopflash (Dr. Bert Vogelstein; Johns Hopkins University); other cell culture medium and reagents (Life Technologies, Inc., Rockville, MD); 17β-estradiol (E2), 4-hydroxytamoxifen (OHT), epidermal growth factor (EGF) and insulin-like growth factor 1 (IGF-1), and epigallocatechin-3-gallate (EGCG) (Sigma Chemical Co., St. Louis, MO); fulvestrant (Tocris Cookson Ltd., Ellisville, MO); Affymetrix Human Genome U133 Plus 2.0 Arrays (Affymetrix, Santa Clara, CA); customized 60-mer promoter arrays were constructed by Agilent Technologies (Palo Alto, CA).

Cell culture and establishment of tamoxifen- and fulvestrant-resistant sublines. Cell media used in this study included growth medium (MEM with 2 mM L-glutamine, 0.1 mM non-essential amino acids, 50 units/ml penicillin, 50 µg/ml streptomycin, 6 ng/ml insulin, and 10% FBS), hormone-free medium (phenol-red free MEM with 2 mM L-glutamine, 0.1 mM mon-essential amino acids, 50 units/ml penicillin, 50 µg/ml streptomycin, 6 ng/ml insulin, and 10% csFBS), and basal medium (phenol-red free MEM with 2 mM L-glutamine, 0.1 mM non-essential amino acids, 50 units/ml penicillin, 50 µg/ml streptomycin, and 3% csFBS). MCF7 human breast cancer cells were purchased from ATCC (Manassas, VA). MCF7 cells cotransfected with pcDNA and

2xERE-pS2-Luc (21) by using LipofectAMINE Plus Reagent were selected in the presence of 0.5 mg/ml geneticin for three weeks. A geneticin-resistant colony that was E2 responsive, as determined by increased luciferase expression and cell proliferation after hormone treatment, was expanded and split into three flasks (10^6 cells/T75 flask) containing different media (Fig. 1S, Supplementary Data): i) growth medium (to maintain a hormone sensitive subline designated as "MCF7"); ii) hormone-free medium supplemented with 10^{-7} M OHT (to establish the tamoxifen-resistant subline, "MCF7-T"); iii) hormone-free medium supplemented with 10^{-7} M fulvestrant (to establish the fulvestrant-resistant subline "MCF7-F"). Cells were continuously cultured under these conditions for 12 months.

Preparation of cell extracts, immunoblotting and luciferase assay. Prior to all experiments, MCF7-T and MCF7-F cells were cultured in hormone-free medium for one week to deplete any residual OHT or fulvestrant. Cells were cultured in basal medium for three days. Preparation of whole cell extracts, immunoblotting, and luciferase analyses were performed as described previously (21, 22). To determine β-catenin activity, cells were transfected with Topflash or Fopflash (23), along with CMV-β-gal as internal control for transcription efficiency. β-catenin activity was determined by dividing the OT-FLASH value by the OF-FLASH value.

Cell proliferation and clonogenicity assays. Cell proliferation assays were performed as described previously (22). To examine clonogenic activity, cells were plated (300

cells/well) in 6-well plates, cultured for two weeks and stained with 0.5% methylene blue in 50% methanol. Colonies that contained ≥50 cells were scored.

RNA preparation and microarray hybridization. Cells were cultured in basal medium for three days and treated with E2 (10^{-8} M) for 4 h. Total RNA was prepared using the QIAGEN RNeasy MiNi Kit. A DNase I digestion step was included to eliminate DNA contamination. cRNA was generated, labeled, and hybridized to the Affymetrix Human Genome U133 Plus 2.0 Arrays by the Center for Medical Genomics at Indiana University School of Medicine (http://cmg.iupui.edu/).

Microarray data analysis and validation. The hybridized Human Genome U133A 2.0 Array was scanned and analyzed using the Affymetrix Microarray Analysis Suite (MAS) version 5.0. The average density of hybridization signals from four independent samples was used for data analysis and genes with signal density less than 300 pixels were omitted from the data analysis. P-values were calculated with two sided t-tests with un-equal variance assumptions, and a p-value less of than 0.001 was considered to be significant. The following pair-wise comparisons were conducted: E2 *vs.* untreated for each sublines to identify E2-responsive genes; untreated MCF7-T or untreated MCF7-F *vs.* untreated MCF7 to identify genes whose basal expression levels were altered in MCF7-T or MCF7-F. The fold change was described as a positive value when the expression level was increased and a negative value when the expression level was reduced. False discovery rate (FDR) was set at 0.1 in the data analysis. To confirm the gene expression data from microarray analysis, qPCR was used to examine the mRNA

levels of a subset of genes (Supplementary data, Fig. S2). The qPCR results showed a high degree of correlation to the microarray data.

Differential Methylation Hybridization (DMH). Genomic DNA was prepared using QIAGEN DNeasy tissue Kit. DMH was performed as described previously (17) using a customized 60-mer oligonucleotide microarrays, which contain ~42,000 CpG-rich fragments from ~12,000 promoters of defined genes. The fold change in methylation density was described as a positive or negative value when methylation density was increased or decreased, respectively, compared to MCF7.

RESULTS

Establishment and characterization of breast cancer cell lines with acquired antiestrogen resistance. The cell line MCF7 is a standard *in vitro* model for hormone-sensitive breast cancer (24). Consequently, we chose this cell line to investigate molecular changes associated with acquired resistance to tamoxifen and fulvestrant. MCF7 cultures are likely heterogeneous in nature (25); thus, to avoid selecting clonal variants with intrinsic drug resistance, we used a single estrogen-responsive MCF7 clone stably transfected with an ERα-responsive luciferase reporter (ERE-pS2-Luc) (21) to derive sublines resistant to tamoxifen (MCF7-T) or fulvestrant (MCF7-F). The stably integrated ERE-pS2-Luc reporter was used to monitor ERα transcriptional activity. Because the three sublines used in the study were derived from a single MCF7 colony, cellular and molecular alterations observed in the drug resistant sublines are likely due to

an adaptive process in response to primary drug action. The overall scheme used to develop our model system is illustrated in Fig. 1S (Supplementary Data).

Cell morphology changes associated with acquired antiestrogen resistance are shown in Fig. 1A. MCF7-T cells were similar to MCF7 cells in appearance, growing as tightly packed colonies with limited cell spreading. MCF7-F cells, by contrast, showed reduced cell-cell contacts, compared to MCF7 or MCF7-T cells, and were loosely attached to the culture surface.

We next examined the expression levels of ERα mRNA and protein in the three sublines by quantitative PCR (qPCR) and immunoblot analyses, respectively (Fig. 1B). To avoid the effects of estrogen and antiestrogens, the cells were cultured in drug-free medium for one week, followed by basal medium for 3 days, before examining ERα content. Compared to MCF7 cells, ERα mRNA levels in MCF7-T and MCF7-F cells were decreased by 50% and 90%, respectively. Immunoblot analysis showed a 2-fold increase in ERα protein level in MCF7-T cells, compared to a 90% decrease in receptor protein levels in MCF7-F cells. ERα transcriptional activity in these sublines was examined by monitoring the expression levels of the stably integrated ERE-pS2-Luc (Fig. 1C). Compared to MCF7, basal luciferase activity was higher in MCF7-T (~2-fold *vs.* MCF7), likely due to the elevated protein level of ERα. E2 treatment increased ERE-pS2-luc activity, which was inhibited by cotreatment with OHT or fulvestrant, in both MCF7 and MCF7-T cells. These observations suggest that ERα retains its transcriptional activity and sensitivity to different ligands in MCF7-T cells. By contrast, basal luciferase activity was dramatically elevated in MCF7-F (~20 fold *vs.* MCF7), and no effect of E2, OHT, or fulvestrant on ERE-pS2-Luc expression was observed (Fig. 1C), demonstrating

that the integrated ERE-pS2-Luc reporter became constitutively activated through an ERα-independent mechanism in the fulvestrant-resistant subline. Together, these results indicate that the acquisition of tamoxifen resistance is associated with retention of functional ERα, whereas acquired fulvestrant resistance is accompanied by loss of ERα protein and E2-induced gene transactivation.

Response of MCF7-T and MCF7-F cells to estrogen, antiestrogens, and growth factors. We next examined growth rates of the three sublines and cell growth in response to E2, OHT, fulvestrant, EGF, and IGF-1 (Fig. 1D). In basal growth medium, doubling times for MCF7 and MCF7-F were 6 and 5 days, respectively. By contrast, MCF7-T cells underwent growth arrest in this medium, showing only a 1.5-fold increase in cell number during a nine-day culture in basal medium, indicating that MCF7-T cells are dependent on a higher concentration of serum or the presence of OHT for proliferation. To compare the sensitivities to E2, OHT and fulvestrant among MCF7, MCF7-T and MCF7-F cells, dose responses were examined. E2 treatment increased the growth rate of MCF7 cells, but showed no effect on MCF7-T or MCF7-F cells. OHT treatment inhibited the growth of MCF7, but not that of MCF7-T or MCF7-F. Fulvestrant inhibited the growth of MCF7, and to a lesser extent MCF7-T, but exhibited no effect on MCF7-F cells. These observations are consistent with previous reports showing that OHT-resistant cells remained responsive to fulvestrant with a reduced sensitivity, while fulvestrant-resistant cells were cross-resistant to OHT (26, 27). Treatment with EGF or IGF-1 increased the growth of MCF7 and MCF7-T cells. However, compared to MCF7 cells, MCF7-T cells were more sensitive to EGF but less sensitive to IGF-1. No effects of either EGF or IGF-

1 on MCF7-F cells were seen. Collectively, these results indicate that acquisition of resistance to tamoxifen and fulvestrant involves differential sensitivity to estrogen, antiestrogens, and growth factors.

Expression profiling of E2-responsive genes. To investigate whether aberrant changes in basal expression patterns and estrogen responsiveness of ERα target genes contribute to antiestrogen resistance, we analyzed gene expression patterns among MCF7, MCF7-T and MCF7-F, untreated or treated with E2 (10^{-8} M) for 4 h, as most direct ERα target genes are either induced or suppressed in that period (28, 29). The Affymetrix Human Genome U133 Plus 2.0 Array, containing 47,000 probe sets for human transcripts, was used. A total of 360, 175 and 7 genes were found to be E2-responsive (fold change≥2, decreased or increased by E2) in MCF7, MCF7-T and MCF7-F cells, respectively (Fig. 2A, Supplementary data, Table S1). Among the 360 E2-responsive genes identified in MCF7 cells, 89 (25%) were also similarly regulated by E2 in MCF7-T cells, while 271 (75%) were no longer inducible by E2 in the MCF7-T cells. Based on these results, we suggest that the acquisition of tamoxifen resistance is associated with altered regulation of a cohort of E2-inducible genes. The development of fulvestrant resistance, by contrast, is associated with almost complete loss of E2-induced gene regulation.

A two-dimensional (Gene tree and Condition Tree) hierarchical clustering program (http://cmg.iupui.edu/mdp/) was used to analyze the expression patterns of the E2-responsive genes in MCF7, MCF7-T, and MCF7-F, untreated or treated with E2 (10^{-8} M, 4 h) (Fig. 2B). Based on similarities in the expression profiles of the E2-responsive genes among sublines (presented as a "Condition Tree" on the top of the matrix in Fig.

2B), MCF7-T and MCF7 cells clustered together and MCF7-F cells clustered on a separate branch, suggesting that MCF7-T cells were more similar to the parental MCF7 than MCF7-F cells.

We then examined MCF7-T and MCF7-F cells for changes in basal expression levels of the 360 E2-responsive genes identified in MCF7 cells (Supplementary data, Table S1). The numbers of E2-upregulated and E2-downregulated genes that showed significant changes in basal expression levels in MCF7-T or MCF7-F cells were presented in Fig. 2C. Among the total of 231 genes displaying altered basal expression in either MCF7-T or MCF7-F cells, only 39 (17%, Fig. 2C, *hatched with white lines*) were coordinately altered in both sublines. These results indicate an association between acquired resistance to tamoxifen and fulvestrant and altered basal expression levels of distinct subsets of E2-responsive genes.

Global gene expression profiles associated with acquired antiestrogen resistance. We performed gene expression profiling of MCF7, MCF7-T and MCF7-F cells after three days of culture in basal medium (Supplementary data, Table S2). We considered only those genes that displayed a 3-fold or greater change in basal expression level in the antiestrogen-resistant sublines. Altered expression of 371 genes was observed in MCF7-T cells, with nearly an equal number of up- and downregulated genes (184 and 187, respectively; Fig. 3A). In MCF7-F cells, altered expression of 2,518 genes was observed, with more genes upregulated (1,753 upregulated *vs.* 765 downregulated; Fig. 3A). Only 138 genes were coordinately altered in both MCF7-T and MCF7-F cells (81 genes upregulated, 57 genes downregulated; Fig. 3A, *shadowed with white lines*), and 233 and

2,380 genes were uniquely altered in MCF7-T and MCF7-F, respectively (Fig. 3A). This result revealed that distinct molecular changes are associated with tamoxifen and fulvestrant resistance. Furthermore, the acquisition of fulvestrant resistance was associated with a dramatic remodeling of global gene expression, with gene upregulation more prevalent that gene downregulation.

Although the functions of the genes with altered expression in either MCF7-T or MCF7-F cells were diverse, they could be organized into different functional categories, using the KEGG database (http://www.genome.ad.jp/kegg/kegg2.html) and Gene Ontology (GO) algorithms (http://www.godatabase.org/cgi-bin/amigo/go.cgi). Signaling pathways coordinately altered at multiple levels and known to be involved in growth regulation are listed in Table 1. In MCF7-T cells, five families of genes were prominently altered: 1) PKA pathway; 2) caveolins; 3) annexins and S100 calcium binding proteins; 4) MAP kinase phosphatases; and 5) inhibitor of differentiation proteins (IDs). In addition, of the 371 altered genes in MCF7-T cells, 40% were E2-responsive genes (Supplementary data, Table S1), suggesting that remodeling of the ERα-target gene network is a mechanism underlying acquisition of tamoxifen resistance. In MCF7-F cells, prominently altered pathways included epidermal growth factor receptors (EGFR and ErbB2) and related proteins, cytokines/cytokines receptors, Wnt/β-catenin pathway, notch pathway, and interferon signaling pathway/interferon-inducible genes (Table 1), showing an overall upregulation of growth-stimulatory pathways in fulvestrant-resistant cells.

Correlation between genes altered in antiestrogen-resistant cells and known prognostic markers of breast tumors. To assess the potential clinical relevance of our findings, we examined the expression levels of multiple breast cancer prognostic markers (30, 31) in MCF7-T and MCF-F. We observed upregulation (fold change≥2; P<0.001) of 16 and 47 poor prognostic markers in MCF7-T and MCF7-F, respectively (Supplementary data, Table S4). Conversely, we observed downregulation of 4 and 9 good prognostic markers in MCF7-T and MCF7-F, respectively (Table S4). Next, we examined the expression levels of genes previously associated with clinical outcome of breast tumors treated with tamoxifen (32-34). In MCF7-T, seven tamoxifen-resistant markers were upregulated, while three tamoxifen-responsive markers were downregulated, (Supplementary data, Table S5). Finally, we examined the expression levels of known ERα signature genes (30, 35). In MCF7-T and MCF7-F, we observed downregulation of 41 and 138 signature genes of ERα-positive tumors, respectively (Supplementary data, Table S6). Conversely, we observed upegulation of 60 and 206 signature genes of ERα-negative tumors in MCF7-T and MCF7-F, respectively (Table S6). Collectively, our observations that subsets of potentially clinically relevant genes are altered in MCF7-T and MCF7-F support the notion that these cell lines may be valuable models for investigating the molecular events underlying the development of antiestrogen resistance in human breast cancer.

DNA methylation profiles associated with acquired resistance. Our recent studies demonstrated that ERα depletion by siRNA in breast cancer cells led to progressive DNA methylation of genes normally regulated by ERα (17). This finding prompted us to

investigate whether long-term treatment with tamoxifen or fulvestrant could cause changes in DNA methylation. Thus, we examined promoter methylation in using differential methylation hybridization (DMH) and a customized 60-mer microarray containing 42,000 CpG-rich fragments from 12,000 promoters of defined genes. Genes showing altered promoter methylation intensities (fold change≥2, *vs.* MCF7) are listed in Supplementary data, Table S3. In MCF7-F cells, 281 genes showed altered promoter methylation, with 240 (86%) hypomethylated genes (Fig. 3B). In MCF7-T, 160 genes showed altered promoter methylation, with 124 (77.5%) hypomethylated genes (Fig. 3B). Comparing the promoter methylation profiles, we found only 16 promoters were commonly hypermethylated or hypomethylated in both resistant sublines (Fig. 3B, *shadowed with white lines*), suggesting that distinct set of promoters are targeted for epigenetic modification by tamoxifen and fulvestrant.

By analyzing the methylation status of the 360 E2-responsive genes identified in MCF7 cells (Supplementary data, Table S1), we found a total of eight genes with an altered methylation in MCF7-T (*ID4* and *FABP5*) and MCF7-F (*FHL2, FUT4, MICAL2, P2RY2, PIK3R3, USP31).* This observation suggests that the acquisition of antiestrogen resistance is not associated with changes in promoter methylation status of early E2-responsive genes.

To correlate changes in promoter methylation and basal gene expression levels, a linear regression analysis was performed. An inverse correlation was observed between promoter methylation intensities and mRNA expression levels ($P<0.05$; Fig. 3C), such as decreased basal expression levels were associated with increased promoter methylation. For a subset of genes listed in Table 2, increased mRNA expression levels were

correlated with hypomethylation or *visa versa* (decreased mRNA expression levels were correlated with hypermethylation). Taken together, these results demonstrate that MCF7-F and MCF7-T display highly divergent DNA methylation patterns; furthermore, promoter hypomethylation was more prevalent in antiestrogen resistant sublines than in MCF7 cells.

EGFR/ErbB2 and Wnt/β-catenin signaling pathways and antiestrogen resistance. As several signaling pathways showed coordinate alteration of multiple components in MCF7-T and MCF7-F (Table 1), we first examined the role of EGFR/ErbB2 in supporting estrogen-independent cell proliferation. Immunoblotting analysis reveled that EGFR is upregulated and activated (phosphorylated) in MCF7-F, and ErbB2 is upregulated and activated (phosphorylated) in both MCF7-T and MCF7-F cells (Fig. 4A, upper panel). Cell proliferation assays demonstrated that 4557W (an inhibitor of both EGFR and ErbB2) and AG879 (an ErbB2-specific inhibitor) both inhibited cell proliferation of MCF7-T and MCF7-F, but not MCF7 (Fig. 4A, lower panels). We also examined the effect of PD15303, an EGFR-specific inhibitor. At 10 μM PD15303, only the growth of MCF7-F was inhibited; however, 30 μM PD15303 completely blocked MCF7-T and MCF7-F cell growth, but only partially inhibited MCF7 growth (Fig. 4A, bottom panel).

Next, we examined the role of the Wnt/β-catenin pathway in supporting estrogen-independent cell growth. Immunoblotting analysis reveled that β-catenin is upregulated in both MCF7-T and MCF7-F, but only activated in MCF7-F, indicated by the presence of β-catenin in the nuclear fraction (Fig. 4B). To inhibit β-catenin activity, we used

epigallocatechin 3-gallate (EGCG) (36). Cell proliferation and clonogenicity assays were used to show that inhibiting β-catenin activity blocked MCF7-F cell growth but not MCF7-T or MCF7 (Fig. 4B, lower panels). Reporter analysis using a Topflash construct (23) confirmed that β-catenin-mediated gene transcription was increased in MCF7-F, which was eliminated by EGCG treatment (Fig. 4B, bottom panel). Taken together, these results show that the EGFR/ErbB2 pathway plays an important role in supporting MCF7-T and MCF7-F cell growth, as well as the involvement of β-catenin activation in fulvestrant-resistance.

DISCUSSION

Based on the unique molecular actions of tamoxifen and fulvestrant, we hypothesized that the two antiestrogens induce distinct adaptive responses in breast cancer cells and subsequently promote the emergence of drug-resistance cells with specific molecular characteristics. To test this possibility, we generated breast cancer cells with acquired resistance to either tamoxifen or fulvestrant and performed global gene expression and DNA methylation analyses on the resistant cells. In our model system, to avoid clonal selection of variants with intrinsic drug resistance from a heterogeneous population, we isolated a single estrogen-responsive MCF7 clone, to subsequently derive the tamoxifen and fulvestrant resistant sublines. Hormone-free medium was used during the selection process to exclude interference from estrogens. Consequently, the cellular and molecular changes identified in our model systems can be considered “acquired traits” in response to tamoxifen and fulvestrant treatment. Although originating from the same MCF7 clone,

the sublines developed strikingly divergent phenotypes (Fig.1) and molecular characteristics (*i.e.*, gene expression and promoter methylation patterns).

In MCF7-T cells, expression of a functional ERα was maintained, and the cells responded to E2 treatment with altered gene expression (Fig. 1B and Table S1). While E2-stimulated cell growth was no longer observed in the MCF7-T subline, the cells retained a transcriptional response to E2 and remained sensitive to growth inhibition by fulvestrant (Fig. 1D), suggesting that ERα signaling continues to contribute to growth regulation after the acquisition of tamoxifen resistance. Comparative analysis revealed that E2-responsive gene profiles were markedly different between MCF7 and MCF7-T (Fig. 2), suggesting that different groups of genes were targeted by ERα in the parental MCF7 cells compared to the tamoxifen resistant subline. Analysis of basal gene expression levels revealed a subset of 371 genes with altered expression in MCF7-T cells; a significant number of these (~40%) were E2-responsive, suggesting that genes normally regulated by ERα are targeted for molecular alteration during acquisition of tamoxifen resistance. Based on these findings, we suggest that breast cancer cells with acquired tamoxifen resistance continue to utilize ERα to support cell growth/survival, but through an altered ER target gene network. Functional analysis of altered genes in MCF7-T cells revealed that several signaling pathways were coordinately upregulated at multiple levels, including protein kinase A (PKA) pathway, caveolins, annexins and S100 calcium binding proteins, MAP kinase phosphatases, and inhibitor of differentiation proteins (Table 1). Deregulation of these pathways has previously been implicated in breast cancer pathogenesis (37-41), but their precise roles in tamoxifen action and acquired resistance remain to be established.

In contrast to MCF7-T cells, the MCF7-F cells showed dramatically reduced expression of ERα and were refractory to E2-induced gene regulation and growth stimulation (Table S1 and Fig. 1). A large number of signature genes of ERα-positive tumors were significantly downregulated in MCF7-F, suggesting that acquired fulvestrant resistance is coupled with the generation of ERα-negative phenotype. One striking observation from the global gene expression analysis is the upregulation of multiple growth-regulatory pathways in MCF7-F cells, including EGFR/ErbB2 and related proteins, cytokines/cytokines receptors, Wnt/β-catenin pathway, and Notch pathway (Table 1). We demonstrated that both EGFR/ErbB2 and Wnt/β-catenin pathways play a role in supporting estrogen-independent cell growth of MCF7-F, the contribution of the other signaling pathways to the development of the resistant phenotype remains unclear.

Although aberrant promoter methylation is an early event in tumorigenesis and frequently observed in breast tumors (42), to our knowledge, a role for DNA methylation in remodeling gene expression patterns associated with acquired antiestrogen resistance has not been reported. Our genome-wide promoter methylation analysis of MCF7-T and MCF7-F cells demonstrated that tamoxifen and fulvestrant can cause hypermethylation or hypomethylation of particular CpG-rich loci, resulting in distinct promoter methylation patterns. We predicted, based on our previous study (17), that inhibition of ERα-signaling would result primarily in gain of methylation on promoter regions of ERα direct target genes, *i.e.*, hypermethylation of CpG-rich loci. In contrast to our hypothesis, the promoter methylation status of only eight E2-responsive genes (*FABP5, FHL2, FUT4, ID4, MICAL2, P2RY2, PIK3R3, USP31*) was found to be altered in the antiestrogen-resistant cells. One possible explanation is that while most early E2-

responsive genes in MCF7 cells are involved in cell growth control, their inactivation by promoter methylation could result in cell growth arrest or death. Thus, only cells without hypermethylation of ERα-target genes, perhaps due to defective DNA methylation, may be able to escape the detrimental effects of antiestrogens. In support of this possibility, promoter hypomethylation was more prevalent than promoter hypermethylation in the antiestrogen-resistant sublines. Intriguingly, our observation agrees with a previous study reporting that the DNA methylation inhibitor 5-azacytidine promoted the generation of antiestrogen resistance colonies from hormone-sensitive breast cancer ZR-75-1 cells (43).

Most current studies on cancer-related DNA methylation have been focused on suppression-linked promoter hypermethylation of tumor suppressors (44). However, a correlation between hypomethylation of promoter regions and transcriptional activation of tumor-promoting genes in tumors has been described (45, 46). Several genes that showed increased basal expression levels and promoter hypomethylation in MCF7-T or MCF7-F cells were found to be upregulated in cancer cells and possess oncogenic activity, such as *CDH2, ID4, ANXA4, BRAF, CTNNB1*, and *Wnt11* (47-50). Taken together, our results suggest that promoter hypomethylation plays a role in the development of antiestrogen resistance. Further studies are required to elucidate how other epigenetic events, such as histone modification and chromatin remodeling, contribute to altered promoter methylation and acquired antiestrogen resistance in breast cancer cells.

In this first study to provide a detailed analysis of the ERα-target gene network, global gene expression and DNA methylation profiles in tamoxifen- and fulvestrant-resistant cells, we show the acquisition of resistance to tamoxifen and fulvestrant involve

distinctly different pathways (summarized in Supplementary data, Fig. S3). Tamoxifen-
485 resistance is associated with the maintenance of the ERα-positive phenotype and utilization of an altered ERα-signaling network to promote cell proliferation/survival. Acquired resistance to fulvestrant is an ERα-independent phenomenon, utilizing multiple growth-stimulatory pathways to establish autocrine-regulated proliferation.

REFERENCES

1. Anderson E. The role of oestrogen and progesterone receptors in human mammary development and tumorigenesis. Breast Cancer Res 2002; 4:197-201.
2. Nicholson RI, Johnston SR. Endocrine therapy--current benefits and limitations. Breast Cancer Res Treat 2005; 93 Suppl 1:S3-10.
3. Bjornstrom L, Sjoberg M. Mechanisms of estrogen receptor signaling: convergence of genomic and nongenomic actions on target genes. Mol Endocrinol 2005; 19:833-842.
4. McDonnell DP, Norris JD. Connections and regulation of the human estrogen receptor. Science 2002; 296:1642-1644.
5. DeNardo DG, Kim HT, Hilsenbeck S, et al. Global gene expression analysis of estrogen receptor transcription factor cross talk in breast cancer: identification of estrogen-induced/activator protein-1-dependent genes. Mol Endocrinol 2005; 19:362-378.
6. Carroll JS, Liu XS, Brodsky AS, et al. Chromosome-wide mapping of estrogen receptor binding reveals long-range regulation requiring the forkhead protein FoxA1. Cell 2005; 122:33-43.
7. Cheng AS, Jin VX, Fan M, et al. Combinatorial analysis of transcription factor partners reveals recruitment of c-MYC to estrogen receptor-alpha responsive promoters. Mol Cell 2006; 21:393-404.
8. Tzukerman MT, Esty A, Santiso-Mere D, et al. Human estrogen receptor transactivational capacity is determined by both cellular and promoter context and

mediated by two functionally distinct intramolecular regions. Mol Endocrinol 1994; 8:21-30.

9. Nawaz Z, Lonard DM, Dennis AP, Smith CL, O'Malley BW. Proteasome-dependent degradation of the human estrogen receptor. Proc Natl Acad Sci U S A 1999; 96:1858-1862.

10. Shiau AK, Barstad D, Loria PM, et al. The structural basis of estrogen receptor/coactivator recognition and the antagonism of this interaction by tamoxifen. Cell 1998; 95:927-937.

11. Wu YL, Yang X, Ren Z, et al. Structural basis for an unexpected mode of SERM-mediated ER antagonism. Mol Cell 2005; 18:413-424.

12. Liu Z, Shi HY, Nawaz Z, Zhang M. Tamoxifen induces the expression of maspin through estrogen receptor-alpha. Cancer Lett 2004; 209:55-65.

13. Gururaj AE, Rayala SK, Vadlamudi RK, Kumar R. Novel mechanisms of resistance to endocrine therapy: genomic and nongenomic considerations. Clin Cancer Res 2006; 12:1001s-1007s.

14. Howell A, Abram P. Clinical development of fulvestrant ("Faslodex"). Cancer Treat Rev 2005; 31 Suppl 2:S3-9.

15. Frasor J, Stossi F, Danes JM, et al. Selective estrogen receptor modulators: discrimination of agonistic versus antagonistic activities by gene expression profiling in breast cancer cells. Cancer Res 2004; 64:1522-1533.

16. Gu Z, Lee RY, Skaar TC, et al. Association of interferon regulatory factor-1, nucleophosmin, nuclear factor-kappaB, and cyclic AMP response element binding

with acquired resistance to Faslodex (ICI 182,780). Cancer Res 2002; 62:3428-3437.

17. Leu YW, Yan PS, Fan M, et al. Loss of estrogen receptor signaling triggers epigenetic silencing of downstream targets in breast cancer. Cancer Res 2004; 64:8184-8192.

18. Jensen BL, Skouv J, Lundholt BK, Lykkesfeldt AE. Differential regulation of specific genes in MCF-7 and the ICI 182780-resistant cell line MCF-7/182R-6. Br J Cancer 1999; 79:386-392.

19. Saxonov S, Berg P, Brutlag DL. A genome-wide analysis of CpG dinucleotides in the human genome distinguishes two distinct classes of promoters. Proc Natl Acad Sci U S A 2006; 103:1412-1417.

20. Feng W, Webb P, Nguyen P, et al. Potentiation of estrogen receptor activation function 1 (AF-1) by Src/JNK through a serine 118-independent pathway. Mol Endocrinol 2001; 15:32-45.

21. Fan M, Long X, Bailey JA, et al. The activating enzyme of NEDD8 inhibits steroid receptor function. Mol Endocrinol 2002; 16:315-330.

22. Fan M, Bigsby RM, Nephew KP. The NEDD8 pathway is required for proteasome-mediated degradation of human estrogen receptor (ER)-alpha and essential for the antiproliferative activity of ICI 182,780 in ERalpha-positive breast cancer cells. Mol Endocrinol 2003; 17:356-365.

23. Korinek V, Barker N, Morin PJ, et al. Constitutive transcriptional activation by a beta-catenin-Tcf complex in APC-/- colon carcinoma. Science 1997; 275:1784-1787.

24. Levenson AS, Jordan VC. MCF-7: the first hormone-responsive breast cancer cell line. Cancer Res 1997; 57:3071-3078.

25. Howell A, Cuzick J, Baum M, et al. Results of the ATAC (Arimidex, Tamoxifen, Alone or in Combination) trial after completion of 5 years' adjuvant treatment for breast cancer. Lancet 2005; 365:60-62.

26. Brunner N, Frandsen TL, Holst-Hansen C, et al. MCF7/LCC2: a 4-hydroxytamoxifen resistant human breast cancer variant that retains sensitivity to the steroidal antiestrogen ICI 182,780. Cancer Res 1993; 53:3229-3232.

27. Brunner N, Boysen B, Jirus S, et al. MCF7/LCC9: an antiestrogen-resistant MCF-7 variant in which acquired resistance to the steroidal antiestrogen ICI 182,780 confers an early cross-resistance to the nonsteroidal antiestrogen tamoxifen. Cancer Res 1997; 57:3486-3493.

28. Lin CY, Strom A, Vega VB, et al. Discovery of estrogen receptor alpha target genes and response elements in breast tumor cells. Genome Biol 2004; 5:R66.

29. Frasor J, Danes JM, Komm B, et al. Profiling of estrogen up- and down-regulated gene expression in human breast cancer cells: insights into gene networks and pathways underlying estrogenic control of proliferation and cell phenotype. Endocrinology 2003; 144:4562-4574.

30. van 't Veer LJ, Dai H, van de Vijver MJ, et al. Gene expression profiling predicts clinical outcome of breast cancer. Nature 2002; 415:530-536.

31. Huang E, Cheng SH, Dressman H, et al. Gene expression predictors of breast cancer outcomes. Lancet 2003; 361:1590-1596.

32. Ma XJ, Wang Z, Ryan PD, et al. A two-gene expression ratio predicts clinical outcome in breast cancer patients treated with tamoxifen. Cancer Cell 2004; 5:607-616.

33. Paik S, Shak S, Tang G, et al. A multigene assay to predict recurrence of tamoxifen-treated, node-negative breast cancer. N Engl J Med 2004; 351:2817-2826.

34. Jansen MP, Foekens JA, van Staveren IL, et al. Molecular classification of tamoxifen-resistant breast carcinomas by gene expression profiling. J Clin Oncol 2005; 23:732-740.

35. Gruvberger-Saal SK, Eden P, Ringner M, et al. Predicting continuous values of prognostic markers in breast cancer from microarray gene expression profiles. Mol Cancer Ther 2004; 3:161-168.

36. Kim J, Zhang X, Rieger-Christ KM, et al. Suppression of Wnt signaling by the green tea compound (-)-epigallocatechin 3-gallate (EGCG) in invasive breast cancer cells. Requirement of the transcriptional repressor HBP1. J Biol Chem 2006; 281:10865-10875.

37. Michalides R, Griekspoor A, Balkenende A, et al. Tamoxifen resistance by a conformational arrest of the estrogen receptor alpha after PKA activation in breast cancer. Cancer Cell 2004; 5:597-605.

38. Razandi M, Oh P, Pedram A, Schnitzer J, Levin ER. ERs associate with and regulate the production of caveolin: implications for signaling and cellular actions. Mol Endocrinol 2002; 16:100-115.

39. Zhang W, Couldwell WT, Song H, et al. Tamoxifen-induced enhancement of calcium signaling in glioma and MCF-7 breast cancer cells. Cancer Res 2000; 60:5395-5400.

40. Camps M, Nichols A, Arkinstall S. Dual specificity phosphatases: a gene family for control of MAP kinase function. Faseb J 2000; 14:6-16.

41. Perk J, Iavarone A, Benezra R. Id family of helix-loop-helix proteins in cancer. Nat Rev Cancer 2005; 5:603-614.

42. Widschwendter M, Jones PA. DNA methylation and breast carcinogenesis. Oncogene 2002; 21:5462-5482.

43. van Agthoven T, van Agthoven TL, Dekker A, Foekens JA, Dorssers LC. Induction of estrogen independence of ZR-75-1 human breast cancer cells by epigenetic alterations. Mol Endocrinol 1994; 8:1474-1483.

44. Alvarez S, Diaz-Uriarte R, Osorio A, et al. A predictor based on the somatic genomic changes of the BRCA1/BRCA2 breast cancer tumors identifies the non-BRCA1/BRCA2 tumors with BRCA1 promoter hypermethylation. Clin Cancer Res 2005; 11:1146-1153.

45. Wu H, Chen Y, Liang J, et al. Hypomethylation-linked activation of PAX2 mediates tamoxifen-stimulated endometrial carcinogenesis. Nature 2005; 438:981-987.

46. Ehrlich M. DNA methylation in cancer: too much, but also too little. Oncogene 2002; 21:5400-5413.

47. Jaggi M, Nazemi T, Abrahams NA, et al. N-cadherin switching occurs in high Gleason grade prostate cancer. Prostate 2006; 66:193-199.

48. Zimmermann J, Liebl R, von Angerer E. 2,5-Diphenylfuran-based pure antiestrogens with selectivity for the estrogen receptor alpha. J Steroid Biochem Mol Biol 2005; 94:57-66.

49. Hoeflich KP, Gray DC, Eby MT, et al. Oncogenic BRAF is required for tumor growth and maintenance in melanoma models. Cancer Res 2006; 66:999-1006.

50. Cowin P, Rowlands TM, Hatsell SJ. Cadherins and catenins in breast cancer. Curr Opin Cell Biol 2005; 17:499-508.

FIGURE LEGEND

Figure 1. Characterization of tamoxifen- and fulvestrant resistant sublines. *A.* Phase contrast photomicrographs of MCF7, MCF7-T and MCF7-F cells. All cells were in log growth phase (10X magnification). *B.* ERα mRNA levels (mean ± SE, n=3) were determined by qPCR and normalized to ERα mRNA level in MCF7 cells (*Bar graph*). ERα protein levels were determined by immunoblotting with a specific ERα antibody. GAPDH was used as loading control. To determine the relative level of ERα in MCF7-F cells, the ERα level in 50 μg MCF7-F protein extract was compared to that in various amounts of MCF7 protein extracts. *C.* ERα transcriptional activity was determined by measuring luciferase expression driven by the stably integrated reporter ERE-pS2-Luc. Cells were treated with indicated doses of E2 alone (*left panel*), 10^{-8} M E2 in combination with indicated doses of OHT (*middle panel*), or 10^{-8} M E2 in combination with indicated doses of fulvestrant (*right panel*). Luciferase activity (unit/μg protein) was normalized with protein concentration and presented as mean ± SE (n=4). *D.* Comparison of cell growth rates among MCF7, MCF7-T and MCF7-F. To determine growth rates in basal medium, cells were plated in 96-well dishes (2000 cells/well) in basal medium for the indicated time, and cell numbers were determined by MTT assay. Relative cell growth rates (drug *vs.* vehicle, mean ± SE, n=6) in the presence of indicated doses of E2, OHT, fulvestrant, EGF and IGF-1 were also examined, and cell numbers were determined by MTT assay after 7-day treatment.

Figure 2. Expression of E2-responsive genes in MCF7, MCF7-T and MCF7-F cells.

A. Venn diagrams showing the numbers of E2-responsive genes in MCF7, MCF7-T and MCF7-F cells. E2-responsive genes were defined as genes whose expression levels were upregulated or downregulated by E2 (10^{-8} M , 4 h) by more than 2-fold and assigned to nine groups: upregulation by E2 in all three sublines, MCF7 and MCF7-T only, MCF7 and MCF7-F only, MCF7 only, and MCF7-T only; downregulation by E2 in MCF7 and MCF7-T only, MCF7 only, MCF7-T only; and MCF7-F only. ***B.*** Two-dimensional hierarchical clustering of E2-responsive genes in MCF7, MCF7-T, and MCF7-F, untreated or E2-treated (10^{-8} M, 4 h). Each row represents a single gene (genes with high expression levels are colored in red; genes with low expression levels in green). The similarities in the expression pattern among sublines are presented as a "Condition Tree" on the top of the matrix. ***C.*** Venn diagrams showing the number of E2-responsive genes that exhibited significant changes in basal expression levels in MCF7-T and MCF7-F cells. The areas hatched with white lines indicate the number of genes commonly altered in both MCF7-T and MCF7-F cells. Cutoff was set as fold change > 2 (upregulated or downregulated, *vs.* MCF7).

Figure 3. Alterations in global gene expression and promoter methylation

A. Venn diagrams showing the number of genes whose basal expression levels were altered (*vs.* MCF7) in MCF7-T and MCF7-F cells. The areas hatched with white line indicate the number of genes commonly altered in both MCF7-T and MCF7-F cells. Cutoff was set as fold change > 3 (upregulated or downregulated, *vs.* MCF7). ***A.*** Venn diagrams showing the number of genes with altered promoter methylation intensity (*vs.*

MCF7) in MCF7-T and MCF7-F cells. The number of genes commonly hypermethylated or hypomethylated in both MCF7-T and MCF7-F cells is shown in the hatched areas (white lines). The cutoff was set as fold change in methylation intensity >2 (decreased or increased, *vs.* MCF7). *C.* Correlation of changes in promoter methylation to gene expression. Genes showing >2-fold change in relative methylation density (horizontal axis) and mRNA level (vertical axis) in comparison with MCF7 are depicted in the figure and divided into four categories: genes with promoter hypomethylation and increased expression (*field a*); genes with promoter hypermethylation and increased expression (*field b*); genes with promoter hypomethylation and decreased expression (*field c*); and genes with promoter hypermethylation and decreased expression (*field d*).

Figure 4. Roles of EGFR/ErbB2 and Wnt/β-catenin pathways in estrogen-independent proliferation of MCF7-T and MCF7-F. *A.* Inhibition of EGFR/ErbB2 activity prevents cell growth of MCF7-T and MCF7-F. EGFR and ErbB2 protein and phosphorylation levels in whole cell lysates were examined by immunoblots. To examine cell growth rates, MCF7 cells (in growth medium), MCF7-T (in hormone-free medium with 100 nM OHT) and MCF-F cells (in hormone-free medium with 100 nM fulvestrant) were treated with EGFR/ErbB2 inhibitors, as indicated. Cell numbers were determined by MTT assay after a 7-day treatment period. Relative cell growth rate (drug *vs.* vehicle) is presented as mean ± SE (n=6). *B.* Inhibition of β-catenin activity prevents cell growth of MCF7-F. Level of β-catenin protein in whole cell lysate and nuclear fraction was examined by immunoblots. Cell growth rates in the presence of EGCG were determined as in *A*. To examine clonogenic activity, cells were treated with EGCG for two weeks.

Colonies contain more than 50 cells were scored. Relative clonogenic activity (drug *vs.* vehicle) was presented as mean ± SE (n=6). To examine β-catenin transcription activity, cell were transfected with Topflash or Fopflash construct and treated with EGCG for 16 h, as indicated. The transcription activity of β-catenin was presented as the ratio of Topflash against Fopflash.

A

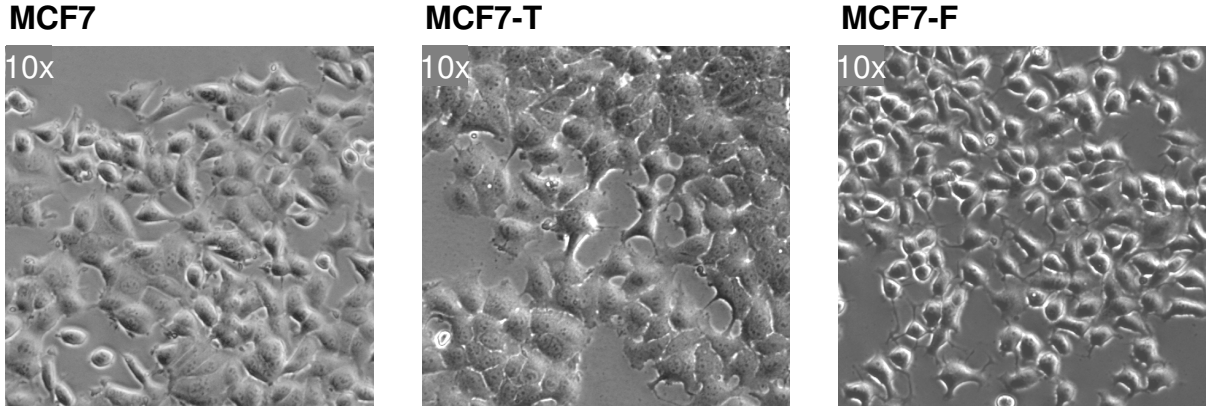

Fan et al., Fig. 1A

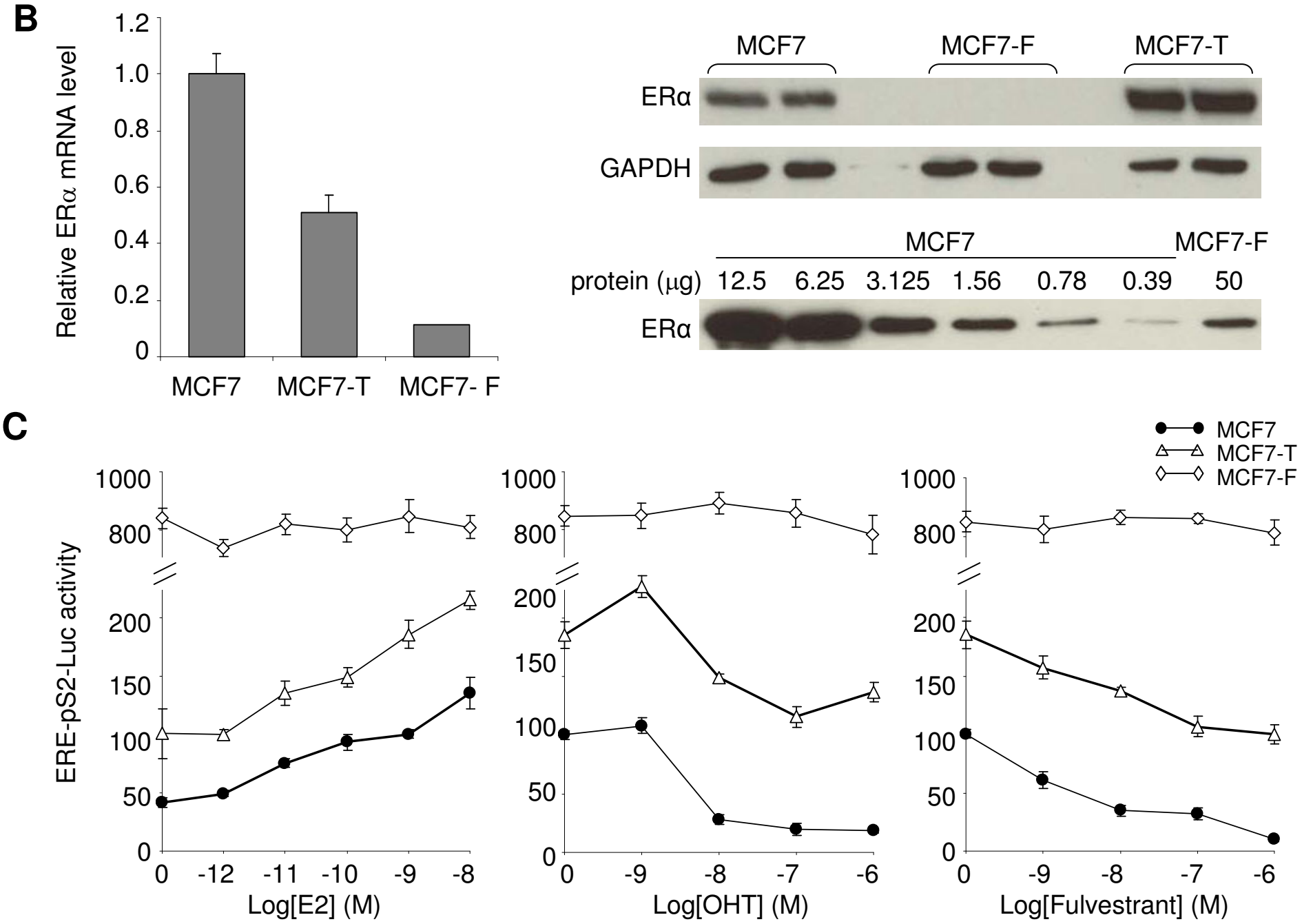

Fan et al., Fig. 1B,C

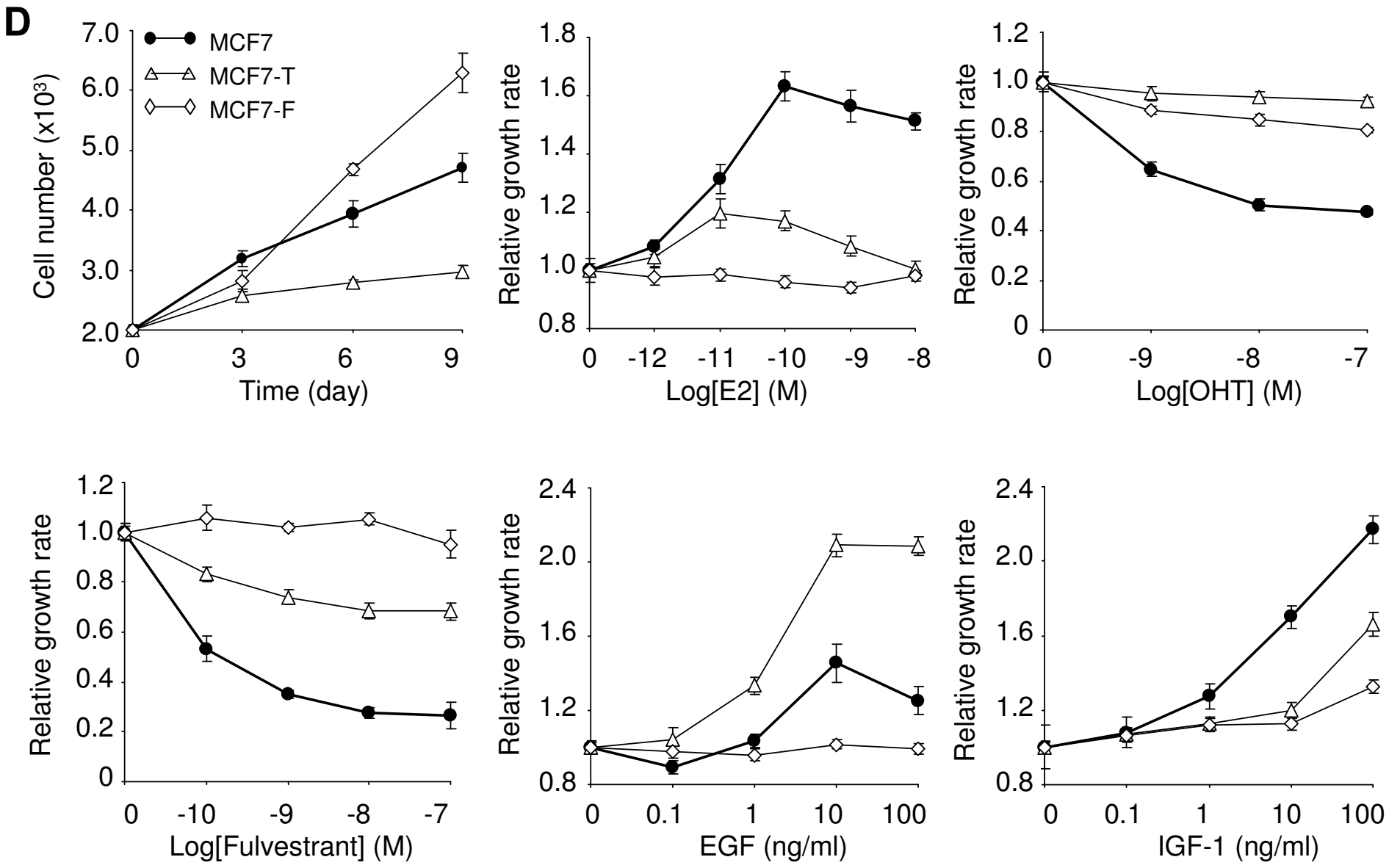

Fan et al., Fig. 1D

A

Genes upregulated by E2

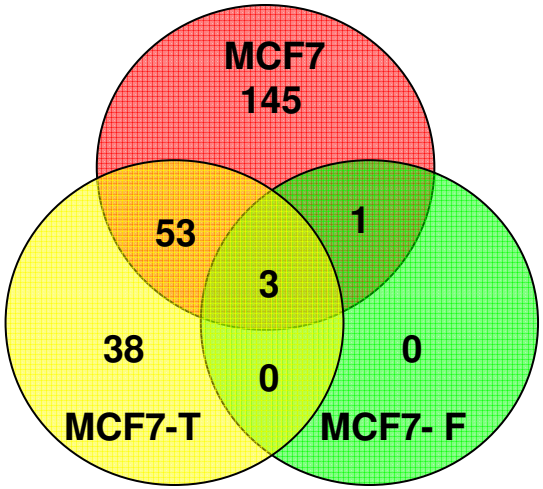

Genes downregulated by E2

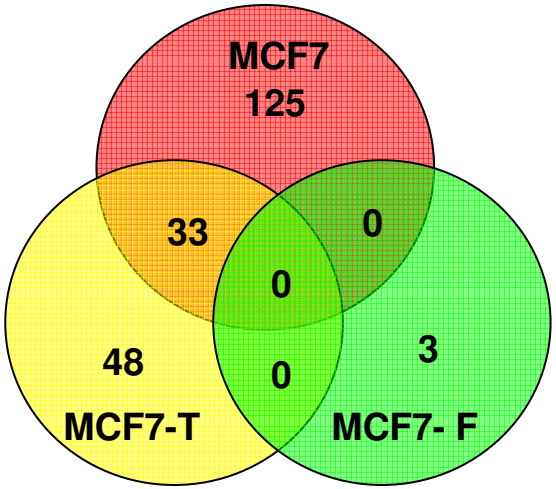

Fan et al., Fig. 2A

B

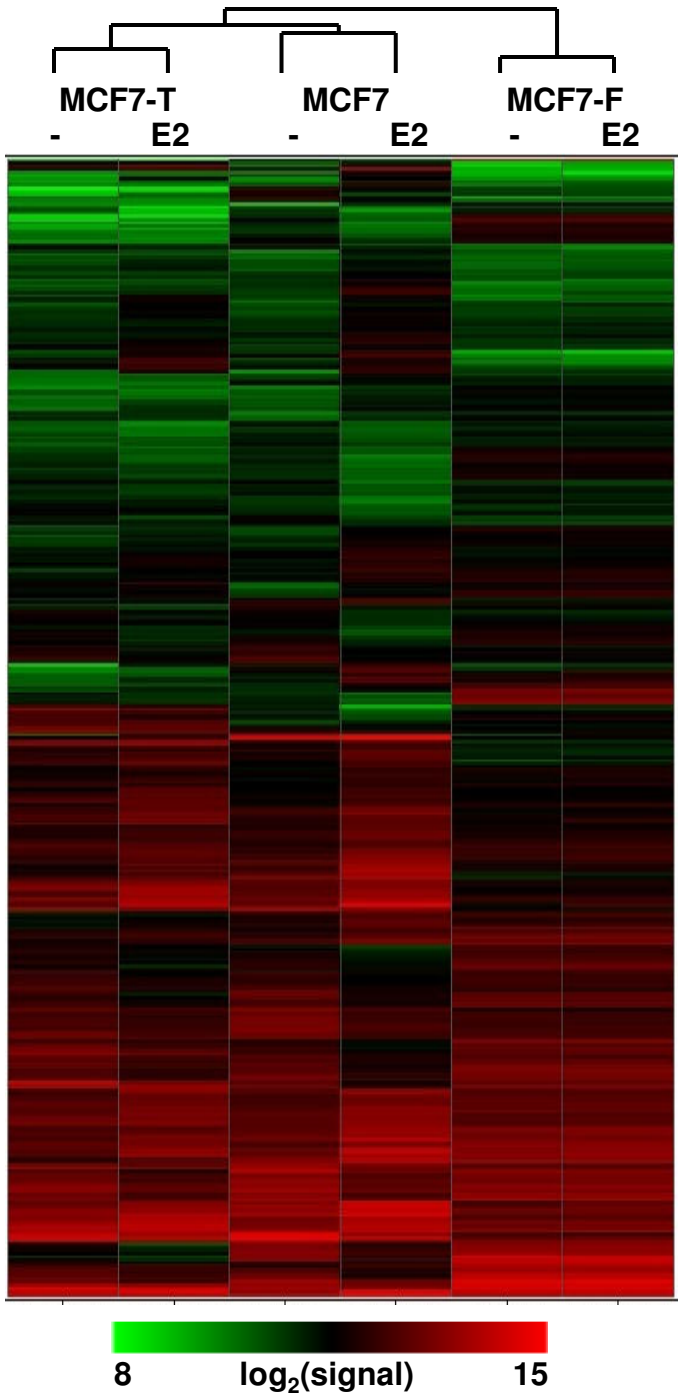

C

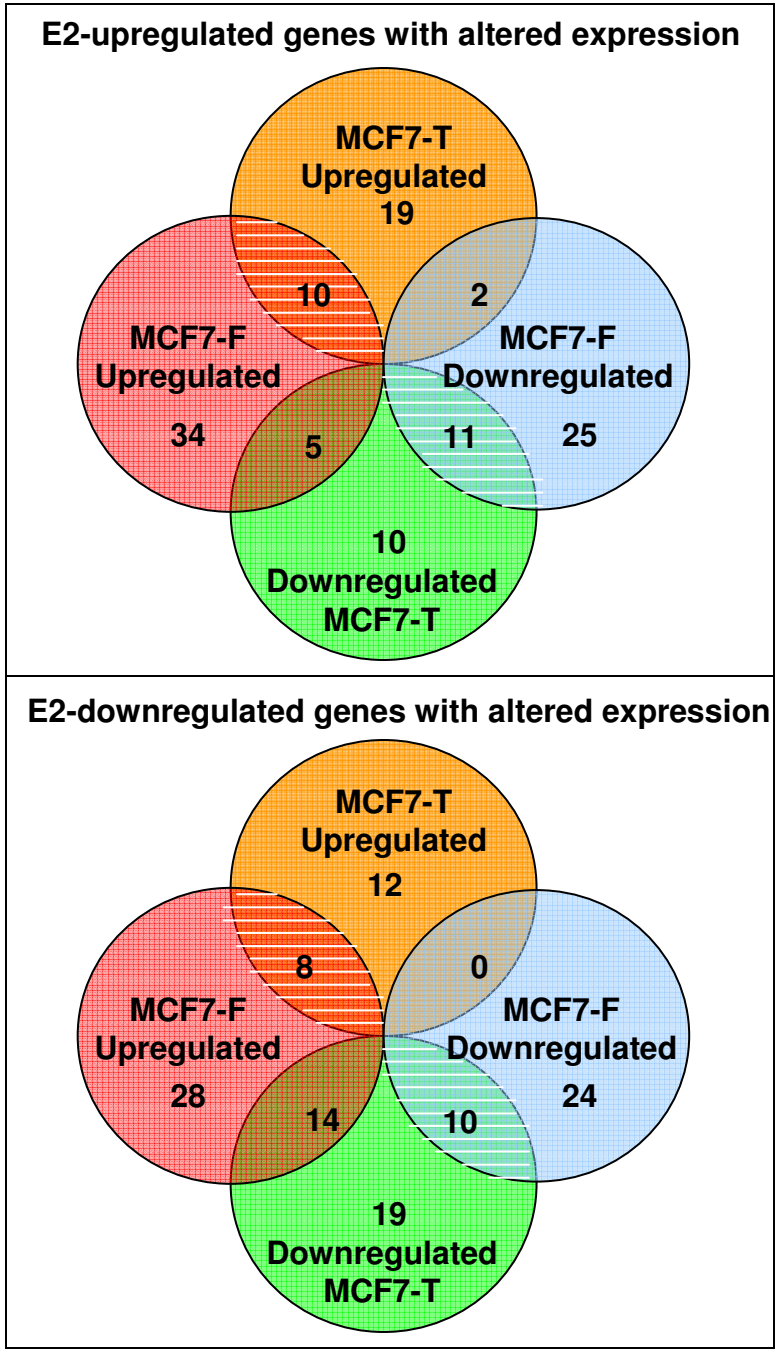

Fan et al., Fig. 2B,C

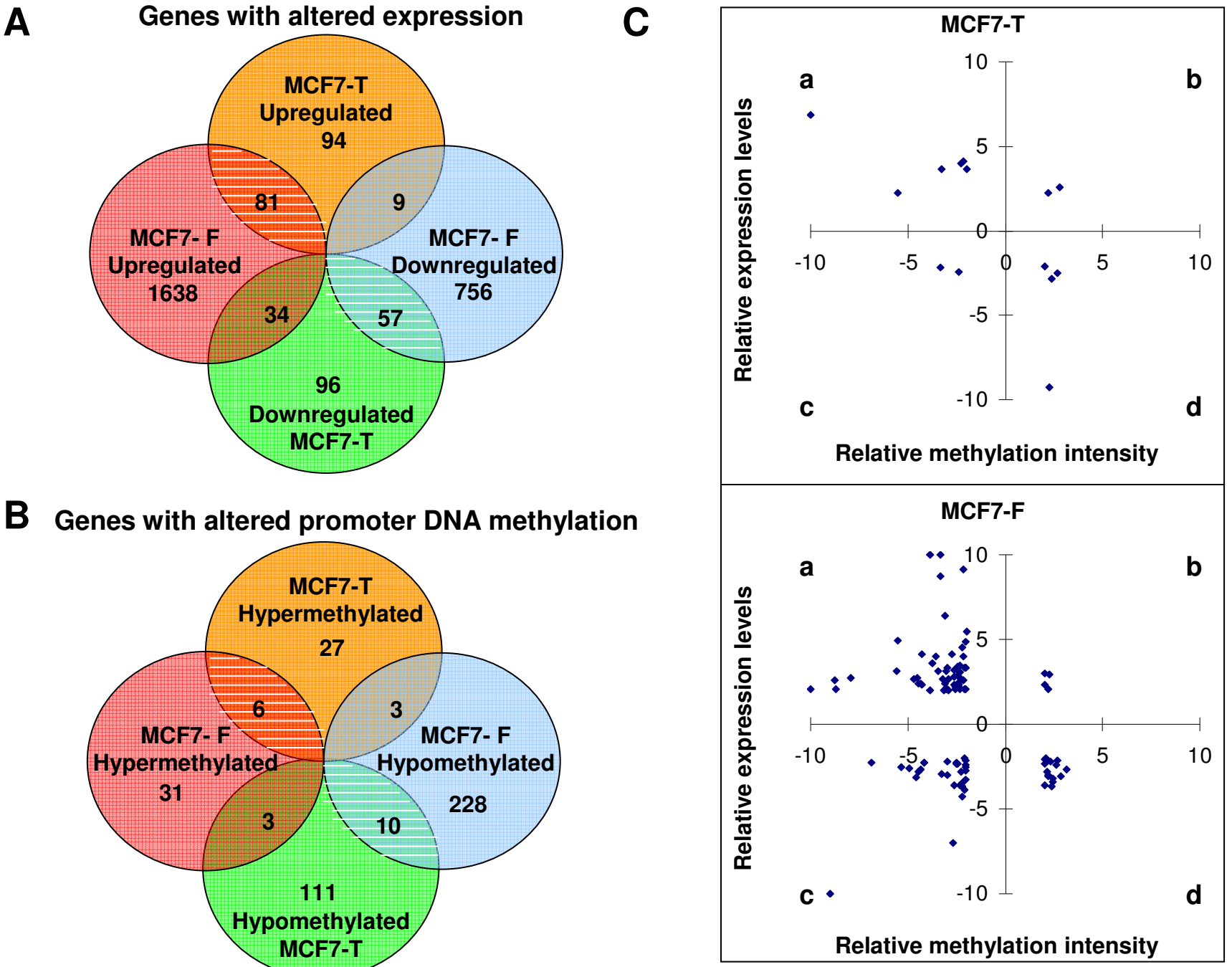

Fan et al., Fig. 3

A

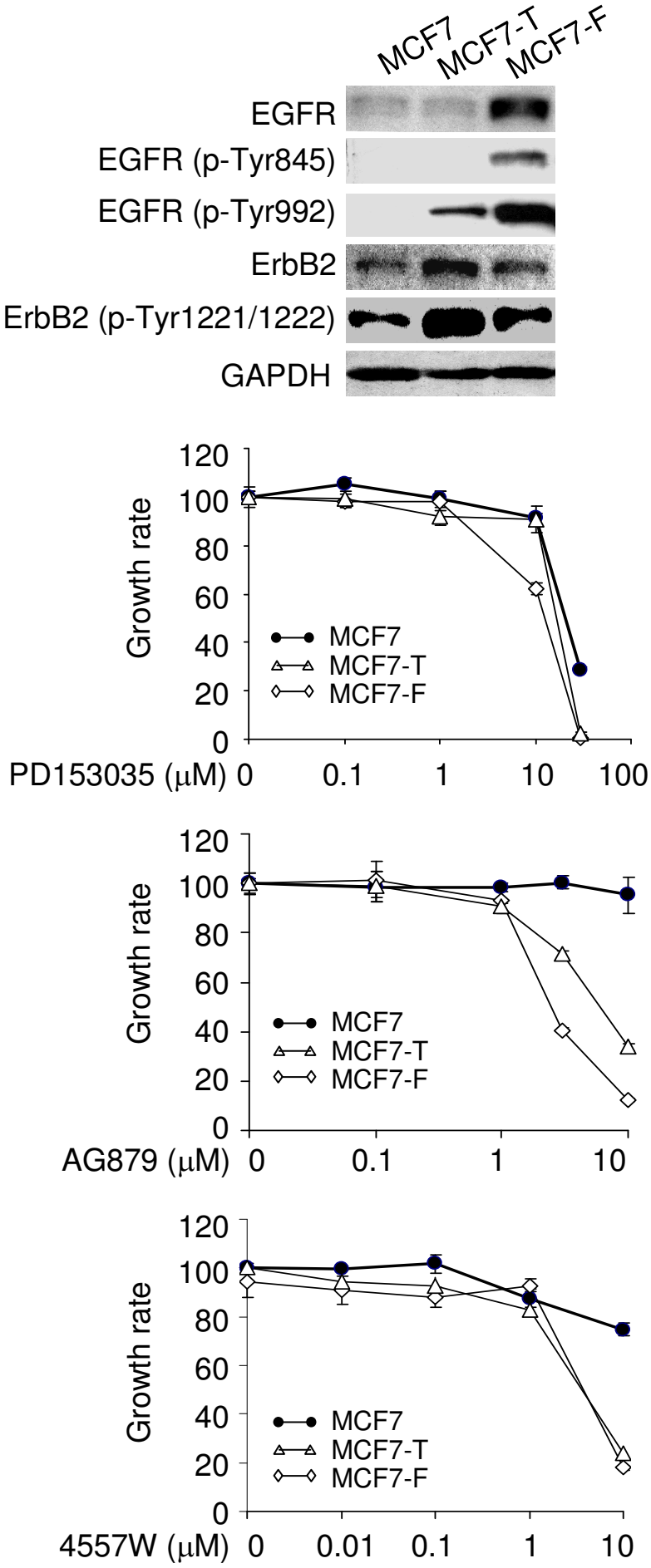

Fan et al., Fig. 4A

B

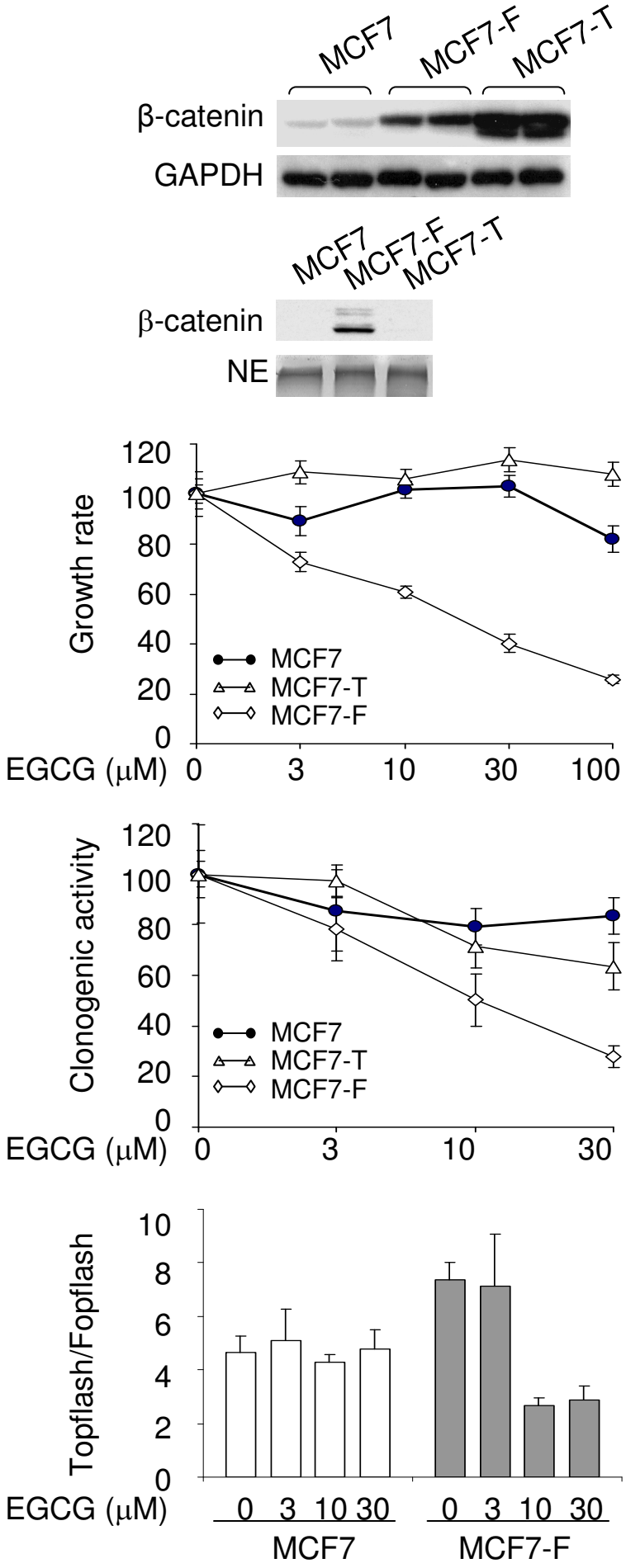

Fan et al., Fig. 4B

Table 1. Cell signaling pathways prominently altered in MCF-T and MCF7-F

		Basal expression (*vs.* MCF7)		
Gene symbol	Genbank	MCF7-T	MCF-F	Description
PKA pathway				
PKIA	NM_181839	-	-4.70	Protein kinase (cAMP-dependent, catalytic) inhibitor alpha
PKIB	NM_181795	-37.26	-33.38	Protein kinase (cAMP-dependent, catalytic) inhibitor beta
PKIG	NM_181805	-2.80	-3.20	Protein kinase (cAMP-dependent, catalytic) inhibitor gamma
PRKACA	NM_002730	-	-2.46	Protein kinase, cAMP-dependent, catalytic, alpha
PRKACB	NM_182948	5.10	4.26	Protein kinase, cAMP-dependent, catalytic, beta
PRKAR2A	NM_004157	-1.54	-2.07	Protein kinase, cAMP-dependent, regulatory, type II, alpha
PRKAR2B	NM_002736	10.39	3.39	Protein kinase, cAMP-dependent, regulatory, type II, beta
Caveolins				
CAV1	NM_001753	-3.56	-1.59	Caveolin 1, caveolae protein, 22kDa
CAV2	NM_198212	-2.53	-2.32	Caveolin 2
Annexins and S100 calcium binding proteins				
ANXA1	NM_000700	-3.04	14.28	Annexin A1
ANXA10	NM_007193	4.65	162.71	Annexin A10
ANXA11	NM_145869	-1.54	-1.88	Annexin A11
ANXA3	NM_005139	-2.25	-1.53	Annexin A3
ANXA4	NM_001153	-1.65	-	Annexin A4
ANXA6	NM_004033	-2.28	-18.63	Annexin A6
ANXA9	NM_003568	-3.52	2.11	Annexin A9
S100A11	NM_005620	-1.79	-2.23	S100 calcium binding protein A11 (calgizzarin)
S100A13	Hs.446592	-4.02	-3.74	S100 calcium binding protein A13
S100A14	NM_020672	-7.11	-3.07	S100 calcium binding protein A14
S100A16	NM_080388	-13.05	-7.30	S100 calcium binding protein A16
S100A4	NM_019554	-2.11	-1.25	S100 calcium binding protein A4
S100A6	NM_014624	-1.97	-2.31	S100 calcium binding protein A6 (calcyclin)
S100P	NM_005980	-4.18	3.40	S100 calcium binding protein P
MAP kinase phosphatase activity				
DUSP23	NM_017823	-1.76	-6.17	Dual specificity phosphatase 23
DUSP4	NM_057158	-4.39	1.23	Dual specificity phosphatase 4
DUSP5	NM_004419	-3.66	-1.26	Dual specificity phosphatase 5
DUSP6	NM_022652	-1.74	3.56	Dual specificity phosphatase 6
Dominant negative helix-loop-helix proteins				
ID1	NM_181353	2.77	2.52	Inhibitor of DNA binding 1, dominant negative helix-loop-helix protein
ID2	NM_002166	-	-2.96	Inhibitor of DNA binding 2, dominant negative helix-loop-helix protein
ID3	NM_002167	2.62	1.25	Inhibitor of DNA binding 3, dominant negative helix-loop-helix protein
ID4	NM_001546	6.86	-	Inhibitor of DNA binding 4, dominant negative helix-loop-helix protein
Epidermal growth factor receptor activity				
EGFR	NM_201284	1.29	3.24	Epidermal growth factor receptor
ERBB2	NM_004448	-	6.61	V-erb-b2 erythroblastic leukemia viral oncogene homolog 2
ERBB3	NM_001982	1.40	7.07	V-erb-b2 erythroblastic leukemia viral oncogene homolog 3 (avian)
TOB1	NM_005749	1.29	-5.03	Transducer of ERBB2, 1
TOB2	NM_016272	-1.34	-3.98	Transducer of ERBB2, 2
Wnt/Frizzled/β-catenin signaling pathway				
WNT11	NM_004626	-	12.64	Wingless-type MMTV integration site family, member 11
WNT5A	NM_003392	11.59	12.91	Wingless-type MMTV integration site family, member 5A
WNT6	NM_006522	-3.47	3.93	Wingless-type MMTV integration site family, member 6
LRP5	NM_002335	-1.17	2.08	Low density lipoprotein receptor-related protein 5
LRP6	NM_002336	-	6.76	Low density lipoprotein receptor-related protein 6
CTNNB1	NM_001904	2.93	4.89	Catenin (cadherin-associated protein), beta 1, 88kDa
FZD7	NM_003507	1.28	2.32	Frizzled homolog 7 (Drosophila)
Notch signaling pathway				
ADAM17	NM_021832	-	9.02	A disintegrin and metalloproteinase domain 17
APH-1A	NM_016022	-	4.94	Anterior pharynx defective 1 homolog A (C. elegans)
JAG1	NM_000214	1.48	5.97	Jagged 1 (Alagille syndrome)
JAG2	NM_145159	3.89	3.09	Jagged 2

Table 1. Cell signaling pathways prominently altered in MCF-T and MCF7-F (continued)

		Basal expression (*vs.* MCF7)		
Gene symbol	Genbank	MCF7-T	MCF-F	Description
Notch signaling pathway				
PSEN1	NM_007319	1.33	7.06	Presenilin 1 (Alzheimer disease 3)
MAML2	NM_032427	-	4.90	Mastermind-like 2 (Drosophila)
NOTCH2	NM_024408	-	3.39	Notch homolog 2 (Drosophila)
NOTCH2NL	Hs.502564	-	6.00	Notch homolog 2 (Drosophila) N-terminal like
Cytokines and cytokine receptors				
ANGPTL4	NM_139314	-	3.60	Angiopoietin-like 4
ANGPTL6	NM_031917	-	10.70	Angiopoietin-like 6
BMPR2	NM_033346	-	3.92	Bone morphogenetic protein receptor, type II (serine/threonine kinase)
CISH	NM_145071	-4.76	-3.03	Cytokine inducible SH2-containing protein
CXCL12	NM_199168	-4.22	1.28	Chemokine (C-X-C motif) ligand 12 (stromal cell-derived factor 1)
CXCR4	Hs.421986	5.15	4.35	Chemokine (C-X-C motif) receptor 4
EFNB2	NM_004093	-4.11	8.50	Ephrin-B2
EGFR	NM_201284	1.29	3.24	Epidermal growth factor receptor
EPHA2	NM_004431	-	5.83	EPH receptor A2
EPHA4	Hs.244624	-1.37	4.39	EphA4
EPHA7	NM_004440	-	23.64	EPH receptor A7
EPHB2	NM_017449	-	9.04	EPH receptor B2
EPHB3	NM_004443	1.23	3.21	EPH receptor B3
EPHB6	NM_004445	1.24	8.92	EPH receptor B6
FGF13	NM_033642	-1.73	-29.30	Fibroblast growth factor 13
FGFR2	NM_023031	-	5.35	Fibroblast growth factor receptor 2
FGFR4	NM_022963	-1.89	-3.82	Fibroblast growth factor receptor 4
FLT3LG	NM_001459	-	4.15	Fms-related tyrosine kinase 3 ligand
GAS6	NM_000820	-	5.45	Growth arrest-specific 6
IFNGR1	NM_000416	-	4.50	Interferon gamma receptor 1
IGF2R	NM_000876	-	4.39	Insulin-like growth factor 2 receptor
IL11RA	NM_147162	-	3.48	Interleukin 11 receptor, alpha
IL13RA1	NM_001560	-1.28	4.16	Interleukin 13 receptor, alpha 1
IL17D	NM_138284	-	-3.20	Interleukin 17D
IL1A	NM_000575	-	3.82	Interleukin 1, alpha
IL1R1	NM_000877	-1.80	-3.44	Interleukin 1 receptor, type I
IL1RAP	NM_134470	-	10.37	Interleukin 1 receptor accessory protein
IL6ST	NM_175767	1.54	3.67	Interleukin 6 signal transducer (gp130, oncostatin M receptor)
IL8	NM_000584	-	3.31	Interleukin 8
INHBB	NM_002193	-5.74	-3.73	Inhibin, beta B (activin AB beta polypeptide)
KITLG	NM_003994	-	5.74	KIT ligand
LIFR	NM_002310	-	13.72	Leukemia inhibitory factor receptor
OSMR	NM_003999	3.69	5.61	Oncostatin M receptor
SOCS2	NM_003877	-	-3.60	Suppressor of cytokine signaling 2
SOCS3	NM_003955	-	-3.42	Suppressor of cytokine signaling 3
SOCS6	NM_004232	-3.03	1.28	Suppressor of cytokine signaling 6
TGFA	NM_003236	-5.94	2.47	Transforming growth factor, alpha
TGFB1I1	NM_015927	3.28	1.27	Transforming growth factor beta 1 induced transcript 1
TGFB2	NM_003238	-1.41	-3.45	Transforming growth factor, beta 2
TGFBR2	NM_003242	-2.00	4.31	Transforming growth factor, beta receptor II (70/80kDa)
TGFBR3	NM_003243	4.14	4.36	Transforming growth factor, beta receptor III (betaglycan, 300kDa)
TNFAIP2	NM_006291	1.27	3.89	Tumor necrosis factor, alpha-induced protein 2
TNFAIP8	NM_014350	-	3.09	Tumor necrosis factor, alpha-induced protein 8
TNFRSF10B	NM_147187	1.31	5.04	Tumor necrosis factor receptor superfamily, member 10b
TNFRSF11B	NM_002546	-8.70	4.38	Tumor necrosis factor receptor superfamily, member 11b (osteoprotegerin)
TNFRSF12A	NM_016639	-3.38	2.02	Tumor necrosis factor receptor superfamily, member 12A
TNFRSF19	NM_148957	-21.63	-13.63	Tumor necrosis factor receptor superfamily, member 19
TNFRSF1A	NM_001065	-	4.67	Tumor necrosis factor receptor superfamily, member 1A
TNFRSF21	NM_016629	-2.97	8.53	tumor necrosis factor receptor superfamily, member 21
TNFRSF25	NM_148974	3.14	5.38	Tumor necrosis factor receptor superfamily, member 25
TNFSF10	NM_003810	-	11.22	Tumor necrosis factor (ligand) superfamily, member 10
TNFSF13	NM_172089	-4.23	-7.18	Tumor necrosis factor (ligand) superfamily, member 12
VEGF	NM_003376	1.20	3.05	Vascular endothelial growth factor

Table 2. Genes with altered expression and promoter methylation in MCF7-T and MCF7-F cells

Gene symbol	Location of methylated loci	Expression level (*vs.* MCF7)	Methylation intensity (*vs.* MCF7)	Description
Overexpressed and hypomethylated in MCF7-T				
CDH2	NM_001792, CDH2:-312	4.14	-2.137	Cadherin 2, type 1, N-cadherin (neuronal)
DIAPH2	NM_007309, DIAPH2:-74	3.64	-3.247	Early lymphoid activation protein
E2F7	NM_203394, E2F7:-116	2.22	-5.525	E2F transcription factor 7
ID4	NM_001546, ID4:247	6.86	-10.000	Inhibitor of DNA binding 4
PCSK9	NM_174936, PCSK9:-28	3.63	-2.004	Proprotein convertase subtilisin/kexin type 9
PRTFDC1	NM_020200, PRTFDC1:-423	3.96	-2.288	Phosphoribosyl transferase domain containing 1
Downregulated and hypermethylated in MCF7-T				
GALNT10	NM_198321, GALNT10:-7	-2.53	2.683	UDP-N-acetyl-alpha-D-galactosamine:polypeptide N-acetylgalactosaminyltransferase 10
NR2F2	NM_021005, NR2F2:-200	-2.12	2.008	Nuclear receptor subfamily 2, group F, member 2
PLEKHA9	NM_015899, PLEKHA9:-51	-2.82	2.363	Pleckstrin homology domain containing, A8
SCUBE2	NM_198473, SCUBE2:-88	-9.30	2.255	Signal peptide, CUB domain, EGF-like 2
Overexpressed and hypomethylated in MCF7-F				
ANXA4	NM_001153, ANXA4:-218	2.04	-2.045	Annexin A4
AP3M2	NM_006803, AP3M2:-438	2.30	-2.451	Adaptor-related protein complex 3, mu 2 subunit
APG9L1	NM_018089, APG9L1:-307	2.18	-2.584	APG9 autophagy 9-like 1 (S. cerevisiae)
APPL	NM_012096, APPL:-43	2.13	-2.320	Adaptor protein containing pH, PTB, and leucine zipper 1
ASB3	NM_015701, ASB3:-146	2.63	-8.772	Ankyrin repeat and SOCS box-containing 3
ASPH	NM_032466, ASPH:-485	4.03	-2.165	Aspartate beta-hydroxylase
ATXN7	NM_025075, ATXN7:-788	2.87	-2.451	Ataxin 7
CBLB	NM_170662, CBLB:-319	2.64	-2.294	Cas-Br-M ecotropic retroviral transforming sequence b
CDW92	NM_080546, CDW92:-128	3.38	-2.427	CDW92 antigen
CENPJ	NM_018451, CENPJ:-279	3.13	-2.370	Centromere protein J
CHD1	NM_001270, CHD1:-1866	2.64	-3.226	Chromodomain helicase DNA binding protein 1
CKAP4	NM_006825, CKAP4:-204	2.39	-4.310	Cytoskeleton-associated protein 4
CORO2A	NM_052820, CORO2A:-219	2.07	-10.000	Coronin, actin binding protein, 2A
CTNNB1	NM_001904, CTNNB1:-49	4.89	-2.049	Catenin (cadherin-associated protein), beta 1, 88kDa
CXCL16	NM_032265|, CXCL16:-174	2.10	-2.591	Chemokine (C-X-C motif) ligand 16
CYB561	NM_001915, CYB561:-225	3.46	-2.342	Cytochrome b-561
CYHR1	NM_145754, CYHR1:-184	2.16	-3.021	Cysteine/histidine-rich 1
EDIL3	NM_005711, EDIL3:-87	10.00	-3.861	EGF-like repeats and discoidin I-like domains 3
FBXL13	NM_031905, FBXL13:-258	2.57	-2.174	F-box and leucine-rich repeat protein 13
FLJ10052	NM_017982, FLJ10052:-476	4.13	-4.274	Sushi domain containing 4
FRAS1	NM_032863, FRAS1:-617	8.74	-3.344	Fraser syndrome 1
GGH	NM_003878, GGH:-423	2.67	-4.695	Gamma-glutamyl hydrolase
GPAM	NM_020918, GPAM:-206	3.05	-2.353	Glycerol-3-phosphate acyltransferase, mitochondrial
GPR51	NM_005458, GPR51:-86	5.45	-2.004	G protein-coupled receptor 51
HIAT1	NM_033055, HIAT1:-203	2.36	-2.618	Hippocampus abundant transcript 1
ITGB1	NM_002211, ITGB1:-48	6.42	-3.115	Integrin, beta 1
ITGB5	NM_002213, ITGB5:-580	3.34	-2.985	Integrin, beta 5
ITM2B	NM_021999, ITM2B:-287	2.08	-3.058	Integral membrane protein 2B
KIFC2	NM_145754, KIFC2:-704	3.12	-3.021	Kinesin family member C2
LRP6	NM_002336, LRP6:-482	2.73	-7.937	Low density lipoprotein receptor-related protein 6
MGC43690	NM_182552, MGC43690:-323	4.01	-3.546	WD repeat domain 27
NAPE	NM_198990, NAPE-PLD:-217	2.68	-2.899	N-acyl-phosphatidylethanolamine-hydrolyzing phospholipase D
NCKAP1	NM_205842, NCKAP1:-177	2.03	-2.899	NCK-associated protein 1
NR1D2	NM_005126, NR1D2:-63	2.47	-2.364	Nuclear receptor subfamily 1, group D, member 2
P2RY2	NM_002564, P2RY2:-115	3.21	-2.653	Purinergic receptor P2Y, G-protein coupled, 2
PAQR3	NM_177453, PAQR3:-141	2.79	-2.604	Progestin and adipoQ receptor family member III
PLCG2	NM_002661, PLCG2:-21	2.01	-3.846	Phospholipase C, gamma 2 (phosphatidylinositol-specific)
PPT2	NM_030651, PPT2:-2776	3.16	-3.460	Palmitoyl-protein thioesterase 2
PSIP1	NM_033222, PSIP1:-659	4.12	-2.740	PC4 and SFRS1 interacting protein 1
RAB24	NM_013237, RAB24:-191	2.05	-2.320	RAB24, member RAS oncogene family
RBM11	NM_144770, RBM11:-174	9.11	-2.151	RNA binding motif protein 11
RCOR3	NM_018254, RCOR3:-586	3.33	-2.110	REST corepressor 3
RYK	NM_002958, RYK:-20	3.35	-2.016	RYK receptor-like tyrosine kinase
SFRS15	NM_020706, SFRS15:-29	3.11	-5.587	Splicing factor, arginine/serine-rich 15
SMYD2	NM_020197, SMYD2:-289	4.93	-5.525	SET and MYND domain containing 2

Table 2. Genes with altered expression and promoter methylation in MCF7-T and MCF7-F cells (continued)

Gene symbol	Location of methylated loci	Expression level *(vs.* MCF7)	Methylation intensity *(vs.* MCF7)	Description
Overexpressed and hypomethylated in MCF7-F				
SS18L1	NM_002792, SS18L1:-729	2.07	-8.696	Synovial sarcoma translocation gene on ch18-like 1
TAF1C	NM_139174|, TAF1C:-114	3.58	-3.731	TBP-associated factor, RNA polymerase I, C,
TM7SF1	NM_003272, TM7SF1:-1135	2.36	-4.255	Transmembrane 7 superfamily member 1
TMPO	NM_003276, TMPO:-98	2.75	-4.484	Thymopoietin
TNFRSF12A	NM_016639, TNFRSF12A:-240	2.02	-3.145	Tumor necrosis factor receptor superfamily, 12A
TRPC1	NM_003304, TRPC1:-46	2.42	-4.464	Transient receptor potential cation channel, C 1
USP31	NM_020718, USP31:-101	4.56	-2.208	Ubiquitin specific protease 31
VKORC1L1	NM_173517, VKORC1L1:-218	3.35	-2.008	Vitamin K epoxide reductase complex, subunit 1-like 1
WDR10	NM_003925, WDR10:-472	2.04	-2.075	WD repeat domain 10
WNT11	NM_004626, WNT11:-3989	10.00	-3.333	Wingless-type MMTV integration site family, member 11
XRN1	NM_019001, XRN1:-43	2.34	-2.392	5'-3' exoribonuclease 1
ZDHHC9	NM_016032, ZDHHC9:-510	2.42	-3.106	Zinc finger, DHHC-type containing 9
Downregulated and hypermethylated in MCF7-F				
BXDC1	NM_032194, BXDC1:-193	-2.22	2.321	Brix domain containing 1
CREB3L4	NM_014437, CREB3L4:-455	-3.58	2.057	CAMP responsive element binding protein 3-like 4
EPPB9	NM_015681, EPPB9:-480	-2.64	3.142	B9 protein
FLJ12671	NM_015997, FLJ12671:-518	-2.00	2.07	Interferon stimulated exonuclease gene 20kDa-like 2
HDGF	NM_004494, HDGF:344	-3.10	2.859	Hepatoma-derived growth factor
MAZ	NM_007317, MAZ:-1107	-2.15	2.664	MYC-associated zinc finger protein
MRPL23	NM_021134, MRPL23:42	-3.43	2.457	Mitochondrial ribosomal protein L23
PCMT1	NM_005389, PCMT1:-134	-2.83	2.166	Protein-L-isoaspartate (D-aspartate) O-methyltransferase
PIK3R3	NM_003629, PIK3R3:-170	-2.98	2.216	Phosphoinositide-3-kinase, regulatory subunit 3
PLSCR3	NM_020360, PLSCR3:-169	-3.68	2.391	Phospholipid scramblase 3
POLR2J	NM_006234, POLR2J:-327	-2.09	2.032	Polymerase (RNA) II (DNA directed) polypeptide J
PTS	NM_000317, PTS:-67	-3.19	2.426	6-pyruvoyltetrahydropterin synthase
PYCARD	NM_013258, PYCARD:295	-3.04	2.239	PYD and CARD domain containing
QIL1	NM_205767, QIL1:208	-2.32	2.025	QIL1 protein
THAP5	NM_012328, THAP5:-37	-2.41	2.647	THAP domain containing 5

THE JOURNAL OF BIOLOGICAL CHEMISTRY VOL. 281, NO. 14, pp. 9607–9615, April 7, 2006

Fulvestrant (ICI 182,780)-dependent Interacting Proteins Mediate Immobilization and Degradation of Estrogen Receptor-α*

Received for publication, October 4, 2005, and in revised form, February 2, 2006 Published, JBC Papers in Press, February 3, 2006, DOI 10.1074/jbc.M510809200

Xinghua Long[‡] **and Kenneth P. Nephew**[‡§¶1]

From the [‡]*Medical Sciences, Indiana University School of Medicine, Bloomington, Indiana 47405 and* [§]*Department of Cellular and Integrative Physiology, Indiana University School of Medicine and* [¶]*Indiana University Cancer Center, Indianapolis, Indiana 46202*

The antiestrogen fulvestrant (ICI 182,780) causes immobilization of estrogen receptor-α (ERα) in the nuclear matrix accompanied by rapid degradation by the ubiquitin-proteasome pathway. In this study we tested the hypothesis that fulvestrant induces specific nuclear matrix protein-ERα interactions that mediate receptor immobilization and turnover. A glutathione *S*-transferase (GST)-ERα-activating function-2 (AF2) fusion protein was used to isolate and purify receptor-interacting proteins in cell lysates prepared from human MCF-7 breast cancer cells. After SDS-PAGE and gel excision, mass spectrometry was used to identify two major ERα-interacting proteins, cytokeratins 8 and 18 (CK8·CK18). We determined, using ERα-activating function-2 mutants, that helix 12 (H12) of ERα, but not its F domain, is essential for fulvestrant-induced ERα-CK8 and CK18 interactions. To investigate the *in vivo* role of H12 in fulvestrant-induced ERα immobilization/degradation, transient transfection assays were performed using wild type ERα, ERα with a mutated H12, and ERα with a deleted F domain. Of those, only the ERα H12 mutant was resistant to fulvestrant-induced immobilization to the nuclear matrix and protein degradation. Fulvestrant treatment caused ERα degradation in CK8·CK18-positive human breast cancer cells, and CK8 and CK18 depletion by small interference RNAs partially blocked fulvestrant-induced receptor degradation. Furthermore, fulvestrant-induced ERα degradation was not observed in CK8 or CK18-negative cancer cells, suggesting that these two intermediate filament proteins are necessary for fulvestrant-induced receptor turnover. Using an ERα-green fluorescent protein construct in fluorescence microscopy revealed that fulvestrant-induced cytoplasmic localization of newly synthesized receptor is mediated by its interaction with CK8 and CK18. In summary, this study provides the first direct evidence linking ERα immobilization and degradation to the nuclear matrix. We suggest that fulvestrant induces ERα to interact with CK8 and CK18, drawing the receptor into close proximity to nuclear matrix-associated proteasomes that facilitate ERα turnover.

Estrogen receptor-α (ERα),[2] a member of the nuclear receptor family, is a ligand-dependent transcription factor that mediates physiological responses to its cognate ligand, 17β-estradiol (E2), in estrogen target tissues such as the breast, uterus, and bone (1). Because ERα is a short-lived protein (half-life of 4–5 h), its cellular levels are strictly regulated (2). Although ERα turnover is a continuous process (2), dynamic fluctuations in receptor levels, mediated primarily by the ubiquitin-proteasome pathway (3–6), occur in response to changing cellular conditions (7–9). In addition, differing ligands have been demonstrated to exert differential effects on steady-state levels of ERα (10, 11). For example, E2 and the "pure" ERα antagonists (*i.e.* ICI 164,384, ICI 182,780, RU 58,668, and ZK-703) (12, 13) induce receptor turnover, whereas the "partial" agonist/antagonist 4-hydroxytamoxifen (4-OHT) stabilizes ERα (14, 15). E2-mediated ERα degradation is dependent on transcription, coactivator recruitment, and new protein synthesis, whereas ICI-induced degradation of ERα is independent of these processes (16–18). Thus, although both E2 and pure antiestrogens induce ERα degradation, their mechanisms of action differ markedly.

In addition to altering ERα stability and turnover, different ligands have been shown to have profoundly distinct effects on receptor mobility and cellular localization. For example, ERα was found localized exclusively in the nucleus after E2 and 4-OHT treatment, whereas ICI caused both nuclear and cytoplasmic receptor localization (13, 19). Stenoien *et al.* (20), using fluorescence recovery after photobleaching, demonstrated that E2, 4-OHT, and ICI treatment resulted in reduced nuclear mobility of ERα tagged with cyan fluorescent protein (20). In that study complete fluorescence recovery was not observed after ICI treatment due to immobilization of ERα to the nuclear matrix (20). Additional studies have further shown a rapid immobilization of the ERα-ICI complex within the nuclear matrix, with sequestration in a salt-insoluble, nuclear compartment (21, 22), although the precise nature of the receptor-nuclear matrix interaction remains unknown.

Fulvestrant (faslodex, ICI 182,780) belongs to a new class of antihormonal therapy for advanced breast cancer called selective estrogen receptor down-regulators (SERDs) (23, 24). SERDs act as potent antagonists by inducing rapid receptor turnover and display no agonist activity in estrogen target tissues. SERDs differ markedly from the class of molecules called selective estrogen receptor modulators (SERMs), such as 4-OHT, that function as either agonists or antagonists, depending upon the target tissue (24). The pure antagonistic property of fulvestrant is due to a steroidal structure containing a long bulky side chain (25), which induces a distinct conformational change in the ligand binding domain of ERα (26), specifically in the position of helix 12 (H12), to prevent receptor dimerization and binding to DNA (27). Because specific mutations in H12 can reverse the pure antiestrogenic properties of fulvestrant (28, 29), H12 may contribute to fulvestrant-induced ERα degradation.

* This work was supported by The American Cancer Society Research and Alaska Run for Women Grant TBE-104125 and the United States Army Medical Research Acquisition Activity Awards DAMD 17-02-1-0418 and -0419. The costs of publication of this article were defrayed in part by the payment of page charges. This article must therefore be hereby marked "*advertisement*" in accordance with 18 U.S.C. Section 1734 solely to indicate this fact.

[1] To whom correspondence should be addressed: Medical Sciences, Indiana University School of Medicine, 302 Jordan Hall, 1001 E. 3rd St., Bloomington, IN 47405-4401. Tel.: 812-855-9445; Fax: 812-855-4436; E-mail: knephew@indiana.edu.

[2] The abbreviations used are: ERα, estrogen receptor-α; CK, cytokeratin; E2, 17β-estradiol; GFP, green fluorescent protein; ICI, ICI 182,780; 4-OHT, 4-hydroxytamoxifen; siRNA, small interference RNA; SERD, selective estrogen receptor down-regulator; GAPDH, glyceraldehyde phosphate dehydrogenase; GST, glutathione *S*-transferase; AF2, activating function-2; wt, wild type; H12, helix 12.

In this study the mechanism of fulvestrant-induced ERα degradation by the ubiquitin-proteasome pathway was investigated. We show that this SERD induces specific ERα cytokeratins CK8·CK18 interactions, the major intermediate filament proteins found in the nuclear matrix and cytoplasm of ERα-positive breast cancer cell lines (30). We further demonstrate that H12 is essential for these cytokeratin interactions and, subsequently, receptor immobilization within the nuclear matrix. Furthermore, we show that fulvestrant-mediated receptor degradation and cytoplasmic localization correlate directly with CK8 and CK18 levels in breast cancer cells. Because proteasomes have been shown to be associated primarily with intermediate filaments (31–33), we suggest that fulvestrant induces specific receptor-cytokeratin interactions in the nuclear matrix, bringing ERα into close proximity to proteasomes for subsequent degradation.

EXPERIMENTAL PROCEDURES

Materials—The following antibodies and reagents were used in this study: anti-ERα (HC20; Santa Cruz Biotechnology, Inc., Santa Cruz, CA) or monoclonal anti-human ERα (Chemicon International, Inc., Temecula, CA); monoclonal anti-human cytokeratin 8 (RCK102; BD Biosciences) and monoclonal anti-human cytokeratin 18 (RCK106; BD Biosciences); monoclonal anti-cytokeratin peptide 8 (Sigma); mouse anti-glyceraldehyde phosphate dehydrogenase (GAPDH) (Chemicon International); glutathione-Sepharose 4 Fast Flow beads (Amersham Biosciences); SuperSignal West Pico chemiluminescent substrate (Pierce); protease inhibitor mixture set III (Calbiochem-Novabiochem); Lipofectamine Plus reagent, Geneticin, and cell culture reagents (Invitrogen); FuGENE (Roche Applied Science); 4-OHT and MG132 (Sigma); ICI 182,780 (Tocris Cookson Ltd., Ellisville, MO); RNase-free DNase I and BL21 (DE3)pLysS competent cells (Promega, Madison, WI).

Plasmid Construction—Wild type ERα pSG5-ERα(HEGO) was kindly provided by Dr. Pierre Chambon (Institut de Génétique et de Biologie Moléculaire et Cellulaire, Strasbourg, France) and GFP-ERα (26) by Dr. Michael Mancini (Baylor College of Medicine, Houston, TX). The ERα helix 12 mutant pRST-7-hER3X (D538N/E542Q/D545N) was kindly provided by Donald McDonnell (Duke University, Durham, NC). pGEX-6P-1-AF2, pGEX-6P-1-AF2ΔF, pGEX-6P-1-AF2ΔFΔH12, and pGEX-6P-1-ERα3X-AF2 were constructed by inserting the PCR DNA fragment of interest into pGEX-6P-1 (BamHI and XhoI site). pcDNA3-ERαΔF, pcDNA3-ERα3XΔF, and pcDNA3-ERαΔFΔH12 were generated by inserting the specific PCR DNA fragment into pcDNA3MycHisA (BamHI and XhoI site). pcDNA3-CK8 was generated by inserting the CK8 PCR DNA fragment into pcDNA3MycHisA (BamHI and XhoI site). pcDNA3-CK18 was generated by inserting CK18 PCR DNA fragment into pcDNA3MycHisA (EcoRI and XhoI site). Cloning results were confirmed by subjecting all constructs to DNA sequencing.

Cell Lines—The human cervical carcinoma HeLa cell line and the breast cancer cell lines MCF-7 and its daughter, C4-12 (ERα-negative, CK8- and 18-positive (34)), are routinely maintained in our laboratory, as described previously (9, 35). MDA-MB-231 and T47D breast cancer cells were purchased from ATCC (Manassas, VA). MDA-MB-231 cells were maintained in Dulbecco's modified Eagle's medium with 50 units/ml penicillin, 50 μg/ml streptomycin, 10 mM Hepes, 6 ng/ml insulin, and 10% fetal bovine serum. T47D cells were maintained in RPMI 1640 medium 2 mM L-glutamine, 1.0 mM sodium pyruvate, 50 units/ml penicillin, 50 μg/ml streptomycin, 10 mM Hepes, 0.2 units/ml insulin, and 10% fetal bovine serum. Before experiments involving transient transfection and hormone treatment, cells were cultured in hormone-free medium (phenol red-free minimum Eagle's medium (MEM) with 5% charcoal-stripped fetal bovine serum) for 3 days.

Stable Transfection of ERα—C4-12 or HeLa cells were transfected with pcDNA-ERα (C4-12/ERα and HeLa/ERα, respectively) using Lipofectamine Plus Reagent and exposed to antibiotic (G418; 0.5 mg/ml) for 3 weeks. Expression of ERα in G418-resistant colonies was verified by immunoblotting with anti-ERα.

Transient Transfection Assay—T47D and HeLa cells were cultured in hormone-free medium for 3 days and transfected with equal amounts of total plasmid DNA (adjusted by the corresponding empty vectors) using Lipofectamine Plus reagent or FuGENE according to the manufacturer's guidelines. Five hours later, the DNA/Lipofectamine mixture was removed, and cells were cultured in hormone-free medium. Unless stated otherwise, 24 h after transfection, cells were treated with the specified drug.

RNA Interference (siRNA)—siRNA transfection reagent, control siRNA, CK8 siRNA, and CK18 siRNA were purchased from Santa Cruz Biotechnology. The CK8 and CK18 siRNAs (singly or both) were transfected into MCF-7 cells according to the manufacturer's protocol; 72 h after transfections, cells were treated with 100 nM ICI 182,780. Whole cell lysates were prepared in 1× SDS sample buffer. Protein levels were examined by Western blotting using specific antibodies.

Preparation of Whole Cell Extracts—Whole cell extracts were prepared by suspending cells in SDS lysis buffer (62 mM Tris, pH 6.8, 2% SDS, 10% glycerol, and protease inhibitor mixture III). After 15 min of incubation on ice, extracts were sonicated, insoluble materials were removed by centrifugation (15 min at 12,000 × *g*), and supernatant protein concentrations were determined using a Bio-Rad protein assay kit.

Preparation of Nuclear Extracts and Nuclear Matrix—Nuclear extract was prepared using a nuclear extraction kit (Active Motif, Carlsbad, CA), according to the manufacturer's protocol. Nuclear matrix was prepared following the procedure described by Coutts *et al.* (30). Briefly, cell nuclei were extracted with nuclear matrix buffer (100 mM NaCl, 300 mM sucrose, 10 mM Tris-HCl, pH 7.4, 2 mM $MgCl_2$, 1% (v/v) thiodiglycol) containing 1 mM phenylmethylsulfonyl fluoride and 0.5% (v/v) Triton X-100. Nuclei were resuspended in digestion buffer (50 mM NaCl, 300 mM sucrose, 10 mM Tris-HCl, pH 7.4, 3 mM $MgCl_2$, 1% (v/v) thiodiglycol, 0.5% (v/v) Triton X-100), digested with DNase I (168 units/ml) for 20 min at room temperature, and then sequentially extracted using 0.25 M ammonium sulfate and 2 M NaCl. Nuclear matrix was resuspended in 1× SDS sample buffer and sonicated.

Western Blot and Quantitation—Whole cell lysates were prepared in 1× SDS sample buffer by sonication, and total protein was separated by SDS-PAGE and transferred to polyvinylidene difluoride membranes. ERα levels were determined by Western blot using a LI-COR (Lincoln, NE) imaging system. The membrane was incubated with primary antibody followed by incubation with infrared dye IR800-labeled goat anti-mouse IgG or IR700-labeled goat anti-rabbit IgG (LI-COR) secondary antibodies and quantitated with LI-COR Odyssey software. For immunoblotting by enhanced chemiluminescence (ECL), primary antibody was detected by horseradish peroxidase-conjugated second antibody and visualized using an enhanced SuperSignal West Pico chemiluminescent substrate.

GST Pull-down Assay—GST pull-down assays were performed as we have described previously (35, 36). To fuse ERα-AF2 with GST, an ERαAF2 PCR fragment (amino acids 297–595) was cloned into the BamHI and XhoI sites of the plasmid pGEX-6P-1 and subjected to DNA sequencing to confirm the correct reading frame. The GST-tagged AF2 was then expressed in BL21 cells and purified as described (36, 37).

Briefly, overnight cultures of BL21 cells containing the plasmid pGEX-6P-1-GST-ERα-AF2 were diluted (1:20), cultured in fresh medium for 2 h, and treated with 0.1 mM isopropyl β-D-thiogalactoside for 3 h. Induced bacteria were then collected by centrifugation and lysed in NETN buffer containing 0.5% Nonidet P-40, 1 mM EDTA, 20 mM Tris, pH 8.0, 100 mM NaCl, and protease inhibitors. GST-ERα-AF2 was purified on glutathione-Sepharose 4 Fast Flow beads (Amersham Biosciences). MCF-7 cell lysates were prepared by sonicating cells in cell lysis buffer (50 mM Tris-HCl, 150 mM NaCl, 1% Nonidet P-40, pH 7.5). Whole cell lysates were then incubated with the glutathione-bound GST-ERα-AF2 in binding buffer (60 mM NaCl, 1 mM EDTA, 20 mM Tris, pH 7.5, 0.05% Nonidet P-40, 1 mM dithiothreitol, 6 mM $MgCl_2$, and 8% glycerol) in the absence or presence of corresponding ligands or vehicle for 3 h at 4 °C. After washing with binding buffer, ERα-AF2-bound proteins were eluted, separated by 10% SDS-polyacrylamide, and visualized by Coomassie Blue. Specific proteins were cut from the gel, eluted, and analyzed by MALDI and liquid chromatography mass spectrometry by the Indiana University Protein Analysis Research Center (Indianapolis, IN).

Co-immunoprecipitation—MCF-7 cell whole cell lysates were prepared in lysis buffer (50 mM Tris, pH 7.4, 150 mM NaCl, 5 mM EDTA, 1% Nonidet P-40, 0.5% Triton X-100, 1 mM Na_3VO_4, protease inhibitor). Whole cell extract was incubated with protein G-agarose for 30 min at 4 °C. After centrifugation at 12,000 × *g* for 15 s, the precleared supernatants were incubated with 5 μl of anti-ERα antibody or IgG at 4 °C for 3 h followed by incubation with 30 μl of protein G-agarose beads for 30 min. The beads were then pelleted by brief centrifugation, washed 3 times with Tris-buffered saline (TBS) and once with TBS containing 0.4 M NaCl, and resuspended in 30 μl of SDS-PAGE loading buffer for SDS-PAGE and Western blotting.

Live Cell Microscopy and Drug Treatment—Live fluorescence microscopy was performed by growing cells on 6-well plates and transfection with GFP-ERα using Lipofectamine or FuGENE and maintained in minimum Eagle's medium with 5% dextran-coated charcoal-stripped fetal bovine serum at 37 °C. Cells were treated with E2 (10 nM), ICI (100 nM), 4-OHT (100 nM), or ICI and cycloheximide (25 μg/ml). Images were taken using a Zeiss Axiovert 40 Inverted Microscope and AxioVision software.

RESULTS

Fulvestrant Induces ERα-Intermediate Filament Protein Interactions—Previously it was shown that treatment of breast cancer cells with the pure antagonist ICI resulted in ERα immobilization and resistance to biochemical extraction within the nuclear matrix (21). For this study we hypothesized that fulvestrant-dependent ERα-interacting proteins in the nuclear matrix were responsible for this phenomena. To identify putative fulvestrant-dependent ERα interacting proteins, cell lysates from human breast cancer MCF-7 cells were incubated with immobilized GST-ERα-activating function-2 (AF2) in the presence of ICI. Interacting proteins were eluted from the beads, separated by SDS-PAGE, and stained with Coomassie Blue. Fulvestrant-specific interacting protein bands (Fig. 1*A*) were excised from the gel and subjected to mass spectrometry (MALDI and liquid chromatography mass spectrometry) analysis, resulting in two of the proteins being identified as cytokeratins 8 and 18 (CK8 and CK18). To validate those findings, Western blot analysis using CK8- or CK18-specific antibodies, was performed to permit conclusive identification of these putative ERα binding partners (Fig. 1, *B* and C). No interaction between ERα and CK8 or CK18 was observed in the presence of either E2 or 4-OHT (Fig. 1). These ERα-CK8·CK18 associations were also stable in the presence of high salt (Fig. 1, *last lane*), consistent with other reports that ERα is insoluble after immobilization by ICI or RU 58668 (21, 38). To further demonstrate an ERα-CK8·CK18 interaction *in vivo*, co-immunoprecipitation was performed using MCF-7 whole cell lysates and an ERα-specific antibody in the absence or presence of fulvestrant. As shown in Fig. 1*D*, CK8 and CK18 were seen in the ERα complex only in the presence of ICI, suggesting that fulvestrant induces an endogenous interaction between ERα and CK8·CK18.

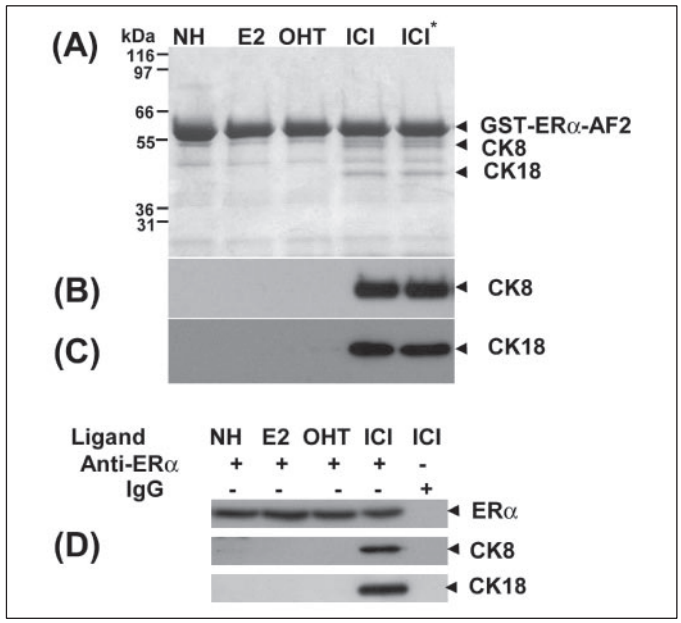

FIGURE 1. *A–C*, purification and identification ICI-dependent ERα-interacting proteins using the GST pull-down assay. Cell lysates were prepared from MCF-7 cells and incubated with immobilized GST-ERα-AF2 in the presence or absence of ligand (1 μM E2, 4-OHT, and ICI; *NH*, no hormone). After SDS-PAGE and gel excision, proteins were identified by mass spectrometry. Results were confirmed by Western blotting using specific antibodies. *A*, Coomassie Blue-stained SDS-polyacrylamide gel of proteins associated with GST-ERα-AF2. *B* and *C*, Western blot confirmation of mass spectrometry using antibodies for CK8 (*B*) or CK18 (*C*). *, sample was also washed with high salt buffer (1 M NaCl). *D*, co-immunoprecipitation of the ERα-CK8·CK18 interaction *in vivo*. ERα was precipitated from MCF-7 cell lysates using an anti-ERα antibody. The presence of CK8·CK18 in the pull-down complex was examined by immunoblotting using antibodies for CK8 or CK18. To assess the amount of precipitated ERα in the complex, the same membrane was then re-probed with ERα antibody. Normal rabbit IgG was used on the negative control. Representative results of two independent experiments, each performed in duplicate, are shown.

Expression of CK8·CK18 in ERα-positive and -negative Cancer Cell Lines—It has been previously shown that both CK8 and CK18 are nuclear matrix-intermediate filament proteins present in ERα-positive cells (30). To investigate whether a correlation exists between expression of ERα and/or CK8·CK18, whole cell lysates were prepared from human breast (MCF-7, T47D, MDA-MB-231) and cervical cancer (HeLa) cell lines. Levels of CK8·CK18 and ERα were determined by Western blot analysis. Differential CK expression was observed between the ERα-positive and -negative cell lines (Fig. 2*A*). Furthermore, CK8 and CK18 protein levels were markedly higher in MCF-7 and T47D (ERα-positive) cells as compared with the ERα-negative MDA-MB-231 and HeLa cells.

Effect of Fulvestrant on the Association of ERα with the Nuclear Matrix and Receptor Degradation—Distinct ligands can specifically affect ERα extractability from the nucleus of breast cancer cells (38). To further characterize the association between ERα and the nuclear matrix in the presence of antiestrogens, MCF-7 and T47D cells (ERα-, CK8-, and CK18-positive) were treated with ICI or 4-OHT followed by isolation of nuclear matrix fractions. Nuclear matrix prepared from MDA-MB-231 (ERα-negative; CK8- and CK18-positive, Fig. 2*A*) was used as a control.

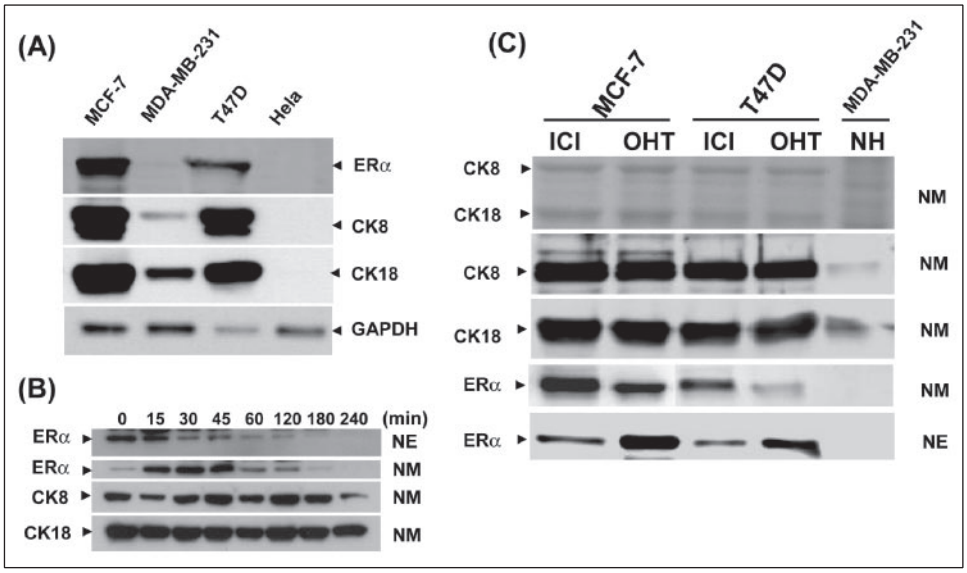

FIGURE 2. *A*, expression of ERα, CK8, and CK18 in cancer cell lines. Whole cell lysates were prepared in 1× SDS sample buffer from the indicated cancer cell lines, subjected to SDS-PAGE electrophoresis, and transferred to membranes. Western blot analysis was performed using specific antibodies for ERα, CK8, and CK18. *B*, fulvestrant induces ERα immobilization to the nuclear matrix and receptor degradation. MCF7 cells were treated with fulvestrant (ICI 182,780; 10 nM) for the indicated times, and nuclear extract (*NE*) or nuclear matrix (*NM*) was prepared as described under "Experimental Procedures." Proteins were separated by SDS-PAGE and analyzed by Western blotting using ERα-, CK8-, and CK18-specific antibodies. *C*, association of ERα with the nuclear matrix in the presence of antiestrogen. Cells were treated with ICI 182,780 or 4-OHT (10 nM for 30 min). Nuclear extract and nuclear matrix was prepared from MCF-7, T47D, and MDA-MB-231 cells, as described under "Experimental Procedures." Proteins were separated by SDS-PAGE and visualized either by Coomassie Blue staining or Western blot analysis using specific antibodies. *Upper panel*, nuclear matrix proteins stained with Coomassie Blue. *Middle panel*, CK8·CK18, ERα levels in NM. *Bottom panel*, ERα levels in nuclear extract. Representative results of two independent experiments, each performed in duplicate, are shown.

In the nuclear matrix of ERα-positive cells, CK8 and CK18 were highly abundant (Fig. 2*C*, *upper panel*, Coomassie Blue; *middle panel*, Western blot). In the presence of ICI, the majority of ERα protein was unextractable and remained tightly associated with the nuclear matrix (Fig. 2*C*); in contrast, in the presence of 4-OHT, ERα was loosely associated with the nuclear matrix, readily extractable, and thus, more abundant in the nuclear extract (Fig. 2*C*, *bottom panel*). These observations are consistent with the result that fulvestrant induces a salt-resistant ERα-CK8 and -CK18 interaction (Fig. 1) and that ERα extractability varies in the presence of different ligands (38).

To monitor ERα immobilization and degradation, nuclear extract and nuclear matrix were prepared from MCF-7 cells treated with fulvestrant for 0–4 h. As shown in Fig. 2*B*, rapid (<30 min) immobilization of ERα from the nuclear extract to the nuclear matrix was observed followed by receptor degradation 1 h after the onset of ICI treatment. In addition, CK8 and CK18 were both localized in the insoluble nuclear matrix (Fig. 2*B*). Taken together, these observations demonstrate that after treatment with fulvestrant, ERα is rapidly sequestered in a salt-insoluble nuclear compartment before being degraded.

Helix 12 Is Required for Fulvestrant-dependent Interaction of ERα with CK8 and CK18 and Antiestrogen-induced Immobilization of ERα to the Nuclear Matrix and Receptor Degradation—Previous studies have suggested a role of two domains of ERα in ICI-induced receptor immobilization and degradation; that is, H12 and the F domain. Furthermore, Katzenellenbogen and coworkers (29) showed that mutations in H12 conferred resistance to ICI-induced degradation. Furthermore, to examine whether these two domains are required for fulvestrant-dependent interactions with CKs, several ERα AF2 mutant GST fusion proteins were constructed; AF2ΔF, with the F domain of AF2 deleted, AF2ΔFΔH12, completely lacking both F domain and helix 12, AF2–3X, with 3 mutated amino acids in H12 (D538N/E542Q/D545N), AF23XΔF, containing H12 mutations and lacking the F domain (Fig. 3*A*). In the presence of fulvestrant, the F domain deletion constructs remained capable of interacting with both CK8 and CK18, demonstrating that the F domain is not required for the ERα-CK interaction (Fig. 3*B*). However, removal of H12 or point mutations introduced into this region completely abolished fulvestrant-induced receptor-CK8·CK18 interactions (Fig. 3*B*). Interestingly, no interaction between ERβ and either CK8 or CK18 was observed after ICI treatment (Fig. 3*B*, *last lane*, *ERβAF2*). In MCF-7 cells (39, 40) and rat efferent ductules (40), ERβ appears to be resistant to fulvestrant-induced degradation, and our results further indicate that the lack of CK interactions may play a role in the inability of fulvestrant to degrade this ER isoform.

Having demonstrated that H12 is required for fulvestrant-induced interaction of ERα with CK8 and CK18, it was of interest to test whether H12 and the F domain are required for ERα immobilization. Plasmids containing wild type ERα (wtERα), ERαΔF, or ERα3X were transfected into the MDA-MB-231 breast cancer cell line (ERα-negative; CK8- and CK18-positive, Fig. 2*A*). Transfected MDA-MB-231 cells were treated with ICI or E2 for 30 min (this short treatment duration causes ERα immobilization but not degradation). Whole cell lysates and nuclear extracts were prepared, and ERα protein levels were determined by Western blot analysis. After E2 treatment, both wtERα and ERαΔF were extractable by nuclear extraction buffer (Fig. 3*C*); however, after treatment with ICI, neither construct was extractable (Fig. 3*C*). No effect of E2 or ICI on the extractability of the mutant ERα3X was observed (Fig. 3*C*). Taken together, these results indicate that H12 is essential for fulvestrant-induced immobilization of ERα to the nuclear matrix.

It was recently demonstrated that mutations in H12 could influence tamoxifen-mediated ERα stability (41). To examine whether H12 contributes to fulvestrant-mediated receptor degradation, T47D breast cancer cells (CK8- and CK18-positive, Fig. 2*A*) were transiently transfected with full-length ERα3X (point-mutated helix 12) or wtERα. Receptor levels were assessed by Western blot analysis after treatment with ICI for 1 h. As shown in Fig. 3*D*, degradation of wtERα, but not ERα3X, was observed after ICI treatment, suggesting that an intact H12 is required for fulvestrant-induced ERα degradation.

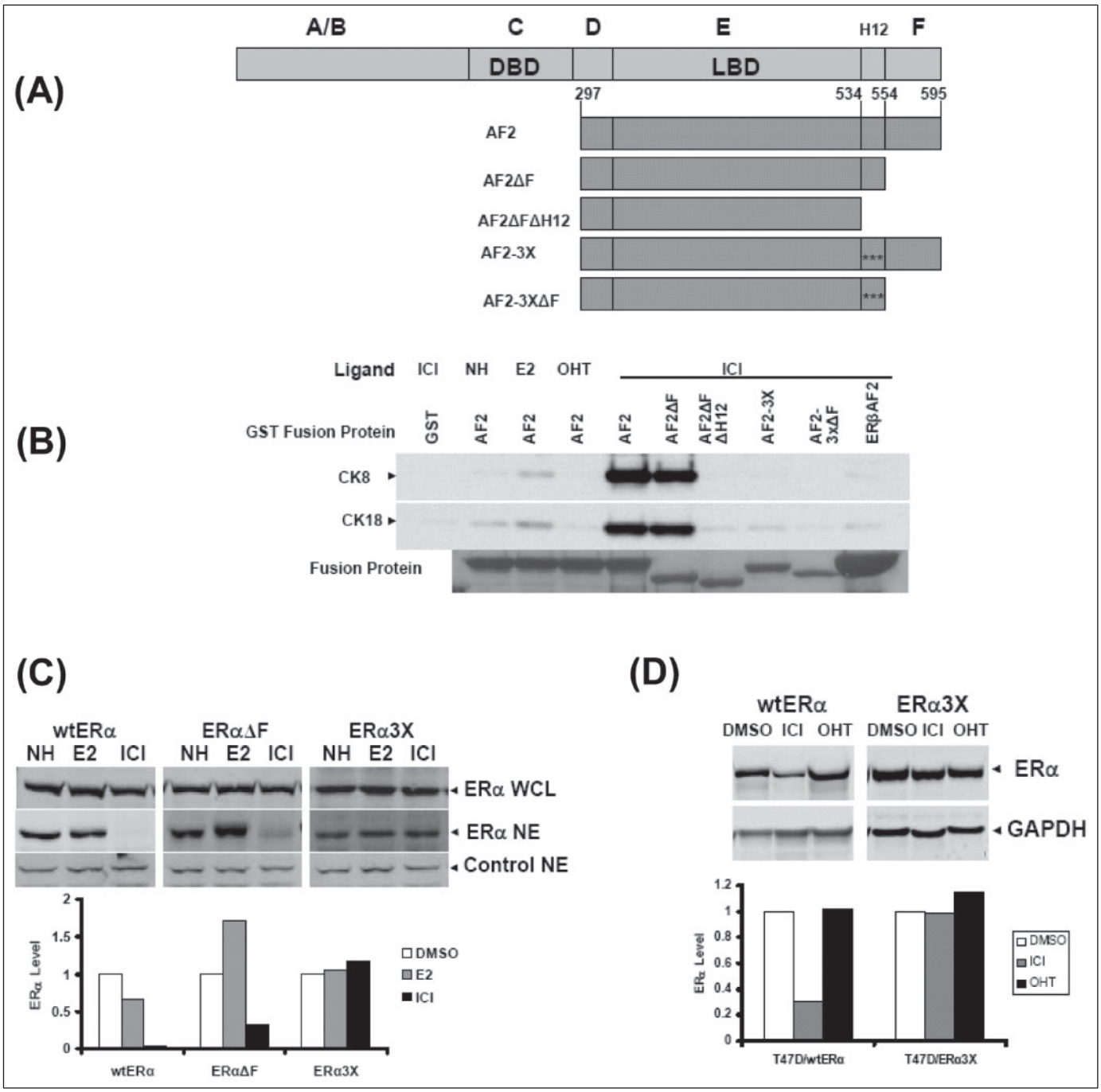

FIGURE 3. *A* and *B*, helix 12 of ERα is essential for receptor interactions with CK8 and CK18. *A*, schematic diagram of ERα and the AF2 constructs used for GST pull-down. *B*, analysis of ERα-AF2 mutants and their interactions with CK8 or CK18. Cell extracts were prepared from MCF-7 cells and incubated with immobilized ERα-AF2 GST fusion proteins in the presence or absence of 1 μM ligand (E2, 4-OHT, and ICI; *NH*, no hormone). Interacting proteins CK8 and CK18 were detected by Western blotting using CK8- or CK18-specific antibodies. *Bottom panel*, Coomassie Blue-stained SDS-polyacrylamide gels of GST fusion proteins. *DBD*, DNA binding domain *LBD*, ligand binding domain. *C*, helix 12, but not the F domain, is required for fulvestrant-induced ERα immobilization. MDA-MB-231 cells were transiently transfected with wtERα, ERαΔF, or ERα-3X and treated with Me_2SO, 100 nM E2, or fulvestrant (ICI) for 30 min. Whole cell lysates and nuclear extracts (*NE*) were prepared as described under "Experimental Procedures." *Upper panel*, ERα levels were measured and analyzed using Western blotting and a LI-COR imaging system, as described under "Experimental Procedures." *Lower panel*, quantitative analysis of ERα protein level in NE, normalized by loading control using LICOR Odyssey software. *DMSO*, dimethyl sulfoxide. *D*, helix 12 is required for fulvestrant-induced ERα degradation. T47D cells were transiently transfected with wtERα and ERα-3X. Transfected cells were treated with either 100 nM fulvestrant (ICI) or 100 nM 4-OHT for 2 h. *Upper panel*, whole cell lysates were prepared as described under "Experimental Procedures," subjected to SDS-PAGE, and transferred to membranes. ERα levels were measured and analyzed using Western blot and a LICOR imaging system, as described under "Experimental Procedures." *Lower panel*, quantitative analysis of Western blot of ERα protein from *panel A*, normalized by GAPDH using LICOR Odyssey software. Representative results of two independent experiments, each performed in duplicate, are shown.

Because the F domain of ERα contains a PEST sequence (residues 555–567), a proposed signal for rapid intracellular breakdown of proteins (42), it was of interest to investigate whether this domain may be involved in fulvestrant-induced ERα degradation. T47D cells were transected with plasmids expressing ERαΔF, ERα3XΔF, or ERαΔFΔH12 and treated with ICI for 1 h. The relative stability of each mutant ERα was then assessed using Western blot analysis using a monoclonal antibody against the N-terminal region of ERα, which recognizes receptors with C-terminal deletions. As shown in Fig. 4, a decrease in the level of ERαΔF protein was observed after ICI treatment;

in contrast, both ERα3XΔF and ERαΔFΔH12 were resistant to fulvestrant-induced degradation. Moreover, ERα3XΔF levels actually increased after treatment with the antiestrogen, likely due to blockage of basal turnover of the mutant receptor (Fig. 4). In support of this possibility, treatment with the proteasome inhibitor MG132, an inhibitor of basal ERα protein turnover (43) increased levels of ERα protein (Fig. 4, *A* and *B*). Collectively, these results indicate that the F domain is not required for fulvestrant-induced ERα degradation, in contrast to H12. Our observations also support those of Pakdel *et al.* (43), who reported that the F domain is dispensable for E2-induced degradation of ERα (43).

Fulvestrant-induced Degradation of ERα Is Dependent on Cellular Levels of CK8 and CK18—Having established that fulvestrant induces an interaction between ERα, the nuclear matrix, and CK8 and CK18, it was important to define the role of these intermediate filaments in antiestrogen-mediated receptor degradation. To test receptor stability in the presence or absence of these CKs, we utilized C4-12 cells, an ERα-negative, CK8·CK18-positive breast cancer cell line derived from MCF-7 (34) and HeLa cells (negative for ERα, CK8, and CK18). These cell lines were stably transfected with wtERα and treated with ICI for 1–4 h; ERα protein levels were then measured by Western blot. After treatment with ICI, marked degradation of ERα was observed in C4-12 cells (Fig. 5*A*) but not in HeLa cells (Fig. 5*B*), indicating that the presence of CK8 and CK18 is essential for receptor turnover by the pure antiestrogen. To investigate the effect of CK8·CK18 overexpression on fulvestrant-induced ERα degradation, HeLa cells (negative for CK8·CK18 and ERα) were co-transfected with CK8 and CK18 (singly or both) along with ERα, and the transfected cells were treated with ICI for 2h. ERα protein levels were subsequently determined by immunoblot analysis. As shown in Fig. 6*A*, overexpression of CK8·CK18 restored the ability of fulvestrant to degrade ERα in HeLa cells. We then examined whether fulvestrant-induced ERα degradation could be inhibited by CK8·CK18-specific small interference RNAs (siRNA). MCF-7 cells (CK8·CK18-positive) were transfected with CK8 or CK18 siRNAs (singly or both) and treated with ICI for 2 h. CK8·CK18 and ERα protein levels were measured by Western blotting. As shown in Fig. 6*B*, CK8·CK18 siRNAs decreased the level of CK8 and CK18, and fulvestrant-induced ERα degradation was less dramatic in these MCF-7 cells.

Cytoplasmic Localization of ERα Is Associated with CK8 and CK18—A unique but poorly understood property of pure antagonists like the ICI compounds (13, 19) and RU 58668 (44) is the induction of cytoplasmic localization of ERα. Intermediate filament proteins CK8 and CK18 have been shown to be located in both the nuclear matrix as well as in the cytoplasm (30). To investigate whether fulvestrant-mediated cytoplasmic localization of ERα is associated with CK8 and CK18, we transfected an ERα-GFP plasmid into CK8- and CK18-positive or -negative cell lines (MCF-7, T47D, or HeLa cells, respectively; Fig. 2). Transfected cells were then treated with ICI in the presence or absence of the protein synthesis inhibitor cycloheximide or the partial antagonist 4-OHT. In untreated cells and cells treated with 4-OHT, expression of ERα-GFP was exclusively nuclear (Fig. 7, *first* and *last columns*, respectively). After treatment of MCF-7 and T47D cells with ICI, dramatic cytoplasmic localization of ERα was observed (Fig. 7, *second column*). This was completely blocked by cycloheximide treatment (Fig. 7, *third column*), consistent with a previous report demonstrating the requirement of new protein synthesis for fulvestrant-induced cytoplasmic ERα localization (44). In contrast to observations in MCF7 and T47D cells, in HeLa cells treated with fulvestrant markedly less cyto-

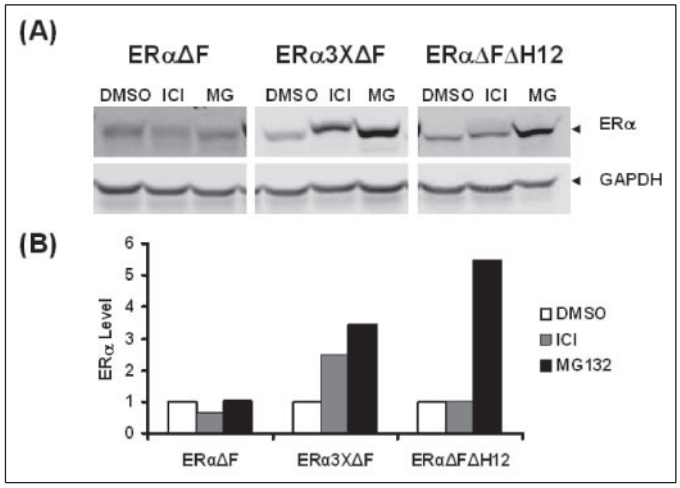

FIGURE 4. **The F domain of ERα is not required for fulvestrant-induced receptor degradation.** T47D cells were transiently transfected with ERαΔF and ERα3XΔF and ERαΔFΔH12 (depicted in Fig. 3) and treated with fulvestrant (100 nM ICI 182,780) or MG132 (5 μM) for 1 h. Whole cell lysates were prepared, and ERα levels were measured and analyzed using Western blotting and a LICOR imaging system, as described under "Experimental Procedures." Western blot image (*A*) and quantitative analysis (*B*) were prepared using normalization to GAPDH and LICOR Odyssey software. Representative results of two independent experiments, each performed in duplicate, are shown. *DMSO*, dimethyl sulfoxide; *MG*, MG132.

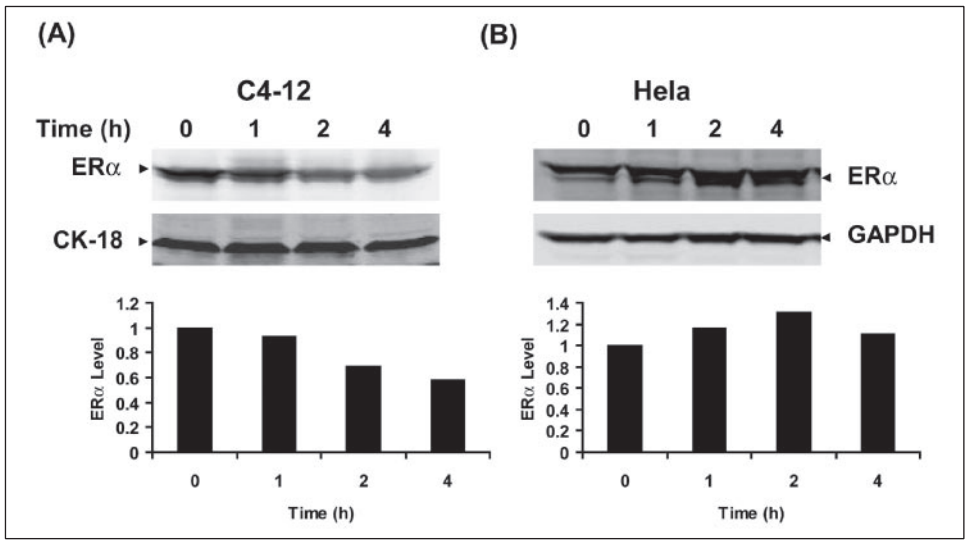

FIGURE 5. **Fulvestrant induces ERα degradation in CK8-, CK18-positive C4-12 cells but not in CK8-, CK18-negative HeLa cells.** C4-12 cells (derived from MCF-7 breast cancer cells) (*A*) and HeLa cells (*B*) were stably transfected with wtERα and treated with fulvestrant (100 nM ICI 182,780) for 1, 2, or 4 h. Whole cell lysates were prepared, subjected to SDS-PAGE, and blotted. ERα levels were measured and analyzed using Western blotting and LICOR imaging system (described under "Experimental Procedures."). *Upper panel*, Western blot image. *Lower panel*, quantitative analysis of Western blot of ERα protein from *panel A*, normalized to GAPDH using LICOR Odyssey software. Representative results of two independent experiments, each performed in duplicate, are shown.

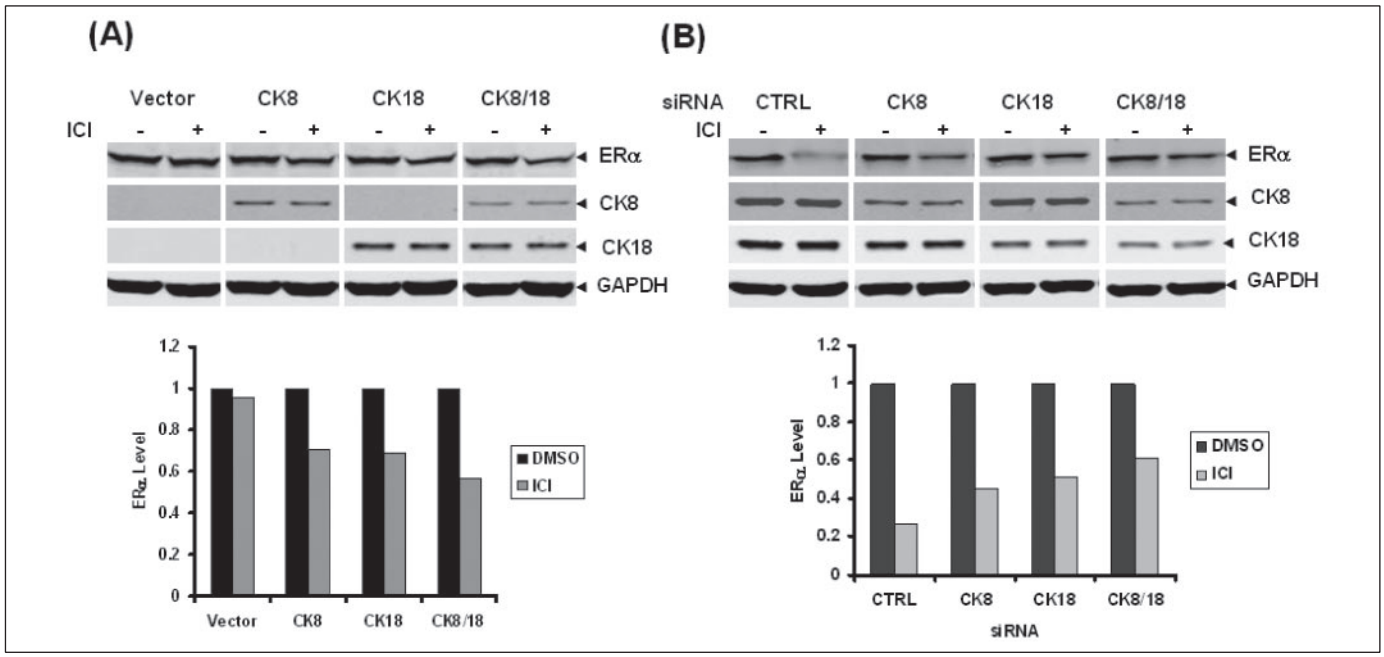

FIGURE 6. **Cytokeratins 8, 18 facilitate fulvestrant-induced ERα degradation.** *A*, HeLa cells (negative for CK8·CK18 and ERα) were transiently transfected with CK8·CK18 (singly or both) and ERα in the absence or presence of fulvestrant (100 nM ICI 182,780). Protein levels were measured and analyzed using Western blotting and LICOR imaging system (described under "Experimental Procedures"). *Upper panel*, Western blot image. *Lower panel*, quantitative analysis of Western blots from *panel A* (normalized to GAPDH using LICOR Odyssey software). *DMSO*, dimethyl sulfoxide. *B*, knockdown of endogenous CK8·CK18 inhibits fulvestrant-induced ERα degradation. MCF-7 cells were transfected with siRNAs for CK8 or CK18 (singly or both) in the absence or presence of fulvestrant (100 nM ICI 182,780). Protein levels were measured and analyzed using Western blotting and LICOR imaging system. *Upper panel*, Western blot image. *Lower panel*, quantitative analysis of Western blots from *panel B* (normalized to GAPDH using LICOR Odyssey software). Representative results of two independent experiments, each performed in duplicate, are shown. *CTRL*, control.

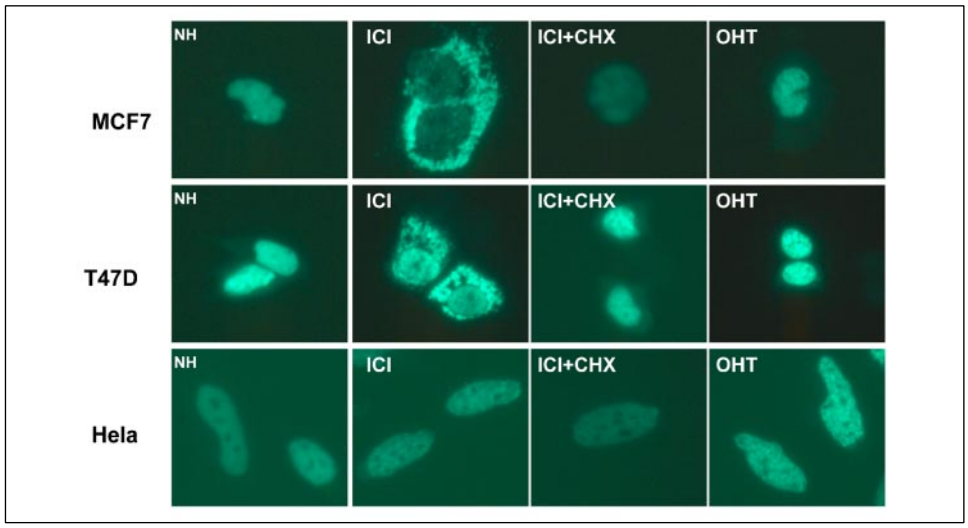

FIGURE 7. **Cytoplasmic localization of ERα after treatment of breast cancer cells with fulvestrant.** MCF7, T47D, and HeLa cells were transiently transfected with pEGFP-C1-hERα and treated with fulvestrant (100 nM ICI 182,780) or fulvestrant plus 25 μg/ml cycloheximide (*CHX*) or 100 nM 4-hydroxytamoxifen (4-OHT) or Me_2SO (*NH*, no hormone). Images were taken 8 h after drug treatment.

plasmic localization was observed based on both the percentage of cells displaying ERα-GFP in the cytoplasm and cytoplasmic ERα-GFP intensity (Fig. 7, *last row*).[3] After 8 h of ICI treatment, most (>50%)[3] MCF-7 and T47D cells showed some degree of cytoplasmic localization; however, <10% of the CK8·CK18-negative HeLa cells displayed cytoplasmic localization, in agreement with a previous report (19). Collectively, these results indicate that the presence of CK8 and CK18 is necessary for fulvestrant-induced cytoplasmic localization of ERα.

DISCUSSION

The antiproliferative effects of fulvestrant (ICI 182,780) on breast cancer cells are due to rapid degradation of ERα protein (12, 21). While the drug acts by immobilizing ERα to the nuclear matrix followed by rapid receptor turnover, the molecular mechanism has not been fully established. In this study we identified two fulvestrant-dependent ERα-interacting proteins, CK8 and CK18, members of the nuclear matrix intermediate filament family of structural proteins (30). We show that CK8 and CK18 are involved in fulvestrant-induced ERα immobilization and degradation, and we further demonstrate that H12 of ERα is essential for the fulvestrant-dependent interaction with CK8 and CK18. Although ERα has long been known to associate with the nuclear matrix (45), our findings are the first demonstration of a fulvestrant-dependent interaction between ERα and intermediate filament proteins in the nuclear matrix. Because proteasomes are closely associated with intermediate filaments (31–33), we suggest that SERD-induced rapid degradation of ERα is due to specific interactions with CK8 and CK18 by

[3] X. Long and K. P. Nephew, unpublished results.

bringing the receptor into close proximity to the 26 S proteasome protein degradation machinery.

Pure antiestrogens, like fulvestrant, can be converted to full estrogen agonists by specific mutations in H12 (28, 29). H12 makes up most of the C-terminal helix within the ligand binding domain of ERα (46) and appears to be required for recruiting coactivators and co-repressors, serving as a "molecular switch" that connects ligands with coregulators (47). This helix is required for ICI-induced immobilization, as demonstrated by Stenoien *et al.* (20) using fluorescence recovery after photobleaching, and mutations in H12 can abrogate E2-mediated degradation (3–6), suggesting that the H12 coactivator binding surface is required for ligand-mediated ERα down-regulation. Furthermore, antiestrogens have been shown to change ERα stability by altering the position of H12 (26). To test whether H12 is essential for receptor-CK8 and -CK18 interactions and, thus, the ability of fulvestrant to immobilize and degrade ERα, we examined the interaction between several GST-ERα-AF2 mutants and CK8 and CK18. Point mutations or deletion of H12, but not loss of F domain function, abolished CK8 and CK18 interactions, demonstrating that the F domain is not required for fulvestrant-induced ERα immobilization. Based on these results, we suggest that in the presence of fulvestrant, H12 interacts with CK8·CK18 and immobilizes ERα within the nuclear matrix for subsequent degradation.

Because the interaction of ERα with CK8 and CK18 is specific for fulvestrant, it is likely that H12 assumes a different position when bound by ICI, as compared with 4-OHT, resulting in receptor degradation *versus* stabilization. Indeed, a recent report showing differences in antiestrogen-induced relocation of hydrophobic residues in H12 strongly supports this possibility (26). Of the ERα antagonists examined, ICI caused the greatest exposure of surface hydrophobicity, whereas 4-OHT caused the least exposure (26). Thus, it seems plausible that ICI-induces a conformational change that allows H12 to interact with CK8 and/or CK18. Nonetheless, it is not clear how an ERα-CK8·CK18 interaction triggers rapid receptor turnover; however, proteasomes have recently been shown to be closely associated with intermediate filaments and, thus, likely facilitate this process (31–33).

It has previously been shown that pure antiestrogens (ICI 182,780, RU 58668) can disrupt ERα nucleocytoplasmic shuttling and cause receptor cytoplasmic localization (13), a process that requires new protein synthesis (19). It is also known that both CK8 and CK18 are located in the cytoplasm and the nuclear matrix (30). In the present study, ERα cytoplasmic localization was observed only in CK8·CK18-positive cells, suggesting that these intermediate filaments play a role in retaining ERα in the cytoplasm after fulvestrant treatment. In support of this hypothesis, Htun *et al.* (19) reported that cytoplasmic retention of ERα varied between breast cancer cell lines, with greater cytoplasmic localization seen in ERα-positive MCF-7 and T47D cells as compared with ERα-negative MDA-MB-231 cells. Although an explanation for this observation was not offered (19), our findings that CK8 and CK18 are differentially expressed in these cell lines provides a plausible rationale. Interestingly, whereas other cytokeratins are present in the nuclear matrix (*e.g.* CK5·CK19), these do not interact with ERα,[3] and the basis for the specificity of ERα for CK8 and CK18 remains unclear.

Although it is well established that the level of ERα in breast tumors is a valuable predictor of a patient's response to antiestrogen therapies such as tamoxifen and fulvestrant (48), CK8 and CK18, via their correlation with tumor differentiation (49), have also been used in cancer diagnosis. Furthermore, up-regulation of CK8·CK18 expression was associated with good prognosis in breast cancer patients (49, 50), whereas their down-regulation was correlated with a poor clinical outcome (51). We have previously shown that breast cancer cells with a disrupted ubiquitin-like NEDD8 pathway can acquire antiestrogen resistance (8) and that tumors from patients who developed resistance to fulvestrant can retain ERα expression (52). Taken together, it seems reasonable to suggest that disruption of ERα degradation may contribute fulvestrant-resistant breast cancer. Because CK8 and CK18 are associated with fulvestrant-mediated ERα degradation, their decreased levels would likely disrupt fulvestrant-mediated ERα immobilization and degradation, which are both essential for the antiproliferative activity of this antiestrogen (8). Thus, we speculate that down-regulation of CK8·CK18 may be involved in fulvestrant resistance; furthermore, a H12 mutant ERα would likely be resistant to fulvestrant-mediated degradation, supporting the observation that H12 mutations can contribute to endocrine-resistant breast cancer (53–56). In conclusion, fulvestrant resistance is clearly multifactorial. We are currently investigating the role of the NEDD8 pathway and the nuclear matrix proteins CK8 and CK18 in antiestrogen-resistant breast cancer.

Acknowledgments—We gratefully acknowledge Dr. Pierre Chambon (Institut de Génétique et de Biologie Moléculaire et Cellulaire, Strasbourg, France) for providing pSG5-ERα (HEGO), Dr. Michael A. Mancini (Baylor College of Medicine, Houston, TX) for GFP-ERα, and Dr. Donald P. McDonnell (Duke University, Durham, NC) for pRST-7-hER3X. We thank Drs. Meiyun Fan and Curtis Balch (Indiana University School of Medicine) for their critical review of this manuscript.

REFERENCES

1. Barkhem, T., Nilsson, S., and Gustafsson, J. A. (2004) *Am. J. Pharmacogenomics* **4,** 19–28
2. Eckert, R. L., Mullick, A., Rorke, E. A., and Katzenellenbogen, B. S. (1984) *Endocrinology* **114,** 629–637
3. Alarid, E. T., Bakopoulos, N., and Solodin, N. (1999) *Mol. Endocrinol.* **13,** 1522–1534
4. El Khissiin, A., and Leclercq, G. (1999) *FEBS Lett.* **448,** 160–166
5. Nawaz, Z., Lonard, D. M., Dennis, A. P., Smith, C. L., and O'Malley, B. W. (1999) *Proc. Natl. Acad. Sci. U. S. A.* **96,** 1858–1862
6. Lonard, D. M., Nawaz, Z., Smith, C. L., and O'Malley, B. W. (2000) *Mol. Cell* **5,** 939–948
7. Reid, G., Denger, S., Kos, M., and Gannon, F. (2002) *Cell. Mol. Life Sci.* **59,** 821–831
8. Fan, M., Bigsby, R. M., and Nephew, K. P. (2003) *Mol. Endocrinol.* **17,** 356–365
9. Fan, M., Nakshatri, H., and Nephew, K. P. (2004) *Mol. Endocrinol.* **18,** 2603–2615
10. Wijayaratne, A. L., and McDonnell, D. P. (2001) *J. Biol. Chem.* **276,** 35684–35692
11. Preisler-Mashek, M. T., Solodin, N., Stark, B. L., Tyriver, M. K., and Alarid, E. T. (2002) *Am. J. Physiol. Endocrinol. Metab.* **282,** 891–898
12. Dauvois, S., Danielian, P. S., White, R., and Parker, M. G. (1992) *Proc. Natl. Acad. Sci. U. S. A.* **89,** 4037–4041
13. Dauvois, S., White, R., and Parker, M. G. (1993) *J. Cell Sci.* **106,** 1377–1388
14. Wijayaratne, A. L., Nagel, S. C., Paige, L. A., Christensen, D. J., Norris, J. D., Fowlkes, D. M., and McDonnell, D. P. (1999) *Endocrinology* **140,** 5828–5840
15. Fan, M., Park, A., and Nephew, K. P. (2005) *Mol. Endocrinol.* **19,** 2901–2914
16. Reid, G., Hubner, M. R., Metivier, R., Brand, H., Denger, S., Manu, D., Beaudouin, J., Ellenberg, J., and Gannon, F. (2003) *Mol. Cell* **11,** 695–707
17. Nardulli, A. M., and Katzenellenbogen, B. S. (1986) *Endocrinology* **119,** 2038–2046
18. Seo, H. S., Larsimont, D., Querton, G., El Khissiin, A., Laios, I., Legros, N., and Leclercq, G. (1998) *Int. J. Cancer* **78,** 760–765
19. Htun, H., Holth, L. T., Walker, D., Davie, J. R., and Hager, G. L. (1999) *Mol. Biol. Cell* **10,** 471–486
20. Stenoien, D. L., Patel, K., Mancini, M. G., Dutertre, M., Smith, C. L., O'Malley, B. W., and Mancini, M. A. (2001) *Nat. Cell Biol.* **3,** 15–23
21. Giamarchi, C., Chailleux, C., Callige, M., Rochaix, P., Trouche, D., and Richard-Foy, H. (2002) *Biochim. Biophys. Acta* **1578,** 12–20
22. Callige, M., Kieffer, I., and Richard-Foy, H. (2005) *Mol. Cell. Biol.* **25,** 4349–4358
23. Howell, A. (2000) *Eur. J. Cancer* **36,** Suppl. 4, 87–88
24. McDonnell, D. P. (2005) *Clin. Cancer Res.* **11,** 871–877
25. Pike, A. C., Brzozowski, A. M., Walton, J., Hubbard, R. E., Thorsell, A. G., Li, Y. L., Gustafsson, J. A., and Carlquist, M. (2001) *Structure (Camb)* **9,** 145–153
26. Wu, Y. L., Yang, X., Ren, Z., McDonnell, D. P., Norris, J. D., Willson, T. M., and Greene, G. L. (2005) *Mol. Cell* **18,** 413–424

27. Fawell, S. E., White, R., Hoare, S., Sydenham, M., Page, M., and Parker, M. G. (1990) *Proc. Natl. Acad. Sci. U. S. A.* **87,** 6883–6887
28. Mahfoudi, A., Roulet, E., Dauvois, S., Parker, M. G., and Wahli, W. (1995) *Proc. Natl. Acad. Sci. U. S. A.* **92,** 4206–4210
29. Montano, M. M., Ekena, K., Krueger, K. D., Keller, A. L., and Katzenellenbogen, B. S. (1996) *Mol. Endocrinol.* **10,** 230–242
30. Coutts, A. S., Davie, J. R., Dotzlaw, H., and Murphy, L. C. (1996) *J. Cell. Biochem.* **63,** 174–184
31. Olink-Coux, M., Arcangeletti, C., Pinardi, F., Minisini, R., Huesca, M., Chezzi, C., and Scherrer, K. (1994) *J. Cell Sci.* **107,** 353–366
32. Arcangeletti, C., Sutterlin, R., Aebi, U., De Conto, F., Missorini, S., Chezzi, C., and Scherrer, K. (1997) *J. Struct. Biol.* **119,** 35–58
33. Arcangeletti, C., De Conto, F., Sutterlin, R., Pinardi, F., Missorini, S., Geraud, G., Aebi, U., Chezzi, C., and Scherrer, K. (2000) *Eur. J. Cell Biol.* **79,** 423–437
34. Oesterreich, S., Zhang, P., Guler, R. L., Sun, X., Curran, E. M., Welshons, W. V., Osborne, C. K., and Lee, A. V. (2001) *Cancer Res.* **61,** 5771–5777
35. Fan, M., Long, X., Bailey, J. A., Reed, C. A., Osborne, E., Gize, E. A., Kirk, E. A., Bigsby, R. M., and Nephew, K. P. (2002) *Mol. Endocrinol.* **16,** 315–330
36. Shibata, H., Nawaz, Z., Tsai, S. Y., O'Malley, B. W., and Tsai, M. J. (1997) *Mol. Endocrinol.* **11,** 714–724
37. Cavailles, V., Dauvois, S., Danielian, P. S., and Parker, M. G. (1994) *Proc. Natl. Acad. Sci. U. S. A.* **91,** 10009–10013
38. Marsaud, V., Gougelet, A., Maillard, S., and Renoir, J. M. (2003) *Mol. Endocrinol.* **17,** 2013–2027
39. Peekhaus, N. T., Chang, T., Hayes, E. C., Wilkinson, H. A., Mitra, S. W., Schaeffer, J. M., and Rohrer, S. P. (2004) *J. Mol. Endocrinol.* **32,** 987–995
40. Oliveira, C. A., Nie, R., Carnes, K., Franca, L. R., Prins, G. S., Saunders, P. T., and Hess, R. A. (2003) *Reprod. Biol. Endocrinol.* **1,** 75
41. Pearce, S. T., Liu, H., and Jordan, V. C. (2003) *J. Biol. Chem.* **278,** 7630–7638
42. Rogers, S., Wells, R., and Rechsteiner, M. (1986) *Science* **234,** 364–368
43. Pakdel, F., Le Goff, P., and Katzenellenbogen, B. S. (1993) *J. Steroid Biochem. Mol. Biol.* **46,** 663–672
44. Devin-Leclerc, J., Meng, X., Delahaye, F., Leclerc, P., Baulieu, E. E., and Catelli, M. G. (1998) *Mol. Endocrinol.* **12,** 842–854
45. Barrack, E. R. (1987) *J. Steroid Biochem.* **27,** 115–121
46. Nettles, K. W., and Greene, G. L. (2005) *Annu. Rev. Physiol.* **67,** 309–333
47. Nettles, K. W., Sun, J., Radek, J. T., Sheng, S., Rodriguez, A. L., Katzenellenbogen, J. A., Katzenellenbogen, B. S., and Greene, G. L. (2004) *Mol. Cell* **13,** 317–327
48. Robertson, J. F. (1996) *Br J. Cancer* **73,** 5–12
49. Schaller, G., Fuchs, I., Pritze, W., Ebert, A., Herbst, H., Pantel, K., Weitzel, H., and Lengyel, E. (1996) *Clin. Cancer Res.* **2,** 1879–1885
50. Abd El-Rehim, D. M., Pinder, S. E., Paish, C. E., Bell, J., Blamey, R. W., Robertson, J. F., Nicholson, R. I., and Ellis, I. O. (2004) *J. Pathol.* **203,** 661–671
51. Iwaya, K., Ogawa, H., Mukai, Y., Iwamatsu, A., and Mukai, K. (2003) *Cancer Sci.* **94,** 864–870
52. Howell, A., Osborne, C. K., Morris, C., and Wakeling, A. E. (2000) *Cancer* **89,** 817–825
53. Graham, M. L., Jr., Krett, N. L., Miller, L. A., Leslie, K. K., Gordon, D. F., Wood, W. M., Wei, L. L., and Horwitz, K. B. (1990) *Cancer Res.* **50,** 6208–6217
54. Dotzlaw, H., Alkhalaf, M., and Murphy, L. C. (1992) *Mol. Endocrinol.* **6,** 773–785
55. Fuqua, S. A., Wiltschke, C., Zhang, Q. X., Borg, A., Castles, C. G., Friedrichs, W. E., Hopp, T., Hilsenbeck, S., Mohsin, S., O'Connell, P., and Allred, D. C. (2000) *Cancer Res.* **60,** 4026–4029
56. Herynk, M. H., and Fuqua, S. A. (2004) *Endocr. Rev.* **25,** 869–898

[CANCER RESEARCH 64, 8184–8192, November 15, 2004]

Loss of Estrogen Receptor Signaling Triggers Epigenetic Silencing of Downstream Targets in Breast Cancer

Yu-Wei Leu,[1] Pearlly S. Yan,[1] Meiyun Fan,[2,3] Victor X. Jin,[1] Joseph C. Liu,[1] Edward M. Curran,[4] Wade V. Welshons,[4] Susan H. Wei,[1] Ramana V. Davuluri,[1] Christoph Plass,[1] Kenneth P. Nephew,[2,3] and Tim H-M. Huang[1]

[1]Human Cancer Genetics Program, Department of Molecular Virology, Immunology, and Medical Genetics, Comprehensive Cancer Center, The Ohio State University, Columbus, Ohio; [2]Medical Sciences, Indiana University School of Medicine, Bloomington, Indiana; [3]Department of Cellular and Integrative Physiology and Obstetrics and Genecology, Indiana University Cancer Center, Indianapolis, Indiana; and [4]Department of Veterinary Biomedical Sciences, University of Missouri, Columbia, Missouri

ABSTRACT

Alterations in histones, chromatin-related proteins, and DNA methylation contribute to transcriptional silencing in cancer, but the sequence of these molecular events is not well understood. Here we demonstrate that on disruption of estrogen receptor (ER) α signaling by small interfering RNA, polycomb repressors and histone deacetylases are recruited to initiate stable repression of the *progesterone receptor* (*PR*) gene, a known ERα target, in breast cancer cells. The event is accompanied by acquired DNA methylation of the *PR* promoter, leaving a stable mark that can be inherited by cancer cell progeny. Reestablishing ERα signaling alone was not sufficient to reactivate the *PR* gene; reactivation of the *PR* gene also requires DNA demethylation. Methylation microarray analysis further showed that progressive DNA methylation occurs in multiple ERα targets in breast cancer genomes. The results imply, for the first time, the significance of epigenetic regulation on ERα target genes, providing new direction for research in this classical signaling pathway.

INTRODUCTION

The steroid hormone estrogen is important for normal breast development, but it is also important for growth and progression of breast cancer. The molecular actions of estrogen are mediated by estrogen receptors (ERs), ERα and ERβ. On ligand binding, ERα functions as a transcription factor by either binding to DNA targets or tethering to other transcription factors, such as AP-1 and SP-1 (1). These molecular interactions have been shown to positively or negatively modulate the activity of ERα downstream genes important to breast epithelial development.

It is known that estrogen signaling regulates the growth of some breast tumors, and antiestrogen therapies can effectively block this growth signaling, resulting in tumor suppression (2). However, most tumors eventually develop resistance to this endocrine therapy, and antiestrogens are mostly ineffective in patients with advanced disease (2). Mechanisms underlying this hormonal resistance are complex, involving intricate interactions between ERα and kinase networks (1, 2). In addition, epigenetic silencing of *ERα* is known to contribute to the antiestrogen resistance (1, 2). An emerging theme not yet investigated in this field is the subsequent influence on the expression of ERα downstream target genes.

Epigenetics can be defined as the study of heritable changes that modulate chromatin organization without altering the corresponding DNA sequence. DNA methylation, the addition of a methyl group to the fifth carbon position of a cytosine residue, occurs in CpG dinucleotides (3) and is a key epigenetic feature of the human genome. These dinucleotides are usually aggregated in stretches of 1- to 2-kb GC-rich DNA, called CpG islands, located in the promoter and first exon of ~60% of human genes (3, 4). Promoter methylation is known to participate in reorganizing chromatin structure and also plays a role in transcriptional inactivation (3, 5). Studies have suggested that the CpG island in an active promoter is usually unmethylated, with the surrounding chromatin displaying an "open" configuration, allowing for the access of transcription factors and other coactivators to initiate gene expression (6–8). Furthermore, transcription factor occupancy may make the promoter inaccessible to repressors or other chromatin-remodeling proteins. In contrast, the CpG island in an inactive promoter may become methylated, with the associated chromatin exhibiting a "closed" configuration. As a result, the methylated area is no longer accessible to transcription factors, disabling the functional activity of the promoter (7, 9, 10).

Recent studies have shown that establishing transcriptional silencing of a gene involves a close interplay between DNA methylation and histone modifications (7, 11). This process may be achieved by recruiting histone-modifying enzymes, such as histone deacetylases, which mediate posttranslational modification at the NH_2 terminus ends of histones (7, 11). As a result, chromatin modifications form distinct patterns, known as the "histone code," that may dictate gene expression (12–14).

Two models have been offered to describe the molecular sequence leading to the establishment of epigenetic gene silencing. One model suggests that histone modifications are the primary initiating event in transient repression (15, 16). DNA methylation subsequently accumulates in the targeted CpG island, creating a heterochromatin environment to establish a heritable, long-term state of transcriptional silencing. However, a second model is that DNA methylation can actually specify unique histone codes for maintaining the silenced state of a gene (17–20). In this case, DNA methylation may precede histone modifications. Clearly, this epigenetic process is complex, and multiple systems may be implemented for genes participating in different signaling pathways.

In this study, we investigated whether the removal of ERα signaling triggers changes in DNA methylation and chromatin structure of ERα target promoters. By using RNA interference (RNAi) to transiently disable ERα in breast cancer cells, we show, for the first time, that polycomb repressors and histone deacetylases assemble on the promoters of interrogated ERα target genes to participate in long-term transcriptional silencing. These events are later accompanied by a progressive accumulation of DNA methylation in the promoter re-

Received 6/9/04; revised 8/27/04; accepted 9/23/04.

Grant support: National Cancer Institute grants R01 CA-69065 (T. Huang) and R01 CA-85289 (K. Nephew); United States Army Medical Research Acquisition Activity, Award Numbers DAMD 17-02-1-0418 and DAMD 17-02-1-0419 (K. Nephew); American Cancer Society Research and Alaska Run for Woman Grant TBE-104125 (K. Nephew); and funds from The Ohio State University Comprehensive Cancer Center-Arthur G. James Cancer Hospital and Richard J. Solove Research Institute (P. Yan and T. Huang).

The costs of publication of this article were defrayed in part by the payment of page charges. This article must therefore be hereby marked *advertisement* in accordance with 18 U.S.C. Section 1734 solely to indicate this fact.

Note: Supplementary data for this article can be found at Cancer Research Online (http://cancerres.aacrjournals.org). T. Huang is a consultant to Epigenomics, Inc., Berlin, Germany.

Requests for reprints: Tim H-M. Huang, Human Cancer Genetics Program, Department of Molecular Virology, Immunology, and Medical Genetics, Comprehensive Cancer Center, The Ohio State University, 420 West 12th Avenue, Columbus, OH 43210. Phone: 614-688-8277; Fax: 614-292-5995; E-mail: huang-10@medctr.osu.edu.

gions of the now silent targets, leaving a heritable "mark" that may be stably transmitted to cell progeny.

MATERIALS AND METHODS

Cell Lines and Clinical Samples. The breast cancer cell line MCF-7 and its derived subline, C4-12, were routinely maintained in our laboratories. For the demethylating treatment, cells were plated at a density of 2×10^6 cells per 10-cm dish and pretreated with 2 or 5 μmol/L 5-aza-2′-deoxycytidine (5-AzadC; Sigma, St. Louis, MO) for 5 days before treatment with 17β-estradiol (E_2; 10 nmol/L, 24 hours). Thirty-two invasive ductal carcinomas were obtained from patients undergoing breast surgery at the Ellis Fischel Cancer Center (Columbia, MO), in compliance with the institutional review board. Seven tumor-free breast parenchymas were used as controls. The ER status of tumor tissue was determined by immunohistochemical staining (21).

Transfection of Estrogen Receptor α Small Interfering RNAs. MCF-7 cells (60% confluent in a 3.5-cm–diameter culture dish) were starved in serum-free medium (minimal essential medium only) for 72 hours, followed by the addition of 10 nmol/L E_2 (E2758; Sigma) for 24 hours. The cells were then transfected with small interfering RNAs (siRNAs) for 4 to 5 hours with DMRIE-C reagent (Invitrogen, Carlsbad, CA). Double-stranded siRNA was generated using the *Silencer* siRNA Construction Kit (Ambion, Austin, TX). The siRNA oligonucleotides designed according to the ERα mRNA sequence (GenBank accession numbers AF_258449, 258450, and 258451) are as follows: (*a*) target sequence 1 (5′-AACCTCGGGCTGTGCTCTTTT), sense strand siRNA primer 5′-CCTCGGGCTGTGCTCTTTTTTCCTGTCTC and antisense strand siRNA primer AAAAGAGCACAGCCCGAGGTTCCTG-TCTC; and (*b*) target sequence 17 (5′-AAACAGGAGGAAGAGCTGCCA), sense strand siRNA primer 5′-ACAGGAGGAAGAGCTGCCATTCCT-GTCTC and antisense strand siRNA primer 5′-TGGCAGCTCTTCCTCCT-GTTTCCTGTCTC.

Media were changed after transfection. The cells were then harvested for total RNA (RNeasy Kit; Qiagen, Valencia, CA) and genomic DNA (QIAamp; Qiagen) isolation at various time periods after siRNA treatment.

Transfection of Estrogen Receptor α Expression Vector. C4-12 cells were transfected with pcDNA-ERα (C4-12/ER) or empty vector (C4-12/vec) using LipofectAMINE Plus Reagent (Life Technologies, Inc., Carlsbad, CA) and then exposed to an antibiotic (G418; 0.5 mg/mL) for 3 weeks. Expression of ERα in G418-resistant colonies was detected by immunoblotting with an anti-ER antibody (Chemicon, Temecula, CA).

Real-Time Reverse Transcription-Polymerase Chain Reaction. Total RNA (2 μg) was treated with DNase I to remove potential DNA contamination and then reverse transcribed using the SuperScript II reverse transcriptase (Invitrogen). Real-time polymerase chain reactions (PCRs) were then performed using puReTaq Ready-To-Go PCR beads (Amersham Biosciences, Piscataway, NJ) and monitored by SYBR Green I (BioWhittaker, Walkersville, MD) using a Smart Cycler Real-Time PCR instrument (Cepheid, Sunnyvale, CA) for 42 cycles. PCR products of the expected size were also visualized on agarose gels stained with ethidium bromide. Alternatively, the reverse transcription-PCR (RT-PCR) reaction was conducted using iQ SYBR Green Supermix (Bio-Rad, Hercules, CA) in an iCycler system (Bio-Rad) for *PR* transcripts (22). The relative mRNA level of a given locus was calculated by Relative Quantitation of Gene Expression (Applied Biosystems, Foster City, CA) with *glyceraldehyde-3-phosphate dehydrogenase* (*GAPDH*) or *β-actin* mRNA as an internal control. The primers used for RT-PCR reactions are listed in Supplementary Table S1.

Immunofluorescence and Western Blot Analysis. MCF-7 cells (2×10^5) treated with or without ERα siRNAs were permeablized with 0.5% Nonidet P-40/PBS and blocked with a 1:100 dilution of horse serum before incubation with primary anti-ERα antibody (1:1,000; mouse monoclonal antibody D-12; Santa Cruz Biotechnology, Santa Cruz, CA). Sample slides were washed with PBS and incubated in the dark with secondary antibody (1:500) conjugated with Texas Red (fluorescent antimouse IgG kit; Vector Laboratories, Burlingame, CA) for 1 hour. The slides were then mounted with Vectashield mounting medium with 4′,6-diamidino-2-phenylindole (Vector Laboratories) and observed under a fluorescence microscope (Zeiss Axioskop 40; Zeiss, Thornwood, NY). Images were captured by the AxioCam HRC camera and analyzed by AxioVision 5.05 software.

Small interfering RNA-treated cells and control cells were lysed in the presence of proteinase inhibitors. One hundred micrograms of protein were subjected to 7% SDS-PAGE and transferred to immunoblot membranes. The membranes were then incubated with mouse anti-ERα (MAB463; Chemicon) and labeled secondary antibody. GAPDH was used a loading control.

Chromatin Immunoprecipitation-Polymerase Chain Reaction. Cultured cells (2×10^6) were cross-linked with 1% formaldehyde and then washed with PBS in the presence of protease inhibitors. The cells were resuspended in lysis buffer, homogenized using a tissue grind pestle to release nuclei, and then pelleted by centrifugation. SDS-lysis buffer from a chromatin immunoprecipitation (ChIP) assay kit (Upstate Biotechnology, Lake Placid, NY) was used to resuspend the nuclei. The lysate was sonicated to shear chromatin DNAs and then centrifuged to remove cell debris. The supernatants were transferred to new tubes and incubated overnight with an antibody against ERα, YY-1, or EZH2 (Santa Cruz Biotechnology); HDAC1, MBD2, or MeCP2 (Upstate Biotechnology); and DMNT1, DNMT3a, or DNMT3b (Imgenex, San Diego, CA). Agarose slurry was then added to the mixture, and the chromatin-bound agarose was centrifuged. The supernatant was collected and used for total input (it serves as a positive control) in the ChIP-PCR assay. After elution, proteins were digested from the bound DNA with proteinase K. Phenol/chloroform-purified DNA was then precipitated and used in ChIP-PCR assays for a *progesterone receptor* (*PR*) promoter region. The primer sequences were 5′-GGCTTTGGGCGGGGCCTCCCTA (sense strand) and 5′-TCTGCTGGCTCCGTACTGCGG (antisense strand). After amplification, ^{32}P-incorporated PCR products were separated on 8% polyacrylamide gels and subjected to autoradiography using a Storm PhosphorImager (Amersham Biosciences).

Methylation-Specific Polymerase Chain Reaction. Genomic DNA (1 μg) from each sample was bisulfite-converted using the EZ DNA Methylation Kit (Zymo Research Corp., Orange, CA), according to the manufacturer's protocol. The converted DNA was eluted with 40 μL of elution buffer and then diluted 50 times for methylation-specific PCR (MSP). The primer sets designed for amplifying the methylated or unmethylated allele of the PR locus are listed in Supplementary Table S2. All PCR reactions were performed in PTC-100 thermocyclers (MJ Research, Watertown, MA) using AmpliTaq Gold DNA polymerase (Applied Biosystems). ^{32}P-incorporated amplified products were separated on 8% polyacrylamide gels and subjected to autoradiography using a Storm PhosphorImager (Amersham Biosciences).

Combined Bisulfite Restriction Analysis. Combined bisulfite restriction analysis (COBRA) was carried out essentially as described previously (23). Bisulfite-modified DNA (~10 ng) was used as a template for PCR with specific primers flanking the interrogated sites (*Taq*I or *Bst*UI) of an ERα downstream target. Primer sequences used for amplification are listed in Supplementary Table S3. After amplification, radiolabeled PCR products were digested with *Taq*I or *Bst*UI, which restrict unconverted DNA containing methylated sites. The undigested control and digested DNA samples were run in parallel on polyacrylamide gels and subjected to autoradiography. The percentage of methylation was determined as the intensity of methylated fragments relative to the combined intensity of unmethylated and methylated fragments.

Chromatin Immunoprecipitation on Chip. MCF-7 cells (2×10^7) were used to conduct ChIP with an antibody specific for ERα following the protocol described (see Chromatin Immunoprecipitation-Polymerase Chain Reaction). After chromatin coimmunoprecipitation, DNA was labeled with Cy5 fluorescence dye and hybridized to a genomic microarray panel containing ~9,000 CpG islands (24). Microarray hybridization and posthybridization washes have been described previously (25). The washed slides were scanned by a Gene Pix 4000A scanner (Axon, Union City, CA), and the acquired microarray images were analyzed with GenePix Pro 4.0 software. This ChIP-on-chip experiment was conducted twice.

Positive CpG island clones were sequenced, and the derived sequences were used to identify putative transcription start sites by Blastn[5] or Blat.[6] Both Genomatrix[7] and TFSEARCH[8] programs were then used to localize the consensus sequences of the estrogen response elements (EREs) and other

[5] http://www.ncbi.nlm.nih.gov/BLAST/.
[6] http://genome.cse.ucsc.edu/cgi-bin/hgBlat.
[7] http://www.genomatix.de/site_map/index.html.
[8] http://www.cbrc.jp/research/db/TFSEARCH.html.

related transcription factor binding sites (AP-1, SP-1, cAMP-responsive element binding protein, and CEBP).

Differential Methylation Hybridization. Differential methylation hybridization (DMH) was performed essentially as described previously (25, 26). Briefly, 2 μg of genomic DNA were digested by the 4-base frequent cutter *Mse*I, which restricts bulk DNA into small fragments but retains GC-rich CpG island fragments (24). H-24/H-12 PCR linkers (5′-AGGCAACTGTGCTATCCGAGGGAT-3′ and 5′-TAATCCCTCGGA-3′) were then ligated to the digested DNA fragments. The DNA samples were further digested with two methylation-sensitive endonucleases, *Hpa*II and *Bst*UI, and amplified by PCR reaction using H-24 as a primer. After amplification, test DNA from siRNA-treated cell lines or clinical samples was labeled with Cy5 (red) dye, whereas control DNA from the mock-transfected cell lines or normal female blood samples was coupled with Cy3 (green) dye. Equal amounts of test and control DNAs were cohybridized to a microarray slide containing 70 ERα promoter targets (average, 500 bp) identified from the ChIP-on-chip results. Posthybridization washing and slide scanning are described above. Normalized Cy5/Cy3 ratios of these loci were calculated by GenePix Pro 4.0.

Shrunken Centroids Analysis. DMH microarray data were analyzed by the procedure described online.[9] This program incorporates graphic methods for automatic threshold choice and centroid classification.

Statistical Analyses. Differences of methylation or mRNA levels in experimental studies were analyzed by a paired *t* test. Methylation differences between two tumor groups were determined with a Pearson's χ^2 test. $P < 0.05$ was considered statistically significant.

RESULTS

RNA Interference Transiently Knocks Down Estrogen Receptor α Expression in Breast Cancer Cells. Although several *in vitro* systems and mouse models are available for analysis of estrogen signaling, to our knowledge, the recently described RNAi (27) has not been actively used in this area of research. We therefore used this technology to specifically repress *ERα* gene expression via targeted RNA degradation (28, 29). Six different *ERα* siRNAs, two of which have sequences homologous to a splice variant, were synthesized (Fig. 1*A*). These siRNAs (40 nmol/L) were individually transfected into MCF-7, an ERα-positive human breast cancer cell line. MCF-7 cells were cultured in the presence of E_2. Quantitative RT-PCR analysis showed that, 24 hours after transfection, two siRNAs, siRNAs 1 and 17, were capable of repressing ERα transcripts (Fig. 1*B*). Specifically for siRNA 1, we observed a >93% decrease of *ERα* mRNA. Immunofluorescence (Fig. 1*C*) and Western blot (Fig. 1*D*) analyses confirmed that this RNAi also dramatically reduced ERα protein synthesis. This inhibitory effect appeared to be transient, and the expression of ERα protein reappeared in cultured cells 4 weeks after RNAi withdrawal (Fig. 1*D*).

Epigenetic Silencing of the *PR* Gene Is Triggered by Estrogen Signal Disruption. We hypothesized that disruption of ERα signaling by siRNA may lead to the silencing of some positively regulated ERα targets governed by epigenetic mechanisms. To this end, a known ERα downstream target, the *PR* gene, was investigated in detail. In Fig. 2*A* and *B*, quantitative RT-PCR analysis showed that by 36 hours after treatment of MCF-7 cells with siRNA 1, the level of *PR* transcripts (PR-A and PR-B) was reduced by >95% (paired *t* test, $P < 0.0001$). Next, ChIP-PCR was performed to determine the status of chromatin remodeling at the 5′-end of the *PR* gene. The protein-DNA complexes were immunoprecipitated with antibodies to ERα or to specific modified histones (acetyl-H3, acetyl-H3-K9, and methyl-H3-K4) known to specify active transcription (7, 30). As shown in Fig. 2*C*, the presence of these active chromatin components was diminished over a period of 36 hours, coinciding with decreased ERα binding to the *PR* promoter region.

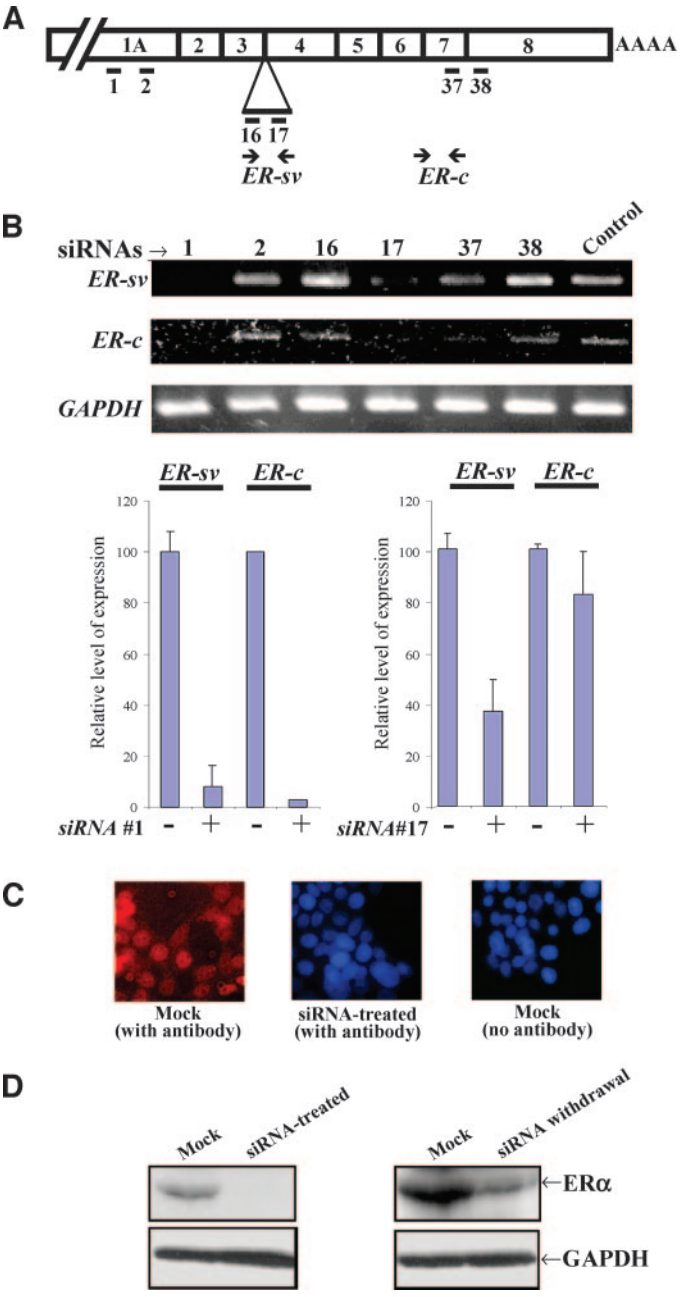

Fig. 1. Down-regulation of *ERα* by siRNAs. MCF-7 ERα-positive human breast cancer cells were transfected with six different double-stranded siRNAs for 4 hours. Cells were left untreated for an additional 24 hours, and total RNA and proteins were then harvested for analysis. Additionally, cells were left untreated for a prolonged period of 3 to 4 weeks (see RNAi withdrawal in *D*), and proteins were harvested for analysis. Mock-treated cells were transfected with vehicle only. *A*, map of *ERα* cDNA. The *ERα* mRNAs were transcribed from several unique first exons and seven other common exons. An additional splice variant (between exons 3 and 4) is also shown. Approximate locations of siRNAs (*1*, *2*, *16*, *17*, *37*, and *38*) are indicated by *bars*. *B*, RT-PCR of *ERα*. PCR primers specifically for the splice variant (*ER-sv*) and the common transcripts (*ER-c*) are indicated by *arrows* in *A*. The *GAPDH* transcript was used as a control. The expression levels of *ER-sv* or *ER-c* were normalized against *GAPDH* (*bottom panel*) by real-time PCR. *C*, immunofluorescence analysis of ERα expression. Small interfering RNA 1- or mock-treated MCF-7 cells were cultured on microscope coverslips and incubated with an ERα antibody. Positive nuclei staining (Texas Red) was seen only in mock-treated cells (with antibody), but not in siRNA 1-treated (with antibody) or mock-treated (without antibody) cells. 4′,6-Diamidino-2-phenylindole was used to counterstain nuclei (*blue*). *D*, Western blot analysis of ERα expression. Cellular protein products from various treatments were harvested and separated by SDS-PAGE for immunoblot analysis with ERα and GAPDH (loading control) antibodies, respectively. Results are representative of at least three independent experiments.

[9] http://www-stat.stanford.edu/~tibs/PAM.

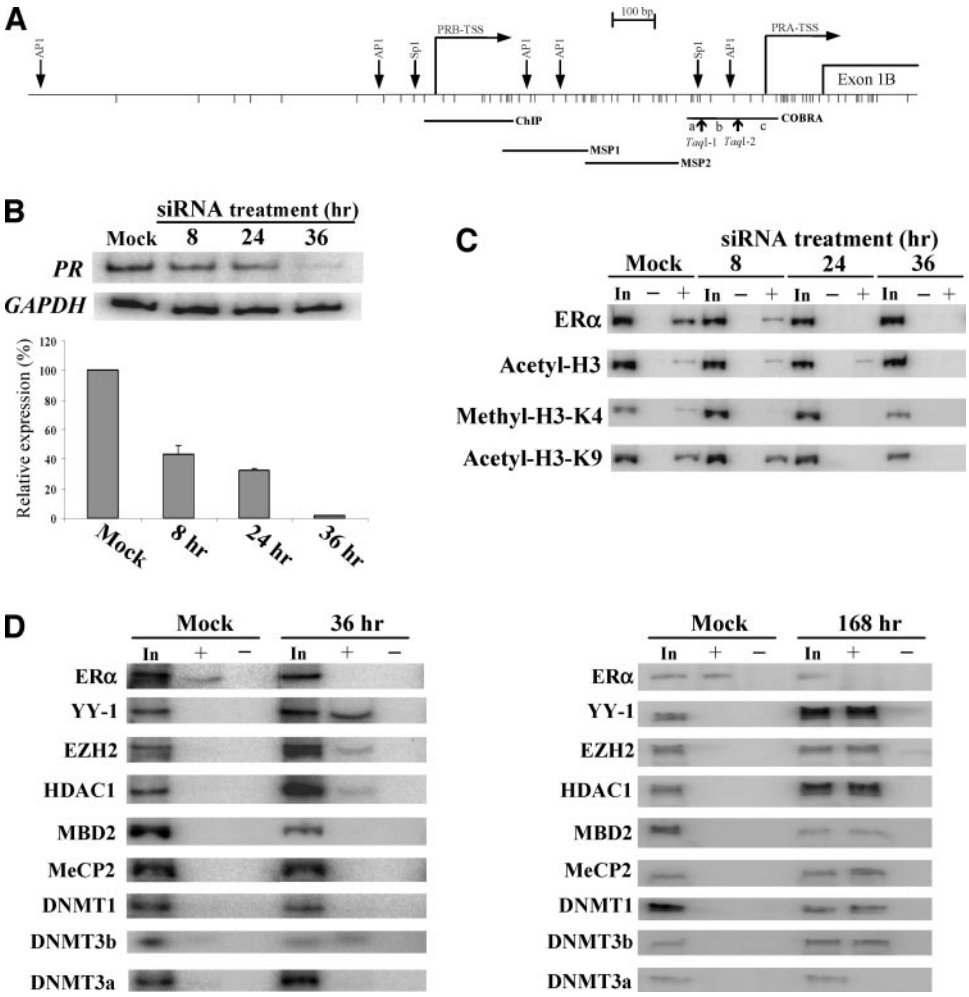

Fig. 2. Loss of estrogen signaling leads to epigenetic silencing of the *PR* gene. *A*, genomic map of the *PR* promoter CpG island. The positions of CpG sites in the genomic sequence are indicated by *thin vertical lines*. The positions of two alternative transcription start sites, *PRA* and *PRB*, respectively, are indicated by *bent arrows*. Potential transcription factor binding sites (AP-1 and Sp1) resulting from a TFSEARCH query (www.cbrc.jp/htbin/nph-tfsearch) are marked by *vertical arrows*. The location of the *PR* promoter fragment used for the ChIP assay and the two regions (MSP1 and MSP2) used for MSP are indicated by *horizontal lines* (see Fig. 3*A*). The region amplified for COBRA is *underlined*, and the *two vertical arrows* indicate the interrogating *Taq*I restriction (TCGA) sites (see Fig. 3*C*). *B*, time course inhibition of PR transcripts by siRNA treatment. MCF-7 cells were transfected with ERα siRNA 1 for the indicated time periods (8, 24, and 36 hours) and harvested for real-time RT-PCR. Mock-transfected cells were harvested at the 36 hour time point. Primers were designed to amplify a common region of the two known *PR* transcripts. Relative levels of *PR* transcripts were normalized against that of the *GAPDH* loading control. Results from three independent experiments are shown as means ± SE. *C*, ChIP-PCR assay for activating chromatin modifications on the PR CpG promoter island. Chromatin DNA was immunoprecipitated with antibodies specific for ERα, acetylated histone H3 (acetyl-H3 and/or acetyl-H3-K9), or dimethyl-H3-K4. DNA fragments were amplified with a primer pair located in a *PR* CpG island region (indicated in *A*). The final radiolabeled products were separated on 6% polyacrylamide gels and subjected to autoradiography. *In*, total input; −, without antibody; +, with antibody. *D*, ChIP-PCR assays for repressive chromatin modifications on the PR promoter CpG island region at 36 and 168 hours after ERα siRNA treatment. Antibodies against polycomb repressors (YY-1 and EZH2), histone deacetylase (HDAC1), methyl-CpG binding proteins (MBD2 and MeCP2), and DNA methyltransferases (DMNT1, DNMT3a, and DNMT3b) were used in ChIP-PCR assays. *In*, total input; −, without antibody; +, with antibody.

We speculated that this initial transcriptional inactivation might trigger further recruitment of repressor molecules to the *PR* promoter CpG island to subsequently establish a long-term silencing state. ChIP-PCR assays were conducted with a panel of antibodies raised for the polycomb repressors YY-1 and EZH2, histone deacetylase HDAC1, methyl-CpG–binding proteins MBD2 and MeCP2, and DNA methyltransferases DMNT1, DNMT3a, and DNMT3b. At 36 hours after siRNA treatment, YY-1 and EZH2 were bound to the promoter region (Fig. 2*D*). These polycomb proteins have previously been shown to target the regulatory regions of *homeobox* genes, the resulting repression of which can be tissue specific and important for early embryonic development (31, 32). Here we demonstrate for the first time that these proteins have an additional role in repressing an ERα target gene. Furthermore, the *PR* promoter was seen, at 36 hours, to recruit HDAC1 (Fig. 2*D*), a protein known to deacetylate histone protein tails, creating a repressive heterochromatin environment in the targeted promoter area (7, 9, 10). However, at this early time point (36 hours), ChIP-PCR analysis did not detect the presence of the DNA methyltransferase DNMT1 in the *PR* promoter CpG island area (Fig. 2*D*), nor did we observe the presence of MBD2 or MeCP2, which are known to bind methylated CpG sites. Only a faint band corresponding to DNMT3b was detected in the *PR* promoter area by 36 hours after ERα siRNA treatment of MCF-7 cells. Except for DNMT3a, the recruitment of these repressive proteins to the *PR* promoter CpG island was evident by 168 hours after siRNA treatment.

To further determine whether the recruitment of these epigenetic components could trigger *de novo* DNA methylation, MSP assays (33) were conducted to survey two 5′-end regions of *PR* at different time periods after siRNA treatment. As shown in Fig. 3*A*, *PR* methylation was detected in amplified bisulfite-treated DNA only at 36 hours after treatment. This observation was independently confirmed by conducting semiquantitative COBRA (23). In the assay, ~10% of MCF-7 cells showed methylation in one (Fig. 2*A*, *TaqI-2*) of the two PR *Taq*I sites analyzed 36 hours after siRNA treatment (Fig. 3*B*). Both of these sites became methylated at a later time point (168 hours) of treatment (Fig. 3*B*). This study implies that acquired DNA methylation is a late event and that the density of DNA methylation may gradually accumulate at the 5′-end of *PR* after disrupting ERα signaling by siRNA.

Next, we determined whether this *acquired* promoter methylation could be observed in ERα-negative breast tumors. COBRA was therefore conducted in 32 primary tumors (16 ERα-negative and 16 ERα-positive tumors) and 7 normal controls (see representative examples in Fig. 3*C*). Consistent with the *in vitro* findings, *PR* promoter hypermethylation occurred more frequently in ERα-negative tumors (45%) than in ERα-positive tumors (10%) (χ^2 test, $P < 0.05$).

Reexpression of *PR* Requires Both Estrogen Signal Restoration and DNA Demethylation. The *in vitro* experimental results described above are based on transient siRNA treatment. To determine whether this signal disruption has a lasting impact on *PR* expression, we took advantage of an ERα-negative cell subline, C4-12, derived from ERα-positive MCF-7 cells by long-term hormonal depletion (34). A recent study has indicated that *PR* gene expression is absent in this cell line (35). We therefore examined whether stably reexpressing ERα could restore *PR* gene activity in several established C4-12

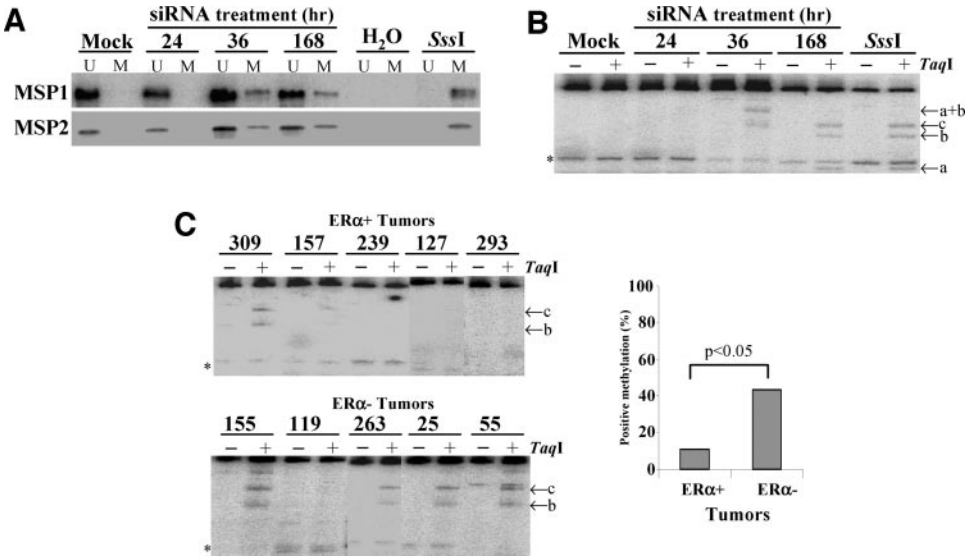

Fig. 3. DNA methylation analysis of the *PR* promoter by MSP and COBRA. *A*, bisulfite-treated DNA samples from siRNA- and mock-treated cells were used for amplification with specific primers for MSP1 and MSP2 (see Fig. 2*A*). Radiolabeled PCR products for unmethylated (*Lanes U*) and methylated (*Lanes M*) DNA strands were separated on 6% polyacrylamide gels. *B*. For COBRA, bisulfite DNA samples from siRNA- and mock-treated cells were amplified and digested with *Taq*I enzyme and then separated on polyacrylamide gels. The digested DNA fragments (*a*, *b*, and *c*) indicated by the *arrows* reflect methylation of *Taq*I restriction sites within the *PR* promoter CpG island (see Fig. 2*A*). An *asterisk* indicates PCR artifact or primer-dimer. *C*, COBRA of *PR* promoter in ERα-positive and -negative breast tumors. The percentage of positive methylation was calculated as the intensity of methylated fragments relative to the combined intensity of unmethylated and methylated fragments (*right panel*). All DNA methylation data shown here are representative of at least three independent experiments.

subclones (C4-12/vec, C4-12/ER#1, C4-12/ER#50, and C4-12/ER#86; see examples in Fig. 4*A*, *inset*).

Treatment of these subclones (*e.g.,* C4-12/ER#86 in Fig. 4*A*) with E_2, however, failed to induce *PR* mRNA expression, demonstrating that reintroduction of ERα alone was insufficient to reactivate expression of a silent *PR* gene. To determine whether loss of *PR* expression was due to DNA methylation, C4-12/vec (*i.e.*, cells stably transfected with empty vector) and C4-12/ER#86 cells were pretreated with 5-AzadC, a DNA demethylating agent, before E_2 treatment. As shown in Fig. 4*A*, sequential treatment with 5-AzadC followed by E_2 resulted in reexpression of *PR* mRNA in C4-12/ER#86 cells, but not in C4-12/vec cells, demonstrating that both ERα expression and DNA demethylation are required to restore PR expression. To further confirm that reactivation of the *PR* gene was due to DNA demethylation, the methylation status of the *PR* promoter CpG island region was examined by MSP (Fig. 4*B*). In contrast to MCF-7 cells in which the *PR* promoter CpG island was unmethylated (Fig. 3*A*), methylation was observed in both C4-12/vec and C4-12/ER cells (Fig. 4*B*, *Lanes 1*, *2*, and *5–10*). However, after treatment with 5-AzadC, *PR* promoter methylation was partially reversed in C4-12/vec cells (Fig. 4*B*, *Lanes 3* and *4*) and completely removed in C4-12/ER#86 cells (Fig. 4*B*, *Lanes 11* and *12*). Together, these results demonstrate that the silencing of *PR* is maintained, in part, by DNA methylation in the ERα-negative C4-12 cells and that reactivation of the *PR* promoter requires both the presence of ERα and DNA demethylation.

DNA Methylation of Multiple Estrogen Receptor α Downstream Targets Is Triggered by Disrupting Receptor Signaling. To determine whether this epigenetically mediated silencing is a generalized event, we used ChIP-on-chip, a novel microarray-based method developed in our laboratory (36, 37), for a genome-wide screening of ERα downstream targets. In this case, we probed a panel of ~9,000 arrayed CpG island fragments with anti-ERα–coimmuo-

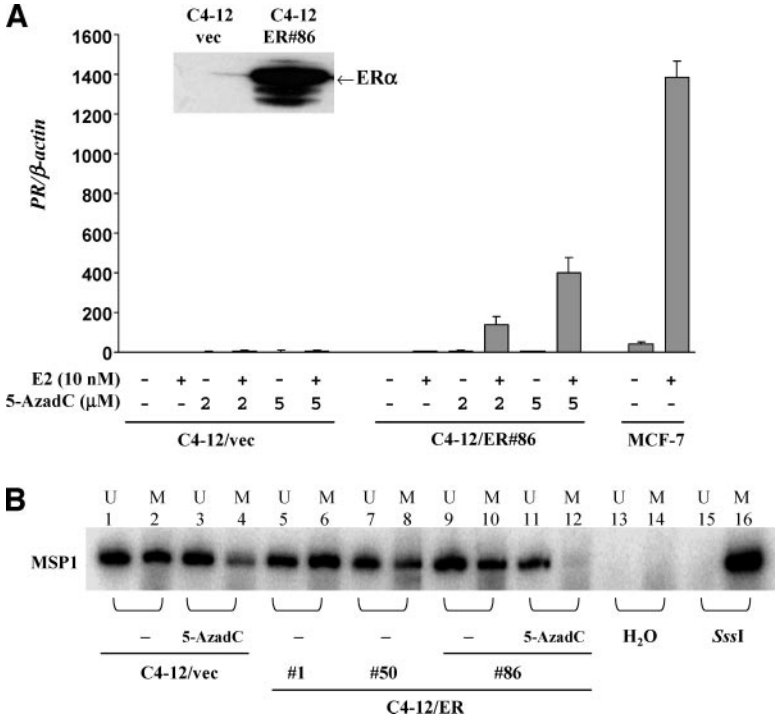

Fig. 4. Treatment of C4-12/ER cells with 5-AzadC restores *PR* mRNA expression. *A*. Expression levels of *PR* mRNA in C4-12/Vec and C4-12/ER cells were determined after treatment with the indicated doses of 5-AzadC for 5 days, followed by 10 nmol/L E_2 for 24 hours. *PR* mRNA levels were measured by quantitative real-time RT-PCR and normalized using *β-actin* mRNA levels. The results ($X\pm$ SE) are shown from two independent experiments, each in triplicate. ERα expression in C4-12 cells #86 (*A*, *inset*) was detected by immunoblotting with an anti-ERα antibody. *B*, analysis of *PR* promoter by MSP assay. Bisulfite-treated DNAs from cells treated with or without 5-AzadC were amplified with specific primers for the *PR* promoter CpG island (*i.e.*, the MSP1 region in Fig. 2*A*). Radiolabeled PCR products for unmethylated (*Lanes U*) and methylated (*Lanes M*) DNA strands were separated on 6% polyacrylamide gels. MSP data shown here are representative of three independent experiments.

precipitated chromatins. Putative target sequences were used to search for the presence of ERα binding motifs, EREs, and other related binding sites (*e.g.,* AP-1, SP-1, cAMP-responsive element binding protein, and CEBP) by using the Genomatrix[7] and TFSEARCH[8] programs. These computational algorithms identified a total of 70 unique ERα promoter targets, which were used to construct a subpanel genomic microarray (see a partial list of the genes in Supplementary Table S4). The previously described DMH method (25, 26) was then used to determine the DNA methylation status of these ERα targets in siRNA-treated *versus* mock-treated MCF-7 cells. Amplicons representing genomic pools of methylated DNAs were prepared from these treated cells using our established protocols (25, 26). Cy5 (red dye)- and Cy3 (green dye)-labeled DNAs were prepared from siRNA- and mock-treated cells, respectively, and cohybridized to microscope slides containing the arrayed 70 unique ERα targets. ERα target loci methylated in siRNA-treated cells, but not in mock-treated cells, were expected to show greater Cy5/Cy3 hybridization signals. This is because methylated CpG sites are protected from methylation-sensitive restriction (*i.e.*, *Hpa*II and *Bst*UI) and could thus be amplified by a linker-PCR approach during amplicon preparation. In contrast, unmethylated CpG sites were restricted by the methylation-sensitive enzymes, could not be amplified by PCR, and were thus devoid of hybridization signals.

To analyze our microarray data, we adapted the "shrunken centroids method" (38) to define the threshold setting for class prediction of methylated ERα target loci. This approach can be used to uniquely define the threshold level that statistically discriminates ERα loci commonly methylated in siRNA-treated cells from the same loci in mock-treated cells. After initial evaluation of the microarray data, we chose the threshold value 2.0 that generates less error (≤0.3) for cross-validation (data not shown). When the cross-validation variances from individual samples were plotted (Fig. 5*A*), many ERα target loci could be used to discriminate between siRNA-treated cells and mock-treated counterparts (manifested as having many loci with no misclassification error) at the 168 hour time point. However, this threshold level was not sufficiently stringent to discriminate between the mock- and siRNA-treated cell samples at 24 or 36 hours (manifested as having very few loci with low misclassification error). In Fig. 5*B*, the actual methylation status of individual loci, in comparison with the predicted centroids, is plotted to present an overall change of DNA methylation at different time periods of siRNA treatment. Relative to the overall predicted centroids, a positive value of a locus

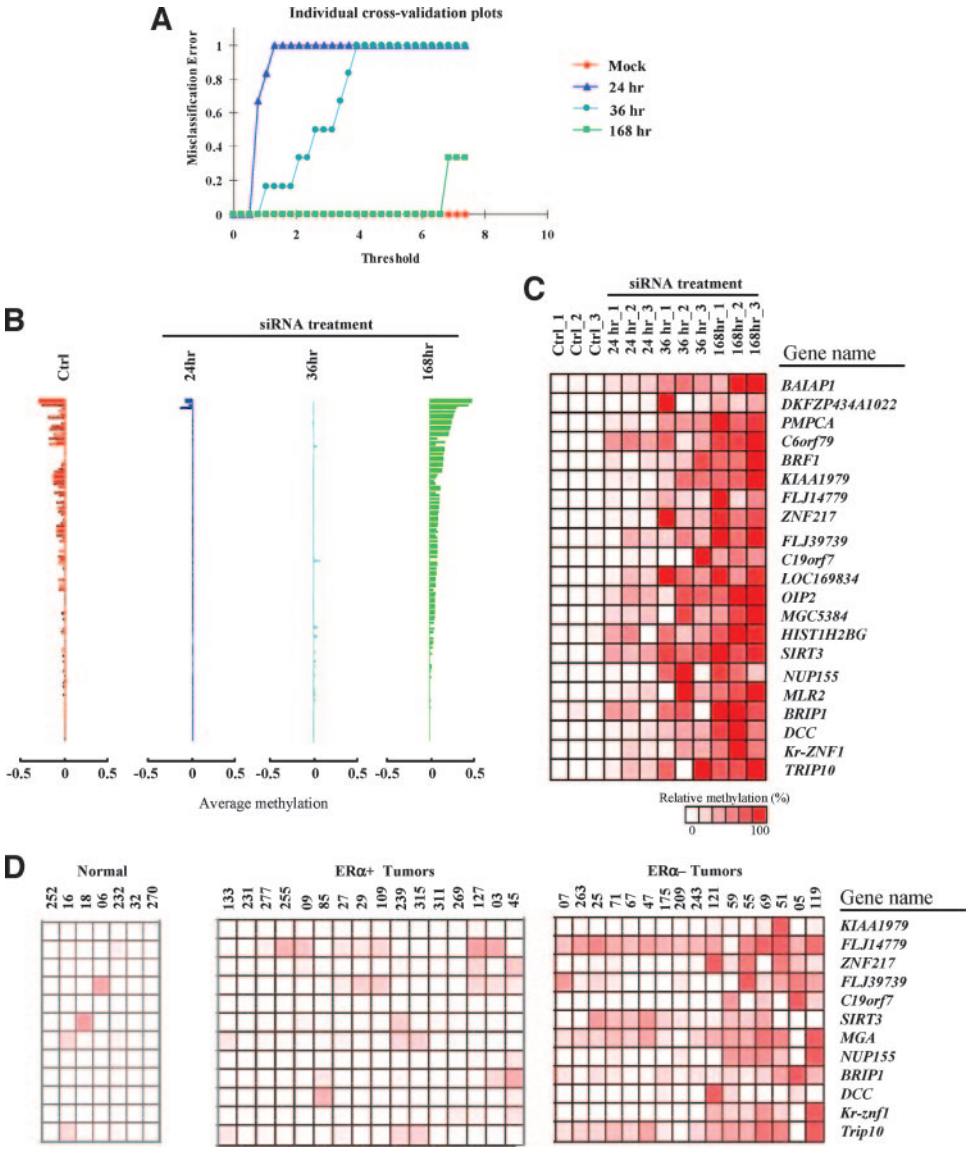

Fig. 5. Acquired DNA methylation in multiple *ERα* downstream targets after estrogen signal disruption. Seventy ERα downstream targets were analyzed by DMH, as described in the text. Fluorescence-labeled methylation amplicons were prepared from siRNA-treated (24, 36, and 168 hours) and mock-treated (168 hours) MCF-7 cells, respectively, and cohybridized to ERα microarray slides. The hybridization output is the measured relative intensity of fluorescence reporter molecules. *A*, test error for different values of shrinkage. Shrunken centroids analysis was conducted using methylation microarray datasets (see detailed description in the text). Tenfold cross-validation was used to estimate the error rate, when a different degree of shrinkage was used to generate the centroids. *B*. Predicted centroids, shown as horizontal units, represent log ratios of DNA methylation. The order of the 70 ERα target loci is arbitrary. Methylation changes were seen only in a few loci at 24 or 36 hours after siRNA treatment; however, a significant methylation change was seen at 168 hours (7 days; $P < 0.05$), displaying positively shrunken values for these 70 loci. *C*, methylation heat map of the 21 selected ERα loci at different time periods after siRNA treatment. These loci were selected because a threshold (threshold = 2; error rate ≤ 0.3) from cross-validation showed fewer errors in methylation microarray experiments. As shown, DNA methylation of these loci accumulates progressively over time (168 hours) after the siRNA treatment. Data shown here represent three independent microarray experiments. *D*, methylation heat map of the top 12 methylated ERα loci in ERα-negative tumors. Microarray-based DMH was conducted in these clinical samples as described in the text. The derived microarray data were analyzed by the shrunken centroids method.

indicates more methylation during the treatment, whereas a negative value indicates less methylation. This shrunken centroids map revealed that *de novo* DNA methylation can be detected in a subset of ERα targets 168 hours after siRNA treatment, but not in cells treated for only 24 or 36 hours after treatment.

To validate the findings of the shrunken centroid analysis, unsupervised cluster analysis was performed on the microarray data, using the top 21 methylated loci selected by machine training ("heat map" shown in Fig. 5*C*). The result reaffirms the shrunken centroid data in that replicates of each treatment type are clustered together and that the level of methylation increased with the extent of siRNA treatment. A paired *t* test revealed that the methylation status of these 21 loci was significantly different ($P < 0.05$) between the mock-treated (ERα-positive) and siRNA-treated (ERα-negative) cells.

This microarray observation was independently validated by conducting expression and DNA methylation analyses on three newly identified ERα downstream targets, *TRIP10*, *Kr-Znf1*, and *DCC*. In general, the decreased levels of these mRNAs preceded the emergence of DNA methylation at their respective promoter CpG islands (Fig. 6*A* and *B*). This epigenetically mediated silencing also indirectly influenced the expression of *MTA3*, a gene known to be regulated via a downstream ERα target and to participate in Mi-2/NuRD nucleosome remodeling (Fig. 6*B*; ref. 39).

DNA Methylation of ERα Downstream Targets is Preferentially Observed in ERα-Negative Tumors. We next determined whether this *in vitro* finding could be seen *in vivo*. DMH was therefore conducted using the aforementioned 32 primary breast tumors and 7 normal controls. The derived microarray data were then analyzed by the shrunken centroid method. Although the methylation results of these 70 ERα target loci did not clearly segregate tumor samples into subclasses, we observed a general trend that methylated loci appear more frequently in ERα-negative tumors than in ERα-positive tumors ($P < 0.05$). Fig. 5*D* presents a heat map of the 12 most methylated loci in the studied breast tumors. As shown, we observed higher overall methylation in the ERα-negative tumors (6 of 16 tumors had >40% methylation in the loci analyzed) than in the ERα-positive tumors (only 1 of 16 tumors achieved the same level of methylation). Also, the total number of loci showing DNA methylation was greater in ERα-negative tumors, when compared with ERα-positive tumors. Only four loci showed a low level of methylation in normal breast samples. Methylation analysis by MSP was further conducted for *TRIP10* in these breast samples (Fig. 6*C*). Consistent with the microarray finding, *TRIP10* promoter hypermethylation was detected in 50% (8 of 16) of ERα-negative tumors but in none of the 16 ERα-positive tumors analyzed (χ^2 test, $P < 0.005$).

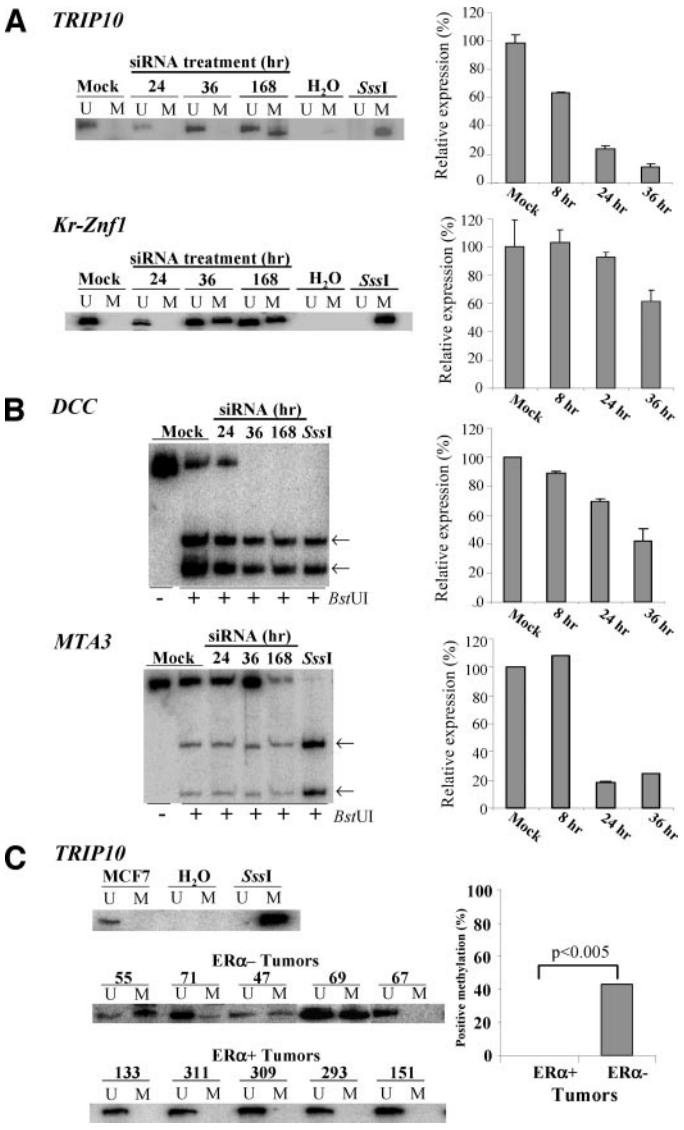

Fig. 6. Methylation and expression analysis of *ERα* target genes. *A*. For methylation-specific PCR assays, bisulfite-treated DNA samples from siRNA- or mock-treated cells were used for amplification with specific primers for *TRIP10* and *Kr-Znf1*, respectively. ^{32}P-labeled PCR products for unmethylated (*Lanes U*) and methylated (*Lanes M*) DNA strands were separated and displayed on 6% polyacrylamide gels (*left panels*). Messenger RNA levels of these genes were measured by quantitative real-time RT-PCR (*right panels*) and normalized using *GAPDH* mRNA expression levels, as described in the text. Results from three independent experiments are shown as means ± SE. The expression level of these genes was significantly reduced by the siRNA treatment (paired *t* test, $P < 0.017$ for *TRIP10* and $P < 0.048$ for *Kr-Znf1*). *B*. For *DCC* and *MTA* genes, COBRA was used to measure DNA methylation. Bisulfite DNA samples were amplified and digested with *Bst*UI enzyme and separated on polyacrylamide gels. The digested DNA fragments shown by *arrows* reflect methylation at the *Bst*UI restriction sites within the *DCC* promoter CpG island (*left panels*). Messenger RNA levels of these genes were measured by quantitative real-time RT-PCR (*right panels*) and normalized using *GAPDH* mRNA expression levels, as described in the text. Results from three independent experiments are shown as means ± SE. The expression level of these genes was significantly reduced by siRNA treatment (paired *t* test, $P < 0.03$ for *DCC* and $P < 0.014$ for *MTA3*). *C*. MSP analysis of the *TRIP10* promoters in 16 ERα-positive and 16 ERα-negative breast tumors. Only representative results are shown.

DISCUSSION

Understanding the sequence of how complex epigenetic events are established can provide important insights into the molecular mechanisms underlying gene silencing in cancer. However, the "chicken and egg" issue of which comes first, DNA methylation, histone modification, or others, is an ongoing debate in the epigenetic research community. Many early studies of this issue come from non-mammalian systems. Mutations in a histone methyltransferase specific for H3-K9 resulted in loss of DNA methylation in *Neurospora crassa* (15, 16), suggesting that histone methylation can initiate DNA methylation. In *Arabidopsis*, it has been shown that CpNpG methylation depends on a histone H3 methyltransferase (40), also indicating that histone methylation can direct DNA methylation. New evidence suggests that the reverse scenario can occur in heterochromatin (41). In this case, a self-reinforcing system is implemented, allowing for feedback from DNA methylation to histone methylation for the long-term maintenance of a heterochromatin state in a gene (41). However, this epigenetic paradigm remains to be explored in mammalian systems. Earlier studies have shown that *in vitro* methylated transgenes can be targets for methyl-CpG–binding proteins, which in turn recruit repressor complexes containing histone deacetylases (17, 18). Fahrner *et al.* (19) suggested that DNA methylation of *hMLH1* can specify unique histone codes for the maintenance of a silenced state. They detected methyl histone 3-lysine 9 in the DNA methylated, transcrip-

tionally silenced promoter CpG island of *hMLH1* in a cancer cell line. Treatment with the DNA demethylating agent 5-AzadC alone, but with not the histone deacetylase inhibitor trichostatin A, resulted in reversal of this repressive histone modification. Taken together, these reports, as well as other studies, imply that in contrast to other organisms, histone modifications may be secondary to DNA methylation in initiating gene silencing in mammalian cells (17, 18, 20, 42).

A study by Bachman *et al.* (43), however, presents a different view with respect to the silencing of the *p16* gene in an experimental system using somatic knockout cells. These authors suggest that chromatin modifications are not totally dependent on prior DNA methylation to initiate gene silencing. In support of this observation, Mutskov and Felsenfeld (44) have recently demonstrated that histone modifications are the primary event associated with the silencing of a transgene, *ILR2*. In this case, a gradual increase in DNA methylation density in and around the *ILR2* promoter was observed after transfection. In contrast to previous observations, these two recent studies therefore suggest that DNA methylation sets up an epigenetic "mark" for the maintenance of long-term silencing, rather than initiating it. Clearly, this epigenetic process is complex and multifaceted, and it is possible that the sequence of epigenetic events for establishing and maintaining the silenced state of a gene can be locus or pathway specific.

The present study suggests that gene inactivation and histone modifications occur before DNA methylation at some ERα target loci. Depicted in Fig. 7 is a hypothetical gene containing an ERE site within the promoter area, the active transcription of which is directly dependent on estrogen signaling. On the removal of this signaling, down-regulation of this gene occurs immediately. Transcriptional repressors (*e.g.,* polycomb proteins) and histone deacetylases are then assembled to its promoter to initiate long-term transcriptional repression. Subsequent recruitment of DNA methyltransferases to the repressor complex methylates CpG sites in the adjacent area. This process may be gradual, with methylation density increasing over time in the targeted area (see the heat map in Fig. 5*C*). The buildup of DNA methylation could set up a heritable mark that may eventually replace some of the original repressors to establish a heterochromatin state of long-term silencing. In this case, reactivation of ERα target genes could no longer be achieved by reestablishing estrogen signaling alone (see the example of *PR* in Fig. 4*A*); it also requires DNA demethylation. In addition to the *PR* gene, we suggest that establishment of epigenetic memory may occur in other critical ERα downstream loci in some breast cancer cells.

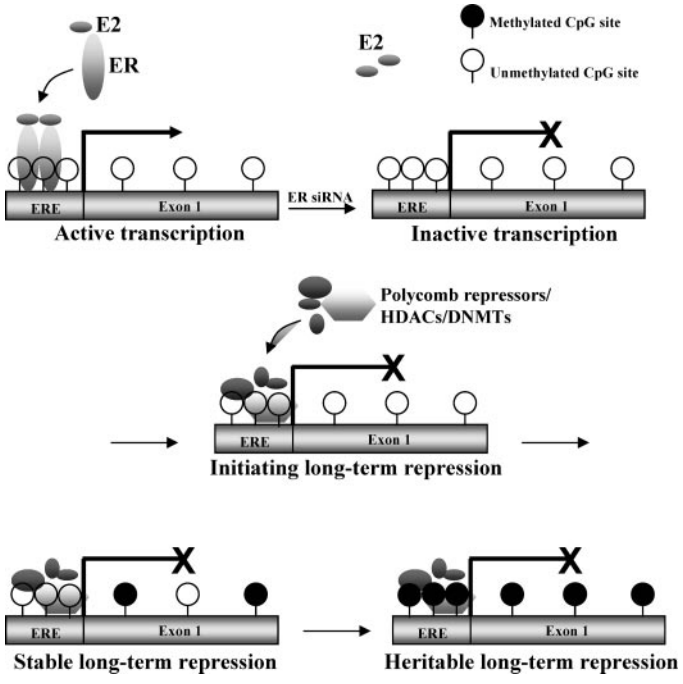

Fig. 7. A proposed model for the epigenetic hierarchy of long-term silencing in *ERα* downstream targets (see further explanation in the text). *HDACs*, histone deacetylases; *DNMTs*, DNA methyltransferases.

The occurrence of DNA methylation in a pathway-specific manner also has a new implication. Altered DNA methylation was originally thought to be a generalized phenomenon arising from a stochastic process in earlier studies (45, 46). This random methylation in tumor suppressor genes at their promoter CpG islands, thus silencing their transcripts, would provide tumor cells with a growth advantage. The specific epigenetic patterns observed in particular cancer types would therefore be derived from clonal selection of the proliferating cells. Some studies (26, 47, 48), however, have indicated that this epigenetic event is not random and that remodeling of the local chromatin structure of a gene may influence its susceptibility to specific DNA methylation. The present study provides some answers to this conundrum. Here we show that dysregulation of normal signaling in cancer cells may result in stable silencing of downstream targets, maintained by epigenetic machinery. This implies that the altered epigenetic condition is pathway specific, rather than a stochastic process in the ERα signaling pathway.

In conclusion, the present study implicates, for the first time, epigenetic influence (*i.e.*, chromatin remodeling and DNA methylation) on transcription of ERα downstream target genes and thus provides a new direction for research in this classical signaling pathway. Unlike irreversible genetic damage, epigenetic alterations are potentially reversible, providing an opportunity for therapeutic intervention in breast cancer. Histone deacetylase inhibitors, alone or together with DNA demethylating agents, may represent novel treatment approaches that could be combined with currently available chemotherapies. Our experimental evidence therefore provides a rationale for such treatment strategies designed to alter aberrant epigenetic processes in hormone-insensitive but receptor-positive breast tumors.

ACKNOWLEDGMENTS

The authors wish to thank Drs. Curt Balch and Phil Abbosh (Bloomington, IN) and Diane Peckham (Columbia, MO) for constructive review of the manuscript.

REFERENCES

1. Schiff R, Massarweh S, Shou J, Osborne, CK. Breast cancer endocrine resistance: how growth factor signaling and estrogen receptor coregulators modulate response. Clin Cancer Res 2003;9:447s–54s.
2. Jensen EV, Jordan VC. The estrogen receptor: a model for molecular medicine. Clin Cancer Res 2003;9:1980–9.
3. Bird A. DNA methylation patterns and epigenetic memory. Genes Dev 2002; 16:6–21.
4. Ehrlich M. Amount and distribution of 5-methylcytosine in human DNA from different types of tissues or cells. Nucleic Acids Res 1982;10:2709–21.
5. Ehrlich M. Expression of various genes is controlled by DNA methylation during mammalian development. J Cell Biochem 2003;88:899–910.
6. Ballestar E, Esteller M. The impact of chromatin in human cancer: linking DNA methylation to gene silencing. Carcinogenesis (Lond) 2002;23:1103–9.
7. Jones PA, Baylin SB. The fundamental role of epigenetic events in cancer. Nat Rev Genet 2002;3:415–28.
8. Nephew KP, Huang TH-M. Epigenetic gene silencing in cancer initiation and progression. Cancer Lett 2003;190:125–33.
9. Baylin SB, Esteller M, Rountree MR, et al. Aberrant patterns of DNA methylation, chromatin formation and gene expression in cancer. Hum Mol Genet 2001;10: 687–92.
10. Rountree MR, Bachman KE, Herman JG, Baylin SB. DNA methylation, chromatin inheritance, and cancer. Oncogene 2001;20:3156–65.

11. Feinberg AP, Tycko B. The history of cancer epigenetics. Nat Rev Cancer 2004;4:143–53.
12. Jenuwein T, Allis CD. Translating the histone code. Science (Wash DC) 2001;293:1074–80.
13. Grunstein M. Histone acetylation in chromatin structure and transcription. Nature (Lond) 1997;389:349–52.
14. Kouzarides T. Histone methylation in transcriptional control. Curr Opin Genet Dev 2002;12:198–209.
15. Tamaru H, Selker EU. A histone H3 methyltransferase controls DNA methylation in Neurospora crassa. Nature (Lond) 2001;414:277–83.
16. Tamaru H, Zhang X, McMillen D, et al. Trimethylated lysine 9 of histone H3 is a mark for DNA methylation in Neurospora crassa. Nat Genet 2003;12:177–85.
17. Eden S, Hashimshony T, Keshert I, Cedar H, Thorne AW. DNA methylation models histone acetylation. Nature (Lond) 1998;394:842.
18. Schubeler D, Lorincz MC, Cimbora DM, et al. Genomic targeting of methylated DNA: influence of methylation on transcription, replication, chromatin structure, and histone acetylation. Mol Cell Biol 2000;20:9103–12.
19. Fahrner JA, Eguchi S, Herman JG, Baylin SB. Dependence of histone modifications and gene expression on DNA hypermethylation in cancer. Cancer Res 2002;62:7213–8.
20. Stirzaker C, Song JZ, Davidson B, Clark SJ. Transcriptional gene silencing promotes DNA hypermethylation through a sequential change in chromatin modifications in cancer cells. Cancer Res 2004;64:3871–7.
21. Yan PS, Rodriguez FJ, Laux DE, et al. Hypermethylation of ribosomal RNA genes in human breast carcinoma. Br J Cancer 2000;82:514–7.
22. Aerts JL, Christiaens MR, Vandekerckhove P. Evaluation of progesterone receptor expression in eosinophils using real-time quantitative PCR. Biochim Biophys Acta 2002;1571:167–72.
23. Laird PW, Xiong Z. COBRA: a sensitive and quantitative DNA methylation assay. Nucleic Acids Res 1997;25:2532–4.
24. Cross SH, Charlton JA, Nan X, Bird AP. Purification of CpG islands using a methylated DNA binding column. Nat Genet 1994;6:236–44.
25. Yan PS, Chen CM, Shi H, et al. Dissecting complex epigenetic alterations in breast cancer using CpG island microarrays. Cancer Res 2001;61:8375–80.
26. Huang TH-M, Perry MR, Laux DE. Methylation profiling of CpG islands in human breast cancer cells. Hum Mol Genet 1999;8:459–70.
27. Elbashir SM, Harborth J, Lendeckel W, et al. Duplexes of 21-nucleotide RNAs mediate RNA interference in cultured mammalian cells. Nature (Lond) 2001;411:494–8.
28. Elbashir SM, Lendeckel W, Tuschl T. RNA interference is mediated by 21- and 22-nucleotide RNAs. Genes Dev 2001;15:188–200.
29. Brummelkamp TR, Bernards R, Agami R. A system for stable expression of short interfering RNAs in mammalian cells. Science (Wash DC) 2002;296:550–3.
30. Geiman TM, Robertson KD. Chromatin remodeling, histone modification, and DNA methylation: how does it all fit together? J Cell Biochem 2002;2002:117–25.
31. Orlando V. Polycomb, epigenomes, and control of cell identity. Cell 2003;112:599–606.
32. Satijn DP, Otte AP. Polycomb-group protein complexes: do different complexes regulate distinct targets? Biochim Biophys Acta 1999;1447:1–16.
33. Herman JG, Graff JR, Myohanen S, Nelkin B, Baylin SB. Methylation-specific PCR: a novel PCR assay for methylation status of CpG islands. Proc Natl Acad Sci USA 1996;93:9821–6.
34. Oesterreich S, Zhang P, Guler RL, et al. Re-expression of estrogen receptor alpha in estrogen receptor alpha-negative MCF-7 cells restores both estrogen and insulin-like growth factor-mediated signaling and growth. Cancer Res 2001;16:5771–7.
35. Xu X, Murdoch FE, Curran EM, Welshons WV, Fritsch MK. Transcription factor accessibility and histone acetylation of the progesterone receptor gene differs between parental MCF-7 cells and a subline that has lost progesterone receptor expression. Gene (Amst) 2004;17:143–51.
36. Weinmann AS, Yan PS, Oberley MJ, Huang T H-M, Farnham PJ. Isolating human transcription factor targets by coupling chromatin immunoprecipitation and CpG island microarray analysis. Genes Dev 2002;16:235–44.
37. Shi H, Wei SH, Leu Y-W, et al. Triple analysis of the cancer epigenome: an integrated microarray system for analyzing gene expression, DNA methylation, and histone acetylation. Cancer Res 2003;63:2164–71.
38. Tibshirani R, Hastie T, Narasimhan B, Chu G. Diagnosis of multiple cancer types by shrunken centroids of gene expression. Proc Natl Acad Sci USA 2002;99:6567–72.
39. Fujita N, Jaye DL, Kajita M, et al. MTA3, a Mi-2/NuRD complex subunit, regulates an invasive growth pathway in breast cancer. Cell 2003;113:207–19.
40. Jackson JP, Lindroth AM, Cao X, Jacobsen SE. Control of CpNpG DNA methylation by the KRYPTONITE histone H3 methyltransferase. Nature (Lond) 2002;416:556–60.
41. Tariq M, Saze H, Probst AV, et al. Erasure of CpG methylation in Arabidopsis alters patterns of histone H3 methylation in heterochromatin. Proc Natl Acad Sci USA 2003;100:8823–7.
42. Lynch CA, Tycko B, Bestor TH, Walsh CP. Reactivation of a silenced H19 gene in human rhabdomyosarcoma by demethylation of DNA but not by histone hyperacetylation. Mol Cancer 2002;1:2.
43. Bachman KE, Park BH, Rhee I, et al. Histone modifications and silencing prior to DNA methylation of a tumor supporessor gene. Cancer Cell 2003;3:89–95.
44. Mutskov V, Felsenfeld G. Silencing of transgene transcription precedes methylation of promoter DNA and histone H3 lysine 9. EMBO J 2004;1:1–12.
45. Jones PA. DNA methylation errors and cancer. Cancer Res 1996;56:2463–7.
46. Pferfer GP, Steigerwald SD, Hansen RS, Gartler SM, Riggs AD. Polymerase chain reaction-aided genomic sequencing of an X chromosome-linked CpG island: methylation patterns suggest clonal inheritance, CpG site autonomy and an explanation of activity state stability. Proc Natl Acad Sci USA 1990;87:8252–6.
47. Feltus FA, Lee EK, Costello JF, Plass C, Vertino PM. Predicting aberrant CpG island methylation. Proc Natl Acad Sci USA 2003;100:12253–8.
48. Costello JF, Fruhwald MC, Smiraglia DJ, et al. Aberrant CpG-island methylation has non-random and tumour-type-specific patterns. Nat Genet 2000;24:132–8.

Molecular Cell *21*, 393–404, February 3, 2006 ©2006 Elsevier Inc. DOI 10.1016/j.molcel.2005.12.016

Combinatorial Analysis of Transcription Factor Partners Reveals Recruitment of c-MYC to Estrogen Receptor-α Responsive Promoters

Alfred S.L. Cheng,[1] Victor X. Jin,[1] Meiyun Fan,[2] Laura T. Smith,[1] Sandya Liyanarachchi,[1] Pearlly S. Yan,[1] Yu-Wei Leu,[3] Michael W.Y. Chan,[1] Christoph Plass,[1] Kenneth P. Nephew,[2] Ramana V. Davuluri,[1] and Tim H.-M. Huang[1,*]

[1] Division of Human Cancer Genetics
Department of Molecular Virology, Immunology and Medical Genetics
Comprehensive Cancer Center
Ohio State University
Columbus, Ohio 43210

[2] Medical Sciences
Indiana University School of Medicine
Bloomington, Indiana 47405

[3] Department of Life Science and Institute of Molecular Biology
National Chung Cheng University
Chia-Yi
Taiwan
Republic of China

Summary

In breast cancer and normal estrogen target tissues, estrogen receptor-α (ERα) signaling results in the establishment of spatiotemporal patterns of gene expression. Whereas primary target gene regulation by ERα involves recruitment of coregulatory proteins, coactivators, or corepressors, activation of these downstream promoters by receptor signaling may also involve partnership of ERα with other transcription factors. By using an integrated, genome-wide approach that involves ChIP-chip and computational modeling, we uncovered 13 ERα-responsive promoters containing both ERα and c-MYC binding elements located within close proximity (13–214 bp) to each other. Estrogen stimulation enhanced the c-MYC-ERα interaction and facilitated the association of ERα, c-MYC, and the coactivator TRRAP with these estrogen-responsive promoters, resulting in chromatin remodeling and increased transcription. These results suggest that ERα and c-MYC physically interact to stabilize the ERα-coactivator complex, thereby permitting other signal transduction pathways to fine-tune estrogen-mediated signaling networks.

Introduction

Estrogen plays pivotal roles in human physiology and breast cancer genesis and progression (McDonnell and Norris, 2002). The biological actions of estrogen are mediated through binding to estrogen receptors (ERs), ERα, and ERβ, which belong to the nuclear receptor superfamily of transcription factors. Intensive studies have revealed multiple mechanisms by which these receptors activate or repress their target genes. Upon ligand activation, ERα-mediated transcription is through binding directly to specific estrogen response elements (EREs) in the promoters of responsive genes (Metivier et al., 2003) or via protein-protein interaction with other promoter bound transcription factors, such as SP1 (Saville et al., 2000), AP1 (DeNardo et al., 2005), or NF-κB (Stein and Yang, 1995). In either case, coactivators or corepressors are further recruited to form a functional receptor complex that specifies transcriptional activities of downstream targets.

Upregulation or downregulation of receptor target genes may occur through complex chromatin remodeling, both in and around the responsive promoters (Metivier et al., 2003; Xu and Li, 2003), and different combinations of histone modifications may act synergistically or antagonistically to affect gene expression (Jenuwein and Allis, 2001). For example, acetylation of lysine 9 at histone H3 (H3-K9) is linked to transcriptional activation (Roh et al., 2005), whereas dimethylation of the same lysine seems to specify transcriptional repression (Peters et al., 2003). In this regard, nuclear coregulators, which often possess chromatin modulating activities, appear to act cooperatively with ERα to establish patterns of gene expression and thus provide considerable functional flexibility in specifying transcriptional activation or repression (McKenna and O'Malley, 2002).

In addition to gene regulation by nuclear ERα, evidence exists for a membrane form of the receptor that may serve to mediate the activities of other intracellular signaling pathways and potentially contribute to both genomic and nongenomic effects of estrogen in various target tissues (Revankar et al., 2005). In this regard, transactivational effects of ERα may also be regulated via independent *trans*-regulatory partners, a much less understood and largely unexplored process. However, given the fact that crosstalk with other signal transduction pathways may allow ERα to regulate gene expression via association with additional transcription factors (Carroll et al., 2005; DeNardo et al., 2005; Saville et al., 2000; Stein and Yang, 1995), specific transcription factor partners could be involved in coregulating gene activities via direct binding to their consensus sequences in the ERα-responsive promoters.

In the present study, we used a genome-wide approach called ChIP-chip (Ren et al., 2000) to identify direct ERα target genes. Chromatin immunoprecipitation of specific protein/DNA complexes was utilized to probe a promoter CpG island microarray panel (Heisler et al., 2005). Based on recent studies demonstrating a correlation between acetylation and dimethylation at H3-K9 with gene activation and repression, respectively (Kondo et al., 2004; Peters et al., 2003; Peterson and Laniel, 2004; Roh et al., 2005), we first classified the ERα-responsive promoters into acetylated and methylated groups. Computational modeling with classification and regression tree (CART) (Breiman et al., 1984) identified 7 *cis*-regulatory modules that discriminate acetylated promoters from methylated promoters and recognized putative transcription factor partners. Experimental validation of the computational findings further identified c-MYC as a positive regulator of the ERα-mediated

*Correspondence: tim.huang@osumc.edu

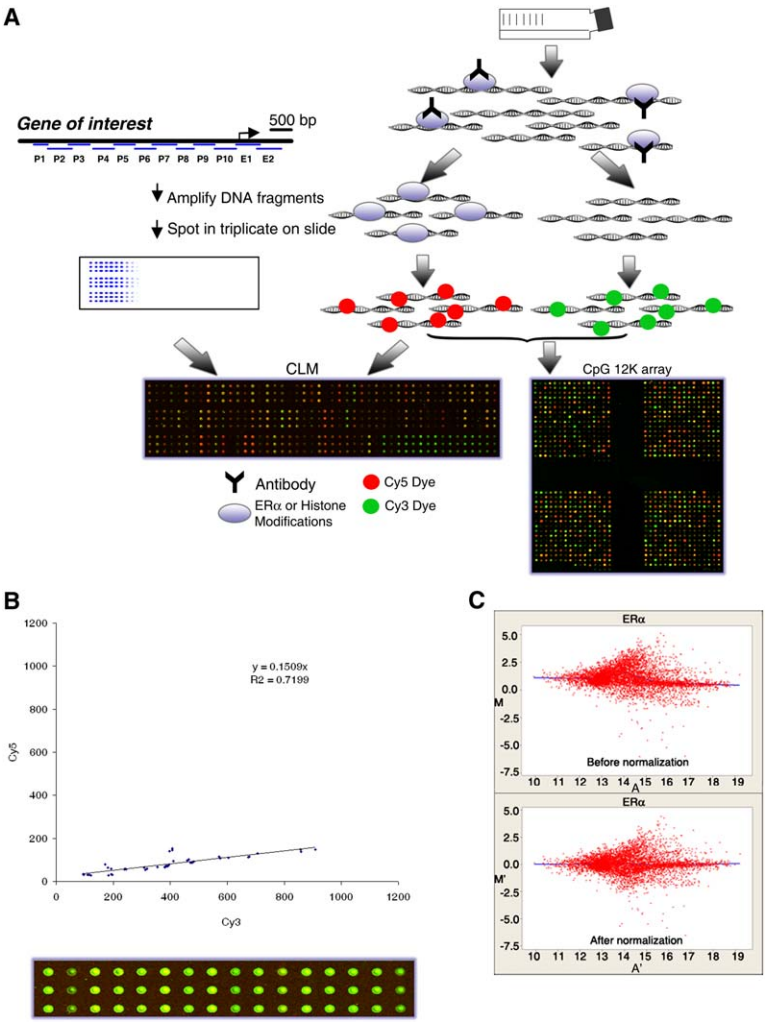

Figure 1. Identification of ERα-Responsive Promoters and Histone Modifications

(A) Schematic diagram of ChIP-chip. Growing cells were crosslinked with formaldehyde, and the sonicated chromatin was immunoprecipitated with a specific antibody. The enriched DNAs were purified, fluorescently labeled, and cohybridized onto two microarray platforms (12K CGI array and CLM) along with an input sample that had been labeled with a different dye. The chromatin landscaping microarray (CLM) contains four known estrogen-responsive promoter regions, each spanning 5 kb upstream (P1 to P10 fragments) and 1 kb downstream (E1 and E2 fragments) of the transcription start site (arrow).

(B) Quality control of CLM. The sonicated chromatin was immunoprecipitated with acetyl-H3-K9 antibody, labeled with Cy5, and cohybridized with Cy3-labeled input. The green spots of 16 repetitive sequences (in triplicate) indicated preferential hybridization with input and not immunoprecipitated DNA (Cy5:Cy3 ratio = 0.15). These data show that the antibody used was specific.

(C) Antibody-specific enrichment in ChIP-chip. Chromatin immunoprecipitated with ERα antibody was labeled with Cy5 and cohybridized with Cy3-labeled input. The Cy5:Cy3 ratio was $\log_2$ transformed and plotted against the signal intensity (M/A plot). The wide spread of the ratios reflects specific enrichment during the immunoprecipitation. The lowess curve (blue line), with 20% of the data used at each point, was overlaid on the plot and used in intensity-dependent normalization. As a confirmation, the lowess curve estimated from the normalized data was nearly a straight line as shown in the lower panel. Similar results were obtained when the enriched immunoprecipitated targets were labeled with Cy3 and the input DNA was labeled with Cy5 (Figure S1).

transcriptional network. c-*MYC* is a well-characterized ERα target gene that plays a critical role in the ability of estrogen to enhance the proliferation of breast cancer cells. Upregulation of c-MYC by ERα resulted in further recruitment of this transcription factor partner to other ERα-responsive promoters and led to target gene activation. Our results demonstrate that integrative ChIP-chip and bioinformatics approaches can be used to interrogate combinatorial control of ERα-regulated transcription, a strategy that can be used to examine additional transcription factor partners.

Results

Histone Modifications Occur Near the Transcription Start Site of ERα-Responsive Promoters upon Estrogen Signaling

ChIP accompanied with microarray screening has become an important approach for comprehensive analysis of transcriptional regulation. We first studied dynamic changes in the chromatin landscape by using a smaller microarray platform of 192 arrayed elements for four known ERα-responsive promoters: *progesterone receptor isoform B (PRB)*, *c-MYC*, *BCL2*, and *ZNF217*. MCF7 breast cancer cells were hormone-deprived for 4 days and then treated for 24 hr with 10 nM 17β-estradiol (E2). Antibodies against specific histone modifications (acetyl-H3-K9 and dimethyl-H3-K9) were used to immunoprecipitate DNAs for microarray hybridization (Figure 1A). For quality control, we tested the specificity of these antibodies, and the lowess-normalized microarray data further confirmed specific enrichment of immunoprecipitated DNAs (Figures 1B and 1C). By using the microarray data, we generated a chromatin map spanning the 5 kb upstream and the 1 kb downstream regions from the transcription start site (TSS) of the four interrogating promoters based on the Ac/Me ratio (i.e., acetyl-H3-K9/dimethyl-H3-K9 (Kondo et al., 2003, 2004). Upon estrogen stimulation, we observed a shift of the Ac/Me ratio of chromatin profiles in the vicinity of the TSS in upregulated *PRB*, *c-MYC*, and *BCL2* promoters (Figure 2). In this case, acquisition of acetylated histones (at lysine 9) and, at the same time, loss of methylated histones tended to occur in a more focal region (~1 kb) around the TSS, a process that may be facilitated by the interaction of ligand bound ERα with various chromatin-modulating proteins (Metzger et al., 2005; Yanagisawa et al., 2002). Two additional regions, located 3 to 5 kb upstream of the *PRB* TSS and 2.5 to 3.5 kb upstream of the *c-MYC* TSS,

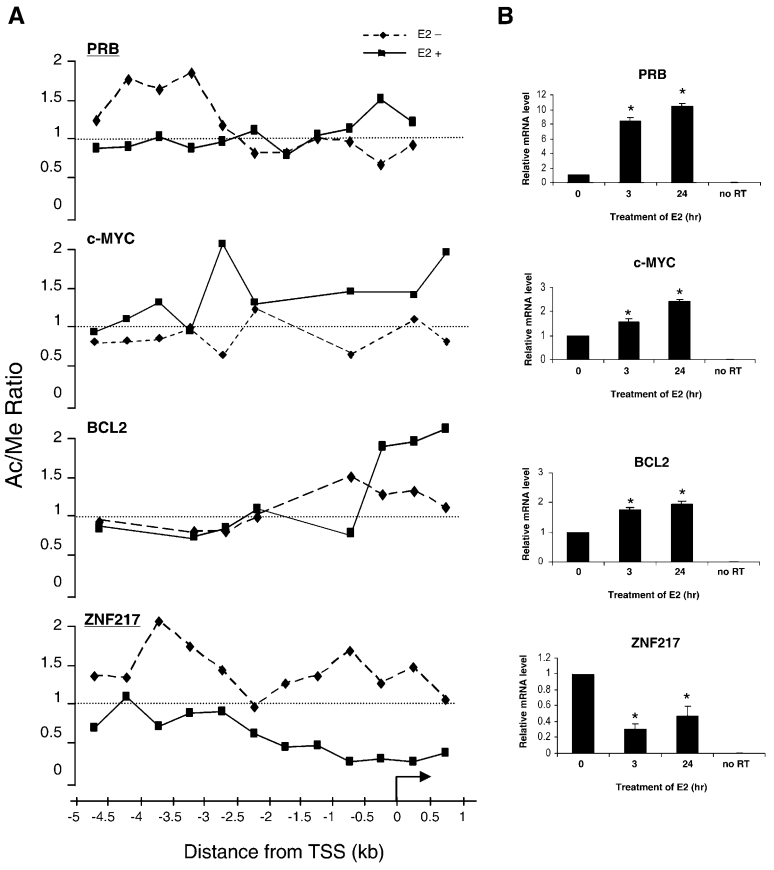

Figure 2. Altered Histone Modifications in the Vicinity of the TSS of ERα-Responsive Promoters

(A) MCF7 cells were maintained in phenol red-free MEM supplemented with 3% charcoal-dextran FBS for 4 days and then were either left untreated or were treated with 10 nM 17β-estradiol (E2) for 24 hr. ChIP assays were performed with antibodies directed against acetyl-H3-K9 (Ac) and dimethyl-H3-K9 (Me), and the dye-coupled DNA was hybridized onto CLM. The microarray signals were determined as described in the Experimental Procedures, and the Ac/Me ratios were plotted for each ERα-responsive promoter region.

(B) MCF7 cells grown as described above were either left untreated or were treated with 10 nM E2 for the indicated time periods. Total RNA was extracted, and the expression of *PRB*, *c-MYC*, *BCL2*, or *ZNF217* genes was analyzed by quantitative RT-PCR. Each error bar represents standard deviation calculated from triplicates. The amplification of sample without reverse transcriptase (RT) served as the negative control. The asterisk indicates $p < 0.05$ (versus untreated cells).

also showed acquisition of more methylated and acetylated histones, respectively, but whether these regions contain functional *cis*-regulatory elements in response to estrogen stimulation remains to be investigated. Interestingly, we observed a wider spread of chromatin changes in a 6 kb region of the *ZNF217* promoter (Figure 2) known to be downregulated by ERα. In this regard, the acquisition of more methylated histones is associated with transcriptional repression of this gene. This chromatin landscaping analysis thus provides an effective approach to assess transcriptional activities of ERα-responsive genes based on their altered chromatin profiles.

ChIP-Chip Analysis Reveals Concerted Action of ERα Binding and Histone Modifications in Responsive Promoters upon Estrogen Stimulation

We performed a series of ChIPs by using a specific antibody against ERα in MCF7 cells treated with E2 for 0, 3, 12, and 24 hr. The immunoprecipitated DNA was used to probe the 12K CGI microarray (Heisler et al., 2005). Because many gene promoters are known to be located near or within CpG islands, this microarray panel is useful for finding new ERα-responsive promoters. We applied Significance Analysis of Microarrays (SAM) to define significant loci (7% false discovery rate), and 83% of these loci attained maximal ERα binding at 3 hr after E2 treatment. Hence, a total of 92 loci were identified as putative targets, which had enrichment signals of >2 at the 3 hr time point in two independent microarray experiments (see also the Supplemental Data, available with this article online, for computational analysis of these loci and Table S1). As shown in a heat map (Figure 3A), maximal binding of ERα to these targets was observed at 3 hr after E2 treatment and returned to near basal levels at the 12 and 24 hr time periods. Minimal or no enrichment signal was observed for the no-antibody control, as compared to immunoprecipitated DNAs hybridized to positive targets (data not shown).

To determine whether these direct ERα target genes were transcriptionally activated or repressed by ligand bound ERα, we performed serial ChIP assays with antibodies against acetyl- and dimethyl-H3-K9 in MCF7 cells treated with E2 for 0, 3, 12, and 24 hr. The immunoprecipitated DNA was used to probe the same CGI microarray, and SAM was used to analyze the chromatin profiles of the 92 target genes. We were able to classify 40 acetylated and 28 methylated targets, suggesting that these targets were upregulated and downregulated by ligand bound ERα, respectively (see also the Supplemental Data for statistical analysis and Table S2). Consistent with the dynamic pattern of ERα binding, the levels of histone modifications (either acetylation or methylation) were maximal at 3 hr after treatment and returned to basal level by 12 and 24 hr (Figures 3B and 3C). The acetylated and methylated targets identified by SAM analysis were located preferentially at the top and the bottom parts of the heat map, ranked by the order of the Ac/Me ratio at the 3 hr time point (Figure 3D). The classification of ERα target genes was also supported by our global gene expression analysis, which showed a positive correlation between histone modification status

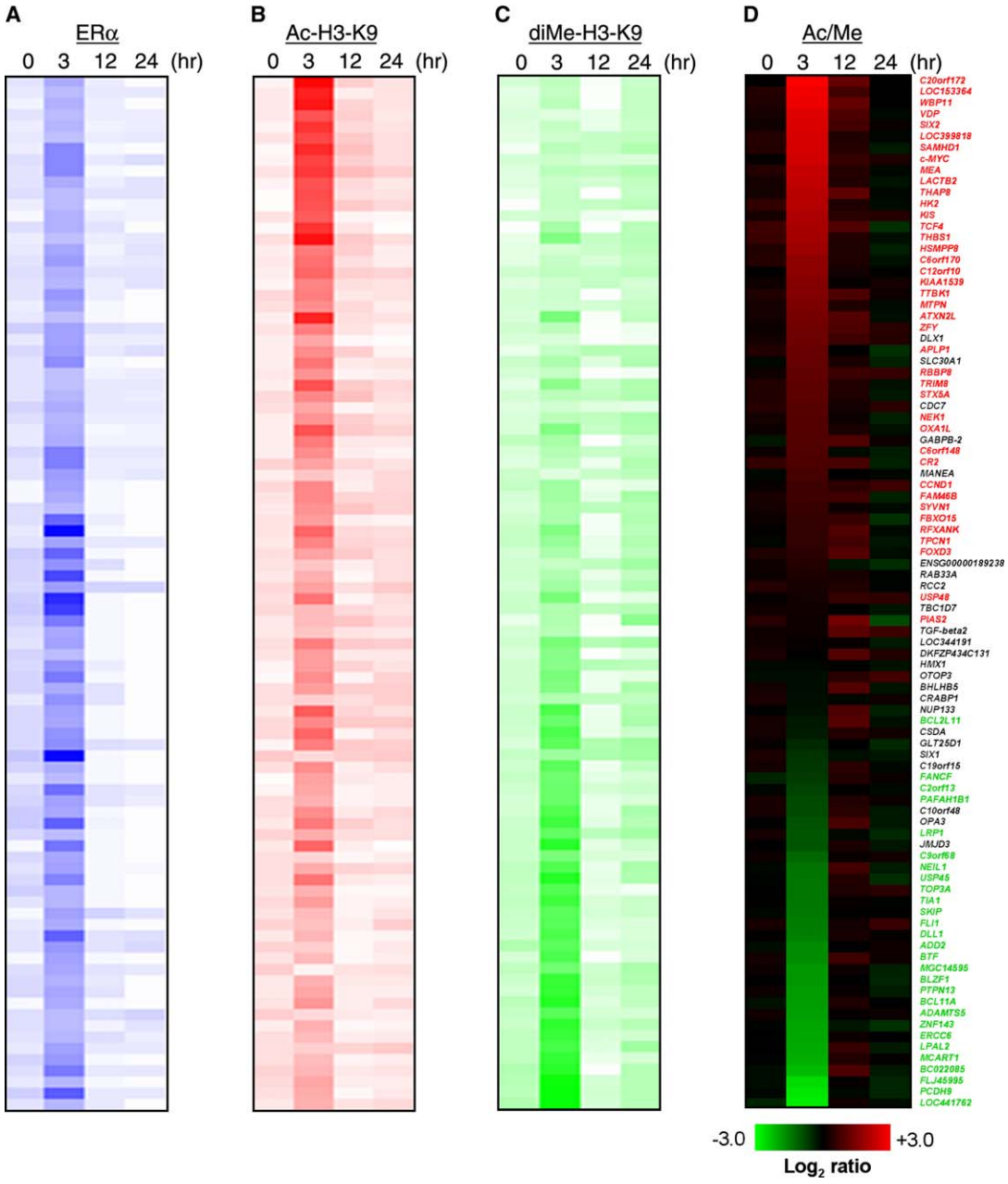

Figure 3. Estrogen Stimulation Induces Dynamic and Concerted ERα Binding and Histone Modifications in Responsive Promoters

(A–C) After E2 treatment for the indicated time periods, MCF7 cells were harvested and ChIP assays were performed with the indicated antibodies. The dye-coupled immunoprecipitated DNA was hybridized onto the 12K CGI microarrays, and the resulting signal ratios of 92 loci are represented in the heat maps.

(D) The Ac/Me ratios of the putative targets are shown. The acetylated and methylated targets identified by SAM are marked in red and green colors, respectively.

(Ac/Me ratio) and transcriptional activity ($p = 0.041$, Fisher's exact test, Table S3).

To validate the microarray findings and determine the presence of ERα binding on promoter targets, we performed quantitative ChIP-polymerase chain reaction (PCR). Immunoprecipitated DNAs were amplified by using paired primers flanking the consensus sequences of EREs predicted by *ERTargetDB* (Jin et al., 2004, 2005). As shown in Figure 4A, eight loci with diverse enrichment signals (*CCND1*, *c-MYC*, *RBBP8*, *CR2*, *THBS1*, *PTPN13*, *BCL11A*, and *PCDH9*) were randomly selected from the 92 putative targets and independently confirmed as ERα-responsive promoters. All these loci showed higher levels (2- to 9-fold) of ERα binding after treating MCF7 cells with E2 for 3 hr. *RASSF1A* showed no binding of ERα in either condition (treated or control) and thus served as a negative control (data not shown). To determine the level of transcription of these loci, ChIP was performed by using an antibody against RNA polymerase II (RNA Pol II) and was quantified by real-time

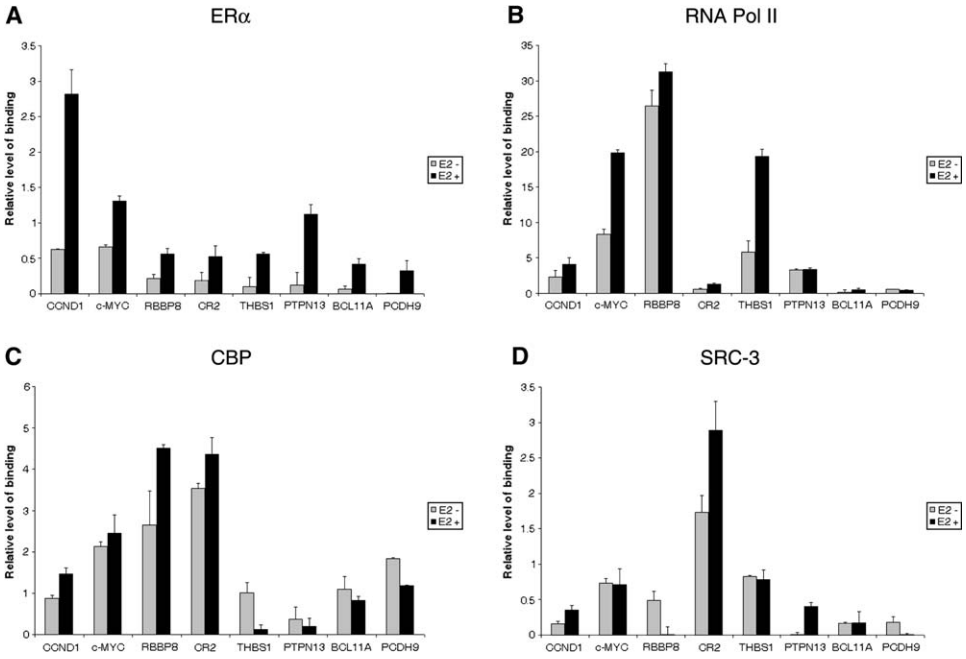

Figure 4. Estrogen Stimulation Recruits ERα, RNA Pol II, and Coactivators to Responsive Promoters

(A–D) MCF7 cells were hormone-starved for 4 days and then either left untreated or were treated with 10 nM E2 for 3 hr. ChIP assays were performed with the indicated antibodies, and the immunoprecipitated DNA corresponding to the responsive promoters was measured by quantitative PCR. Quantitation of binding was determined as a percent of input DNAs, and each error bar represents standard deviation calculated from triplicates.

PCR. Estradiol-enhanced RNA Pol II association was detected in *CCND1*, *c-MYC*, *RBBP8*, *CR2*, and *THBS1* genes (Figure 4B). Although the degree of enhancement varied among the different promoters, the results demonstrate that E2-induced ERα binding positively regulates transcription of these genes. In contrast, E2 treatment did not promote RNA Pol II binding at *PTPN13*, *BCL11A*, and *PCDH9*. Because ligand bound ERα can recruit coactivators, including CBP and SRC-3, to specific chromatin regions for remodeling (McKenna and O'Malley, 2002), we examined the association of these coactivators with the ERα-responsive promoters. In *CCND1*, *RBBP8*, and *CR2*, which all displayed enhanced RNA Pol II association after E2 treatment, CBP or SRC-3 was also recruited to these chromatin regions (Figures 4C and 4D). There was no change in CBP/SRC-3 binding at *c-MYC*, and CBP binding at *THBS1* decreased, indicating that other coactivators may be recruited to these promoters after E2 treatment. In contrast, for those loci with no change in RNA Pol II binding, coactivator recruitment decreased or was unchanged after E2 treatment (the exception being SRC-3 binding at *PTPN13*). Our data demonstrate that estrogen stimulation results in the recruitment of ERα and CBP/SRC-3 to specific promoters and enhances the association of RNA Pol II, and these findings agree with previous observations by Klinge et al. (2004) that different ERE sequences modulate the interaction of ligand bound ERα with coactivators.

Next, we correlated the effect of ERα and coactivator(s) binding on changes of chromatin and expression status in these responsive genes. Consistent with the ChIP-chip results, five loci (*CCND1*, *c-MYC*, *THBS1*, *RBBP8*, and *CR2*) showed 3- to 15-fold increases of Ac/Me ratios and 2- to 3-fold increases of mRNA levels after E2 treatment (Figure 5A). Except for *CR2*, increased levels of histone acetylation and decreased levels of histone methylation of the target genes usually coincided with the timing (at 3 hr) of ERα binding to their respective promoters. In *CR2*, the chromatin response was delayed (observed at the 24 hr time point) relative to ERα binding, which may reflect the heterogeneous nature of some responsive loci. It is also possible that the critical region is not located in or near the predicted ERE of the *CR2* promoter. Predicted to be downregulated by ChIP-chip analysis, the chromatin of *BCL11A*, *PCDH9*, and *PTPN13* showed an overall decrease in Ac/Me ratios (0.1- to 0.7-fold) after E2 treatment (Figure 5B), accompanied by a 2- to 3-fold decrease in their mRNA level. Taken together, these validation studies generally confirm the validity of microarray findings and support the collaborative action of ERα and coactivator(s) binding and chromatin remodeling on these promoters after E2 stimulation.

Computational Modeling Reveals Seven Modules of Combinatorial Control that Predict Transcriptional Activities of Responsive Promoters upon Estrogen Stimulation

The combinatorial theory of gene regulation by transcription factors states that transcription factors act cooperatively to mediate target gene activation (Wasserman and Sandelin, 2004). Accordingly, the identification of the putative *cis*-regulatory modules in different sets of responsive promoters enable the discovery of synergistically interacting transcription factors that are involved in crosstalk with the ERα signaling pathway. To identify transcription factor partners involved in the

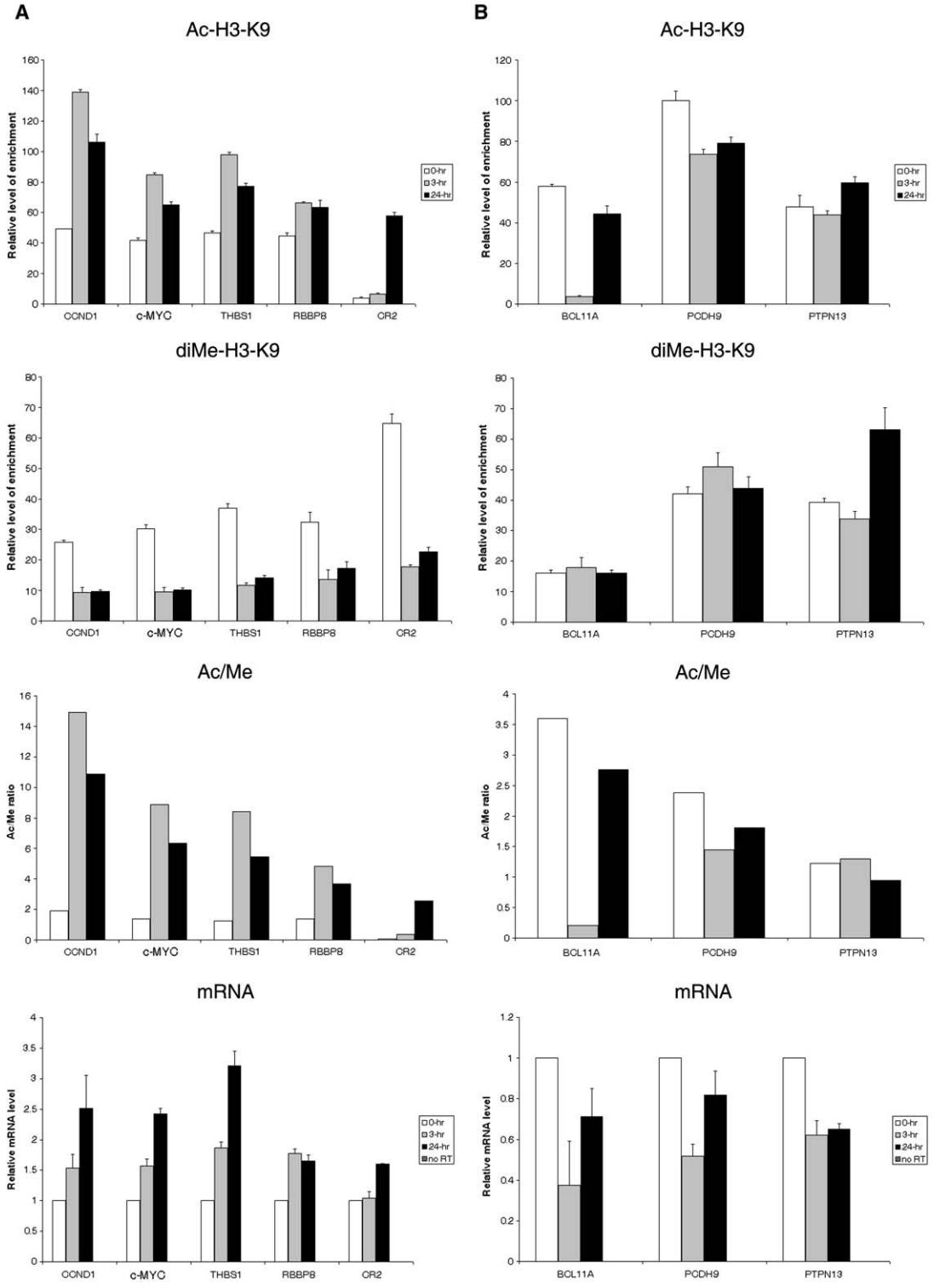

Figure 5. Chromatin Profiles Correlate with Expression Status in Estrogen-Responsive Genes

(A) After E2 treatment for the indicated time periods, MCF7 cells were harvested and ChIP assays were performed with antibodies directed against acetyl-H3-K9 and dimethyl-H3-K9. The immunoprecipitated DNA corresponding to the upregulated targets was measured by quantitative PCR. Quantitation of specific histone modifications was determined as a percent of input DNAs, and each error bar represents standard deviation calculated from triplicates. The Ac/Me ratios of the targets are also shown. mRNA expression at the indicated time points was determined by quantitative RT-PCR (the lowest panels). Each error bar represents standard deviation calculated from triplicates. The amplification of sample without RT served as the negative control.

(B) Quantitative ChIP-PCR and RT-PCR results for the downregulated targets are shown.

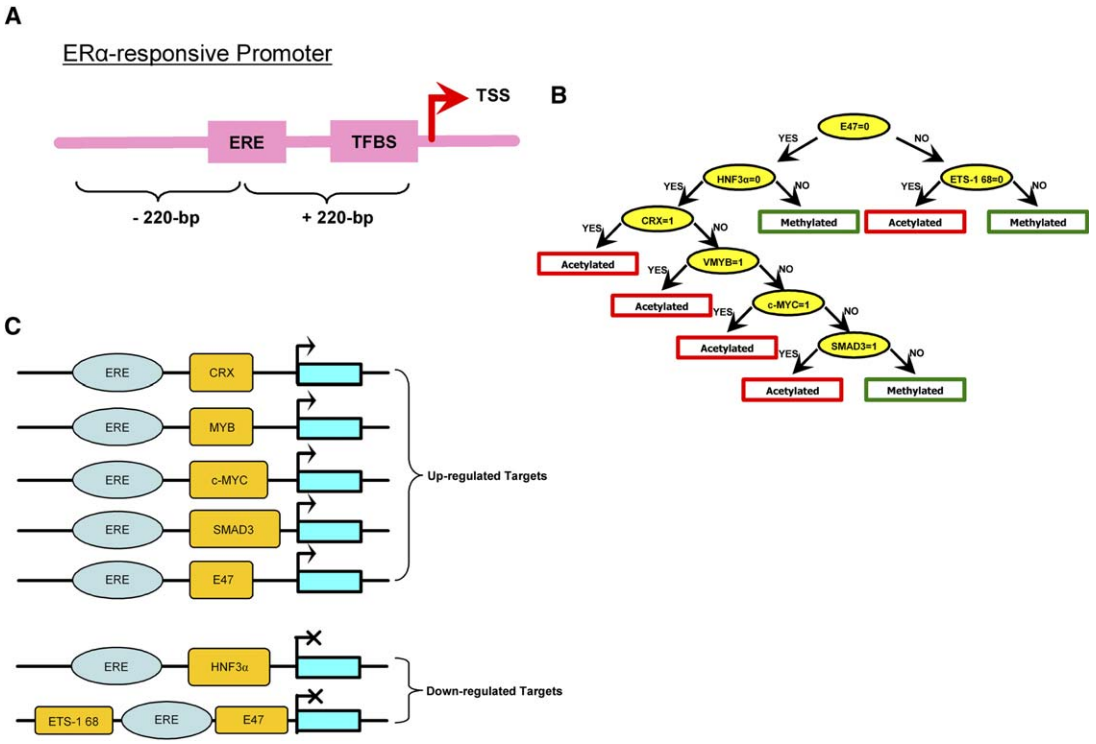

Figure 6. Computational Modeling Reveals *cis*-Regulatory Modules in Estrogen-Responsive Promoters

(A) ERα-responsive promoter sequences from −220 to +220 bp around the predicted ERE were used to construct a computational model to identify overrepresented TFBSs.

(B) A CART model that discriminates between ERα upregulated (more acetylated) and downregulated (more methylated) targets.

(C) *cis*-regulatory modules of ERα upregulated and downregulated target genes identified by the CART model.

regulation of acetylated and methylated ERα target genes, a computational model that distinguishes these two sets of promoters was constructed by using ERα target promoter sequences from −220 to +220 bp around the ERE (Figure 6A). CART analysis initially identified 20 of the most important transcription factor binding sites (TFBSs) from 140 TFBSs (with at least 35% occurrence in either type of targets) in the TRANSFAC database. A minimal-cost tree was constructed based on these transcription factor binding sites as the categorical predictor variables (Figure 6B). The prediction rate, based on 10-fold crossvalidation, was 80% for acetylated targets and 100% for methylated targets. Based on the discovery of overrepresented TFBSs identified by CART, five *cis*-regulatory modules, i.e., ERE+CRX, ERE+MYB, ERE+c-MYC, ERE+SMAD3, and ERE+E47, were identified for upregulated (i.e., more acetylated) targets, and two modules (ERE+HNF3α and ERE+E47+ETS-1 68) were identified for downregulated (i.e., more methylated) targets (Figure 6C). Overall, the bioinformatics analyses identified seven distinct *cis*-regulatory modules for upregulated or downregulated ERα target genes. These results suggest that specific transcription factor partners are involved in the ERα-regulated transcription network.

c-MYC Is a Positive Regulator of ERα-Regulated Transcriptional Activation

Next, we experimentally verified the prediction results by CART. In one of the *cis*-regulatory modules, c-MYC binding sites were found to be located near (13–214 bp) EREs of 13 ERα-responsive promoters (Figure 7A and Table S4). Because c-MYC is an important transcription factor regulated by ERα in breast cancer (Dubik et al., 1987), we examined the role of c-MYC in ERα-regulated transcriptional activation. First, we determined if c-MYC was recruited to ERα-responsive promoters. Quantitative ChIP-PCR analysis showed that after E2 treatment for 3 hr, a 2- to 4-fold increase of c-MYC binding was seen in 11 of the ERα target genes tested (*LOC153364*, *HK2*, *RCC2*, *GABPB2*, *SYVN1*, *DLX1*, *VDP*, *SAMHD1*, *RBBP8*, *CR2*, and *MEA*) (Figure 7B). No c-MYC binding was detected in a negative control gene, *RASSF1A* (data not shown). Because TRRAP functions as a c-MYC-interacting coactivator that mediates histone acetyltransferase recruitment and c-MYC-dependent oncogenesis (McMahon et al., 1998; Park et al., 2001), its association with the same subset of loci was examined. Quantitative ChIP-PCR showed that E2 treatment caused a concordant increase of TRRAP binding at six of the 11 loci (*GABPB2*, *DLX1*, *VDP*, *RBBP8*, *CR2*, and *MEA*) (Figure 7C). These data suggest that estrogen stimulation results in the recruitment of c-MYC and the coactivator TRRAP to a subset of ERα-responsive promoters.

The association of TRRAP, which physically interacts with c-MYC (McMahon et al., 1998) and ERα (Yanagisawa et al., 2002), with ERα-responsive promoters containing a c-MYC binding site and ERE in close proximity implies a functional interaction between c-MYC and

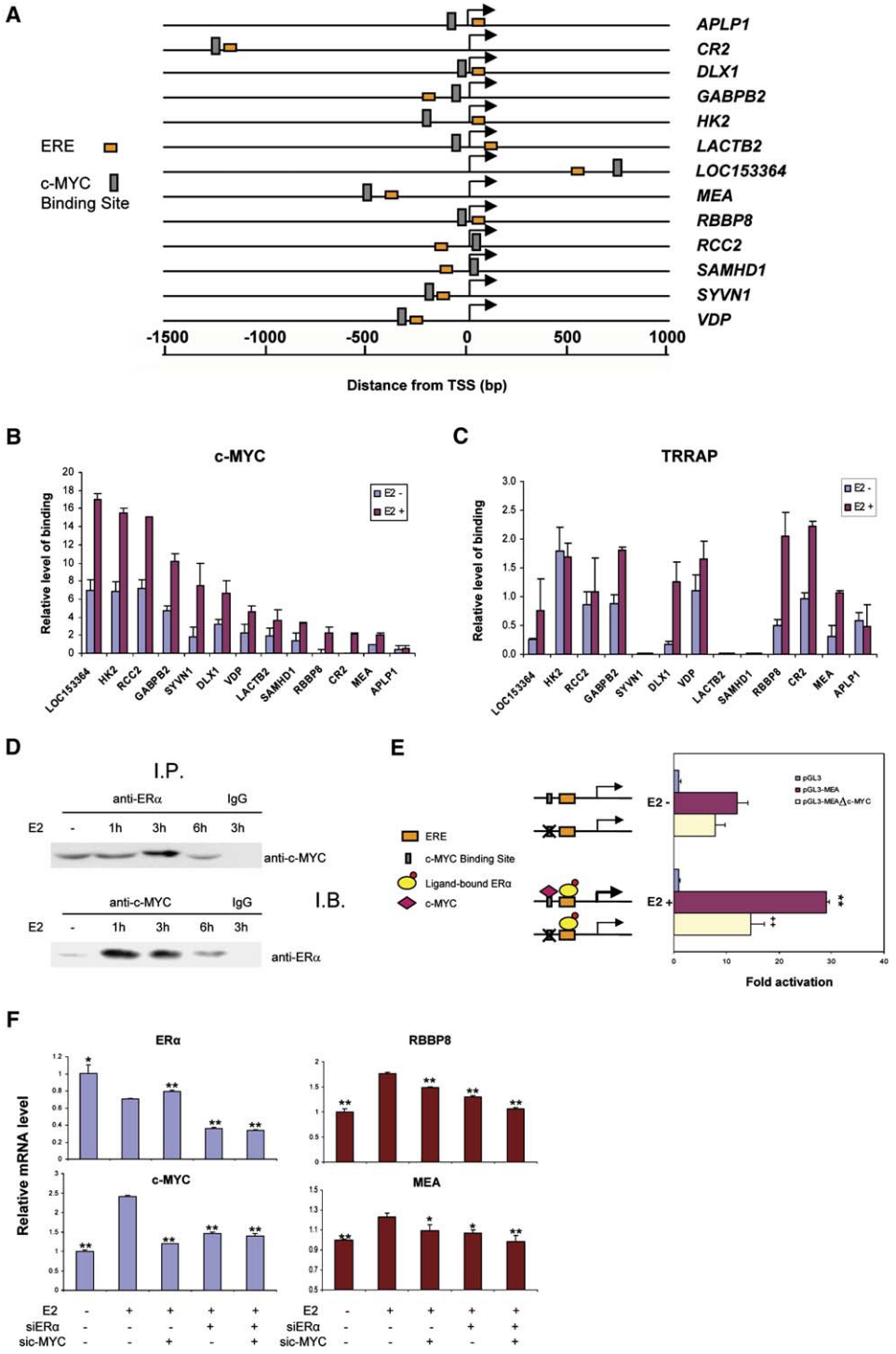

Figure 7. ERα and c-MYC Coregulate Estrogen-Responsive Genes

(A) Schematic diagram showing the relative locations of ERE motifs (orange boxes) and c-MYC binding sites (gray boxes) in a subset of estrogen-responsive genes.

(B and C) MCF7 cells were hormone-starved for 4 days and either left untreated or were treated with 10 nM E2 for 3 hr. ChIP assays were performed with the indicated antibodies, and the immunoprecipitated DNA corresponding to the estrogen-responsive promoters was measured by quantitative PCR. Quantitation of binding was determined as a percent of input DNAs, and each error bar represents standard deviation calculated from triplicates.

(D) Estrogen stimulation enhances the interaction between ERα and c-MYC in the nucleus of MCF7 cells. MCF7 cells were hormone-starved for 3 days and treated with 10 nM E2 for the indicated time periods. Nuclear extracts were prepared and immunoprecipitated with the indicated antibodies or rabbit IgG (negative control). Precipitates were subjected to immunoblotting with antibodies against ERα or c-MYC as indicated. Representative results from three independent experiments are shown. Abbreviations are as follows: I.P., immunoprecipitation; I.B., immunoblot.

(E) The c-MYC binding site of the ERα-responsive promoter is important for transcriptional activation. MCF7 cells that were hormone-starved for

ERα. We used coimmunoprecipitation assays to examine the association of c-MYC and ERα in the nucleus in response to E2 treatment. Treatment of MCF7 cells with E2 for 3 hr increased the amount of c-MYC in the immunoprecipitated ERα complex (Figure 7D, upper panel). In the reciprocal experiment, the amount of ERα in the complex immunoprecipitated with the c-MYC antibody was increased after E2 treatment for 1 and 3 hr (Figure 7D, lower panel). Consistent with these observations, ERα and c-MYC protein levels in the nucleus were increased at 1 and 3 hr after E2 treatment, as shown by immunoblotting (Figure S2).

As predicted by CART, further recruitment of c-MYC to ERα-responsive promoters caused transcriptional activation (Figure 6C). To examine if the c-MYC binding site confers estrogen responsiveness, a deletion mutant of the *MEA* promoter, which contains a c-MYC binding site and ERE (Figure 7A), was constructed. Estrogen treatment increased the transcriptional activity of the wild-type *MEA* promoter >2-fold ($p < 0.005$, Figure 7E). However, the estrogen responsiveness of the *MEA* promoter was abolished in the absence of the c-MYC binding site ($p < 0.005$, Figure 7E). To further validate ERα and c-MYC coregulation in a subset of ERα-responsive promoters, siRNAs directed against *ERα* and/or *c-MYC* were transfected into estrogen-treated MCF7 cells. Quantitative RT-PCR analysis showed a 50% knockdown of *ERα* mRNA by 48 hr after transfection of *ERα* siRNA (Figure 7F). Interestingly, *ERα* siRNA treatment also resulted in a 40% knockdown of *c-MYC* mRNA, further supporting a positive regulatory role of ERα on *c-MYC* transcription. *c-MYC* siRNA treatment resulted in a 50% knockdown of *c-MYC* mRNA. When the cells were simultaneously treated with both siRNAs, *ERα* and *c-MYC* mRNA levels were reduced by 50% and 40%, respectively. In all of the 11 ERα-responsive genes that showed increased c-MYC binding (>2-fold) upon E2 treatment (Figure 7B), *c-MYC* siRNA treatment significantly ($p < 0.05$) reduced their mRNA levels (12% to 57%, data not shown). The mRNA levels of two ERα-responsive genes, *RBBP8* and *MEA*, were decreased ($p < 0.05$) by individual siRNA treatments (Figure 7F). More importantly, combined siRNAs treatment further reduced ($p < 0.005$) *RBBP8* and *MEA* mRNA levels, indicating that ERα and c-MYC coregulate these responsive targets at the transcriptional level.

Discussion

Estrogen signaling has been intensively studied for the last 20 years, and the complexity of this classical transduction pathway is beginning to be unraveled. The architecture of the estrogen regulatory network can be categorized into single-component and multicomponent inputs. In the single-component input model, downstream target genes are activated or suppressed upon promoter binding of the ERα complex, triggering a cascade of downstream events and forming a regulatory feedback loop for ERα-mediated actions. Perhaps more likely, however, is that estrogen signaling regulates downstream gene activity through the multicomponent inputs. In support of this latter possibility, experimental evidence exists for crosstalk between ERα signaling and multiple transduction pathways, including HER2, PI3K/Akt, IGF-IR, Src, or MAPK (Osborne et al., 2005). Furthermore, estrogen signaling, which controls the balance of growth and apoptosis in normal breast epithelial cells, becomes disrupted in breast cancer cells, resulting in preferential utilization of these other transduction pathways, contributing to abnormal cell proliferation. Therefore, comprehensive identification and characterization of downstream promoters can provide deeper insight into the hierarchy of ERα-mediated regulatory networks.

In the present study, the ability of ChIP-chip to identify in vivo direct target promoters of a transcription factor has allowed us to define specific targets directed by the ERα regulatory network. Our genome-wide approach used a CpG island microarray to identify 92 putative ERα-responsive promoters. The microarray platform used in this study contains 4500-5000 single-copy CpG promoters (Heisler et al., 2005), and ERα was found to bind to ~2% of the promoters in MCF7 breast cancer cells, a proportion similar to genomic binding of other transcription factors (Odom et al., 2004; Ren et al., 2002). Because acetylation and dimethylation at histone 3 lysine 9 correlate with gene activation and repression (Kondo et al., 2004; Peters et al., 2003; Peterson and Laniel, 2004; Roh et al., 2005), respectively, we utilized the same CpG island microarray to determine the histone modification status of ERα target promoters as a surrogate for transcriptional activity. Furthermore, by using an integrated bioinformatics approach, we have identified seven *cis*-regulatory modules containing combinatorial binding patterns for additional transcription factors in ERα-responsive promoters. These transcription factor partners, including CRX, MYB, c-MYC, SMAD3, E47, HNF3α, and ETS-1, are known to be involved in breast carcinogenesis (Lacroix and Leclercq, 2004; Lincoln and Bove, 2005; Matsuda et al., 2001; Rushton et al., 2003), consistent with the notion that ERα plays a role in promoting the development of breast cancer cells.

Of the above ERα transcriptional partners, we have demonstrated a previously unknown coregulatory role of c-MYC for a subset of ERα-responsive genes. The c-MYC protein, an important regulator of many cellular processes including proliferation and apoptosis (Pelengaris et al., 2002), is overexpressed in human breast carcinoma (Berns et al., 1992; Bland et al., 1995). Our observations that estrogen treatment of MCF7 breast cancer cells results in ERα nuclear translocation, receptor

3 days were transfected with the indicated *MEA* luciferase reporter constructs and a Renilla luciferase plasmid and treated with or without 10 nM E2 for 24 hr, and the luciferase activity was analyzed. Each error bar represents standard deviation calculated from triplicates. The double asterisk and ++ indicate $p < 0.005$ (versus untreated and E2-treated wild-type *MEA* luciferase reporter construct, respectively).

(F) ERα and c-MYC coregulate ERα-responsive genes. MCF7 cells were transfected with 25 nM of siRNAs targeting *c-MYC* and/or *ERα*. After being hormone-starved for 3 days, the cells were either left untreated or were treated with 10 nM E2 for 3 hr. The expression of *c-MYC*, *ERα*, *RBBP8*, and *MEA* mRNA was determined by quantitative RT-PCR. Each error bar represents standard deviation calculated from triplicates. The asterisk represents $p < 0.05$ and the double asterisk indicates $p < 0.005$ (verses cells treated with E2 only).

recruitment to the *c-MYC* promoter, increased *c-MYC* gene transcription, and elevated c-MYC protein level in the nucleus are in agreement with a recent report (Park et al., 2005); furthermore, we demonstrated estrogen-induced recruitment of c-MYC to certain ERα bound promoters (Figure 7B and Table S4). Notably, as these promoters contain both ERE and c-MYC binding elements located in close proximity to one another, we went on to show that ERα and c-MYC physically interact in MCF7 cells and that estrogen stimulation further enhances the ERα/c-MYC interaction (Figure 7D). We speculate that this physical interaction is mediated via bridging factors, including TRRAP, which interact with AF-2 of ERα via LxxLL motifs (Yanagisawa et al., 2002) and with the c-MYC N terminus via a separate domain (McMahon et al., 1998). In fact, estrogen stimulation increases the association of TRRAP with some of the ERα/c-MYC bound promoters (Figure 7C). However, it should also be pointed out that three promoters showed no TRRAP binding (Figure 7C), indicating that coactivators other than TRRAP may bridge ERα/c-MYC interaction on these promoters. Previous studies have demonstrated that TRRAP forms a structural core for the assembly and recruitment of histone acetyltransferase complexes involved in transcriptional activation by ERα (Yanagisawa et al., 2002) and c-MYC (Park et al., 2001). Collectively, these observations are consistent with our findings that estradiol-induced corecruitment of ERα, c-MYC, and TRRAP to ERα-responsive promoters is associated with hyperacetylated H3-K9 and increased transcriptional activity (Figures 5A, 7E, and 7F). This scenario—the stabilization of ERα-coactivator interactions by adjacent transcription factor partners—could allow other signal transduction pathways to fine-tune ERα-mediated transcription.

In summary, we have taken an integrated, genome-wide approach to define complex networks directed by ERα. Our results indicated that a physical interaction between ERα and c-MYC is needed for activation of a subset of ERα-responsive promoters. This action may orchestrate the growth of breast cancer cells in response to the mitogenic estrogen signal. This finding exemplifies the power of combining both experimental and bioinformatics methods to identify regulatory elements in complex signaling networks. Our integrative approach should be broadly applicable to the elucidation of regulatory networks of other transcription factors.

Experimental Procedures

Reagents and Antibodies

17β-estradiol (E2), aminoallyl-dUTP, and formaldehyde were purchased from Sigma (St. Louis, MO). Culture media and fetal bovine serum (FBS) were obtained from Invitrogen (Carlsbad, CA) and Hyclone (South Logan, UT), respectively. The antibodies used in chromatin immunoprecipitation are as follows and were purchased from Santa Cruz Biotechnology (Santa Cruz, CA): ERα (D-12), c-MYC (N-262), RNA Pol II (H-224), CBP (C-20), SRC-3 (C-20), and TRRAP (T-17). The antibodies against acetyl-K9 of histone 3 (AcH3K9, 06-942) and dimethyl-K9 of histone 3 (diMeH3K9, ab-7312) were obtained from Upstate Biotechnology (Lake Placid, NY) and Abcam (Cambridge, MA), respectively.

Chromatin Immunoprecipitation Microarray

MCF7 cells were maintained in minimum essential medium (MEM) supplemented with 10% FBS, 100 units/ml penicillin/streptomycin, 2 mM L-glutamine, 6 μg/ml insulin, and 0.4 mM HEPES. The cells were hormone-starved for 4 days in phenol-red free MEM supplemented with 3% charcoal-dextran-treated FBS followed by treatment with 17β-estradiol (E2; 10 nM) for 0, 3, 12, and 24 hr. Two millions cells were crosslinked with 1% formaldehyde for 12 min, and chromatin immunoprecipitation was performed by using a ChIP assay kit (Upstate Biotechnology) as described previously (Leu et al., 2004). Incorporation of aminoallyl-dUTP into 2 μg ChIP-DNA, control no-antibody DNA, or input DNA was conducted with the BioPrime DNA Labeling System (Invitrogen). Cy5 and Cy3 fluorescent dyes (Amersham, Buckinghamshire, UK) were coupled to ChIP/no-antibody DNA and input DNA, respectively, and were cohybridized to two microarray platforms. Chromatin landscaping microarray contains four ERα-responsive promoter regions, each spanning 5 kb upstream and 1 kb downstream from the transcription start sites of these genes. For each gene, a 6 kb region was covered by 12 DNA fragments with an average size of 500 bp, designated as promoter 1 to promoter 10 (P1–P10) and exon 1 to exon 2 (E1–E2). These fragments and 16 control repetitive sequences were amplified by PCR and spotted in triplicate to UltraGAPS-coated slides (Corning, Acton, MA) by using the Affymetrix GMS 417 Arrayer (Affymetrix, Santa Clara, CA). The spotted slides were UV crosslinked and stored in a desiccator.

For global analysis, dye-coupled DNA was also hybridized onto microscopic slides containing 12,192 arrayed DNA fragments (http://data.microarrays.ca/cpg/; Heisler et al., 2005). Microarray hybridization and posthybridization washes have been described previously (Kondo et al., 2004; Yan et al., 2001). The washed slides were scanned by a GenePix 4000A scanner (Axon, Union City, CA), and the acquired microarray images were analyzed with GenePix Pro 6.0 software (Axon). Two independent experiments were performed for each time point treatment and antibody.

Statistical Analysis

After excluding the spots flagged for bad quality, signal ratios were $\log_2$ transformed and normalized by using intensity-dependent normalization (Yang et al., 2002). In order to identify putative ERα targets, the loci were first filtered by SAM analysis (Tusher et al., 2001) by using multiclass comparison with four E2 treatment time points (0, 3, 12, and 24 hr). The target loci were then identified by a signal ratio cutoff of 2 at the 3 hr time point in both independent experiments. To identify acetylated and methylated loci among the putative targets in the ChIP-chip experiments with antibodies against acetyl- and dimethyl-H3-K9, SAM analysis was performed on the 92 target loci as a two-class unpaired time course.

Quantitative ChIP-PCR

To confirm candidate ERα target genes determined by ChIP-chip, PCR primers targeting a region within 200 bp of the predicted ERE were used to measure the amount of this sequence in anti-ERα-immunoprecipitated samples by quantitative PCR with SYBR Green-based detection (Applied Biosystems, Foster City, CA). Experimental quantitative ChIP-PCR values were normalized against values obtained by a standard curve (50 to 0.08 ng, 5-fold dilution, $R^2 > 0.99$) constructed by input DNA with the same primer set. The same method was used to determine binding levels of other factors and enrichment levels of histone modifications. For some target genes (*BCL11A*, *PCDH9*, and *PTPN13*) in which the predicted ERE is located >2 kb upstream of the TSS, additional primers, targeted to a region within 500 bp of the TSS, were designed to measure histone modifications. Specific primers for amplification are available upon request.

RNA Extraction and Quantitative RT-PCR

Total RNA was prepared from sampled cells by the TriZol reagent (Invitrogen). Two μg RNA was treated with DNase I (Invitrogen) to remove potential DNA contamination and then was reverse transcribed with SuperScript II reverse transcriptase (Invitrogen). Quantitative RT-PCR was performed by using SYBR Green (Applied Biosystems) as a marker for DNA amplification on a 7500 Real-Time PCR System apparatus (Applied Biosystems). The relative mRNA level of a given locus was calculated by relative quantitation of gene expression (Applied Biosystems) with *GAPDH* or *β-actin* mRNA (based on amplification efficiency) as an internal control.

Statistical analyses were carried out by using a two-tailed t test. Specific primers for amplification are available on request.

RNA Interference

MCF7 cells (2.5×10^5) were seeded in a 6 well plate and cultured in phenol-red free MEM supplemented with 3% charcoal-dextran-treated FBS overnight. The next day, cells were transfected with predesigned siRNAs against *c-MYC* (catalog number 143591, Ambion, Austin, TX) and/or *ERα* (catalog number M-3401, Upstate Biotechnology) at 25 nM by using TransIT-TKO transfection reagent (Mirus, Madison, WI) according to the manufacturer's protocol. After 2 days, the cells were treated with or without 10 nM E2 for 3 hr, and then total RNA was harvested for quantitative RT-PCR analysis, as described above.

Coimmunoprecipitation

MCF7 cells were hormone-starved for 3 days and then treated with 10 nM E2 for the indicated time periods. Nuclear extracts were prepared with a Nuclear Extract Kit (Active Motif, Carlsbad, CA) and diluted to 1 mg protein/ml with buffer containing 50 mM Tris-HCl and 150 mM NaCl. Nuclear extracts (0.5 mg) were precleared with protein G agarose (30 μl) for 30 min and incubated overnight with anti-c-MYC (1 μg; 9E10, Santa Cruz), anti-ERα (1 μg, Ab-10, Lab Vision Corporation, Fremont, CA), or rabbit IgG (1 μg; Santa Cruz). Immunocomplexes were precipitated with protein G agarose (50 μl) for 1 hr and washed three times with buffer containing 50 mM Tris-HCl, 150 mM NaCl, and 1% NP40. The immunoprecipitated proteins were dissolved in 20 μl SDS-PAGE loading buffer and subjected to immunoblotting analysis with the indicated antibodies.

Transfection and Luciferase Assay

The upstream promoter region (−303 to +472 bp) of *MEA*, including the c-MYC binding site and ERE located at −12 and +155 bp, respectively, was cloned into the luciferase reporter plasmid pGL3 (Dual-Luciferase Reporter Assay System, Promega Corporation, Madison, WI). The c-MYC binding site deletion mutant (pGL3-MEAΔc-MYC) was then generated by site-directed mutagenesis (QuikChange II XL Site-Directed Mutagenesis Kit, Stratagene, La Jolla, CA) and verified by DNA sequencing. MCF7 cells that were hormone-starved for 3 days at 70% confluence were transfected with 1μg of the indicated luciferase reporter constructs and 60 ng of Renilla luciferase plasmid by using Superfect Transfection Reagent (Qiagen, Hilden, Germany) in 6 well plates. The cells were then treated with or without 10 nM E2 for 24 hr, and luciferase activity was analyzed. Luciferase activity was normalized by Renilla value and represented as fold activation relative to the activity obtained by the pGL3 basic construct alone.

Computational Modeling

The OMGProm database (Palaniswamy et al., 2005) was used to retrieve promoter sequences of orthologous pairs for the candidate ERα target genes identified by ChIP-chip. The program *ERTarget*, developed previously by us (Jin et al., 2004, 2005), was used to identify the direct ERα targets by analyzing the promoter sequences. Briefly, the *ERTarget* program discriminates direct ERα target promoters from nontargets by scanning for ERE and combinatorially associating other TFBSs conserved in human-mouse orthologous promoters. We used a similar approach to discriminate acetylated ERα target promoters from methylated ERα target promoters. CART (Breiman et al., 1984) analysis was employed to classify acetylated and methylated ERα target promoters. The resulting model was a highly interpretable decision tree for *cis*-regulatory modules identification. Because CART is a relatively unstable regression method with high variance, further experiments were needed to verify the prediction (see also the Supplemental Data for detailed CART description). All possible TFBSs predicted by MATCH (Kel et al., 2003) using the position weight matrices (PWM) from the TRANSFAC database (Wingender et al., 2000) were considered as binary predictor variables, either 1 or 0, depending on presence or absence within a −220 bp to +220 bp region of a predicted ERE (see Equation 1, Figure 6A). A distance of 220 bp is the approximate distance between adjacent nucleosomal linkers and the optimal distance for short-range looping in chromatin (Ringrose et al., 2003). The "Gini" method was selected as the splitting method for growing the tree, and the 10-fold cross validation method was used to obtain the minimal tree (see Equation 2). The analysis was performed on the commercially available CART software (Salford Systems, San Diego, USA) and used the following equations:

$$D = \left\{ y_i, x_{i1}, \ldots x_{ik} \ldots, x_{iM} \right\}_1^N \quad (1)$$

Where D is a collection of TFs; y_i is the class label for acetylated (equal to 1) and methylated (equal to 0) promoters; x_{ik} is the binary value of TF k that represents presence (equal to 1) or absence (equal to 0) of its binding site within the neighborhood of ERE; N is the number of promoters; M is the number of TFs.

For a node t and classes (1,…, k), Gini index is defined as:

$$GINI(t) = 1 - \sum_j P(j/t)^2 \quad (2)$$

Where $P(j/t)$ is the relative part of class j at node t.

Supplemental Data

Supplemental Data include Supplemental Methods and Results, four tables, four figures, and Supplemental References and can be found with this article online at http://www.molecule.org/cgi/content/full/21/3/393/DC1/.

Acknowledgments

This work was supported in part by National Cancer Institute grants P50 CA113001 and R01 CA-69065; U.S. Army Medical Research awards DAMD 17-02-1-0418 and DAMD17-02-1-0419; American Cancer Society Research and Alaska Run for Woman Grant TBE-104125; and by funds from The Ohio State University Comprehensive Cancer Center-Arthur G. James Cancer Hospital and Richard J. Solove Research Institute. V.X.J. is partly supported by an Up on the Roof postdoctoral fellowship at the Division of Human Cancer Genetics of The Ohio State University.

Received: August 9, 2005
Revised: November 2, 2005
Accepted: December 21, 2005
Published: February 2, 2006

References

Berns, E.M., Klijn, J.G., van Putten, W.L., van Staveren, I.L., Portengen, H., and Foekens, J.A. (1992). c-myc amplification is a better prognostic factor than HER2/neu amplification in primary breast cancer. Cancer Res. *52*, 1107–1113.

Bland, K.I., Konstadoulakis, M.M., Vezeridis, M.P., and Wanebo, H.J. (1995). Oncogene protein co-expression. Value of Ha-ras, c-myc, c-fos, and p53 as prognostic discriminants for breast carcinoma. Ann. Surg. *221*, 706–718.

Breiman, L., Friedman, J.H., Olshen, R.A., and Stone, C.J. (1984). Classification and Regression Trees (New York, NY: Chapman & Hall).

Carroll, J.S., Liu, X.S., Brodsky, A.S., Li, W., Meyer, C.A., Szary, A.J., Eeckhoute, J., Shao, W., Hestermann, E.V., Geistlinger, T.R., et al. (2005). Chromosome-wide mapping of estrogen receptor binding reveals long-range regulation requiring the forkhead protein FoxA1. Cell *122*, 33–43.

DeNardo, D.G., Kim, H.T., Hilsenbeck, S., Cuba, V., Tsimelzon, A., and Brown, P.H. (2005). Global gene expression analysis of estrogen receptor transcription factor cross talk in breast cancer: identification of estrogen-induced/activator protein-1-dependent genes. Mol. Endocrinol. *19*, 362–378.

Dubik, D., Dembinski, T.C., and Shiu, R.P. (1987). Stimulation of c-myc oncogene expression associated with estrogen-induced proliferation of human breast cancer cells. Cancer Res. *47*, 6517–6521.

Heisler, L.E., Torti, D., Boutros, P.C., Watson, J., Chan, C., Winegarden, N., Takahashi, M., Yau, P., Huang, T.H., Farnham, P.J., et al. (2005). CpG Island microarray probe sequences derived from a physical library are representative of CpG Islands annotated on the human genome. Nucleic Acids Res. *33*, 2952–2961.

Jenuwein, T., and Allis, C.D. (2001). Translating the histone code. Science *293*, 1074–1080.

Jin, V.X., Leu, Y.W., Liyanarachchi, S., Sun, H., Fan, M., Nephew, K.P., Huang, T.H., and Davuluri, R.V. (2004). Identifying estrogen receptor alpha target genes using integrated computational genomics and chromatin immunoprecipitation microarray. Nucleic Acids Res. *32*, 6627–6635.

Jin, V.X., Sun, H., Pohar, T.T., Liyanarachchi, S., Palaniswamy, S.K., Huang, T.H., and Davuluri, R.V. (2005). ERTargetDB: an integral information resource of transcription regulation of estrogen receptor target genes. J. Mol. Endocrinol. *35*, 225–230.

Kel, A.E., Gossling, E., Reuter, I., Cheremushkin, E., Kel-Margoulis, O.V., and Wingender, E. (2003). MATCH: A tool for searching transcription factor binding sites in DNA sequences. Nucleic Acids Res. *31*, 3576–3579.

Klinge, C.M., Jernigan, S.C., Mattingly, K.A., Risinger, K.E., and Zhang, J. (2004). Estrogen response element-dependent regulation of transcriptional activation of estrogen receptors alpha and beta by coactivators and corepressors. J. Mol. Endocrinol. *33*, 387–410.

Kondo, Y., Shen, L., and Issa, J.P. (2003). Critical role of histone methylation in tumor suppressor gene silencing in colorectal cancer. Mol. Cell. Biol. *23*, 206–215.

Kondo, Y., Shen, L., Yan, P.S., Huang, T.H., and Issa, J.P. (2004). Chromatin immunoprecipitation microarrays for identification of genes silenced by histone H3 lysine 9 methylation. Proc. Natl. Acad. Sci. USA *101*, 7398–7403.

Lacroix, M., and Leclercq, G. (2004). About GATA3, HNF3A, and XBP1, three genes co-expressed with the oestrogen receptor-alpha gene (ESR1) in breast cancer. Mol. Cell. Endocrinol. *219*, 1–7.

Leu, Y.W., Yan, P.S., Fan, M., Jin, V.X., Liu, J.C., Curran, E.M., Welshons, W.V., Wei, S.H., Davuluri, R.V., Plass, C., et al. (2004). Loss of estrogen receptor signaling triggers epigenetic silencing of downstream targets in breast cancer. Cancer Res. *64*, 8184–8192.

Lincoln, D.W., 2nd, and Bove, K. (2005). The transcription factor Ets-1 in breast cancer. Front. Biosci. *10*, 506–511.

Matsuda, T., Yamamoto, T., Muraguchi, A., and Saatcioglu, F. (2001). Cross-talk between transforming growth factor-beta and estrogen receptor signaling through Smad3. J. Biol. Chem. *276*, 42908–42914.

McDonnell, D.P., and Norris, J.D. (2002). Connections and regulation of the human estrogen receptor. Science *296*, 1642–1644.

McKenna, N.J., and O'Malley, B.W. (2002). Combinatorial control of gene expression by nuclear receptors and coregulators. Cell *108*, 465–474.

McMahon, S.B., Van Buskirk, H.A., Dugan, K.A., Copeland, T.D., and Cole, M.D. (1998). The novel ATM-related protein TRRAP is an essential cofactor for the c-Myc and E2F oncoproteins. Cell *94*, 363–374.

Metivier, R., Penot, G., Hubner, M.R., Reid, G., Brand, H., Kos, M., and Gannon, F. (2003). Estrogen receptor-alpha directs ordered, cyclical, and combinatorial recruitment of cofactors on a natural target promoter. Cell *115*, 751–763.

Metzger, E., Wissmann, M., Yin, N., Muller, J.M., Schneider, R., Peters, A.H., Gunther, T., Buettner, R., and Schule, R. (2005). LSD1 demethylates repressive histone marks to promote androgen-receptor-dependent transcription. Nature *437*, 436–439.

Odom, D.T., Zizlsperger, N., Gordon, D.B., Bell, G.W., Rinaldi, N.J., Murray, H.L., Volkert, T.L., Schreiber, J., Rolfe, P.A., Gifford, D.K., et al. (2004). Control of pancreas and liver gene expression by HNF transcription factors. Science *303*, 1378–1381.

Osborne, C.K., Shou, J., Massarweh, S., and Schiff, R. (2005). Crosstalk between estrogen receptor and growth factor receptor pathways as a cause for endocrine therapy resistance in breast cancer. Clin. Cancer Res. *11*, 865s–870s.

Palaniswamy, S.K., Jin, V.X., Sun, H., and Davuluri, R.V. (2005). OMGProm: a database of orthologous mammalian gene promoters. Bioinformatics *21*, 835–836.

Park, J., Kunjibettu, S., McMahon, S.B., and Cole, M.D. (2001). The ATM-related domain of TRRAP is required for histone acetyltransferase recruitment and Myc-dependent oncogenesis. Genes Dev. *15*, 1619–1624.

Park, K.J., Krishnan, V., O'Malley, B.W., Yamamoto, Y., and Gaynor, R.B. (2005). Formation of an IKKalpha-dependent transcription complex is required for estrogen receptor-mediated gene activation. Mol. Cell *18*, 71–82.

Pelengaris, S., Khan, M., and Evan, G. (2002). c-MYC: more than just a matter of life and death. Nat. Rev. Cancer *2*, 764–776.

Peters, A.H., Kubicek, S., Mechtler, K., O'Sullivan, R.J., Derijck, A.A., Perez-Burgos, L., Kohlmaier, A., Opravil, S., Tachibana, M., Shinkai, Y., et al. (2003). Partitioning and plasticity of repressive histone methylation states in mammalian chromatin. Mol. Cell *12*, 1577–1589.

Peterson, C.L., and Laniel, M.A. (2004). Histones and histone modifications. Curr. Biol. *14*, R546–R551.

Ren, B., Robert, F., Wyrick, J.J., Aparicio, O., Jennings, E.G., Simon, I., Zeitlinger, J., Schreiber, J., Hannett, N., Kanin, E., et al. (2000). Genome-wide location and function of DNA binding proteins. Science *290*, 2306–2309.

Ren, B., Cam, H., Takahashi, Y., Volkert, T., Terragni, J., Young, R.A., and Dynlacht, B.D. (2002). E2F integrates cell cycle progression with DNA repair, replication, and G(2)/M checkpoints. Genes Dev. *16*, 245–256.

Revankar, C.M., Cimino, D.F., Sklar, L.A., Arterburn, J.B., and Prossnitz, E.R. (2005). A transmembrane intracellular estrogen receptor mediates rapid cell signaling. Science *307*, 1625–1630.

Ringrose, L., Rehmsmeier, M., Dura, J.M., and Paro, R. (2003). Genome-wide prediction of Polycomb/Trithorax response elements in Drosophila melanogaster. Dev. Cell *5*, 759–771.

Roh, T.Y., Cuddapah, S., and Zhao, K. (2005). Active chromatin domains are defined by acetylation islands revealed by genome-wide mapping. Genes Dev. *19*, 542–552.

Rushton, J.J., Davis, L.M., Lei, W., Mo, X., Leutz, A., and Ness, S.A. (2003). Distinct changes in gene expression induced by A-Myb, B-Myb and c-Myb proteins. Oncogene *22*, 308–313.

Saville, B., Wormke, M., Wang, F., Nguyen, T., Enmark, E., Kuiper, G., Gustafsson, J.A., and Safe, S. (2000). Ligand-, cell-, and estrogen receptor subtype (alpha/beta)-dependent activation at GC-rich (Sp1) promoter elements. J. Biol. Chem. *275*, 5379–5387.

Stein, B., and Yang, M.X. (1995). Repression of the interleukin-6 promoter by estrogen receptor is mediated by NF-kappa B and C/EBP beta. Mol. Cell. Biol. *15*, 4971–4979.

Tusher, V.G., Tibshirani, R., and Chu, G. (2001). Significance analysis of microarrays applied to the ionizing radiation response. Proc. Natl. Acad. Sci. USA *98*, 5116–5121.

Wasserman, W.W., and Sandelin, A. (2004). Applied bioinformatics for the identification of regulatory elements. Nat. Rev. Genet. *5*, 276–287.

Wingender, E., Chen, X., Hehl, R., Karas, H., Liebich, I., Matys, V., Meinhardt, T., Pruss, M., Reuter, I., and Schacherer, F. (2000). TRANSFAC: an integrated system for gene expression regulation. Nucleic Acids Res. *28*, 316–319.

Xu, J., and Li, Q. (2003). Review of the in vivo functions of the p160 steroid receptor coactivator family. Mol. Endocrinol. *17*, 1681–1692.

Yan, P.S., Chen, C.M., Shi, H., Rahmatpanah, F., Wei, S.H., Caldwell, C.W., and Huang, T.H. (2001). Dissecting complex epigenetic alterations in breast cancer using CpG island microarrays. Cancer Res. *61*, 8375–8380.

Yanagisawa, J., Kitagawa, H., Yanagida, M., Wada, O., Ogawa, S., Nakagomi, M., Oishi, H., Yamamoto, Y., Nagasawa, H., McMahon, S.B., et al. (2002). Nuclear receptor function requires a TFTC-type histone acetyl transferase complex. Mol. Cell *9*, 553–562.

Yang, Y.H., Dudoit, S., Luu, P., Lin, D.M., Peng, V., Ngai, J., and Speed, T.P. (2002). Normalization for cDNA microarray data: a robust composite method addressing single and multiple slide systematic variation. Nucleic Acids Res. *30*, e15.

Accession Numbers

A microarray dataset has been submitted to the GEO database, which is a MIAME compliant repository, under accession number GSE3987.

Breast Cancer Res Treat
DOI 10.1007/s10549-006-9353-2

ORIGINAL PAPER

Characterization of molecular and structural determinants of selective estrogen receptor downregulators

Meiyun Fan · Emily L. Rickert · Lei Chen · Syed A. Aftab · Kenneth P. Nephew · Ross Weatherman

Received: 7 June 2006 / Accepted: 20 July 2006

Abstract Antiestrogens used for breast cancer therapy can be categorized into two classes that differ in their effect on estrogen receptor (ER) alpha stability. The selective estrogen receptor modulators (SERMs) stabilize ER alpha and the selective estrogen receptor downregulators (SERDs) cause a decrease in cellular ER alpha levels. A clinically relevant antiestrogen, GW7604, appears to work through a SERD-like mechanism, despite sharing the same molecular scaffold as 4-hydroxytamoxifen, a SERM. In order to investigate potential structural features of GW7604 responsible for SERD activity, GW7604 and two analogs were synthesized using a new, improved synthetic route and tested for their effects on ER alpha function and cell proliferation. The two analogs, which have an acrylamide or a methyl vinyl ketone replacing the acrylic acid group of GW7604, display lower binding affinity for ER alpha than GW7604, but show similar antagonism of estradiol-induced activation of ER alpha-mediated transcription as GW7604 and inhibit estradiol-induced proliferation of the MCF-7 cell line with a similar potency as GW7604. Unlike GW7604, neither analog has a significant effect on cellular ER alpha levels, suggesting that the carboxylate is a key determinant in GW7604 action and, for the first time, showing that this group is responsible for inducing ER alpha degradation in breast cancer cells.

Keywords Antiestrogen · GW5638 · GW7604 · Estrogen receptor degradation · Selective estrogen receptor downregulator · Selective estrogen receptor modulator · Tamoxifen

Introduction

Tamoxifen (Fig. 1) antiestrogen therapy is one of the first and most effective treatments for the treatment and prevention of estrogen receptor (ER) positive breast cancer. Another antiestrogen, fulvestrant, has recently entered the clinic in the United States (Fig. 1). Dramatic differences between tamoxifen and fulvestrant at both the cellular and structural level have been demonstrated [1]. Tamoxifen, which belongs to a class of compounds known as selective estrogen receptor modulators (SERMs), stabilizes ER alpha and causes a slight increase in receptor levels; in contrast, fulvestrant causes rapid ER alpha degradation, leading some to classify compounds such as fulvestrant as selective estrogen receptor downregulators (SERDs) [2]. These differences in mechanism of action of SERMs and SERDs appear to extend to the mechanisms of resistance to these compounds [3]. Many tumors that acquire tamoxifen resistance but remain ER positive are still sensitive to fulvestrant. As a result, there is much interest in finding other compounds with SERD-like mecha-

Electronic Supplementary Material Supplementary material is available to authorised users in the online version of this article at http://dx.doi.org/10.1007/s10549-006-9353-2.

M. Fan · L. Chen · K. P. Nephew
Department of Medical Sciences, Indiana University School of Medicine, Bloomington, IN, USA

E. L. Rickert · S. A. Aftab · R. Weatherman (✉)
Department of Medicinal Chemistry and Molecular Pharmacology and the Purdue Cancer Center, Purdue University, 575 Stadium Mall Drive, West Lafayette, IN 47907 , USA
e-mail: rossw@pharmacy.purdue.edu

Journal : 10549 | Dispatch : 4-8-2006 | Pages : 8
Article No. : 9353 | ☐ LE | ☐ TYPESET
MS Code : BREA1501 | ☑ CP | ☑ DISK

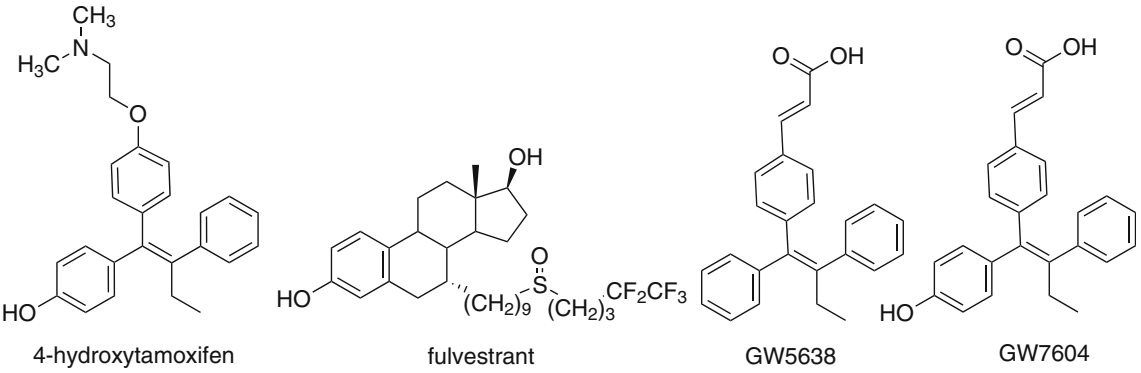

Fig. 1 4-hydroxytamoxifen, fulvestrant, GW5638 and GW7604

nisms and understanding how those compounds cause estrogen receptor degradation.

Two antiestrogens under clinical investigation, GW5638 and its hydroxylated metabolite GW7604 (Fig. 1), have been identified to possess SERD activity similar to fulvestrant and the ability to inhibit the growth of tamoxifen-resistant breast tumors [4, 5]. In contrast to fulvestrant, GW7604 possesses a nonsteroidal structure with a triphenylethylethylene core similar to 4-hydroxytamoxifen. However, GW7604 contains an acrylic acid side chain extending from the triphenylethylethylene core, instead of the basic amine-containing side chain of 4-hydroxytamoxifen (Fig. 1). Exploring the relative importance of the acrylic acid side chain in the overall SERD profile of the GW7604 compound could give insight into the structural determinants for distinguishing SERM and SERD mechanisms and lead to the design of improved antiestrogen therapies for tamoxifen-resistant tumors. In this report, we describe the synthesis and characterization of two new GW7604 analogs and demonstrate that although the carboxylate of GW7604 is essential for eliciting the degradation of ER alpha, this group is not essential for inhibiting the proliferation of breast cancer cells.

Methods

Synthesis of 7604 analogs

The detailed synthetic procedures and characterization for the compounds used in this work can be found in the supplementary material.

ER alpha binding assay

Commercially available fluorescent polarization based competition binding assays (Invitrogen) were used to determine the relative affinity of the GW7604 analogs. Briefly, serial dilutions of the different compounds were prepared in ES2 screening buffer (100 mM potassium phosphate, pH7.4, 100 μg/ml bovine gamma globulin) and 50 μl of each concentration was aliquoted into three wells of a black 96 well assay plate. Fifty microliters of a solution containing 20 nM recombinant ER alpha and 2 nM of a proprietary fluorescent ER ligand (Fluormone-ES2) were added to each well. The plate was incubated for 2 h at room temperature (in the dark with shaking). Fluorescence polarization signals were then measured using a Packard Fusion fluorimeter. The data were fit to a single binding site competition curve by nonlinear regression analysis (Prism 4 software package, Graphpad software). K_i values were determined from the average of 3 different experiments and calculated using a K_D = 4 nM for Fluormone binding to ER alpha.

Transcriptional reporter assays

MCF7/ERE-Luc cells, derived from MCF7 cells stably transfected with a luciferase report construct driven by the estrogen responsive element in *pS2* promoter (ERE-pS2-Luc) [6], were seeded in steroid-free medium for 3 days prior to drug treatment. Cell lysates were prepared with passive lysis buffer (Promega Corp., Madison, WI) and luciferase activity determined using the Luciferase Assay System (Promega). Luciferase activity was normalized against total cellular protein and expressed as the mean unit/mg protein ± SE of three independent experiments.

MCF7 proliferation assays

MCF7 cells (2000/well) were plated in 96-well dishes in steroid-free medium and treated with various doses of

Journal : 10549 Dispatch : 4-8-2006 Pages : 8
Article No. : 9353 LE TYPESET
MS Code : BREA1501 CP DISK

drugs. Cell numbers were determined by MTT assay after 3, 6, 9, and 12 days of drug treatment.

ER alpha stability assays

MCF7 cells (5×10^5/dish) were plated in 60-mm dishes in steroid-free medium for 3 days prior to drug exposure. Whole cell extracts were prepared by suspending cells in 0.1 ml of lysis buffer (62 mM Tris, pH 6.8, 2% sodium dodecyl sulfate; 10% glycerol; 10 μl protease inhibitor cocktail set III). After sonication (3×10 sec), insoluble material was removed by centrifugation (15 min at 12,000 *g*), and protein concentration in the supernatant was determined using the Bio-Rad Laboratories, Inc. protein assay kit. The protein extracts were mixed with 1/4 vol of 5× electrophoresis sample buffer and boiled for 5 min at 90 C. Protein extract (50 μg per lane) was then fractionated by SDS-PAGE, transferred to polyvinylidene difluoride membrane, and probed with antibodies. Primary antibody was detected by horseradish peroxidase-conjugated second antibody and visualized using enhanced SuperSignal West Pico Chemiluminescent Substrate (Pierce Chemical Co., Rockford, IL). The band density of exposed films was evaluated with ImageJ software (http://rsb.info.nih.gov/ij/).

Results

Design and Synthesis of GW7604 Analogs

Although GW5638 and its 4-hydroxylated analog GW7604 share many structural similarities with tamoxifen and 4-hydroxytamoxifen, they appear to modulate ER alpha activity by different mechanisms. Structural information garnered from a crystallographic study with GW5638 bound to the ligand binding domain (LBD) of ER alpha suggests that the acrylic acid side chain of GW5638 induces helix 12 of the LBD to adopt a conformation distinct from the conformation induced by 4-hydroxytamoxifen [7]. The carboxylic acid of the acrylic acid side chain of GW5638 appears to be involved in hydrogen bonds with a bound water molecule and the side chain of aspartate 351 and the backbone amide of leucine 536. The acrylic acid side chain of GW5638 has been shown previously to be important in the overall function of the compound—GW5638 analogs possessing an acrylamide side chain showed equivalent uterotrophic activity as tamoxifen in immature rats compared to the non-uterotrophic activity of 5638 [8]. Furthermore, modification of the acrylic acid side chain to either an acrylamide or a vinyl methyl ketone altered the activity of ER alpha at a specific AP-1 regulated promoter [9].

The unique effects of the acrylamide and methyl vinyl ketone analogs of GW5638, combined with the fact that the 4-hydroxylated compound GW7604 showed significantly more potent activity than GW5638, led to the design of a new synthesis to make a novel acrylamide derivative and remake the methyl vinyl ketone derivative of GW7604. The previously reported synthesis of GW7604 and its methyl vinyl ketone derivative was found to be inadequate for the needs of this study due to two very poor yielding steps that were intractable to optimization—the protection of the phenol as a tetrahydropyran acetal and the formation of a vinyl bromide intermediate. As a result, a new synthesis was designed that relied on a high yielding Friedel–Crafts acylation and Grignard coupling reaction to generate the triphenylethylene core (Fig. 2) [10, 11]. The dehydration generated both stereoisomers of the double bond, but after deprotection of the phenol, the double bond of the triphenylethylene interconverted readily at room temperature, as had been shown previously [9]. That work also showed that only one isomer of GW5638 had biological activity, so it is highly likely that ER alpha only bound to the *E* isomer of these GW7604 analogs. The remainder of the synthesis followed previously reported work to readily generate GW7604 and 7604-ket and a novel analog, 7604-NH2.

Estrogen receptor binding assays

After synthesizing the compounds, we first determined whether the modifications altered the binding affinity to ER alpha. Using a fluorescence polarization-based competition assay with purified full-length ER alpha, the K_i values were determined to be 27 ± 10 nM for GW7604, 240 ± 35 nM for 7604-NH2 and 210 ± 30 nM for 7604-ket (Fig. 3). The K_i determined for GW7604 and 7604-ket are consistent with previous studies [9]. The binding data suggest that although altering the carboxylic acid to either a carboxamide or a methyl ketone reduces the affinity of the ligand for ER alpha significantly ($P < 0.01$, one-way ANOVA test with Dunnett's post-test), the compounds possess sufficient receptor affinity to perform cell-based experiments.

Estrogen receptor transcriptional activity

After testing the binding affinity, we examined the ability of these compounds to modulate ER alpha

Journal : 10549 Dispatch : 4-8-2006 Pages : 8
Article No. : 9353 LE TYPESET
MS Code : BREA1501 CP DISK

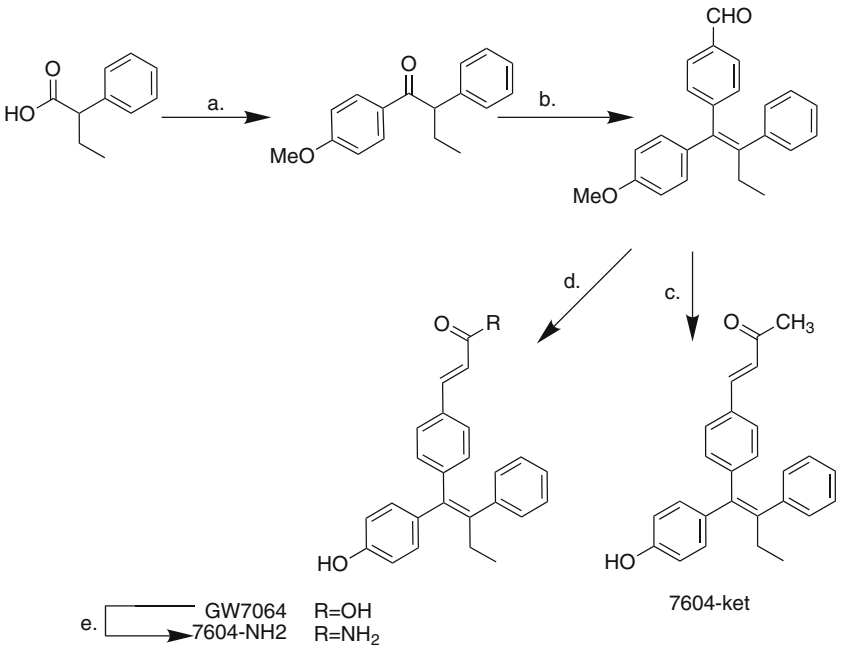

Fig. 2 Synthetic scheme for the preparation of 7604 analogs. (**a**) 2-phenylbutyric acid, trifluoroacetic acid anhydride, phosphoric acid, anisole, 10 C, 100% yield, (**b**) (i)., THF, magnesium, 4-bromobenzaldehyde diethyl acetal; H_3O^+(ii). HCl, ethanol, reflux, 76% yield. (**c**) (i). diethyl (2-oxopropyl)phosphonate, potassium bis(trimethylsilyl)amide, THF, –78 C to room temp. (ii). BBr_3, CH_2Cl_2, 0 C, 54% yield. (**d**) (i).trimethlyphosphonoacetate, potassium bis(trimethylsilyl)amide, THF, –78 C to room temp. (ii). KOH, EtOH/THF,

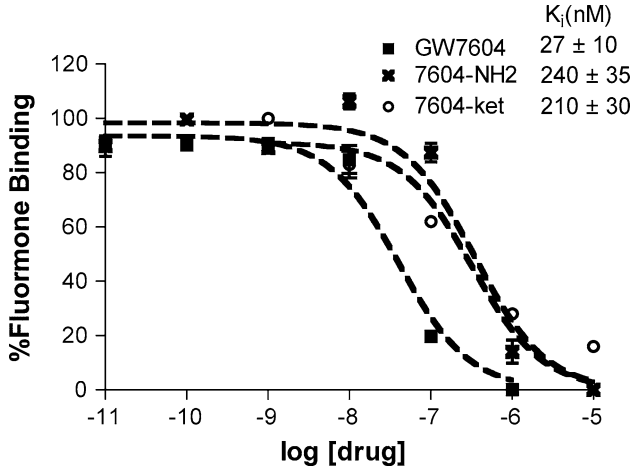

Fig. 3 Binding of 7604 analogs to ER alpha 2 nM of Fluormone ES2 was incubated with recombinant ER alpha in the presence of various concentrations of 7604 analogs and the extent of displacement of fluorescent ligand measured using fluorescence polarization

transcriptional activity inside cells by using MCF7 breast cancer cells stably transfected with an ERE-pS2-Luc construct [6]. All three GW7604 compounds acted as antagonists but showed different potencies, depending on whether hormone was present or absent. In the absence of E2, inhibition of basal reporter gene activity by 7604-NH2 was greater than GW7604 or 7604-ket. However, GW7604 displayed greater inhibition of E2-induced reporter gene activity than 7604-NH2 and 7604-ket (Fig. 4). Consistent with the ER alpha receptor binding data, both 7604-NH2 and 7604-ket were significantly less potent than GW7604 at antagonizing E2-induced transcription of the stably integrated ERE-pS2-Luc reporter.

Receptor stability

One of the most interesting properties of GW7604 is its ability to induce ER alpha degradation after binding to the receptor [12]. In order to determine whether the carboxylic acid group was important in inducing degradation, ER alpha levels were measured in MCF7 cells after treatment with the various analogs. As shown in Fig. 5, GW7604 induced ERα degradation in a dose dependent manner, but the acrylamide and methyl vinyl ketone analogs did not induce degradation to nearly the same extent. Even with extended incubation times, the extent of ER alpha degradation induced by the acrylamide and the methyl vinyl ketone was much less than the degradation induced by GW7604. Taken together, these observations indicate that the carboxylate moiety of GW7604 is essential for its selective estrogen receptor degradation properties.

Journal : 10549 Dispatch : 4-8-2006 Pages : 8
Article No. : 9353 LE TYPESET
MS Code : BREA1501 CP DISK

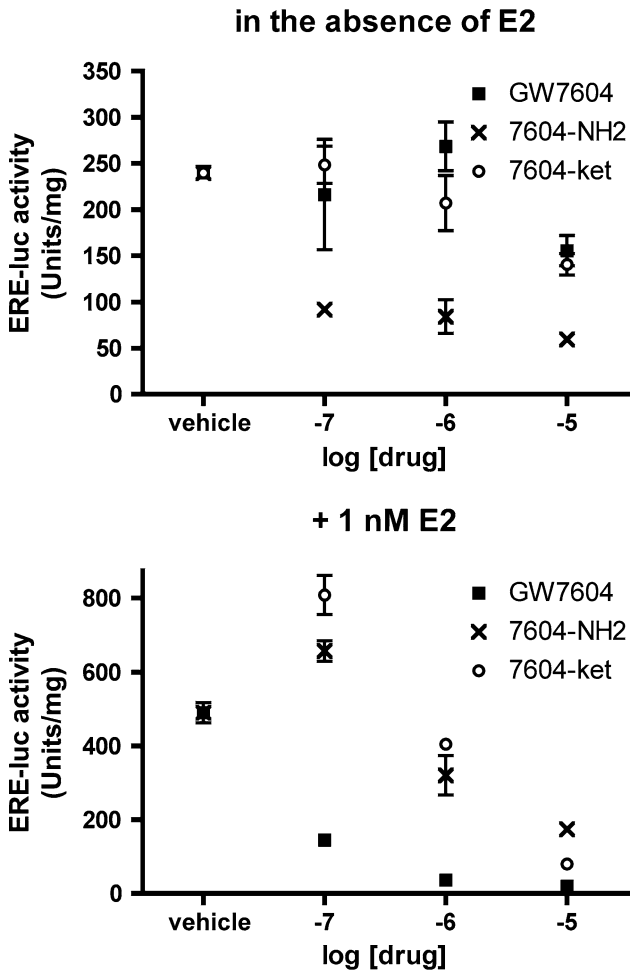

Fig. 4 Effect of 7604 analogs on ER alpha transcription activity. MCF7/ERE-Luc cells were seeded in hormone-free medium for three days, then treated with 7604 analogs as indicated, in the absence or presence of 1 nM E2. Luciferase activity was examined at 24 h after drug treatment. Luciferase activities are normalized against total cellular protein and expressed as the mean units/mg protein ± SE of three independent experiments

Proliferation assays

Because the extent of ER alpha degradation induced by the two GW7604 analogs was not significant, it was unclear whether these compounds would still inhibit estrogen-induced proliferation of breast cancer cells. A standard MTT cell proliferation was performed using MCF-7 cells grown in hormone free media (Fig. 6). In the absence of estradiol, GW7604 and 7604-ket, but not 7604-NH2, significantly inhibited basal cell growth at high doses (10^{-7}–10^{-6} M, $P < 0.05$ versus vehicle, student's *t*-test). In the presence of 1 nM estradiol, however, inhibition of cell growth was observed for all three compounds at approximately the same concentrations, suggesting that the two 7604 analogs act as antiestrogens in the breast, even though they do not induce ER alpha degradation in a fashion similar to GW7604.

Discussion

Selective estrogen receptor degradation represents an emerging, clinically validated paradigm in designing antiestrogen treatments for breast cancer. One major benefit to using a SERD such as fulvestrant compared to using a SERM such as tamoxifen is that SERDs have been found to still effectively treat some ER alpha-positive, tamoxifen-resistant breast cancers [13]. Thus, compounds that induce ER alpha degradation may be used to extend the period of time that breast cancer patients can be treated successfully with antiestrogen therapies, presumably by using different SERMs, aromatase inhibitors and SERDs in succession [14].

While fulvestrant is considered an effective therapeutic agent for treatment of advanced breast cancer [1, 13], a major problem at the current time is poor bioavailability, thereby requiring monthly intramuscular injections for drug delivery. In addition, the synthesis of fulvestrant is lengthy and difficult to modify in order to study structure-activity relationships related to the ability of the drug to induce ER alpha degradation. Due to the difficulty of working with fulvestrant, the finding that GW7604 induced ER alpha degradation provided an excellent opportunity to study the molecular mechanisms of SERD activity.

Even though both fulvestrant and GW7604 induce ER alpha degradation, these compounds are significantly different molecules. Fulvestrant is a steroidal compound with an extremely long, flexible extending side chain, whereas GW7604 has a rigid, nonsteroidal structure and an extending side chain that terminates in a carboxylic acid—a rarity in compounds that target the ER alpha. The fact that both of these compounds could induce ER alpha degradation was initially puzzling. However, the crystal structures of GW5638 and fulvestrant bound to the ER alpha ligand binding domain (LBD) were recently reported [7, 15], revealing that receptor conformations induced by both compounds exposed hydrophobic residues, which are normally ''packed'' inside the LBD, to the surrounding solvent. Exposed hydrophobic patches on the protein surface are known targeting signals for protein degradation [16], and fulvestrant and GW5638 induce this repositioning of hydrophobic residues through different mechanisms. The long side chain of fulvestrant blocks any interaction of helix 12 with the rest of the LBD, resulting in exposure of the hydrophobic core of the receptor binding pocket to solvent. In contrast, GW5638 causes less disruption of helix 12 than fulvestrant, but the carboxylic acid of GW5638 forms hydrogen bonds with the amide backbone of Leu536

Journal : 10549 Dispatch : 4-8-2006 Pages : 8
Article No. : 9353 LE TYPESET
MS Code : BREA1501 CP DISK

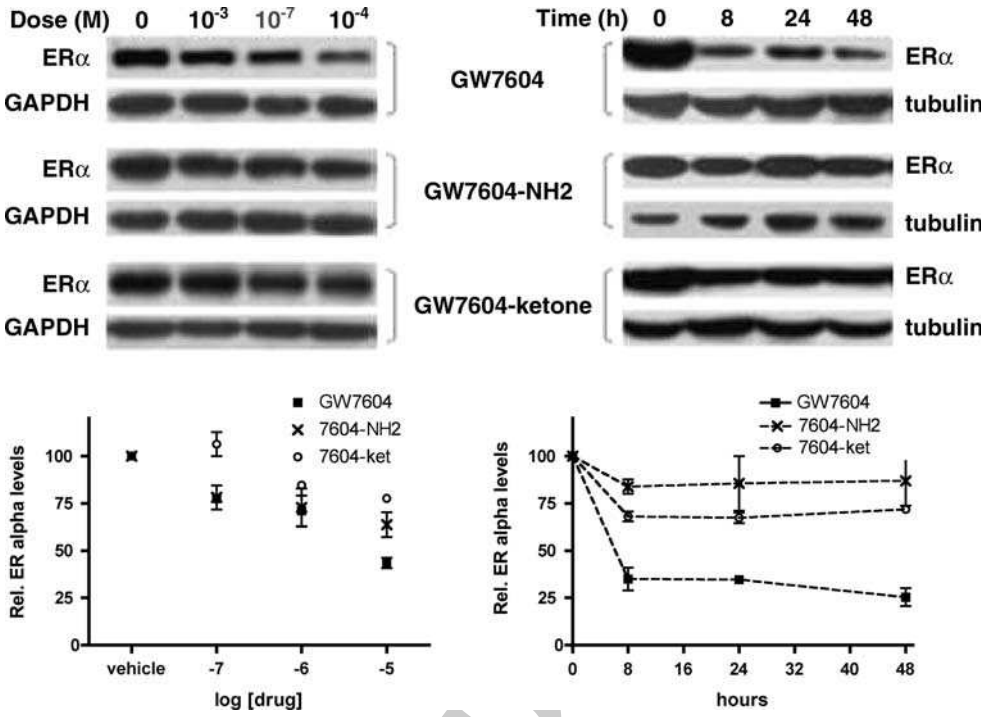

Fig. 5 Effects of 7604 analogs on ER alpha stability. MCF7 cells were seeded in hormone-free medium for three days, then treated with 7604 analogs for various times as indicated. ER alpha levels in whole cell extracts were determined by immunoblotting with anti-ERα antibody. GAPDH or tubulin was used as the loading control. Representative results of experiments performed in duplicate are shown. Relative ER alpha levels (versus untreated cells) are shown in the corresponding histogram

and Tyr537, tethering that region of helix 12 closer to the ligand binding pocket and distorting the positioning of the other hydrophobic residues of helix 12 (Fig. 7). This key interaction between the carboxylic acid and the residues of helix 12 led us to explore the effect of changing that carboxylic acid on the function of GW7604.

The analysis of the GW5638-ER alpha LBD structure suggests that the acrylic acid group on GW5638 is protonated. If this is true, then converting the carboxylic acid of GW7604 to a carboxamide is a fairly conservative change. The carboxamide is not exactly isosteric with the carboxylic acid and the protons on the carboxamide are much less acidic, but the carboxamide is still capable of hydrogen bonding and could potentially hold the helix 12 backbone in the same degradation-inducing conformation when bound in the binding site. Converting the carboxylic acid to a methyl ketone would generate a compound capable of fitting into the binding pocket but unable to engage in the same number of hydrogen bonds as the carboxylic acid of GW7604. The ketone would likely not be able to maintain the necessary contacts with backbone amide hydrogens in helix 12 to induce degradation.

Making conservative changes in the carboxylic acid moiety proved to be deleterious when the ER alpha binding affinity of the two analogs was measured. Both analogs bound to the receptor with lower affinity but the equilibrium dissociation constants were still in the nanomolar range, suggesting that the modifications were still mostly compatible with the binding pocket. Both analogs also inhibited ER alpha mediated transcription from an ERE-controlled promoter, another indication that the compounds were able to disrupt the normal packing of helix 12 to form the coactivator binding pocket. Even though the two analogs do show some differences with GW7604 from the viewpoint of binding and transcriptional regulation, the two analogs differed significantly from GW7604 in terms of effects on ER alpha stability. GW7604 induced ER alpha degradation in a dose dependent and time dependent manner, whereas the two analogs had minimal effects on ER alpha levels. Overall, this difference did not have a significant effect on the ability of the two analogs to inhibit estradiol-induced MCF7 proliferation, as both GW7604-ket and 7604-NH2 inhibited cell growth to nearly the same extent as GW7604. For both the ERE transcriptional assays and the cell proliferation assays, the different effects seen for the 3 compounds in the absence of estradiol are not easily rationalized, but we speculate that these differences reflect the ability of the compounds to induce distinctive conformational changes in ER alpha that affect basal levels of activity.

Ultimately, these results suggest that modification of the carboxylate moiety of GW7604 converts the mechanism of action from a SERD-like mechanism found with fulvestrant to a SERM-like mechanism found with tamoxifen and raloxifene. Comparing the binding modes of the side chain extension of GW5638

Journal : 10549 Dispatch : 4-8-2006 Pages : 8
Article No. : 9353 LE TYPESET
MS Code : BREA1501 CP DISK

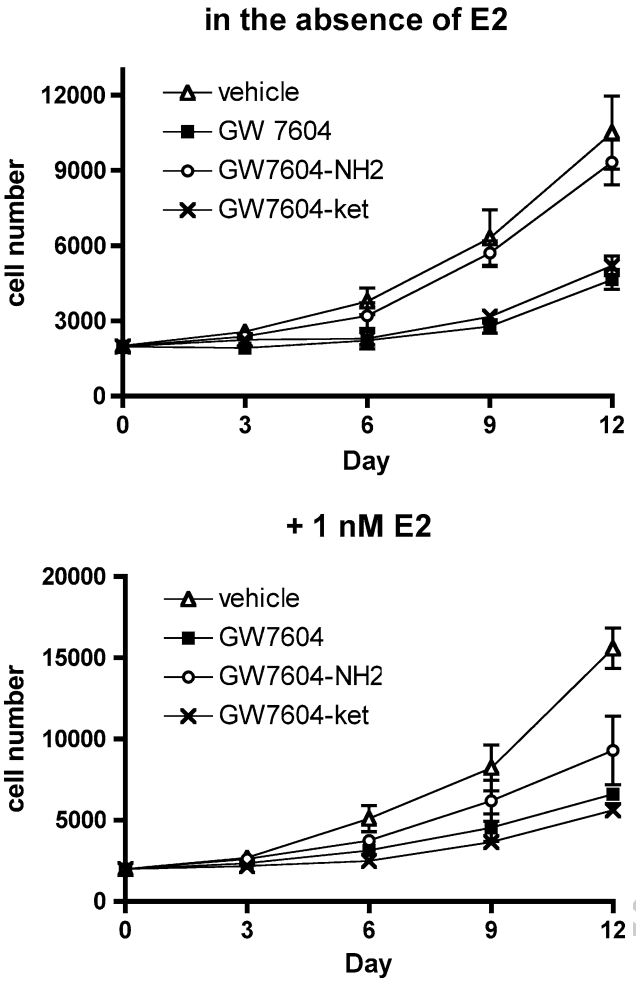

Fig. 6 Effect of 7604 Analogs on MCF7 cell growth. MCF7 cells were seeded in hormone-free medium and treated with 7604 analogs as indicated, in the absence or presence of 1 nM E2. Seven days after treatment, cell number was determined by MTT assay. Experiments were performed twice in triplicate

and 4-hydroxtamoxifen with ER alpha (Fig. 7) shows that GW5638 is able to make hydrogen bond contacts with the helix 12 backbone protons whereas 4-hydroxytamoxifen does not. It is likely that the acrylamide and methyl vinyl ketone analogs are also unable to make the necessary number of hydrogen bonds to the helix 12 backbone, either due to steric effects or lack of appropriate hydrogen bond donor or acceptor groups. Because GW7604-ket and 7604-NH2 likely interact with Asp351, helix 12 can still be displaced and antagonize transcription in a manner similar to 4-hydroxytamoxifen, i.e., a more "SERM-like" mechanism of action. The analogs do not induce ER alpha degradation, indicating that repositioning of helix 12 into a conformation that exposes hydrophobic residues does not occur.

In conclusion, we have characterized the activity of two new antiestrogens and demonstrated, for the first time using very slight chemical changes, the conversion of an antiestrogenic compound and "ER downregulator" into a SERM and "receptor stabilizer". The implications of our findings may have clinical significance. Breast tumors that become resistant to one antiestrogen class often maintain sensitivity to another class of antiestrogens. Based on our observations, we suggest that two distinct classes of therapeutics can be derived from one tight binding lead structure. Modifications that allow for additional interactions between the ligand and receptor appear to be key determinants for designing new ER downregulators (i.e. SERDs) with potential clinical use. Such interactions, which also cause a slight unfolding of the LBD, expose hydrophobic residues to solvent. Unfortunately, at this time, there are no general rules for eliciting such

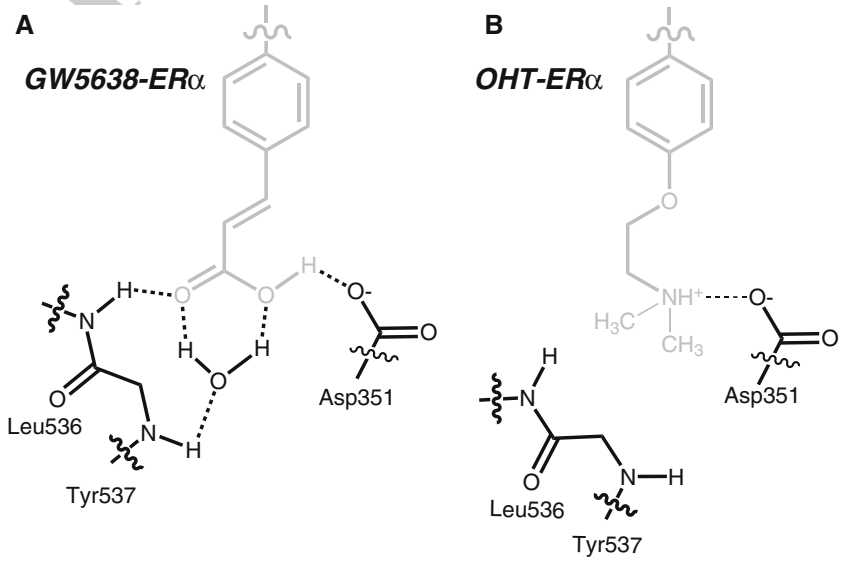

Fig. 7 Binding of GW5638 and 4-hydroxytamoxifen side chains. Cartoon schematic of the interactions between the side chains of the ER alpha ligand binding domain with the side chain extension of (**A**) GW5638 and (**B**) 4-hydroxytamoxifen. Triphenylethylethylene core and side chain residues of Leu537 and Tyr537 are omitted for clarity. Dashed lines represent hydrogen bonds

Journal : 10549 Dispatch : 4-8-2006 Pages : 8
Article No. : 9353 LE TYPESET
MS Code : BREA1501 CP DISK

unfolding, and further study into the mechanistic differences between different types of antiestrogens is needed in order to extend the usefulness of high affinity pharmacophores.

Acknowledgements RVW acknowledges the Purdue Cancer Center, the Indiana Elks Charities and the Army Breast Cancer Research Program (BC030507) for supporting this work. KPN gratefully acknowledges the following agencies for supporting this work: the Walther Cancer Institute, U.S. Army Medical Research Acquisition Activity, Award Numbers DAMD 17-02-1-0418 and DAMD17-02-1-0419; American Cancer Society Research and Alaska Run for Woman Grant TBE-104125

References

1. Robertson JF (2004) Selective oestrogen receptor modulators/new antioestrogens: a clinical perspective. Cancer Treat Rev 30:695-706
2. Osborne CK, Wakeling A, Nicholson RI (2004) Fulvestrant: an oestrogen receptor antagonist with a novel mechanism of action. Br J Cancer 90(Suppl 1):S2–6
3. Normanno N, Di Maio M, De Maio E et al (2005) Mechanisms of endocrine resistance and novel therapeutic strategies in breast cancer. Endocr Relat Cancer 12:721–747
4. Willson TM, Norris JD, Wagner BL et al (1997) Dissection of the molecular mechanism of action of GW5638, a novel estrogen receptor ligand, provides insights into the role of estrogen receptor in bone. Endocrinology 138:3901–3911
5. Wijayaratne AL, Nagel SC, Paige LA et al (1999) Comparative analyses of mechanistic differences among antiestrogens. Endocrinology 140:5828–5840
6. Fan M, Long X, Bailey JA et al (2002) The activating enzyme of NEDD8 inhibits steroid receptor function. Mol Endocrinol 16:315–330
7. Wu YL, Yang X, Ren Z et al (2005) Structural basis for an unexpected mode of SERM-mediated ER antagonism. Mol Cell 18:413–424
8. Willson TM, Henke BR, Momtahen TM et al (1994) 3-[4-(1,2-Diphenylbut-1-enyl)phenyl]acrylic acid: a non-steroidal estrogen with functional selectivity for bone over uterus in rats. J Med Chem 37:1550–1552
9. Weatherman RV, Clegg NJ, Scanlan TS (2001) Differential SERM activation of the estrogen receptors (ERalpha and ERbeta) at AP-1 sites. Chem Biol 8:427–436
10. Eaddy III, JF, Heyer D, Katamreddy SR et al (2005) Preparation of acyloxydiphenylbutenylcinnamates as estrogen receptor modulator prodrugs
11. Smyth TP, Corby BW (1998) Toward a clean alternative to Friedel-Crafts acylation: In situ formation, observation, and reaction of an acyl bis(trifluoroacetyl)phosphate and related structures. J Org Chem 63:8946–8951
12. Wijayaratne AL, McDonnell DP (2001) The human estrogen receptor-alpha is a ubiquitinated protein whose stability is affected differentially by agonists, antagonists, and selective estrogen receptor modulators. J Biol Chem 276:35684–35692
13. Robertson JF, Come SE, Jones SE et al (2005) Endocrine treatment options for advanced breast cancer–the role of fulvestrant. Eur J Cancer 41:346–356
14. Shao W, Brown M (2004) Advances in estrogen receptor biology: prospects for improvements in targeted breast cancer therapy. Breast Cancer Res 6:39–52
15. Pike AC, Brzozowski AM, Walton J et al (2001) Structural insights into the mode of action of a pure antiestrogen. Structure (Camb) 9:145–153
16. Bohley P (1996) Surface hydrophobicity and intracellular degradation of proteins. Biol Chem 377:425–435

Journal : 10549 | Dispatch : 4-8-2006 | Pages : 8
Article No. : 9353 | ☐ LE | ☐ TYPESET
MS Code : BREA1501 | ☑ CP | ☑ DISK